

AFFTC-TIH-90-001

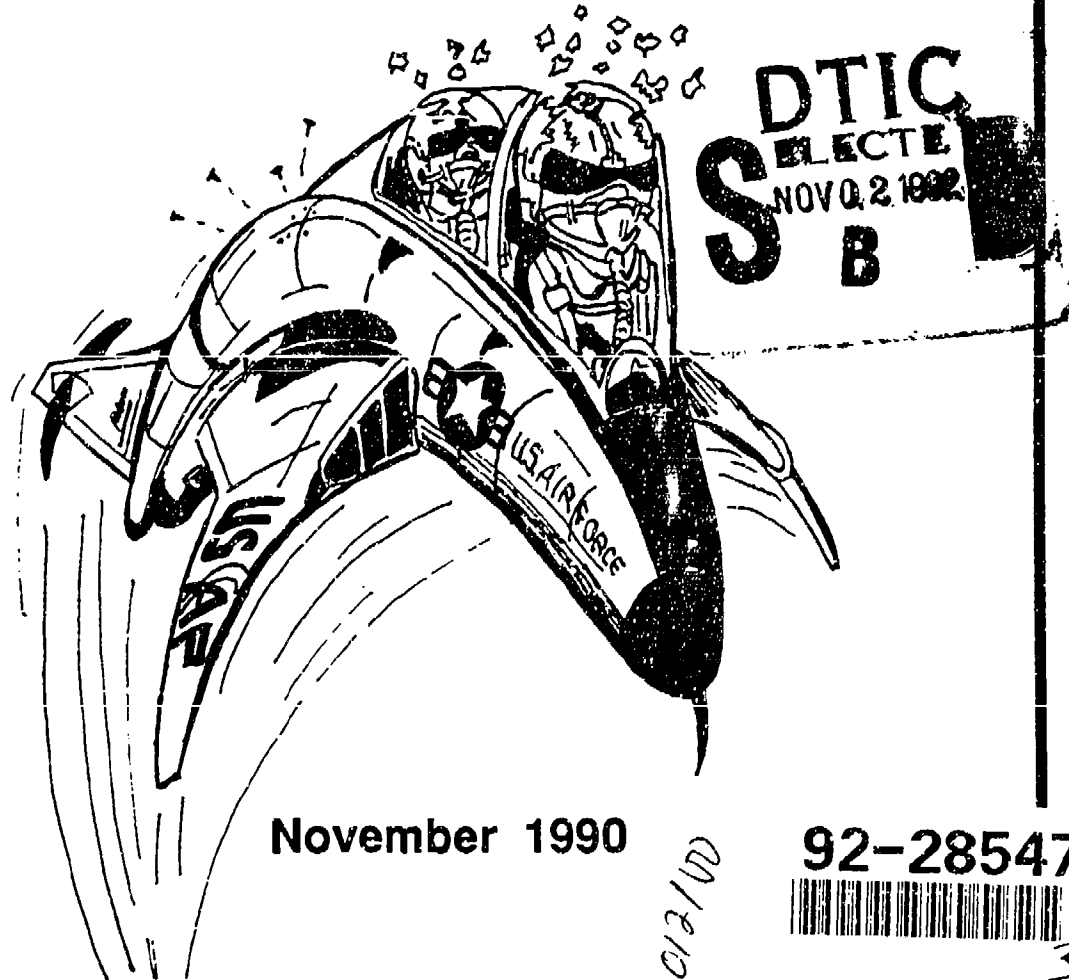
AD-A257 262



# STRUCTURES FLIGHT TEST HANDBOOK

Captain William J. Norton

A  
F  
F  
T  
C



Approved for public release; distribution unlimited.

AIR FORCE FLIGHT TEST CENTER  
EDWARDS AIR FORCE BASE, CALIFORNIA  
AIR FORCE SYSTEMS COMMAND  
UNITED STATES AIR FORCE

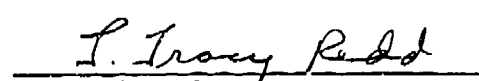
92 10 30 027

This handbook, TIH-90-001, Structures Flight Test Handbook, was prepared as an aid to engineers at the Air Force Flight Test Center, Edwards Air Force Base, California, 93523-5000.

Prepared by:

  
WILLIAM J. NORTON  
Captain, USAF  
Flight Test Engineer

This handbook has been reviewed  
and is approved for publication:  
15 November 1990

  
L. TRACY REDD  
Chief  
Structural Dynamics Branch

  
ROGER C. CRANE  
Chief Engineer  
6510 Test Wing

Do not return; retain or destroy.

## PREFACE

The STRUCTURES FLIGHT TEST HANDBOOK was written principally as a training aid for new engineers assigned to the Air Force Flight Test Center (AFFTC), Edwards AFB, California. Experienced structural flight test engineers may find the hand book useful as a reference and resource guide only.

The handbook is intended to provide a "broad-brush" overview of the many disciplines encompassed by the structures flight test field. It provides the basic knowledge and introduction required for the new engineer to become productive in the briefest time possible. It assumes knowledge of at least undergraduate engineering concepts. Underlying assumptions, applicable standards and regulations, common testing approaches, rules of thumb, and examples are provided in each area. Development or equations are minimized with specific references to readily available texts or handbooks provided for those who need to develop a more complete understanding of the supporting mathematics. The HANDBOOK is not intended as a textbook so supplemental reading should become a normal practice for the structures engineer. A comprehensive index is provided for quick reference and each chapter contains a list of nomenclature for that chapter. An attempt has been made to make the HANDBOOK more readable than a textbook.

Despite its necessary limitations, the HANDBOOK fills a long-suffered gap in one crucial area of flight test engineering. It will be updated or revised as the structures personnel at the AFFTC see a need or as readers suggest. If the reader finds any omission or errors, this may be corrected by recommending the changes to the author or the current Handbook Manager.

DTIC QUALITY INSPECTED 1

Accession For	
NTIS GRA&I	<input checked="" type="checkbox"/>
DTIC TAB	<input type="checkbox"/>
Unclassified	<input type="checkbox"/>
Justification	
By _____	
Distribution/	
Availability Codes	
Dist.	Avail and/or Special
A-1	

## **ACKNOWLEDGEMENTS**

A great many people are to thank for making this handbook possible. The number who helped, either directly or indirectly, are too numerous to list here. However, a few are due special mention. The personnel of the Air Force Flight Test Center (AFFTC) Structural Dynamics Branch, of whom I have proudly count myself a part, are to be thanked for the many tedious readings and re-readings of the manuscript and their very helpful comments. Most of all, I owe a great deal to Mr. Tracy Redd, the Branch Chief, who taught me so much, not all of it about engineering, and tolerated my atypical behavior during the time I worked for him. Many of the other engineers at AFFTC also contributed comments on drafts of the HANDBOOK, most notably Mr. Jim Ford, Mr. Al Webb, Mr. Russ Lenz, Mr. Wayne Olsen, and Mr. Tom Twisdale. In other USAF organizations I must thank Ms. Mary Marshall of the 3246th Test Wing, Maj. Dan Gleason of the USAF Test Pilot School, and Mr. Dave Denner of the Aeronautical Systems Division. Among this nation's outstanding aerospace companies I owe thanks to Mr Carl Johnson and Mr. Bob Pearson of McDonnel-Douglas and the remarkable Mr. Alex Mackenzie of North American Rockwell. A special thanks to Mr. Mike Kehoe of the NASA Ames/Dryden Flight Research Facility. I am especially grateful to Ms. Mary Bradley and Mr. Joe Stroface who caught many grammatical errors and who helped to make this publication look so professional.

Bill Norton  
November 1990

# TABLE OF CONTENTS

	<u>Page No.</u>
PREFACE . . . . .	iii
ACKNOWLEDGMENTS . . . . .	iv
1.0 BASICS OF AIRCRAFT	
1.1 INTRODUCTION . . . . .	1-1
1.2 GEOMETRY . . . . .	1-1
1.2.1 WING GROUP . . . . .	1-1
1.2.2 TAIL GROUP . . . . .	1-3
1.2.3 FUSELAGE GROUP . . . . .	1-6
1.2.4 LANDING GEAR GROUP . . . . .	1-6
1.2.5 MISCELLANEOUS . . . . .	1-8
1.3 SYSTEMS . . . . .	1-8
1.3.1 PROPULSION . . . . .	1-10
1.3.2 HYDRAULICS . . . . .	1-13
1.3.3 ELECTRICAL . . . . .	1-13
1.3.4 ENVIRONMENTAL CONTROL SYSTEM . . . . .	1-13
1.3.5 FUEL . . . . .	1-15
1.3.6 FLIGHT CONTROLS . . . . .	1-15
1.3.7 COCKPIT GROUP . . . . .	1-15
1.3.8 WEAPONS . . . . .	1-20
NOMENCLATURE . . . . .	1-22
REFERENCES . . . . .	1-22
2.0 AERODYNAMICS AND FLIGHT MECHANICS	
2.1 INTRODUCTION . . . . .	2-1
2.2 BASIC AERODYNAMICS . . . . .	2-1
2.2.1 THE ATMOSPHERE . . . . .	2-1
2.2.2 ALTITUDE AND AIRSPEED MEASUREMENT . . . . .	2-4
2.2.3 AIRFLOW VISUALIZATION . . . . .	2-6
2.2.4 SUPERSONIC FLIGHT . . . . .	2-7
2.2.5 GENERATION OF LIFT . . . . .	2-8
2.2.6 GENERATION OF DRAG . . . . .	2-9
2.2.7 AERODYNAMIC MODELING . . . . .	2-11
2.3 BASIC FLIGHT MECHANICS . . . . .	2-12
2.3.1 REFERENCE SYSTEM . . . . .	2-13
2.3.2 WEIGHT AND BALANCE . . . . .	2-13
2.3.3 STATIC STABILITY . . . . .	2-14
2.3.4 DYNAMIC STABILITY . . . . .	2-16

## TABLE OF CONTENTS (Continued)

	Page No.
2.3.5 AEROELASTIC EFFECTS ON STABILITY AND CONTROL . . . . .	2-17
NOMENCLATURE . . . . .	2-17
REFERENCES . . . . .	2-18
3.0 MATERIALS	
3.1 INTRODUCTION . . . . .	3-1
3.2 CHARACTERISTICS . . . . .	3-1
3.2.1 STRESS . . . . .	3-1
3.2.2 STRAIN . . . . .	3-1
3.2.3 STRESS ANALYSIS . . . . .	3-4
3.2.4 THERMAL EFFECTS . . . . .	3-5
3.3 COMPOSITES . . . . .	3-5
3.4 FAILURE MODES . . . . .	3-7
3.4.1 CREEP . . . . .	3-8
3.4.2 WORK-HARDENING . . . . .	3-8
3.4.3 DELAMINATION . . . . .	3-8
3.4.4 CRACKING . . . . .	3-8
3.4.5 FATIGUE . . . . .	3-8
3.4.6 CORROSION . . . . .	3-8
3.5 INSPECTIONS . . . . .	3-9
3.5.1 STRESS VISUALIZATION . . . . .	3-9
3.5.2 DYE PENETRATION . . . . .	3-10
3.5.3 MAGNETIC PARTICLES . . . . .	3-10
3.5.4 X-RAY . . . . .	3-10
3.5.5 ULTRASONICS . . . . .	3-10
3.5.6 EDDY CURRENT . . . . .	3-10
3.6 DEFINITIONS . . . . .	3-10
NOMENCLATURE . . . . .	3-11
REFERENCES . . . . .	3-11
4.0 BASIC STRUCTURAL DYNAMICS	
4.1 INTRODUCTION . . . . .	4-1
4.2 BASIC SYSTEM ELEMENTS . . . . .	4-1
4.3 SIMPLE SYSTEM MODELS . . . . .	4-3
4.3.1 FREE RESPONSE CASE . . . . .	4-4
4.3.2 FORCED RESPONSE CASE . . . . .	4-7
4.4 SUPPLEMENTAL CONCEPTS . . . . .	4-10
4.4.1 RESPONSE RELATIONSHIPS . . . . .	4-10

## TABLE OF CONTENTS (Continued)

	<u>Page No.</u>
4.4.2 COMPLEX MODES . . . . .	4-11
4.4.3 BEATING . . . . .	4-12
4.4.4 HARMONICS . . . . .	4-13
4.4.5 JUMP PHENOMENA . . . . .	4-13
4.5 MODAL ANALYSIS . . . . .	4-13
4.5.1 MULTI-DEGREE OF FREEDOM SYSTEMS . . . . .	4-13
4.5.2 COORDINATE TRANSFORMATION AND SOLUTION . . . . .	4-15
NOMENCLATURE . . . . .	4-17
REFERENCES . . . . .	4-19
 5.0 LOADS	
5.1 INTRODUCTION . . . . .	5-1
5.2 MANEUVER LOADS . . . . .	5-2
5.2.1 LOADS GROUND TESTS . . . . .	5-7
5.2.2 LOADS FLIGHT TESTS . . . . .	5-8
5.2.2.1 INSTRUMENTATION . . . . .	5-8
5.2.2.2 MANEUVERS . . . . .	5-10
5.2.2.3 ANALYSIS . . . . .	5-11
5.3 GUST LOADS . . . . .	5-12
5.3.1 GUST LOADS FLIGHT TESTS . . . . .	5-12
5.4 LOAD ALLEVIATION SYSTEMS . . . . .	5-13
5.5 LANDING GEAR . . . . .	5-14
5.5.1 GEAR LOADS . . . . .	5-14
5.5.2 GEAR SHIMMY . . . . .	5-17
NOMENCLATURE . . . . .	5-17
REFERENCES . . . . .	5-18
 6.0 FLUTTER	
6.1 INTRODUCTION . . . . .	6-1
6.2 DESCRIPTION . . . . .	6-1
6.2.1 FLUTTER EXAMPLES . . . . .	6-3
6.2.2 FLUTTER SUPPRESSION . . . . .	6-6
6.3 FLUTTER PREDICTION . . . . .	6-6
6.3.1 K-METHOD . . . . .	6-9
6.3.2 PK-METHOD . . . . .	6-10
6.3.3 P-METHOD . . . . .	6-12
6.3.4 OTHER METHODS . . . . .	6-12
6.4 OTHER AEROELASTIC PHENOMENA . . . . .	6-13

## TABLE OF CONTENTS (Continued)

	<u>Page No.</u>
6.4.1 PANEL FLUTTER . . . . .	6-13
6.4.2 BUZZ . . . . .	6-13
6.4.3 STALL FLUTTER . . . . .	6-14
6.4.4 DIVERGENCE . . . . .	6-14
6.4.5 CONTROL REVERSAL . . . . .	6-15
6.4.6 LIMIT CYCLE OSCILLATION . . . . .	6-15
6.4.7 BUFFET . . . . .	6-15
6.4.8 MECHANICAL VIBRATION . . . . .	6-16
6.4.9 DYNAMIC RESPONSE . . . . .	6-16
6.4.10 AEROTHERMOELASTICITY . . . . .	6-16
6.5 PRELIMINARY GROUND TESTS . . . . .	6-16
6.5.1 WIND TUNNEL TESTS . . . . .	6-18
6.5.2 GROUND VIBRATION TEST . . . . .	6-18
6.6 FLUTTER FLIGHT TESTS . . . . .	6-18
6.6.1 EXCITATION . . . . .	6-18
6.6.1.1 PULSE . . . . .	6-19
6.6.1.2 SWEEP . . . . .	6-19
6.6.1.3 BURST-AND-DECAY . . . . .	6-22
6.6.1.4 PYROTECHNIC . . . . .	6-22
6.6.1.5 AIR TURBULENCE . . . . .	6-23
6.6.2 PROCEDURES . . . . .	6-23
6.7 DATA REDUCTION . . . . .	6-26
6.8 STORES FLUTTER TESTING . . . . .	6-27
6.9 RULES OF THUMB . . . . .	6-27
NOMENCLATURE . . . . .	6-29
REFERENCES . . . . .	6-29
 7 0 GROUND VIBRATION TESTS	
7.1 INTRODUCTION . . . . .	7-1
7.2 OVERVIEW . . . . .	7-1
7.3 UNDERLYING ASSUMPTIONS . . . . .	7-2
7.4 PREPARATION . . . . .	7-2
7.4.1 CONFIGURATION . . . . .	7-3
7.4.2 REDUCING NONLINEARITIES . . . . .	7-3
7.4.3 PRELOADS . . . . .	7-4
7.5 AIRCRAFT SUSPENSION . . . . .	7-4
7.6 ELECTRODYNAMIC SHAKERS . . . . .	7-5
7.6.1 CHARACTERISTICS . . . . .	7-5

## TABLE OF CONTENTS (Continued)

	Page No.
7.6.1.1 PHYSICAL FEATURES . . . . .	7-5
7.6.1.2 SELECTION . . . . .	7-7
7.6.2 SUSPENSION . . . . .	7-7
7.6.3 ATTACHMENT TO STRUCTURE . . . . .	7-8
7.6.4 IMPEDANCE MISMATCH . . . . .	7-9
7.7 TRANSDUCER INSTALLATION . . . . .	7-12
7.8 EXCITATION TECHNIQUES . . . . .	7-12
7.8.1 OPERATING INPUTS . . . . .	7-12
7.8.2 TRANSIENT . . . . .	7-13
7.8.2.1 IMPACT . . . . .	7-13
7.8.2.2 STEP RELAXATION . . . . .	7-16
7.8.3 SINE WAVEFORMS . . . . .	7-16
7.8.3.1 SINE SWEEP . . . . .	7-17
7.8.3.2 SINE DWELL . . . . .	7-18
7.8.3.3 CHIRP . . . . .	7-18
7.8.4 RANDOM . . . . .	7-18
7.8.4.1 PURE RANDOM . . . . .	7-18
7.8.4.2 PSEUDO-RANDOM . . . . .	7-19
7.8.4.3 PERIODIC RANDOM . . . . .	7-19
7.8.4.4 BURST RANDOM . . . . .	7-20
7.9 LINEARITY CHECK . . . . .	7-20
7.10 SURVEYS . . . . .	7-20
7.11 MODAL RESULTS . . . . .	7-22
7.11.1 MULTI-POINT DATA . . . . .	7-22
7.11.2 MODE VISUALIZATION . . . . .	7-23
7.11.3 ORTHOGONALITY CHECKS . . . . .	7-23
NOMENCLATURE . . . . .	7-27
REFERENCES . . . . .	7-27
 8.0 AEROSERVOELASTICITY	
8.1 INTRODUCTION . . . . .	8-1
8.2 CONTROL THEORY . . . . .	8-3
8.2.1 BASIC CONCEPTS . . . . .	8-3
8.2.2 COMPENSATION . . . . .	8-6
8.2.3 REPRESENTATIONS . . . . .	8-6
8.2.3.1 ROOT-LOCUS . . . . .	8-6
8.2.3.2 BODE . . . . .	8-8
8.2.3.3 NYQUIST AND POLAR . . . . .	8-10

## TABLE OF CONTENTS (Continued)

	<u>Page No.</u>
8.3 ANALYSIS . . . . .	8-12
8.4 GROUND TESTS . . . . .	8-12
8.5 FLIGHT TESTS . . . . .	8-15
8.5.1 NOTCH FILTER . . . . .	8-15
NOMENCLATURE . . . . .	8-18
REFERENCES . . . . .	8-19
9.0 VIBRO-ACOUSTICS	
9.1 INTRODUCTION . . . . .	9-1
9.2 GENERAL VIBRATION . . . . .	9-2
9.3 FUNDAMENTALS OF SOUND . . . . .	9-2
9.4 MEASUREMENT OF SOUND . . . . .	9-3
9.5 FLIGHT TESTS . . . . .	9-8
9.5.1 PRELIMINARY GROUND TESTS . . . . .	9-8
9.5.2 TEST CONCEPTS . . . . .	9-9
9.5.3 DATA ANALYSIS . . . . .	9-9
NOMENCLATURE . . . . .	9-9
REFERENCES . . . . .	9-13
10.0 INSTRUMENTATION	
10.1 INTRODUCTION . . . . .	10-1
10.2 STRAIN GAGES . . . . .	10-2
10.2.1 SELECTION . . . . .	10-2
10.2.2 MEASUREMENT . . . . .	10-3
10.2.3 CALIBRATION . . . . .	10-5
10.2.4 INSTALLATION . . . . .	10-7
10.3 ACCELEROMETERS . . . . .	10-7
10.3.1 SELECTION . . . . .	10-8
10.3.2 MEASUREMENT . . . . .	10-10
10.3.3 CALIBRATION . . . . .	10-10
10.3.4 INSTALLATION . . . . .	10-10
10.4 FORCE TRANSDUCERS . . . . .	10-11
10.5 PRESSURE SENSORS . . . . .	10-13
10.6 MICROPHONES . . . . .	10-13
10.7 OTHER COMMON TRANSDUCERS . . . . .	10-13
10.7.1 THERMOCOUPLES . . . . .	10-16
10.7.2 DISPLACEMENT TRANSDUCERS . . . . .	10-16
10.7.3 TIME CODE GENERATORS . . . . .	10-16

# TABLE OF CONTENTS (Continued)

	Page No.
10.7.4 DISCRETES . . . . .	10-18
10.8 INSTRUMENTATION SYSTEMS . . . . .	10-18
10.8.1 FM SYSTEMS . . . . .	10-20
10.8.2 PCM SYSTEMS . . . . .	10-20
NOMENCLATURE . . . . .	10-20
REFERENCES . . . . .	10-24
 11.0 FREQUENCY RESPONSE DATA ANALYSIS	
11.1 INTRODUCTION . . . . .	11-1
11.2 TIME DOMAIN . . . . .	11-1
11.2.1 LOGARITHMIC DECREMENT METHOD . . . . .	11-2
11.2.2 LOGARITHMIC (PEAK) AMPLITUDE METHOD . . . . .	11-2
11.2.3 MULTIPLE DEGREE OF FREEDOM RESPONSES . . . . .	11-2
11.2.4 RANDOM DECREMENT METHOD . . . . .	11-4
11.2.5 CORRELATION FUNCTIONS . . . . .	11-5
11.2.6 LISSAJOUS FIGURES . . . . .	11-6
11.3 FREQUENCY DOMAIN . . . . .	11-9
11.3.1 FOURIER TRANSFORMATIONS . . . . .	11-9
11.3.2 AUTO SPECTRUMS . . . . .	11-12
11.3.3 POWER SPECTRAL DENSITY . . . . .	11-13
11.3.4 HALF POWER METHOD . . . . .	11-13
11.3.5 OTHER COMMON PRESENTATIONS . . . . .	11-17
11.3.6 TRANSFER FUNCTIONS . . . . .	11-20
11.3.7 COHERENCE FUNCTION . . . . .	11-21
11.3.8 CO/QUAD METHOD . . . . .	11-22
11.3.9 NYQUIST PLOTS AND CIRCLE FIT . . . . .	11-22
11.3.10 LAPLACE (S-PLANE) TRANSFORMATION . . . . .	11-23
11.3.11 BODE PLOTS . . . . .	11-26
11.3.12 Z-PLANE TRANSFORMATION . . . . .	11-28
NOMENCLATURE . . . . .	11-29
REFERENCES . . . . .	11-30
 12.0 SIGNAL PROCESSING	
12.1 INTRODUCTION . . . . .	12-1
12.2 RESOLUTION . . . . .	12-1
12.2.1 FREQUENCY RESOLUTION . . . . .	12-1
12.2.2 DAMPING RESOLUTION . . . . .	12-2
12.2.3 AMPLITUDE RESOLUTION . . . . .	12-2

## TABLE OF CONTENTS (Continued)

	<u>Page No.</u>
12.2.4 RANGING . . . . .	12-4
12.3 ERROR . . . . .	12-4
12.3.1 QUANTIZATION . . . . .	12-4
12.3.2 ALIASING . . . . .	12-4
12.3.3 LEAKAGE . . . . .	12-6
12.3.4 OTHER SOURCES OF ERROR . . . . .	12-6
12.4 PROCESSING TECHNIQUES . . . . .	12-8
12.4.1 WINDOWING . . . . .	12-8
12.4.1.1 HANNING WINDOW . . . . .	12-8
12.4.1.2 FLAT TOP WINDOW . . . . .	12-9
12.4.1.3 UNIFORM WINDOW . . . . .	12-9
12.4.1.4 FORCE WINDOW . . . . .	12-9
12.4.1.5 EXPONENTIAL WINDOW . . . . .	12-9
12.4.2 ENSEMBLE AVERAGING . . . . .	12-13
12.4.2.1 RMS AVERAGING . . . . .	12-13
12.4.2.2 LINEAR AVERAGING . . . . .	12-13
12.4.2.3 OVERLAP AVERAGING . . . . .	12-13
12.4.3 ADDING AND SUBTRACTING SPECTRA . . . . .	12-13
12.4.4 ZOOM TRANSFORM . . . . .	12-14
12.4.5 ZERO INSERTION . . . . .	12-14
12.4.6 DECIMATION . . . . .	12-14
12.4.7 CUT-OFF . . . . .	12-16
12.4.8 FILTERING . . . . .	12-16
NOMENCLATURE . . . . .	12-18
REFERENCES . . . . .	12-18
 13.0 FLIGHT TESTING AT AFFTC	
13.1 INTRODUCTION . . . . .	13-1
13.2 RESPONSIBLE ORGANIZATIONS . . . . .	13-1
13.3 AIRCRAFT MODIFICATIONS . . . . .	13-2
13.3.1 ANALYSIS . . . . .	13-2
13.3.2 FLIGHT TESTS . . . . .	13-2
13.4 TEST PLANNING . . . . .	13-3
13.4.1 PRELIMINARY PLANNING . . . . .	13-3
13.4.2 THE TEST PLAN . . . . .	13-4
13.4.3 THE REVIEW CYCLE . . . . .	13-4
13.4.4 FINAL PREPARATIONS . . . . .	13-5
13.5 CONDUCT OF THE TEST . . . . .	13-5

## TABLE OF CONTENTS (Concluded)

	<u>Page No.</u>
13.5.1 PRE-FLIGHT BRIEFING . . . . .	13-5
13.5.2 CONTROL ROOM OPERATIONS . . . . .	13-6
13.6 TEST REPORTS . . . . .	13-6
NOMENCLATURE . . . . .	13-6
REFERENCES . . . . .	13-7
INDEX . . . . .	I-1

# LIST OF ILLUSTRATIONS

<u>Figure</u>	<u>Title</u>	<u>Page No.</u>
CHAPTER 1.0		
1.1	Wing Planform Definitions . . . . .	1-2
1.2	Wing Incidence . . . . .	1-2
1.3	Anhedral and Dihedral Definition . . . . .	1-3
1.4	Wing Control Surfaces . . . . .	1-4
1.5	Tail Group and Control Surfaces . . . . .	1-5
1.6	The Canard and Delta Wing . . . . .	1-5
1.7	Fuselage Group . . . . .	1-7
1.8	Fuselage Station and Butt Line Definition . . . . .	1-8
1.9	Typical Landing Gear . . . . .	1-9
1.10	Typical Turbine Engine . . . . .	1-11
1.11	Typical Supersonic Inlet . . . . .	1-12
1.12	Typical Engine Exhaust Nozzle . . . . .	1-14
1.13	Aerial Refueling Boom and Receptacle System . . . . .	1-16
1.14	Aerial Refueling Probe and Drogue System . . . . .	1-17
1.15	Typical Mechanical Control System . . . . .	1-18
1.16	Typical Fighter/Trainer Cockpit . . . . .	1-19
1.17	Example Weapon Pylon and Store Ejector Rack . . . . .	1-21
CHAPTER 2.0		
2.1	Relationship of Airspeed Forms with Altitude . . . . .	2-5
2.2	Streamlines Around an Airfoil . . . . .	2-6
2.3	Pressure Distribution on an Airfoil . . . . .	2-6
2.4	Shocks . . . . .	2-7
2.5	Airfoil Geometry Terminology . . . . .	2-8
2.6	Lift Generation on an Airfoil . . . . .	2-8
2.7	Example of Circulation . . . . .	2-10
2.8	Wing Tip Vortices . . . . .	2-10
2.9	Example Vortex Generator Installation . . . . .	2-10
2.10	Example of Aerodynamic Paneling of an Aircraft . . . . .	2-12
2.11	Basic Aircraft Reference System . . . . .	2-13
2.12	Statically Stable Airplane cg and a.c. Relationship and Tail Load . . . . .	2-14
CHAPTER 3.0		
3.1	Basic Loading and Stresses . . . . .	3-2

# LIST OF ILLUSTRATIONS (Continued)

<u>Figure</u>	<u>Title</u>	<u>Page No.</u>
3.2	Material Deformation Under Load	3-3
3.3	Shear Strain Illustration	3-3
3.4	Example Stress-Strain Curve	3-4
3.5	Example Finite Element Model - X-29A Wing Structure	3-6
3.6	Examples of Composites	3-7
3.7	Example S-N Diagram	3-9

## CHAPTER 4.0

4.1	Basic Spring Element	4-1
4.2	Basic Damper Element	4-2
4.3	Basic Mass Element	4-2
4.4	Example of Combined Basic Elements	4-3
4.5	Example Structural Model	4-3
4.6	Free-Body Diagram of Figure 4.5	4-4
4.7	Example of an Over-Damped Displacement Response	4-5
4.8	Example of an Under-Damped Displacement Response	4-6
4.9	Example of an Undamped Displacement Response	4-6
4.10	Example of a Divergent Displacement Response	4-6
4.11	Typical Magnitude Response Showing Effect of Resonance and Damping	4-8
4.12	Definition of Phase Angle	4-9
4.13	Typical Phase Angle Response Showing Effect of Resonance and Damping	4-9
4.14	Relationship of Displacement, Velocity, and Acceleration	4-10
4.15	Vibration Nomograph for Sinusoidal Motion	4-12
4.16	The Beating Phenomena	4-14
4.17	The Jump Phenomena	4-14
4.18	Example Multidegree of Freedom System	4-14
4.19	Beam Bending Problem with Mode Shapes	4-18

## CHAPTER 5.0

5.1	Forces Acting on an Aircraft in a Level Turn	5-3
5.2	Forces Acting in a 90° Roll Attitude	5-3
5.3	Significance of the V-n Diagram	5-4
5.4	Example Maximum Loads Related to V-n Plot	5-4

## LIST OF ILLUSTRATIONS (Continued)

<u>Figure</u>	<u>Title</u>	<u>Page No.</u>
5.5	V-g Diagrams - T-38A (Symmetric) . . . . .	5-5
5.6	Example Load Factor Limits Chart - T-38A . . . . .	5-6
5.7	Example Loads Strain Gage Installation - F-15 Wing . . . . .	5-9
5.8	Example Loads Cross-Plot . . . . .	5-11
5.9	Comparison of DLL and Gust Load Factor with Weight . . . . .	5-13
5.10	MLC Test Results for L-1011 (71% of Semispan) . . . . .	5-14
5.11	Typical Runway Repair Landing Gear Testing Profiles . . . . .	5-16

### CHAPTER 6.0

6.1	Collar's Aeroelastic Triangle of Forces . . . . .	6-2
6.2	Example Wing Flutter Model - F/A-18 . . . . .	6-8
6.3	Example Aircraft Flutter Model - F-15 STOL . . . . .	6-8
6.4	Example V-G Diagram . . . . .	6-11
6.5	Example V-f Diagram . . . . .	6-11
6.6	Stagnation Temperatures . . . . .	6-17
6.7	Diagram of Flutter Investigation During Development . . . . .	6-17
6.8	Wand Flutter Exciter System . . . . .	6-20
6.9	Electrodynamic Exciter . . . . .	6-21
6.10	Vane or Flutteron Exciter . . . . .	6-22
6.11	Flutter Expansion Example . . . . .	6-24
6.12	Example Store Flutter Instrumentation Installation . . . . .	6-28

### CHAPTER 7.0

7.1	Schematic of GVT Equipment Arrangement . . . . .	7-6
7.2	Characteristics of a Driving Point Measurement . . . . .	7-10
7.3	Characteristics of a Cross Point Measurement . . . . .	7-11
7.4	Influence of Impact Hammer Tips . . . . .	7-14
7.5	Influence of Impact Hammer Weight and Force, Hammer b With More Weight Than Hammer a . . . . .	7-15
7.6	Effect of Sine Sweep Rate on Data . . . . .	7-17
7.7	Characteristics of Various Random Signal Types . . . . .	7-19
7.8	Example of a GVT Survey Grid . . . . .	7-21
7.9	Example Wing Second Bending Mode Shape Presentations	7-24

### CHAPTER 8.0

8.1	Example Sensor Placement Considerations - Fuselage Second Vertical Bending . . . . .	8-2
-----	---	-----

## LIST OF ILLUSTRATIONS (Continued)

<u>Figure</u>	<u>Title</u>	<u>Page No.</u>
8.2	Example Determination of Sensor Locations . . . . .	8-2
8.3	Open-Loop System Diagram . . . . .	8-4
8.4	Closed-Loop System Diagram . . . . .	8-4
8.5	Example MIMO System - Aircraft Lateral-Directional Control System . . . . .	8-4
8.6	Block Diagram Algebra . . . . .	8-5
8.7	Typical Pole-Zero Plot . . . . .	8-7
8.8	Root-Locus Plot for Figure 8-7 . . . . .	8-8
8.9	Bode Plot for Equation 8-6 . . . . .	8-9
8.10	Determining Phase and Gain Margin from a Bode Plot . . . . .	8-9
8.11	Phase and Gain Margin from a Polar Plot . . . . .	8-11
8.12	Aeroservoelastic Analysis Flow Diagram . . . . .	8-11
8.13	Example Notch Filter . . . . .	8-16
8.14	Effects of Notch Filter a. Undesirable Response . . . . . b. Undesirable Response Attenuated by Notch Filter . . . . .	8-17

### CHAPTER 9.0

9.1	Wavelength Versus Frequency of Sound in Air . . . . .	9-2
9.2	Sound Fields . . . . .	9-5
9.3	Sound Attenuation in Air . . . . .	9-5
9.4	Summing Sound Pressure Levels . . . . .	9-7
9.5	Subtracting Sound Pressure Levels . . . . .	9-7
9.6	Effect of Measurement Time on SPL Results . . . . .	9-7
9.7	Example Sound Contour Pattern . . . . .	9-10
9.8	Illustration of Octave and Third-Octave Segmentation of Frequency Spectrum . . . . .	9-11
9.9	Illustration of Octave and Third-Octave SPL versus a Fourier Transform Presentation . . . . .	9-11
9.10	Example of SPL Test Data versus Specification Level . . . . .	9-12

### CHAPTER 10.0

10.1	Typical Uniaxial Strain Gage Configuration . . . . .	10-3
10.2	Other Common Strain Gage Configurations a. Bi-Axial Gage . . . . . b. Delta Rosette Gage . . . . . c. Rectangular Rosette Gage . . . . .	10-3

## LIST OF ILLUSTRATIONS (Continued)

<u>Figure</u>	<u>Title</u>	<u>Page No.</u>
	d. Spiral Gage . . . . .	10-3
10.3	Typical Wheatstone Bridge Circuit . . . . .	10-5
10.4	Example Strain Gage Applications for Loads Measurements - X-29 Wing and Canard . . . . .	10-6
10.5	Example Strain Gage Installation . . . . .	10-8
10.6	Common Piezoelectric Accelerometer Components . . . . .	10-9
10.7	Three Common Accelerometer Configurations a. Compression (Upright) . . . . . b. Compression (Inverted) . . . . . c. Shear Mode . . . . .	10-9 10-9 10-9
10.8	Example of Shim Mounted Accelerometer . . . . .	10-12
10.9	Force Transducer Components . . . . .	10-12
10.10	Common Force Transducer Configurations a. Compression-Tension-Impact . . . . . b. Force Link . . . . . c. Quartz Force Ring . . . . .	10-14 10-14 10-14
10.11	Pressure Transducer Components . . . . .	10-14
10.12	Typical Small Piezoelectric Pressure Transducer . . . . .	10-15
10.13	Common Measurement Microphones and Components . . . . .	10-15
10.14	Example SCR Slow Code Trace . . . . .	10-17
10.15	Typical Instrumentation System Configuration . . . . .	10-19
10.16	Basic FM System Components . . . . .	10-21
10.17	Basic PCM System Components . . . . .	10-22
10.18	Example of PCM Encoding . . . . .	10-23
10.19	Illustration of Commutator Function . . . . .	10-23

## CHAPTER 11.0

11.1	Damped Impulse Response Time History . . . . .	11-3
11.2	Log Amplitude Plot . . . . .	11-3
11.3	MDOF Impulse Response Function . . . . .	11-3
11.4	Random Excitation Response Time History . . . . .	11-4
11.5	a. Original Random Response Time History (SDOF) . . . . . b. Associated Auto-Correlation Function . . . . .	11-7 11-7
11.6	Sample Lissajous Construction . . . . .	11-7
11.7	Lissajous Displays for Sinusoidal Inputs at Various Frequency Ratios . . . . .	11-8

## LIST OF ILLUSTRATIONS (Continued)

<u>Figure</u>	<u>Title</u>	<u>Page No.</u>
11.8	Important Lissajous Figures a. Line, Positive 45° Slope, In Phase . . . . . b. Line, Negative 45° Slope, 180° Out of Phase . . . . . c. Circle, 90° Out of Phase . . . . .	11-8 11-8 11-8
11.9	Typical Fourier Transformation Results . . . . .	11-10
11.10	Half Power Damping from a Non-Squared FRF . . . . .	11-14
11.11	Half Power Method from a Squared FRF . . . . .	11-15
11.12	Half Power Applied to Decibel Scale (non-Squared FRF) . . . . .	11-15
11.13	Half Power Method Using an IFFT for Smoothing a. Original PSD . . . . . b. Bandpass Filter Isolation of Single Mode from a. . . . . c. IFT of b. Showing Exponential Window Notation . . . . . d. Resulting PSD Showing Half Power Analysis . . . . .	11-16 11-16 11-16 11-16
11.14	Common Data Presentations . . . . .	11-18
11.15	Modal Parameters from Simple Response Plots . . . . .	11-19
11.16	Diagram of Transfer Function Operation . . . . .	11-20
11.17	Example of Ordinary Coherence Function . . . . .	11-21
11.18	CO/QUAD Elements . . . . .	11-23
11.19	Determining Damping From Real or Imaginary Response . . . . .	11-24
11.20	3-Axis Frequency Response Plot . . . . .	11-24
11.21	SDOF Nyquist Plot . . . . .	11-25
11.22	Nyquist Plot Analysis . . . . .	11-25
11.23	S-Plane Representations (SDOF) . . . . .	11-25
11.24	Example S-Plane (Root-Locus) Analysis (SDOF) . . . . .	11-27
11.25	Magnitude and Phase Diagrams . . . . .	11-27
11.26	SDOF Bode Plot . . . . .	11-28
11.27	Example Z-Plane . . . . .	11-29

## CHAPTER 12.0

12.1	Points Required to Define a Mode . . . . .	12-3
12.2	Illustration of Minimum Damping Resolution . . . . .	12-3
12.3	Illustration of Worst-Case Amplitude Error . . . . .	12-3
12.4	Examples of Aliasing Error . . . . .	12-5
12.5	Aliasing Fold-Down Chart . . . . .	12-5
12.6	Distorted Waveform Producing Leakage . . . . .	12-7
12.7	Illustration of Leakage Error . . . . .	12-7
12.8	Application of Hanning Window . . . . .	12-10

## LIST OF ILLUSTRATIONS (Concluded)

<u>Figure</u>	<u>Title</u>	<u>Page No.</u>
12.9	Comparison of Hanning and Flat Top Windows . . . . .	12-10
12.10	Flat Top Window . . . . .	12-11
12.11	Uniform Window . . . . .	12-11
12.12	Application of Force Window . . . . .	12-12
12.13	Application of Exponential Window . . . . .	12-12
12.14	Illustration of Overlap Averaging and Result . . . . .	12-15
12.15	Example of Zoom Transform Application . . . . .	12-15
12.16	Filter Characteristics . . . . .	12-17
12.17	A Bank of Hanning Passbands . . . . .	12-17

## LIST OF TABLES

<u>Table</u>	<u>Title</u>	<u>Page No.</u>
2.1	The Standard Atmosphere . . . . .	2-2
7.1	Comparisons of GVT Excitation Forms . . . . .	7-13
7.2	Example C-17A Modes . . . . .	7-25
7.3	Example AFTI F-111 Modes . . . . .	7-25
7.4	Example T-46 Modes . . . . .	7-26
8.1	Gain and Phase Margin Requirements . . . . .	8-14
9.1	Octave and Third-Octave Passbands . . . . .	9-4

# CHAPTER 1.0

## BASICS OF AIRCRAFT

### 1.1 INTRODUCTION

Because many of the engineers undertaking structures flight testing have no experience with aircraft, a basic introductory chapter is felt to be necessary. The object of the chapter is to introduce you to the basic nomenclature of modern aircraft. Many books have been written encompassing all of the variations in aircraft design, but such is not the purpose here. Instead, only common design features will be presented. Special purpose aircraft like flying boats and helicopters are not covered. If engineers are uncertain of the function of some aspect of the aircraft they are working with then they are encouraged to ask others. Additional reading in this area is recommended and several fine publications are listed in the reference section at the end this chapter. Aeronautical engineers or experience flight test engineers may find this chapter rudimentary and may wish to skip it altogether.

### 1.2 GEOMETRY

Every part and feature of an aircraft serves some function which may not be obvious even to knowledgeable aeronautical engineers. This section will address some of the more typical design features without detailed explanation of the reasons why things are done one way or another. The author seeks only to make the structures engineer conversant in the language associated with aviation.

#### 1.2.1 WING GROUP

A top view of an aircraft wing is called the **planform**. There are a number of common terms applied to the planform. The **sweep** refers to the angle between a line perpendicular to the fuselage centerline and a line half way between the leading and trailing edges of the wing (the **mean chord line**). Leading and trailing edge sweep may also be referenced and may change along the span. The **wing span (b)** is measured from wing tip to wing tip perpendicular to the fuselage centerline (see Figure 1.1). Some wings have pivoting mechanisms that permit the sweep to be changed (variable geometry).

Positions along the wing are measured in inches from the fuselage centerline and are referred to as **Wing Stations (WS)**, Figure 1.1. For example, a pylon located in the same place on both wings may be at WS 34.5, or 34.5 inches from the fuselage centerline.

Wings may be **tapered**, having a larger chord at the root or base than at the tip, and also have tapered thickness. Planform taper is often referred to as the **taper ratio**, the ratio between the root and the tip chord. **Aspect ratio (A)** is defined as

$$A = b^2/S \quad (1.1)$$

where S is the planform area.

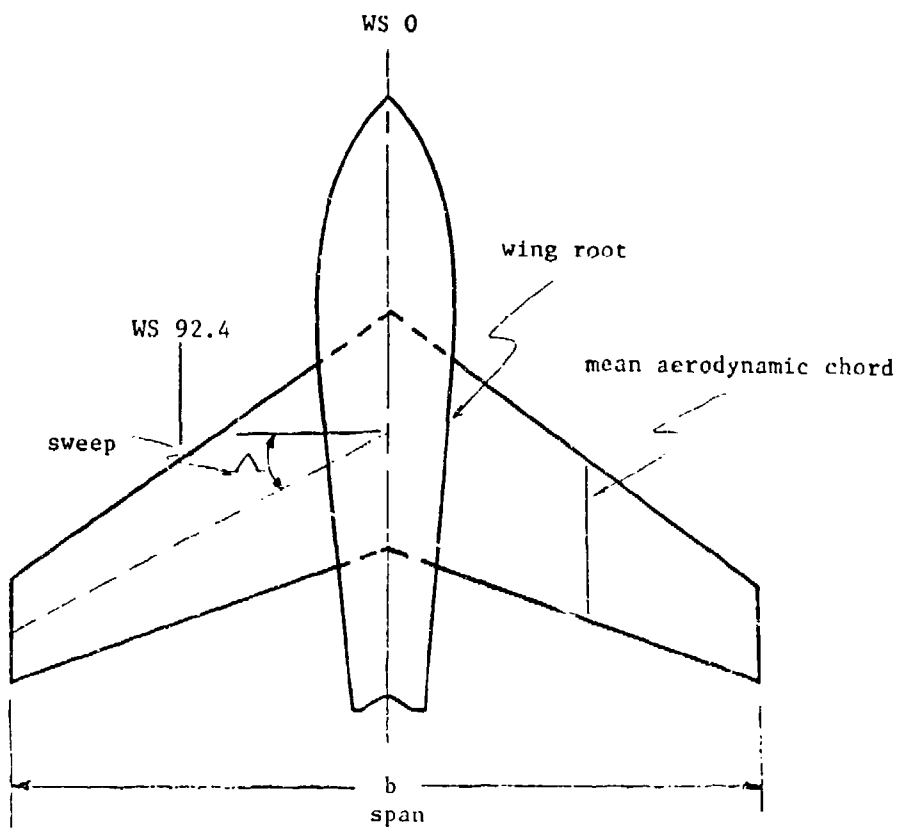


Figure 1.1 Wing Planform Definitions

**Incidence** refers to the angle between the centerline of the aircraft and a line between the leading and trailing edges of a section of the wing (see Figure 1.2). A wing may be twisted along the span with the incidence increasing (**washin**) or decreasing (**washout**) toward the tip. A wing may be mounted low on the fuselage, mid fuselage, or on top of the fuselage depending upon ground clearance requirements or aerodynamic features. They may be canted upward (**dihedral**) or downward (**anhedral**, see Figure 1.3), although the latter is more common in tail surfaces. Some wings may have vertical surfaces at the tips which are called **winglets**.

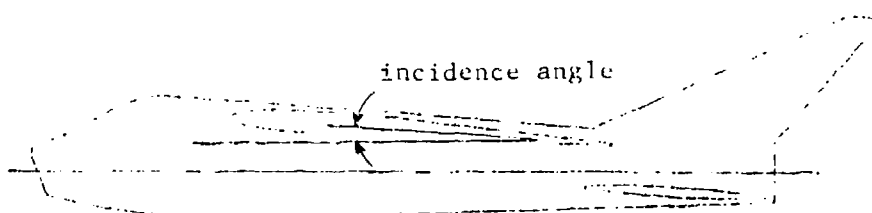


Figure 1.2 Wing Incidence

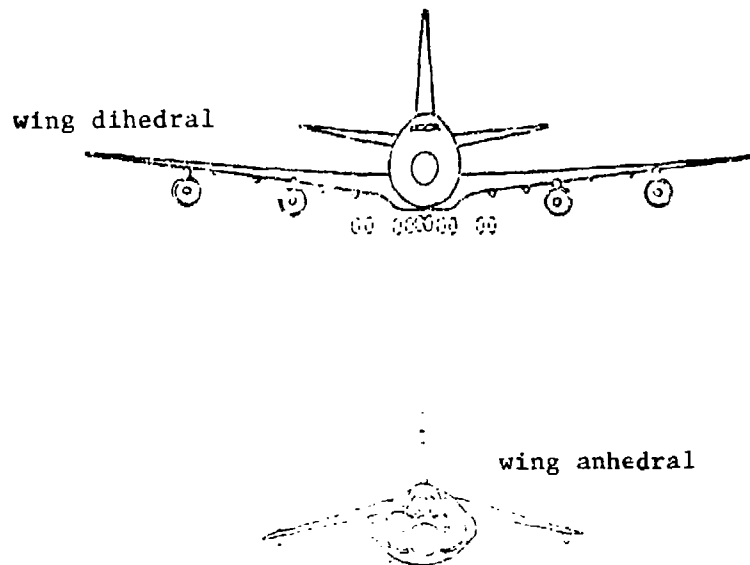


Figure 1.3 Anhedral and Dihedral Definition

A wing will have a number of movable control surfaces (Figure 1.4). One or more trailing edge surfaces near the tip of the wing are **ailerons** and move differentially between sides to cause the airplane to roll about its longitudinal axis. A similar device near the root is called a **flap** and will deploy symmetrically downward. This allows the plane to fly more slowly without stalling (see Section 2.2.5). Flaps may have multiple parts with slots in between and may slide out on rails. Fighter type aircraft may have flaps that do move asymmetrically like ailerons for roll control and are then referred to as **flaperons**. Surfaces similar to flaps may be placed at the leading edge of the wing (leading edge flaps or slats). Large panels may be designed to pivot out from the top or bottom of the wing (**spoilers**) to slow the aircraft or to produce rolling moments (the B-1B is an example of this). Many control surfaces will have much smaller movable surfaces near its trailing edge. These are **trim tabs** and may assist in moving the surface or to keep it deflected with less mechanical effort.

### **1.2.2 TAIL GROUP**

An aircraft tail unit or **empennage** normally consists of a **vertical stabilizer** or fin (one or two) and two **horizontal stabilizers** (see Figure 1.5). The vertical surface(s) usually includes a trailing edge control device called a **rudder**. The rudder causes the nose of the aircraft to yaw in the same direction as the side the tailing edge of the rudder moves (some roll will likely also occur). The horizontal surfaces may contain trailing edge control devices called **elevators**. Elevators cause the nose of the aircraft to rise or fall in a sense coincident with the elevator motion. Fighter type aircraft may have all-moving horizontal stabilizers called **stabilators** or **stabs** which can move together for elevator action or differentially for rolling motion. Other aircraft with elevators may have horizontal stabilizers that rotate through a small arc for trimming action. Rudders and elevators may have trim tabs like ailerons. The anhedral and dihedral explained earlier also applies to horizontal stabilizers.

Tail arrangements may vary markedly but there are some common designs worthy of mention. The "T" tail has a single horizontal stabilizer at the top of the vertical stabilizer. Mid-fin designs have been used but the horizontal surface placed at the base of the fin or on the bottom of the tail is most common. If the aircraft has two vertical surfaces they may be perpendicular

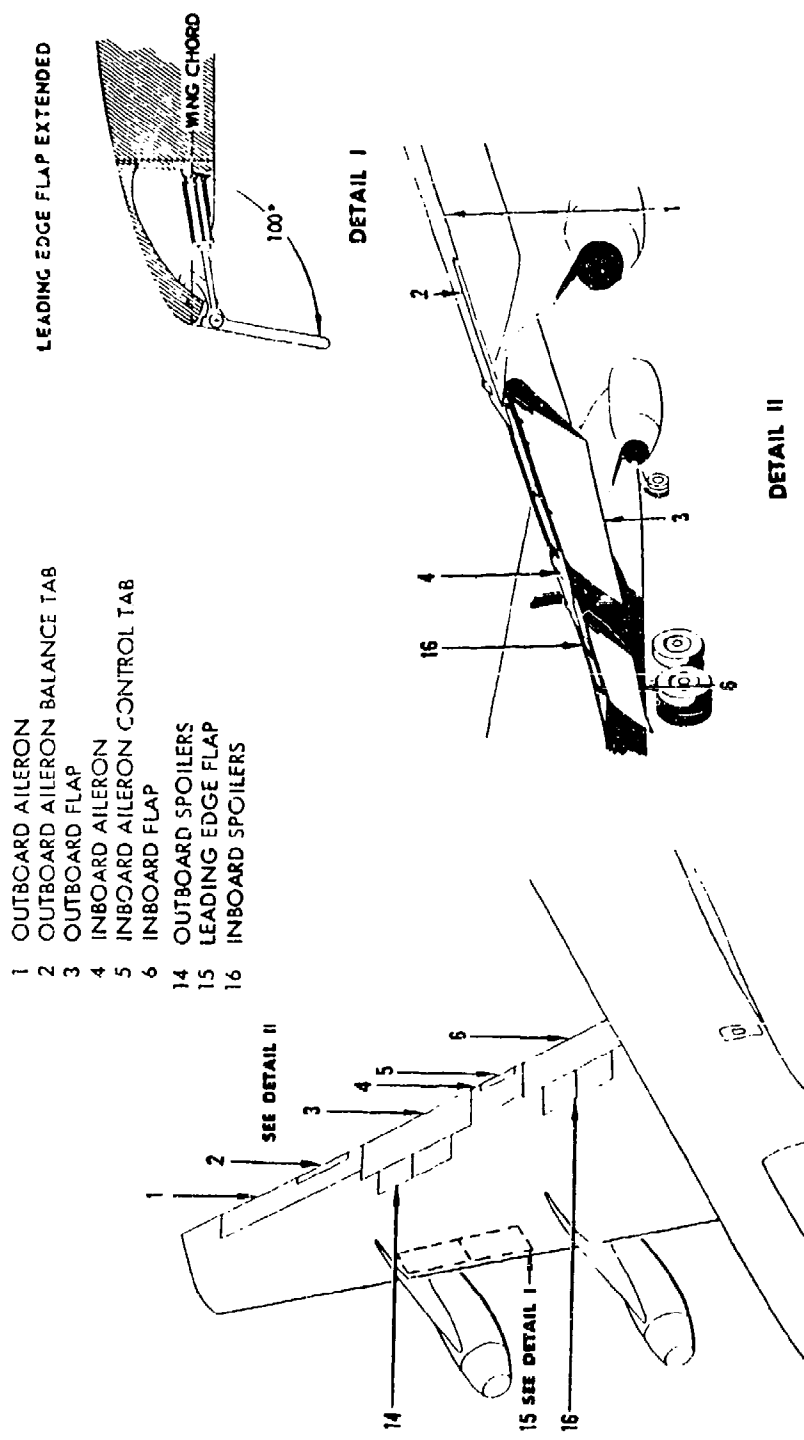
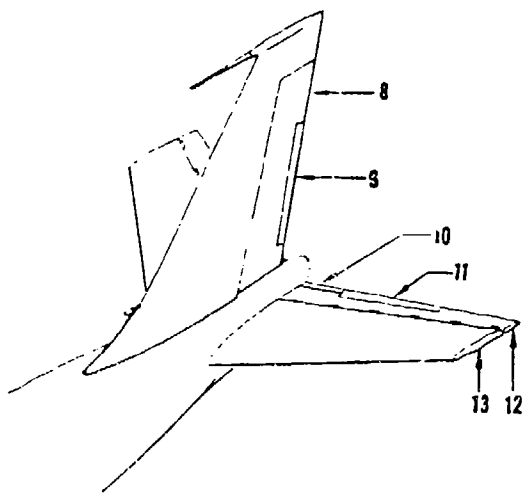


Figure 1.4 Wing Control Surface



8 RUDDER  
9 RUDDER CONTROL TAB  
10 STABILIZER ACTUATED TAB  
11 ELEVATOR CONTROL TAB  
12 ELEVATOR  
13 ADJUSTABLE HORIZONTAL STABILIZER

Figure 1.5 Tail Group and Control Surface

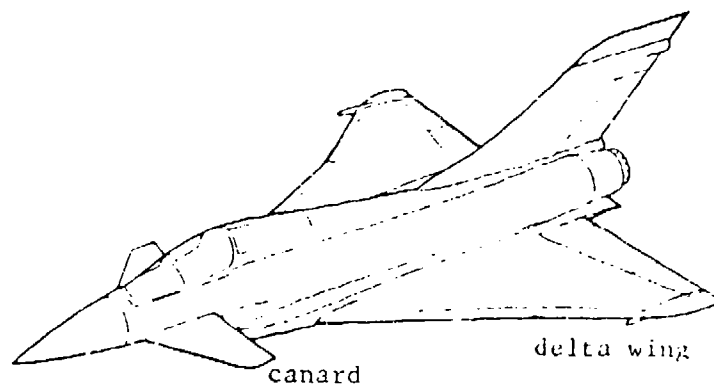


Figure 1.6 The Canard and Delta Wing

to the fuselage or canted in or out some amount. A few aircraft have used a "V" tail arrangement which uses just two surfaces to perform the functions of the vertical and horizontal stabilizers. Such an arrangement may have control surfaces which perform the functions of rudders and elevators and are appropriately called **ruddervators**.

Things attached to the top of the fuselage are typically referred to as **dorsal** (dorsal fairing, for example) and on the bottom as **ventral** (ventral antenna, for example). One or more small vertical surfaces may project below the tail and are called **ventral fins**. Some airplanes may not have any horizontal surfaces at all (tailless aircraft). Such aircraft will usually have a large wing extending far back on the fuselage or have horizontal surfaces forward of the wings called **canards** (Figure 1.6). For the later case, the wing trailing edge control surfaces have to perform both elevator and aileron or flap actions. They are referred to as **elevons**. The canards may be fixed, all-moving, or have trailing edge control devices. Canards serve a similar purpose to that of the aft-mounted horizontal stabilizer and have been mounted in many positions on the forward fuselage.

### **1.2.3 FUSELAGE GROUP**

The fuselage is the central structure to which the wing and tail are attached and contains the cockpit, perhaps the engine(s) and landing gear, and most of the aircraft systems (see Figure 1.7).

The nose of the fuselage will usually consist of the **radome** behind which lies the radar (see Section 1.3.7). The radome is an aerodynamic fairing made of material through which radar waves will easily propagate. The cockpit, which contains the aircrew, is next in line toward the rear and will have a canopy or windscreens and perhaps some escape hatches. The wings and tail are attached as shown in the figures. If the engine(s) are within the fuselage then the air inlet(s) (see Section 1.3.1) will be on the fuselage.

A surface that protrudes into the airstream on command to create drag (see Section 2.2.6) and slow the aircraft, a **speedbrake** or **airbrake**, may be included in the fuselage structure (although split aileron speed brakes are also used). Many access and inspection panels will be found on the fuselage to get at the avionics and other systems. The tail of fighter air vehicles may include a **tail hook** which rotates down on command. It serves to snag an arresting cable across the runway in an emergency to slow the airplane in the event of a wheel brake failure. Braking parachutes may also be housed in the tail area and have been used on very large aircraft.

Positions on the fuselage are referenced both vertically and longitudinally in inches (Figure 1.8). The vertical positions are from a **Water Line (WL)** which is generally some major longitudinal structural member. Water line numbers will be positive up and negative below the WL. The main gear axle may be at WL -67.3, or 67.3 inches below the water line datum. Longitudinal positions are called **Fuselage Stations (FS)** or **Butt (Buttock) Line (BL)** and are measured from some convenient datum, generally ahead of the nose of the airplane, and positive aft. The main gear axle may also be at FS 133.4.

### **1.2.4 LANDING GEAR GROUP**

The aircraft will usually have wheels attached to struts which extend from the fuselage, wings, or engine pods (**nacelles**) by means of hydraulics. This is the landing gear and must absorb most of the shock of the landing impact (hydraulically or pneumatically) as well as provide a means of stopping the plane (Figure 1.9). The wheel brakes typically consist of

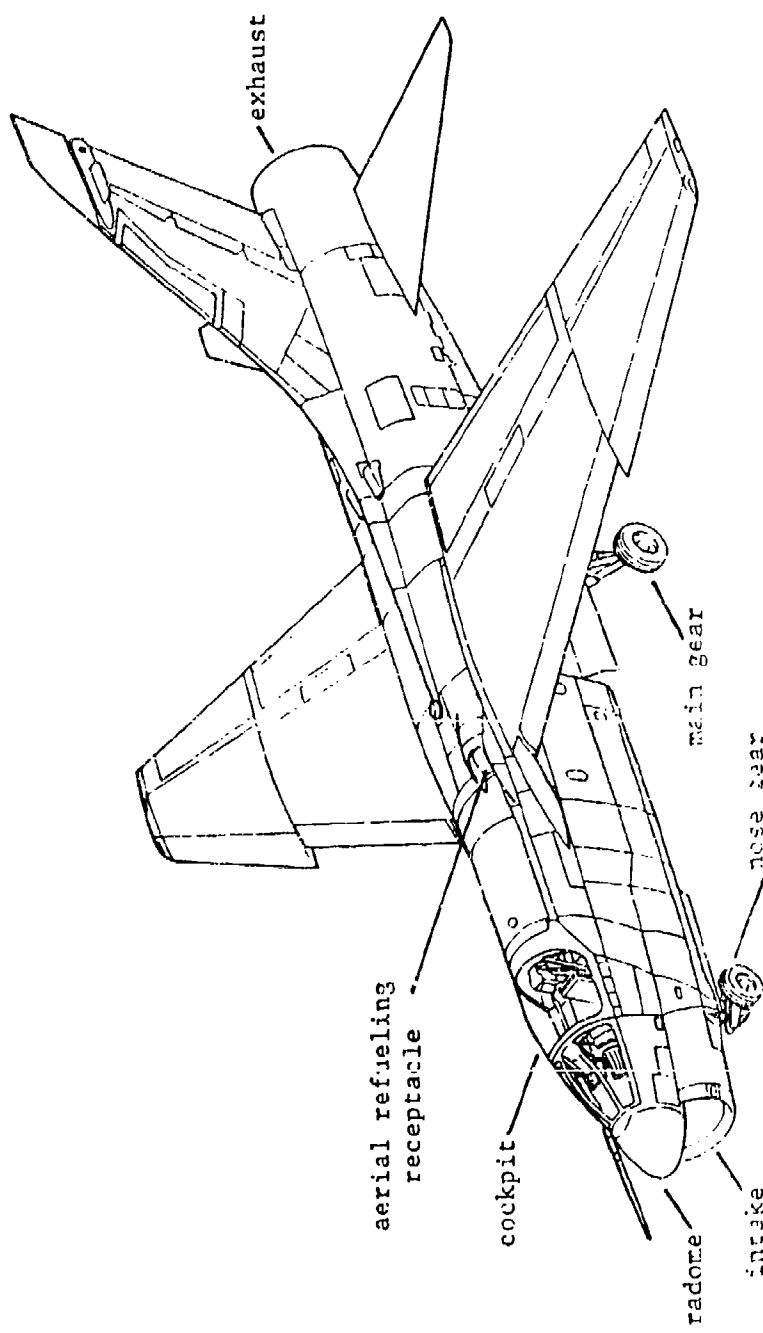


Figure 1.7 Fuselage Group

multiple disc brake assemblies which are hydraulically actuated. The gear will most often be designed to retract out of the airstream to reduce drag. The tricycle gear arrangement is most popular with a nose gear and twin main gear assemblies. Some planes have small gear assemblies near the wing tips called **outriggers**.

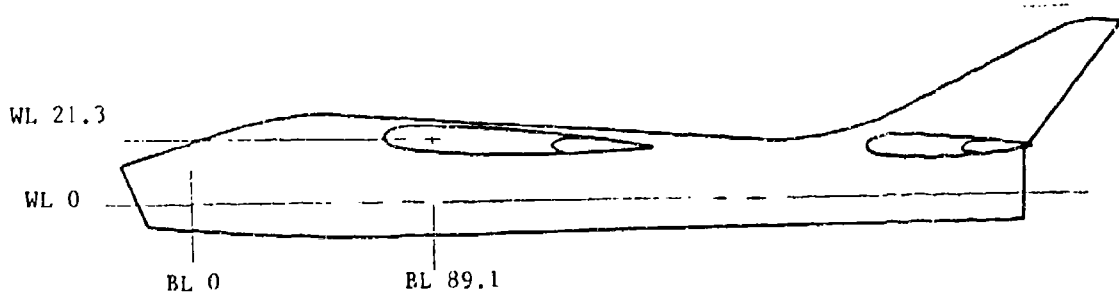


Figure 1.8 Fuselage Station and Butt Line Definition

### **1.2.5 MISCELLANEOUS**

Fillets are fairings that smoothly transition one surface to another at a junction, such as at the root of the wing or where an engine nacelle joins the wing. Strakes may be small surfaces that extend ahead of a leading edge such as at the root of the vertical stabilizer. Other strakes may be very small surfaces protruding from a larger surface to straighten air flow.

## **1.3 SYSTEMS**

Modern military aircraft have become exceedingly complex machines with a myriad of different systems that must work together at the command of the aircrew and onboard computers. Some of the more common systems will be covered in a brief manner. The individual systems of the test aircraft may need to be studied in various levels of detail as required for the test program being conducted. At least a broad familiarization with the major systems is recommended for even the most superficial flight tests. Do not hesitate to ask for manuals and question the aircrew, maintenance personnel, and other engineers if you are uncertain of particular aspects of a system.

Most of the aircraft systems are controlled through electronic "boxes" scattered throughout the aircraft. Such boxes are collectively called **avionics** and are connected through miles of wires and cable bundles. Computers will control systems with like functions and may be called **flight computers** or **mission computers**. Signals from these myriad systems may come together at a central point called a **data bus** where they may be sent to displays, the computers, or monitored during flight tests. Many avionics systems will also have associated external antennas, both flush and blade types. Electronic equipment can generate considerable heat which can be self-damaging. To avoid this damage the equipment is cooled by conditioned air or liquid provided by an **environmental control system (ECS)**, described in Section 1.3.4.

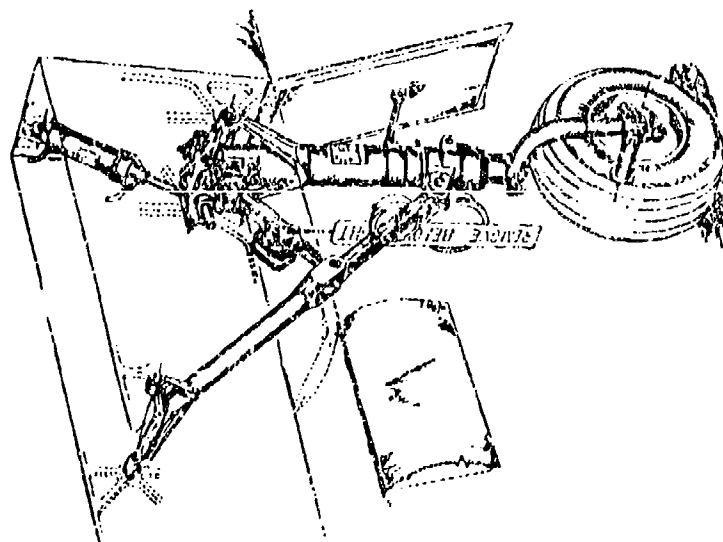
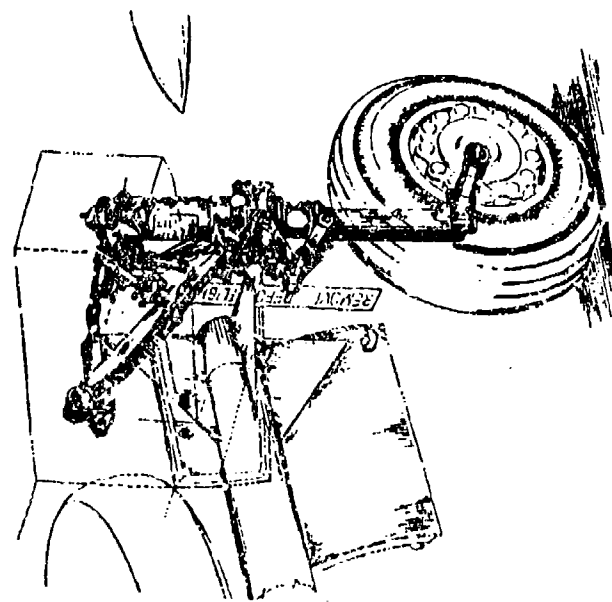


Figure 1.9 Typical Landing Gear

### **1.3.1 PROPULSION**

There are only a few types of power plants that are typically used in high performance military aircraft. These are the **turbojet**, **turbofan** and **turboprop** engines which share many identical parts. The reciprocating engine, such as is in a car, will not be covered. Figure 1.10 shows the principle features of the turbine aircraft engine, the individual sections often being referred to by station numbers, as shown. Each engine has specific performance characteristics in terms of fuel demand and rated thrust. These characteristics will determine the choice of engine for the specific aircraft and mission.

The most forward element of the turbofan engine is the **fan** section. This section consists of one or more rows of rotating, radially-mounted airfoil blades (see Section 2.2.5) which increase the velocity and pressure of the air downstream. A forward row of blades may be fixed and serve only to pass the airflow at the proper angle into the engine. Some of this air will be exhausted directly out of the engine nacelle (or into the primary exhaust stream for fighter-type turbofan engines) and the rest channeled into the core of the engine. The amount of air ducted out versus that ducted into the core is defined as the **bypass ratio**. A high bypass ratio engine will tend to be fat, with a very large fan section, and are common on transport-type aircraft. In this case the fan provides most of the thrust. The low bypass engine can be found in fighter applications with the core providing most of the thrust. In a turbojet engine there is no fan section at all.

The turboprop uses propeller blades to do the same job as a fan section but none of the downstream flow is ducted into the core. In fact, the propeller may be connected to the core of the engine only by a gear case which reduces the rotational speed of the core shaft to a speed compatible with propeller aerodynamics (avoiding supersonic tip speeds). The core exhaust typically produces less than 15 percent of a turboprop's thrust.

The engine **inlet** or **intake** plays a very important role in the engine performance (Figure 1.11). In all cases, the inlet attempts to produce an ideal pressure distribution at the face of the compressor or fan section. Many engine installations will have very simple, fixed geometry inlets because the airplane is restricted to subsonic speeds. In the case of supersonic flight, the inlet will slow the incoming air to subsonic conditions before the flow encounters fan or compressor blades. This is done by positioning one or more shock waves (see Section 2.2.4) and may involve movable ramps or a movable cone within the inlet.

The engine core begins with the **compressor** section which consists of many rows or stages of alternating fixed (**stator**) and rotating blades which greatly increase the pressure of the air. The air then enters the **combustion section** that mixes fuel with the air and burns the mixture to raise the temperature and velocity of the flow. The **turbine** section, several rows of stators and rotary turbine blades, extracts energy from the flow to drive the compressor and fan through the drive shaft which runs through the center of the engine. Turbofan engines have two compressors (the first being the fan) and two turbines, called the high pressure and low pressure components. The fan is tied to the aft, low pressure turbine by a separate, nested shaft which turns at a slower speed than the core components. The second compressor and initial turbine are the high pressure core components and operate on its own, higher speed shaft.

Bleed air is extracted from the high pressure compressor for use by the ECS (see Section 1.3.4) and for other auxiliary functions. The high pressure compressor, the initial turbine section, may also be connected to an **accessory gearbox** which, through reduction gearing, drives hydraulic pumps and the aircraft electrical generators.

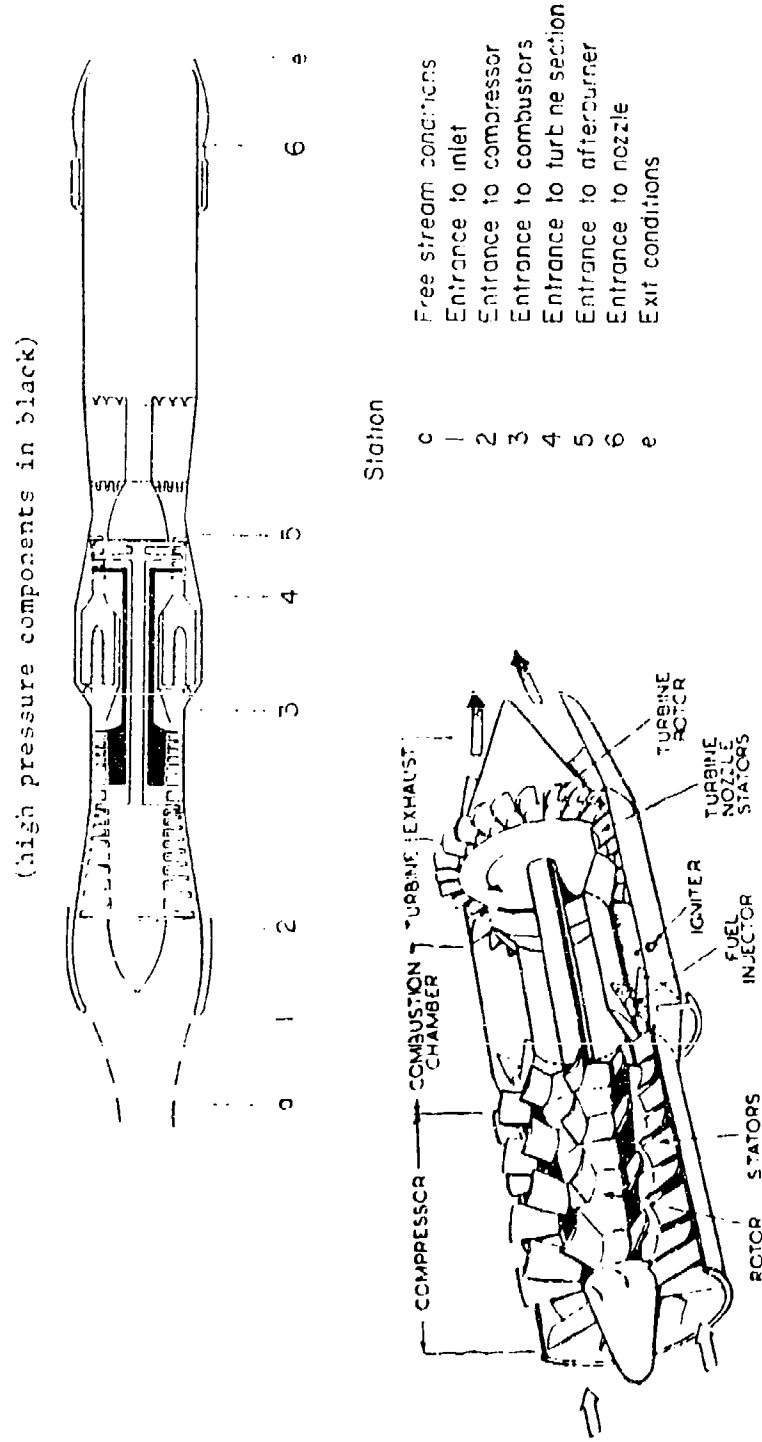


Figure 1-10 Typical Turbine Engine

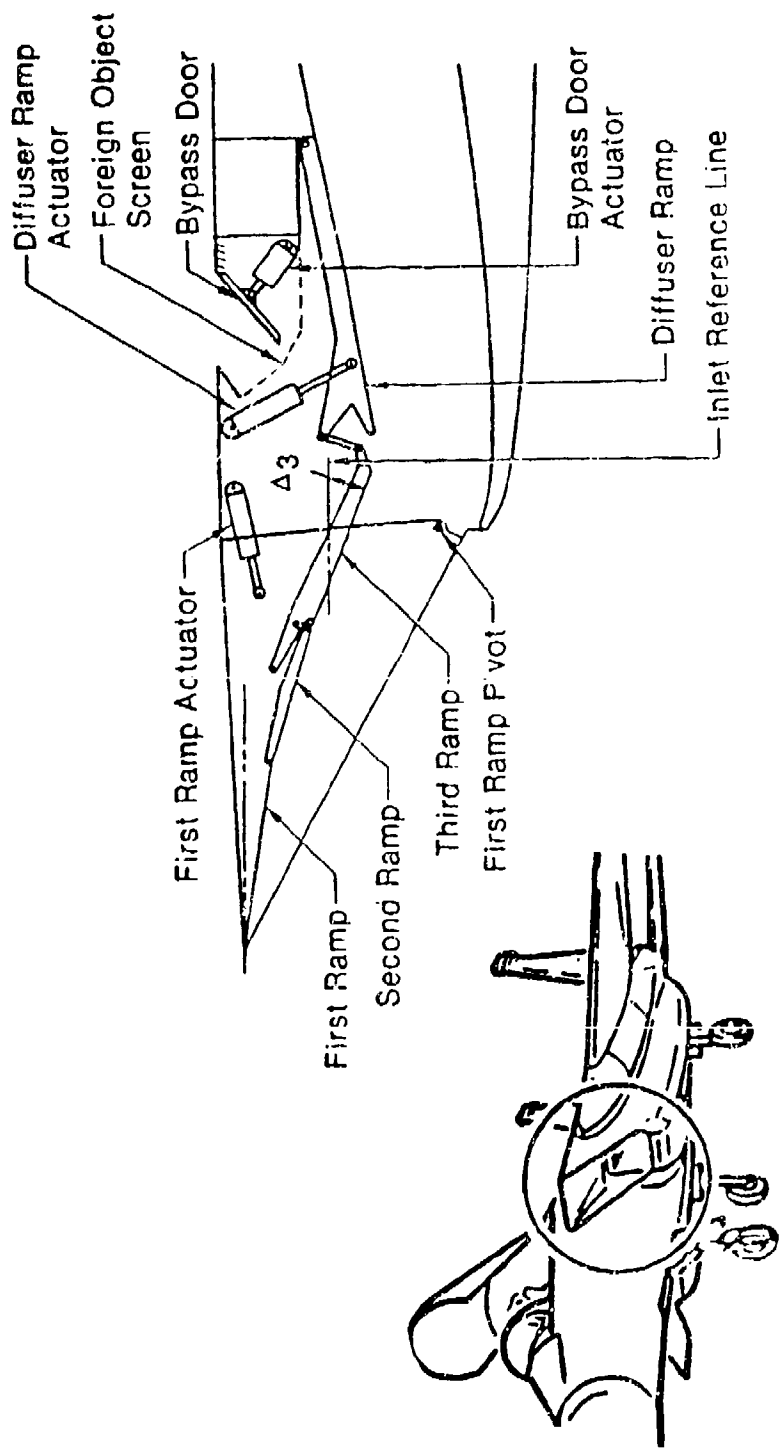


Figure 1.11 Typical Supersonic Inlet

The **nozzle** or **diffuser** at the aft end of the engine is also very important (Figure 1.12). The exhaust nozzle provides the final acceleration of the air through a venturi as it exits the engine. Some fuel may be added as the flow leaves the turbine and ignited (the **afterburner** or **augmentor**) to greatly increase the thrust (and also the fuel flow). The nozzle will likely be able to change its exit area so that the exit pressure approaches the ambient conditions, a critical parameter for efficient production of thrust. Nozzles may incorporate some form of **thrust reverser** to serve as a deceleration mechanism and **thrust vectoring** for an additional flight control.

### **1.3.2 HYDRAULICS**

Hydraulics are used to move heavy appendages against gravity and air pressure. The hydraulic fluid, which is typically highly inflammable, is contained in **reservoirs** and accumulators and moved by engine-driven or electric motor-driven pumps through valves and hydraulic pressure lines throughout the aircraft. Hydraulics typically move control surfaces, airbrakes, and the landing gear through rams or actuators. Because of the criticality of these systems the failure of a hydraulic system is often an emergency situation and will require the plane to return to base immediately. During ground check-outs or maintenance during which the engines are not operating, an external hydraulic pump cart is used.

### **1.3.3 ELECTRICAL**

Many of the aircraft systems are electrically powered. This power is typically derived from **generators** driven by the engine(s) as an accessory. When the engines are not operating, batteries will supply power briefly for a few essential systems. On the ground, a motor in a ground generator cart will supply power through a ground power receptacle until the engines have been started. Some aircraft have their own onboard independent generator for power before engine start and to power the engine starters themselves. These are called **auxiliary power units** or **APUs**. In the event of a failure of all the engines in flight, a small **ram air turbine** (RAT) may be deployed. This is a propeller generator driven by the outside air flow.

The power is distributed to the various aircraft systems through one or more **electrical buses**. Separate buses for ac and dc power are typical. Some systems are dedicated to particular buses or generators so that partial electrical failures may effect only selective systems. Power to individual systems can be cut by pulling **circuit breakers**, the most important of which are generally within reach of the aircrrew.

### **1.3.4 ENVIRONMENTAL CONTROL SYSTEM**

Most modern military aircraft are equipped with an environmental control system (ECS). It serves the following functions: distribution of engine compressor bleed air to components and subsystems such as pressurization of inflatable seals; air conditioning and pressurization of the cockpit or cabin, equipment compartments, and the avionics; anti-icing or de-icing of flight surfaces, engine inlets and ram air scoops; removal of rain, snow, ice, frost, fog, dust and insect residue from transparent surfaces and sensor windows; pressurization of hydraulic system fluid reservoirs and miscellaneous equipment; and purging of gun gas and vapor or fuel from air refueling manifolds (see next section).

Environmental control system air conditioning for the avionics circulates cooled air or fluid. Air is originally obtained through ram air scoops on the skin of the plane and is carried

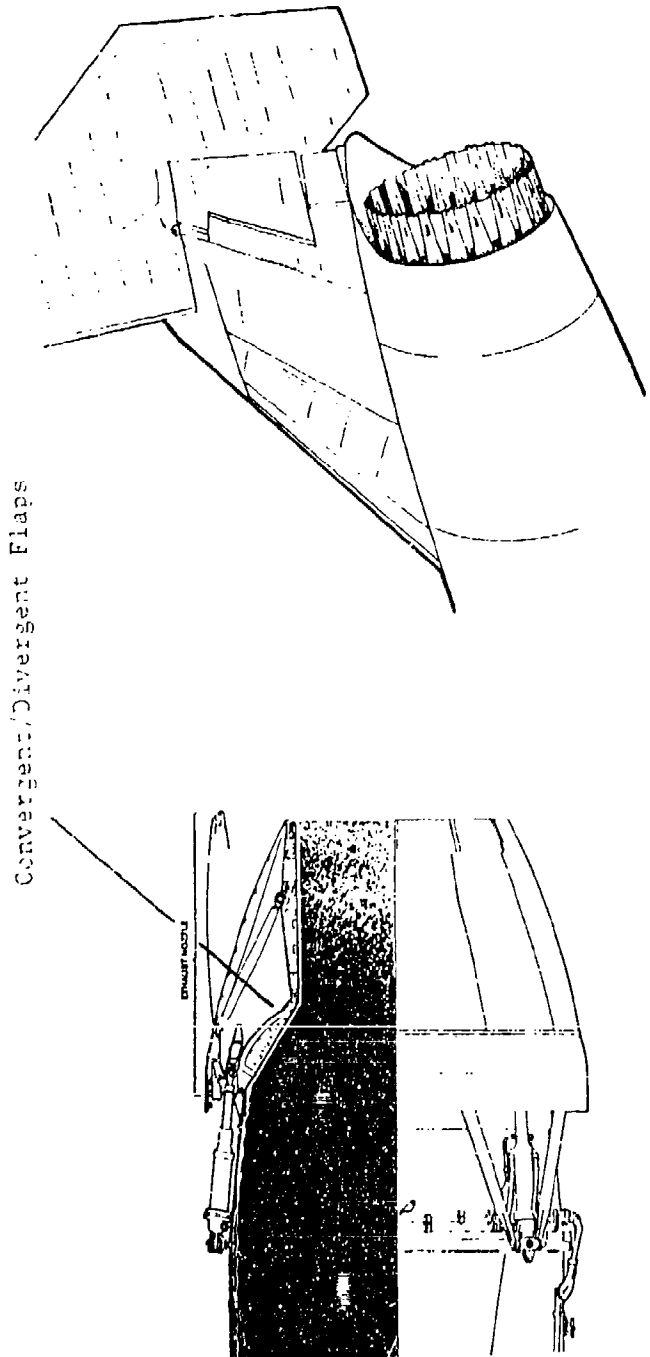


Figure 1.12 Typical Engine Exhaust Nozzle

throughout the aircraft through ducting to the avionics. On the ground, before taxi or during check-outs, this cooling air is provided by ground carts through hoses connected to special ports in the aircraft.

### **1.3.5 FUEL**

Fuel to run the engine(s) is typically contained in a number of flexible bladders or metal cells within the structure of the wings and fuselage, or within "drop" tanks attached to pylons beneath the wings or the fuselage. The tanks are usually interconnected to allow the transfer of fuel to the engines and between tanks for weight and balance considerations (see Section 2.3.2). The fuel is transferred through fuel lines by fuel pumps, frequently located in the tanks themselves. Major junctions of fuel lines are called manifolds.

Aircraft are refueled or defueled on the ground through one or more refueling points and fuel is pumped onboard under pressure. Many aircraft can be refueled in flight from a tanker (aerial refueling or AR). The USAF method is the "boom" refueling method by which the tanker connects a steerable, telescoping boom with a fuel tube and refueling nozzle into a receptacle on the "receiver" aircraft (Figure 1.13). Other services and countries use the "probe and drogue" system in which the receiver flies a probe with a nozzle attached to the plane into a "basket" or drogue trailing from the tanker on a retractable hose (Figure 1.14).

### **1.3.6 FLIGHT CONTROLS**

Pilot commands to the control surfaces which change the aircraft's attitude and flight path are carried from the control column (stick) for vertical and lateral control and the rudder pedals for directional inputs by push rods, cables, pulleys and bellcranks (Figure 1.15). Weights and springs within the system will give the pilot the "feel" or feedback needed to properly judge the amount of input required. In most cases the pilot does not directly move the surface but opens and closes hydraulic valves which ports the correct amount of hydraulic fluid under pressure to move the surface. The flight control computer will often mix motions of several control surfaces in different axes to achieve the desired aircraft response.

Many newer aircraft have electronic flight controls that interpret the pilot's commands and generate signals to move the control surfaces (or hydraulic valves) as appropriate. In this case there is no mechanical connection between the stick and rudder pedals and the control surfaces themselves. This is the so called "fly-by-wire" concept. Almost all aircraft have autopilots that perform basic functions like keeping the wings level and maintaining the assigned heading with the pilot making no control input. They can also automatically guide the airplane on approach-to-landing paths by tying into navigation radio signals. More sophisticated systems can be programmed to fly pre-selected routes and even perform an entire mission including weapons release without pilot intervention.

### **1.3.7 COCKPIT GROUP**

The cockpit contains life support equipment for the pilot plus the controls and instruments needed to operate the aircraft and perform its mission. A typical cockpit arrangement is shown in Figure 1.16.

Except for transport aircraft, the crew will be seated in ejection seats. These are seats that can be propelled by a rocket out of the aircraft on command if the occupant is endangered with

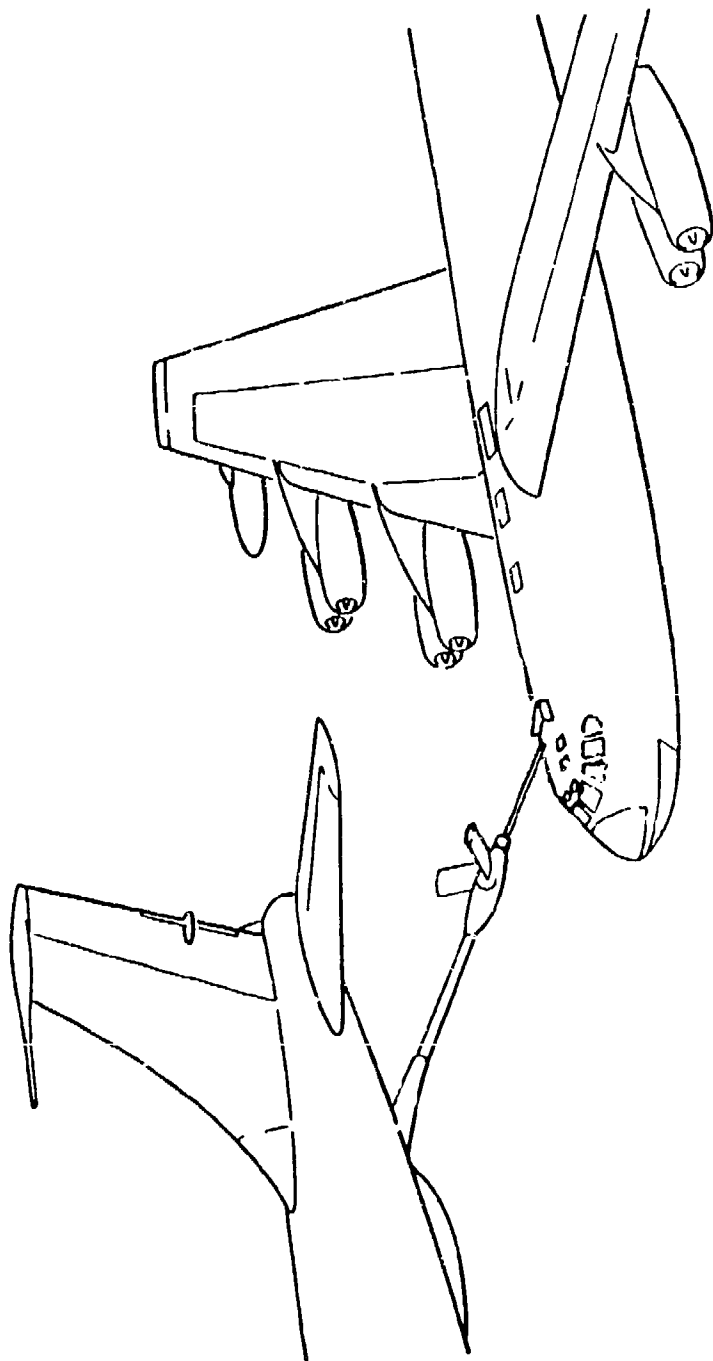


Figure 1.13 Aerial Refueling Boom and Receptacle System

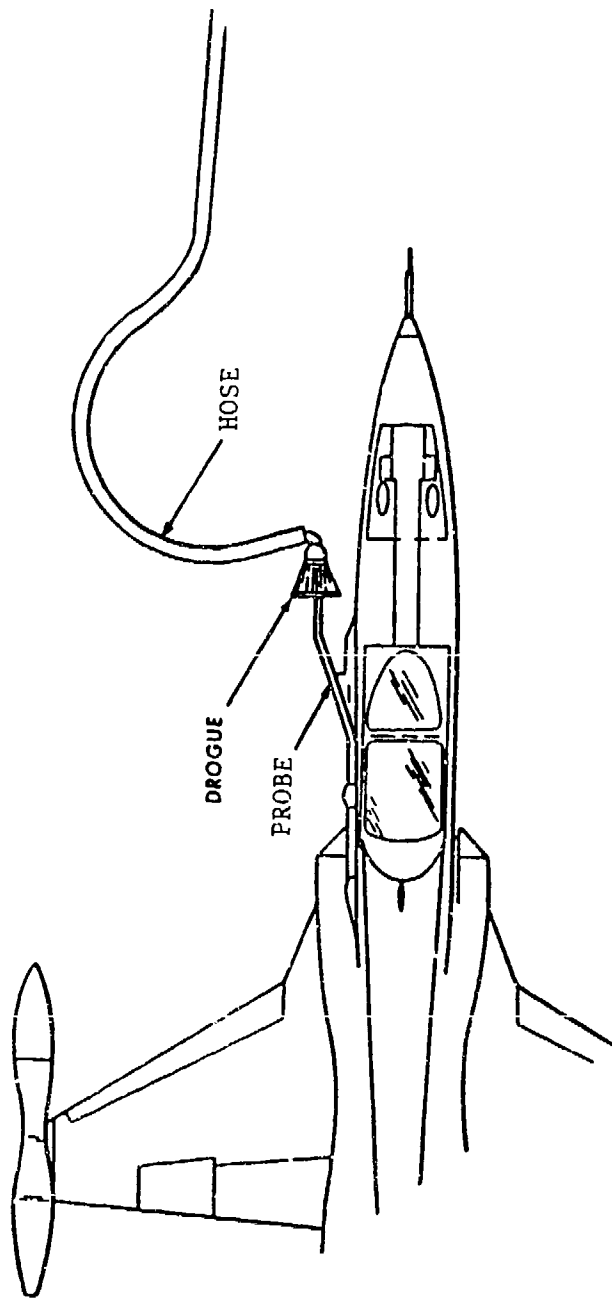


Figure 1.14 Aerial Refueling Probe and Drogue System

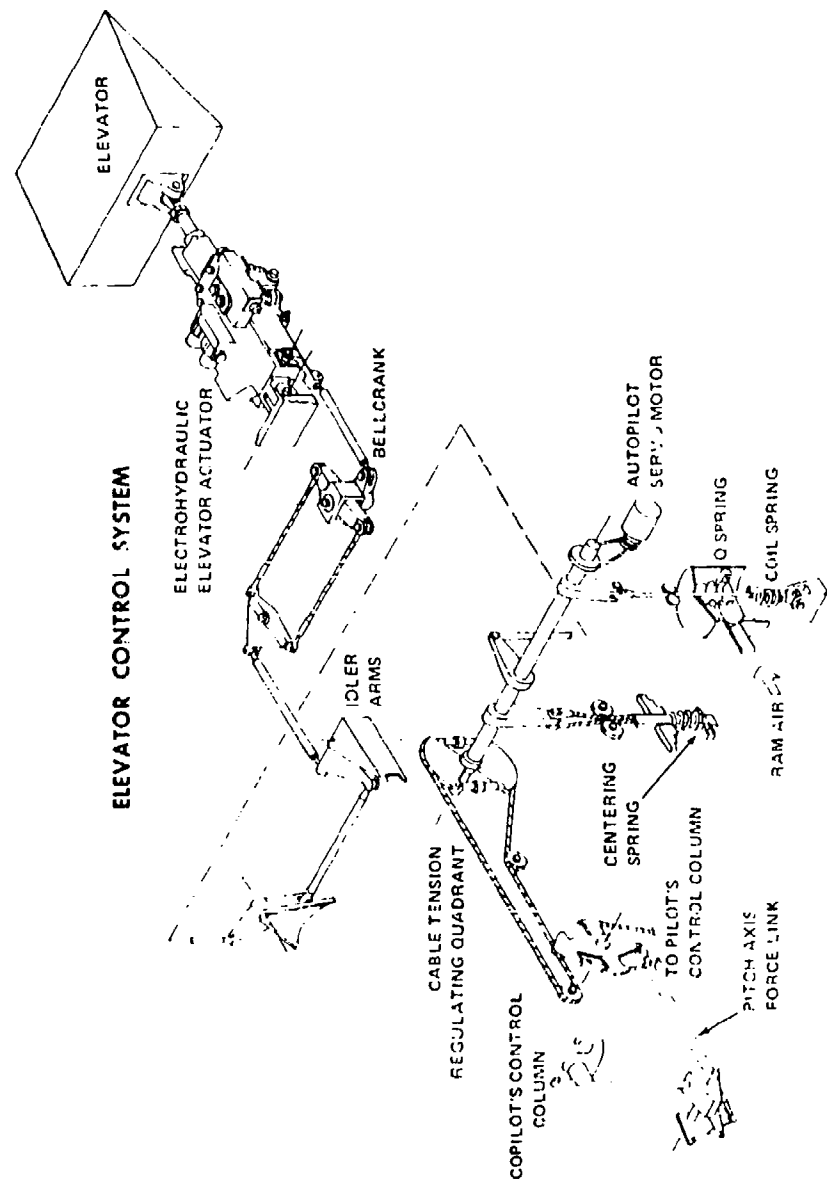


Figure 1.15 Typical Mechanical Control System

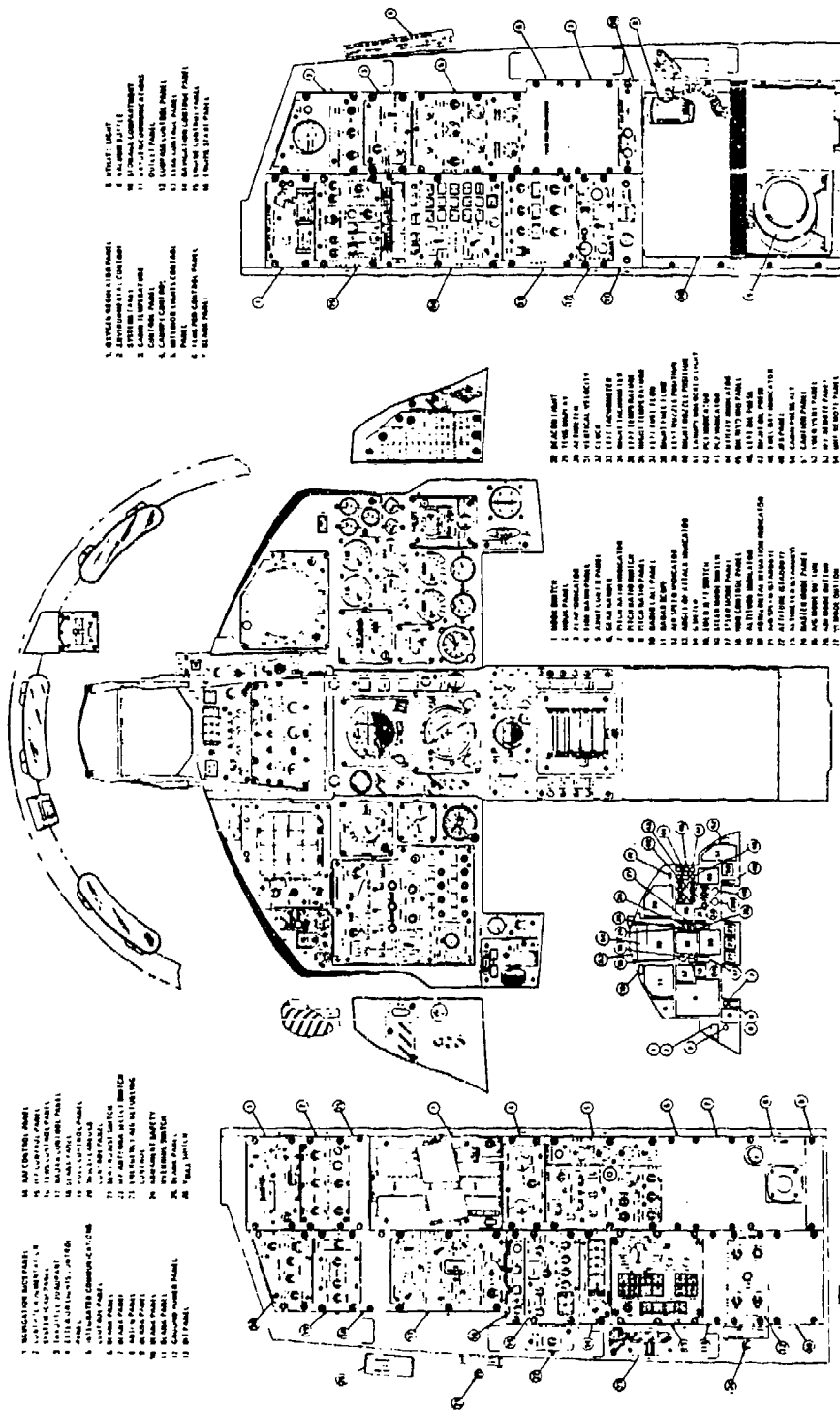


Figure 1.16 Typical Fighter/Trainer Cockpit

imminent harm. An onboard oxygen system provides breathing air to the crew under pressure at high altitude. A separate pressurized air system is available in fighter-type aircraft to inflate the g-suit which the crew wear on their lower extremities to increase their tolerance to withstand high accelerations (see Section 5.2.2).

The primary flight instruments are the **altimeter** which displays the aircraft's height as a function of barometric pressure (many aircraft have another altimeter which uses a radar reflection), the **airspeed indicator** which shows the plane's speed relative to the surrounding air, the **rate-of-climb indicator** which displays the rate of ascent or descent as a function of changing ambient pressure, and the **attitude indicator** which shows the plane's orientation relative to the earth's gravity center by use of gyros. The principle engine indicators can include the **engine pressure ratio** (EPR, the ratio of turbine discharge to inlet pressure), the **core rotational speed** (in a turbofan, N1 for the low pressure components and N2 for the high pressure), an **inter-turbine temperature** (ITT or FITT between the low pressure and high pressure turbines in a turbofan engine), **nozzle pressure ratio** (NPR, the ratio of the pressure at the exit of the turbine to the pressure at the throat of the venturi), **exhaust gas temperature** (EGT, at the exit of the turbine section) and the **fuel flow rate**. The primary engine control is the throttle to adjust the engine rotational speed and select afterburner operation. Many of the most recent aircraft have all of these displays integrated on one or more **multipurpose displays** (MPDs), or a TV or other type screen, and only a few separate backup instruments.

The aircraft will have many radios at the disposal of the crew. One or more transceivers of the UHF, VHF and HF types are common. Special purpose non-verbal radios will include a **transponder** that shows ground radar controllers the altitude and identity of the aircraft, and the **Identification Friend-or-Foe** (IFF) which transmits an encoded signal. An **intercom** or **interphone** permits conversation between the crew members and carries the cockpit audio tones and warnings. There may be a couple of navigation radios with associated displays to show the plane's distance, bearing or relative location from a ground transmitter station. Most military aircraft also have a gyroscopic or laser **inertial navigation system** (INS) with its associated display. Much of this navigation data is displayed on a **Horizontal Situation Indicator** (HSI).

The cockpit will include many other displays to show system status, fault warnings, offensive and defensive systems status, and mission information. Many aircraft also have a **Heads-Up Display** (HUD) which reflects the most fundamental data on a glass plate in front of the pilot within the field of view when looking out the forward windscreens. A radar display is also included in the cockpit. The radar may be designed to track other aircraft or to show the weather or terrain on the radar display in the cockpit.

### **1.3.8 WEAPONS**

Military aircraft typically carry some form of weaponry, many times external to the structure. Guns are usually internal and fire through a gun port. Large drums of ammunition will be stored within the aircraft. Many weapons that are released from the machine are carried either internally in a bay (bomb or weapons bay) or externally, attached directly to the structure or on pylons fixed to the underside of the wing or fuselage that stand them away from the structure for aerodynamic reasons (Figure 1.17).

Bombs and missiles may be attached to racks that in turn attach to pylons. The racks will have an attachment and release mechanism and perhaps a wire harness through which power and commands are transmitted. Missiles may be guided or unguided (rockets) and be an air-to-ground or air-to-air weapon. Chaff (small strips of metal) and flares are often also carried

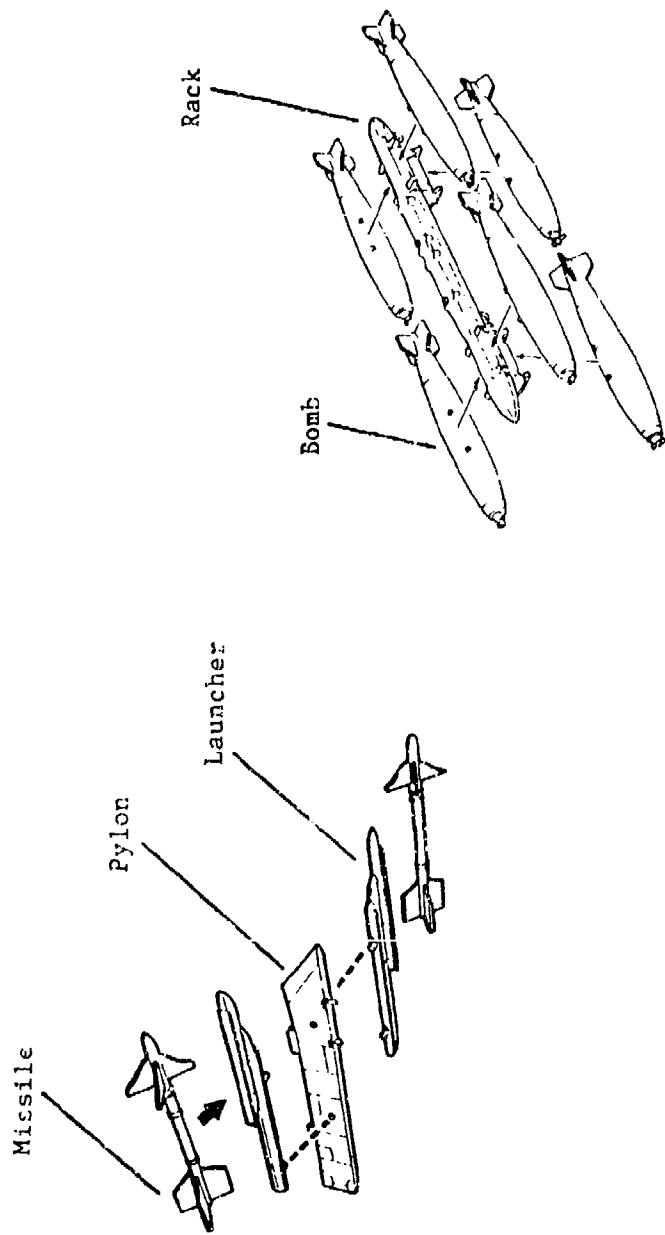


Figure 1.17 Example Weapon Pylon and Store Ejector Rack

as defensive measures. Many forms of radio transmitters and receivers are also carried as an offensive or defensive form of **electronic warfare (EW)**

## NOMENCLATURE

A	aspect ratio
APU	auxiliary power unit
AR	aerial refueling
ac	alternating current
BL	butt line
b	wing span
dc	direct direct
ECS	environmental control system
EGT	exhaust gas temperature
EPR	engine pressure ratio
EW	electronic warfare
ITT	inter-turbine temperature
FS	fuselage station
HSI	horizontal situation indicator
HUD	heads-up display
IFF	identification friend-or-foe
INS	inertial navigation system
ITT	inter-turbine temperature
MPD	multipurpose display
N1	low pressure core rotational speed
N2	high pressure core rotational speed
NPR	nozzle pressure ratio
RAT	ram air turbine
S	wing area
WL	water line
WS	wing station

## REFERENCES

1. Hurt, H.H., Jr., *Aerodynamics for Naval Aviators*, NAVWEPS 00-80T-80, US Navy, January 1965.
2. Gunston, Bill and Spick, Mike, *Modern Air Combat*, Crescent Books, New York, New York, 1983.
3. Stinton, Darrol, *The Anatomy of the Aeroplane*, Granada Publishing Limited, London, England, 1980.
4. Stinton, Darrol, *The Design of the Airplane*, Van Nostrand Reinhold Company, New York, New York, 1983.
5. Whitford, Ray, *Design for Air Combat*, Jane's Publishing Company, London, England, 1987.

# CHAPTER 2.0

## AERODYNAMICS AND FLIGHT MECHANICS

### 2.1 INTRODUCTION

Many engineers who first begin working in aircraft structures flight testing have only a rudimentary understanding of aerodynamics and aircraft control. Because in flight the aerodynamic forces are the predominant structural forcing function, it is important that the structures flight test engineer become versed in aerodynamic theory. Aircraft dynamics can also play an important role in structural dynamics. During flight testing the engineer will be exposed to many terms and concepts for which this chapter will serve as an introduction.

This chapter will provide an extremely broad and simplistic introduction to aerodynamics and aircraft control. The reader is strongly encouraged to pursue the subject further by reviewing the suggested references, particularly Reference 2, which provides a thorough but easily understood overview.

### 2.2 BASIC AERODYNAMICS

#### 2.2.1 THE ATMOSPHERE

The aerodynamic forces and moments acting upon an aircraft in flight is due in large part to the properties of the air in which it flies. Of primary importance is the static pressure at the point in the sky where the aircraft is flying. Pressure ( $P$ ) is dependent upon temperature and density of the fluid (the air). Recall the Perfect Gas Law

$$P = \rho R t \quad (2.1)$$

where  $\rho$  is the density,  $t$  is the absolute temperature, and  $R$  is the gas constant. Since density and temperature, in general, decrease with altitude and are influenced by humidity and other weather phenomena, it is clear that the pressure distribution within the atmosphere is far from homogeneous.

Air pressure is often defined in inches of mercury (in. Hg) as in a barometer reading (barometric pressure). A useful conversion is

$$1 \text{ in. Hg} = 0.49 \text{ psi} \quad (2.2)$$

Another useful concept is the standard lapse rates or variation of temperature and pressure with altitude in the lower atmosphere where most "airbreathing" flight occurs. They are

$$(1 \text{ in. Hg})/(1000 \text{ ft}) \quad (2.3)$$

$$(2^\circ\text{C})/(1000 \text{ ft}) \quad (2.4)$$

In order to provide a predictable change of atmospheric properties with altitude, a Standard Atmosphere (or standard day condition) has been defined (see Table 2.1). By correcting

**Table 2.1**  
**The Standard Atmosphere**

Altitude Z. ft	Temperature $T. {}^{\circ}\text{R}$	Pressure $P.$ lb/ft <sup>2</sup>	Density $\rho.$ lb sec <sup>2</sup> /ft <sup>4</sup>	Speed of sound. ft/sec
0	518.69	2116.2	2.3769 <sup>-3</sup>	1116.4
1,000	515.12	2040.9	2.3081	1112.6
2,000	511.56	1967.7	2.2409	1108.7
3,000	507.99	1896.7	2.1752	1104.9
4,000	504.43	1827.7	2.1110	1101.0
5,000	500.86	1760.9	2.0482	1097.1
6,000	497.30	1696.0	1.9869 <sup>-3</sup>	1093.2
7,000	493.73	1633.1	1.9270	1089.3
8,000	490.17	1572.1	1.8685	1085.3
9,000	486.61	1512.9	1.8113	1081.4
10,000	483.04	1455.6	1.7556	1077.4
11,000	479.48	1400.0	1.7011 <sup>-3</sup>	1073.4
12,000	475.92	1346.2	1.6480	1069.4
13,000	472.36	1294.1	1.5961	1065.4
14,000	468.80	1243.6	1.5455	1061.4
15,000	465.23	1194.8	1.4962	1057.4
16,000	461.67	1147.5	1.4480 <sup>-3</sup>	1053.3
17,000	458.11	1101.7	1.4011	1049.2
18,000	454.55	1057.5	1.3553	1045.1
19,000	450.99	1014.7	1.3107	1041.0
20,000	447.43	973.27	1.2673	1036.9
21,000	443.87	933.26	1.2249 <sup>-3</sup>	1032.8
22,000	440.32	894.59	1.1836	1028.6
23,000	436.76	857.24	1.1435	1024.5
24,000	433.20	821.16	1.1043	1020.3
25,000	429.64	786.33	1.0663	1016.1

**Table 2.1**  
**The Standard Atmosphere (Continued)**

Altitude Z, * ft	Temperature <i>T</i> , °R	Pressure <i>P</i> , lb/ft <sup>2</sup>	Density <i>ρ</i> , lb sec <sup>2</sup> /ft <sup>4</sup>	Speed of sound, ft/sec
26,000	426.08	752.71	1.0292 <sup>-4</sup>	1011.9
27,000	422.53	720.26	9.9311 <sup>-4</sup>	1007.7
28,000	418.97	688.96	9.5801	1003.4
29,000	415.41	658.77	9.2387	1000.13
30,000	411.86	629.66	8.9068	994.85
31,000	408.30	601.61	8.5841 <sup>-4</sup>	990.54
32,000	404.75	574.58	8.2704	986.22
33,000	401.19	548.54	7.9656	981.88
34,000	397.64	523.47	7.6696	977.52
35,000	394.08	499.34	7.3820	973.14
36,000	390.53	476.12	7.1028 <sup>-4</sup>	968.75
37,000	389.99	453.86	6.7800	968.08
38,000	389.99	432.63	6.4629	968.08
39,000	389.99	412.41	6.1608	968.08
40,000	389.99	393.12	5.8727	968.08
41,000	389.99	374.75	5.5982 <sup>-4</sup>	968.08
42,000	389.99	357.23	5.3365	968.08
43,000	389.99	340.53	5.0871	968.08
44,000	389.99	324.62	4.8493	968.08
45,000	389.99	309.45	4.6227	968.08
46,000	389.99	294.99	4.4067 <sup>-4</sup>	968.08
47,000	389.99	281.20	4.2008	968.08
48,000	389.99	268.07	4.0045	968.08
49,000	389.99	255.54	3.8175	968.08
50,000	389.99	243.61	3.6391	968.08
51,000	389.99	232.23	3.4692 <sup>-4</sup>	968.08
52,000	389.99	221.38	3.3072	968.08
53,000	389.99	211.05	3.1527	968.08
54,000	389.99	201.19	3.0055	968.08
55,000	389.99	191.80	2.8652	968.08
56,000	389.99	182.84	2.7314 <sup>-4</sup>	968.08
57,000	389.99	174.31	2.6039	968.08
58,000	389.99	166.17	2.4824	968.08
59,000	389.99	158.42	2.3665	968.08
60,000	389.99	151.03	2.2561	968.08

information such as aircraft performance data to this standard a justified comparison can be made to other data with the effects of atmospheric variations removed. These variations are often defined as the ratios:

$$\delta = P/P_s \quad (2.5)$$

$$\sigma = \rho / \rho_s \quad (2.6)$$

$$\theta = t/t_s \quad (2.7)$$

where the subscript s denotes standard day sea level conditions.

## 2.2.2 ALTITUDE AND AIRSPEED MEASUREMENT

Aircraft altimeters are calibrated for the standard atmosphere and are essentially sensitive barometers that indicate altitude in the standard atmosphere. However, they normally have the means of correcting the readings for the local pressure conditions. Setting the instrument to the local barometric pressure will allow it to display **density altitude**. If the standard day pressure of 29.92 in. Hg is used then a **pressure altitude** will be read. To reduce the level of standardization corrections necessary for test data, the pressure altitude is normally used in flight test.

The measurement of airspeed is done with the difference of total and static pressures. The **total pressure** ( $P_T$ ) is the sum of the static and dynamic pressures, as defined by the **Bernoulli Equation** (assuming incompressible air)

$$P_T = P + \rho V^2/2 \quad (2.8)$$

which is constant, and where the **dynamic pressure term** ( $q$ ) is

$$q = \rho V_t^2/2 = \rho_s V_e^2/2 \quad (2.9)$$

where  $V_t$  refers to true airspeed and  $V_e$  refers to equivalent airspeed, both defined shortly. The dynamic pressure is an important measure of the force acting on a flight vehicle. Measurement of the static pressure is normally done on the aircraft fuselage where the pressure field is corrupted by the presence of the aircraft itself. This produces what are called **position errors**. When the **indicated airspeed** (IAS or KIAS when given in nautical air miles per hour or knots) is corrected for instrument and position errors it is called **calibrated airspeed** (CAS or KCAS). The error may be additive or subtractive, so CAS could be higher or lower than IAS. The position error can be significantly reduced by sensing the pitot-static pressures at the tip of a boom (pitot-static boom) extending ahead of the aircraft or on a tube stabilized with a cone which trails behind the aircraft (trailing cone). The errors are determined with an **airspeed calibration test** (see Reference 1). **Equivalent airspeed** (EAS or KEAS) is the correction of CAS for compressibility effects. This correction is necessary during flight near and beyond the speed of sound (see Section 2.2.4). These corrections are negative, so EAS is always less than CAS above sea level (Figure 2.1). A final correction will produce **true airspeed**, or TAS. This is a correction for air density changes with altitude, defined as

$$V_t = V_e / \sqrt{\sigma} \quad (2.10)$$

which makes TAS greater than EAS above sea level.

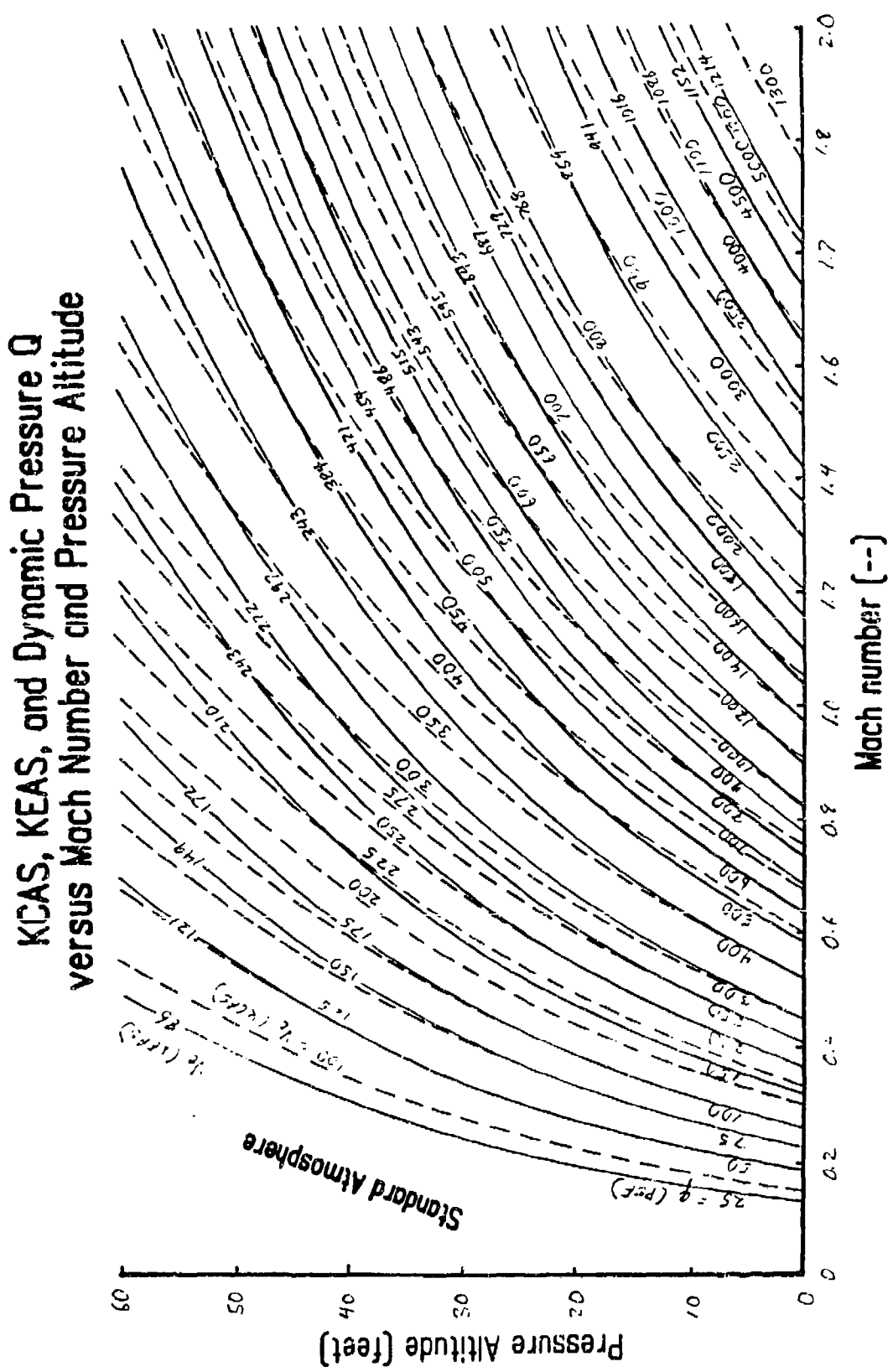


**Figure 2..1 Relationships of Airspeed Forms with Altitude**

### **2.2.3 AIRFLOW VISUALIZATION**

In an effort to more fully understand the airflow about and pressure distribution on an object in flight, a system of flow visualizations has been developed.

The **streamline** is the most basic element of the visualization system. It shows the direction of travel and path of air molecules in the presence of a body (see Figure 2.2). Closely spaced streamlines imply high velocity and widely spaced streamlines imply a lower velocity. Where the streamline ends on the surface the velocity is zero. This is called a **stagnation point**. During flight testing it is possible to see the direction of the flow by taping an array of **tufts** (short strips of yarn, perhaps with a small cone attached) to the area of interest on the surface of the aircraft. A turbulent flow would be seen as violently disturbed tufts.

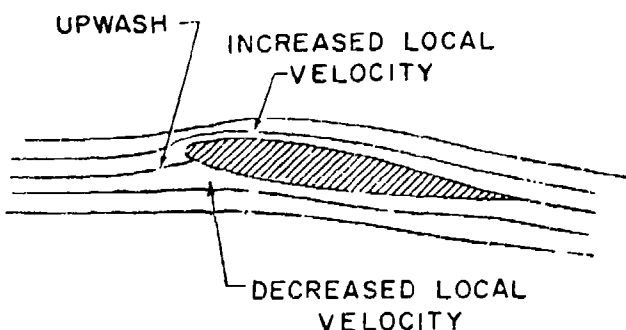


Figure 2.2 Streamline Around an Airfoil

The pressure distribution on the body is shown by a series of arrows (see Figure 2.3). Long arrows indicate a large pressure and small short arrows lower pressure. Arrows pointing toward the body imply a positive pressure (greater than the surrounding static pressure) and those pointing away from the body imply a negative pressure (lower than static). A change in pressure along a portion of the body is called a **pressure gradient**.

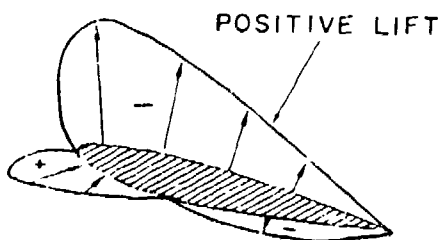


Figure 2.3 Pressure Distribution on an Airfoil

More recently, computer-generated images show colored or shaded zones, each representing different ranges of pressure, velocity, or surface temperature. Shock waves (next section) can be seen and photographed during wind tunnel tests using a system of polarized light and lenses called **Schlieren**. The shocks appear as shadows or "fringes" in the photograph.

## 2.2.4 SUPERSONIC FLIGHT

Pressure (or density) waves in the atmosphere (or any fluid), generated by the motion of a body within the atmosphere, travel at the speed of sound for the fluid. An object traveling at or greater than the speed of sound will be displacing the air molecules faster than they can propagate ahead of the object. The air will pile up into a wave of highly compressed air called a **shock wave**. This phenomena results in a fundamental change in aircraft aerodynamics and requires a separate review.

Flight above the speed of sound is called supersonic flight. Airspeeds can be related to the speed of sound through **Mach numbers (M)**, defined as

$$M = V_t/a = V_e/(a\sqrt{\sigma}) \quad (2.11)$$

where  $a$  is the speed of sound.

Since the speed of sound decreases with altitude, at least up to 36,000 ft (see Table 2.1 and Figure 2.1), an aircraft would have to travel much faster (relative to the earth) and be subjected to much higher dynamic pressures to fly at Mach 1.0 (supersonic) at sea level than at 30,000 ft altitude. Because of the fundamental difference between supersonic and subsonic flight (less than the speed of sound) it is convenient to use Mach numbers for aircraft capable of supersonic flight.

It has been found convenient to make further definitions of airspeed relative to the speed of sound. Supersonic speeds will typically begin to occur at some points on the surface of the aircraft (called the **critical Mach number**) at about 0.85M. From here to about 1.2M some subsonic flow will still be present on the aircraft and this is called the **transonic speed range**. There are important performance and control impacts on an aircraft as it enters the transonic region and this is the most challenging flight regime to analyze with any precision. The **hypersonic range** is considered to begin at about 3.0M.

There are different types of shock waves, dependent upon the geometry of the body within the flow (Figure 2.4). The **normal shock** occurs ahead of a blunt body. The flow is decelerated aft of the shock to subsonic flow with a great increase in static pressure and density. The **oblique shock** is formed at an acute corner of the body. The flow turns to follow the body and is decelerated with a rise in pressure and density. At an oblique corner an expansion wave will occur to turn the flow but with an increase in Mach number but a decrease in pressure and density. The position and geometry of the shock wave is dependent upon the body and the Mach number. Shocks are often unsteady and their movement can effect control and aeroelasticity.

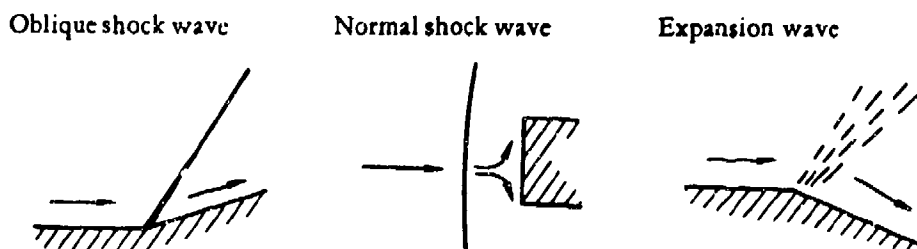


Figure 2.4 Shocks

## 2.2.5 GENERATION OF LIFT

The primary lifting surface on an aircraft is the wing. The section (cross- section) or **airfoil** of the wing is the most critical aspect of the wing that determines its lift characteristics. Some of the airfoil geometry is defined in Figure 2.5 and other definitions relative to lift generation in Figure 2.6.

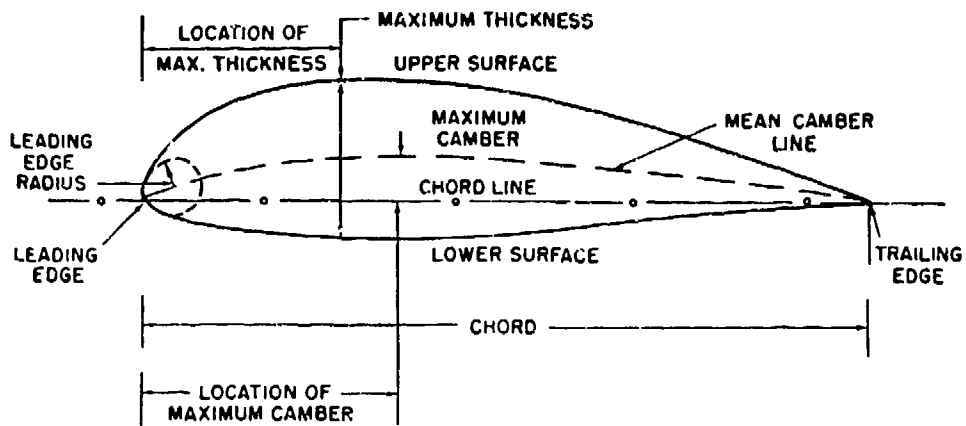


Figure 2.5 Airfoil Geometry Terminology

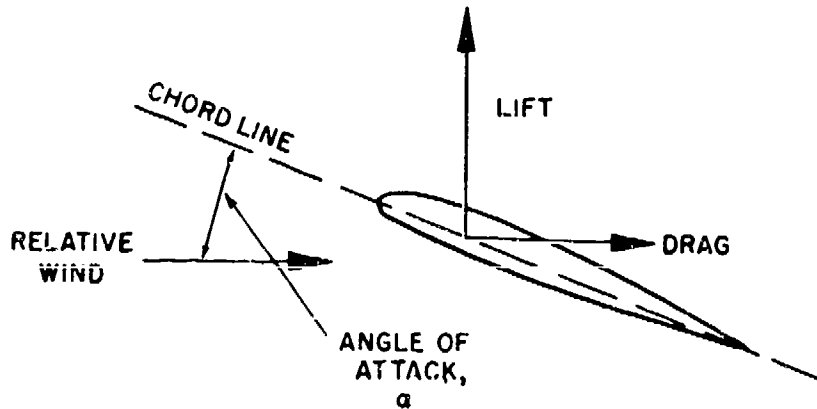


Figure 2.6 Lift Generation on an Airfoil

The simplest explanation of how an airfoil generates lift is the velocity increase of the air as it flows over the **cambered** upper surface. As the airfoil is propelled through the air (seen from the perspective of the airfoil as air flowing past the surface), the air molecules immediately adjacent to the surface are displaced against molecules further removed from the surface which resist the displacement by virtue of their inertia and friction with surrounding molecules. The result is an increase in velocity over the airfoil by venturi effect, with the cambered airfoil and surrounding air acting as the constricting walls of a venturi. This velocity increase results in a

drop in static pressure on the top of the wing for the total pressure to remain constant (see equation 2.8). However, more complex events must also occur. The presence of the airfoil and the aircraft in general produces an **upwash** effect ahead of the surface and then a **downwash** aft of it. The consequence of this is the production of **circulation** in the flow, essential for lift (see Figure 2.7). The flow of high pressure air around the wing tip to the low pressure region on top of the wing contributes to this circulation by producing a helical flow pattern called a **tip vortex** (see Figure 2.8).

Some of the flow near the surface (the **boundary layer**) will be smooth (**laminar**) but eventually trips to a **turbulent layer** further aft on the body. The lift on a wing will increase with angle of attack (AOA, see Figure 2.6) until the pressure gradient on the top of the wing becomes so severe that it overcomes the surface viscous forces that hold the boundary layer attached to the surface and it separates with chaotic flow resulting aft of this point. The **separated flow** over the wing generally results in a sudden loss of lift called **stall**. Up to this point the lift to AOA relationship is linear. Near and at stall this relationship is no longer linear. To achieve this stall AOA in level flight generally requires a comparatively slow speed or a maneuver in which the nose of the plane has been pulled up sharply with respect to the incident air flow. The lift of the wing can be defined in a non-dimensional coefficient form (the **lift coefficient**  $C_L$ ) as

$$C_L = L/(qS) \quad (2.12)$$

where  $S$  is the projected area of the wing.

All of the lift generated by the wing effectively acts at one point called the **center of pressure** (c.p.). Changes in lift produced by wind gusts or changes in AOA effectively act at the point called the **aerodynamic center** (a.c.). The importance of these concepts will be discussed further in Section 2.3.2

It may occasionally be useful to induce flow disturbances in an effort to energize the flow and thus delay separation. This can be done with strips on the leading edge of the wing or, more commonly on high performance aircraft, **vortex generators** (VGs). Vortex generators are small metal tabs attached vertically to the surface and angled to the flow. They are generally arranged in a line or some other pattern (see Figure 2.9). A **flow straightener** does exactly what the name implies in an effort to induce the flow into a certain pattern. As an example, the F-101 was encountering a bothersome buffeting at cruise that was isolated to adverse flow on the aft fuselage interacting with the engine efflux. The solution was a small sheet metal tab attached at the periphery of each engine nozzle at the location necessary to divert the flow into a more suitable pattern.

The boundary layer, the separation and reattachment of the flow, perhaps induced by structural motion, and the shedding of vortices has a frequency content associated with it. This **unsteady flow** is a critical aspect of aeroelasticity but is still not well understood.

## **2.2.6 GENERATION OF DRAG**

Drag is the sum of the components of aerodynamic force vectors acting on the aircraft that are opposite to the relative wind. This force must be overcome by thrust to achieve flight. The initial introduction to drag was in Figure 2.6 as that portion of the wing normal lift force on the airfoil parallel to the relative wind. This is termed **induced drag**, or that drag produced as a result of producing lift.

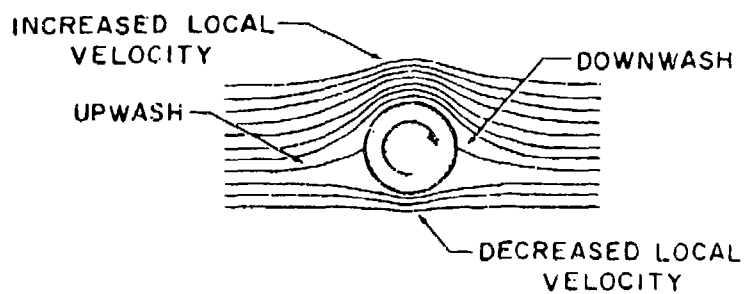


Figure 2.7 Example of Circulation

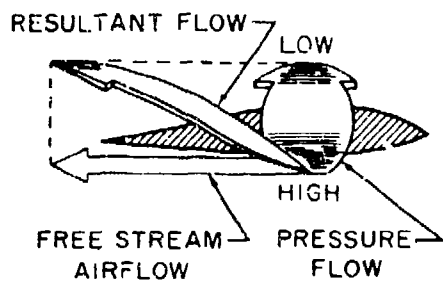


Figure 2.8 Wing Tip Vortices

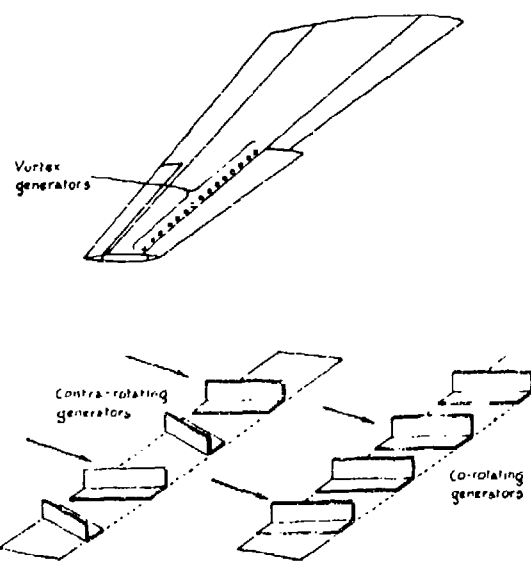


Figure 2.9 Example Vortex Generator Installation

Because air is viscous, the boundary layer (see Section 2.2.5) will produce a resistance to the passage of the air vehicle. This resistance is termed **skin friction drag** and can be reduced by reducing the surface area of the aircraft and by making the surface smoother. A laminar boundary layer has an even velocity profile and is desirable because of its low skin friction drag. As the flow extends down stream on the body skin friction will eventually cause the flow to trip to a turbulent state which is thicker and has higher friction, thus more drag. The separation of this flow usually occurs on an aft portion of a part of the aircraft and produces a low pressure zone that acts in the drag direction. This is called **form drag** and together with skin friction drag makes up the **profile drag**.

The characteristics of flow in the vicinity of two surfaces joined at acute angles can produce a drag called **interference drag**. A fairing at this junction can sometimes reduce this drag. This drag combined with profile drag produces a drag termed **parasite drag**. The pressure distribution associated with shocks (see Section 2.2.4) can also act opposite to the direction of flight and produce what is called **wave drag**. Total drag ( $D$ ) would be the sum of the parasite, wave and induced drag. The total drag can also be expressed in nondimensional **drag coefficient ( $C_D$ )** form as

$$C_D = D/(qS) \quad (2.13)$$

### **2.2.7 AERODYNAMIC MODELING**

The design of high performance aircraft has become so complex, time consuming and expensive that considerable effort must be expended in computer analysis of design options long before wind tunnel models or test aircraft are constructed. A critical element of this analysis is the mathematical modeling of the aerodynamics of a proposed configuration. This modeling must represent the pressure distribution, lift, drag, vortex shedding, etc., faithfully enough that control derivatives (see Section 2.3.3) may be derived and aeroelastic forcing functions confidently applied to the structural model.

The field of mathematical aerodynamic modeling is collectively known as **Computational Fluid Dynamics (CFD)**. This field is so complex as to generally require graduate and often doctorate level education to understand and implement. Only a general introduction to the techniques used will be presented so that the engineer will understand the level of effort and principles involved.

The basis of the modeling methods are mathematically-contrived fluid flow elements. These may include a **source** (flow from an infinitesimal singularity), a **sink** (flow into a singularity), a **doublet** (flow into and out of a singularity simultaneously), vortices and circulation. A series of these elements at different strengths are distributed on the surface of the numerical model of the vehicle surface or a part of the vehicle. The objective is to have these elements interact in such a way as to force the modeled airstream to flow tangent to the modeled surface as streamlines would, while faithfully replicating downwash and to produce other necessary flow characteristics. The pressure distribution and thus lift and drag forces can then be determined. Unsteady aerodynamics require the introduction of a periodic formulation. Large matrix operations and numerical integrations are involved in CFD which makes the computer operations very costly. There are a number of well known modeling techniques that an engineer should understand at least in a broad sense. Only the most common methods will be discussed.

**Lifting line theory** is generally restricted to lifting surfaces only. It involves dividing the surface into chordwise strips or panels and superimposing vortices on the panels, normally at

the quarter chord. A series of vortices may be used at a number of points along the chord of each panel, thus creating a lattice pattern on the surface. The influence of each vortex upon all others is a fundamental aspect of this method. The distribution may be restricted to just the mean camber line of a wing or be distributed over an entire enclosed representation of the wing. The distribution of the flow elements on complex surface curvatures can also be done in ways for which analysis techniques are known, such as elliptical, parabolic and hyperbolic distributions. Minor variations on this technique are also known as **strip theory**, **vortex sheets**, and **doublet lattice**.

A similar approach can be extended to the entire aircraft but with many more of the flow model elements employed. An example of such modeling is shown in Figure 2.10. Compressibility effects can be accounted for to some extent but shocks cannot be modeled by these methods. This restricts these methods to no higher than transonic velocities. Supersonic flow can be accounted for in several ways, the most popular being the **Mach Box** method in which the influence of a conical shock is accounted for in each of many boxes superimposed on the surface. Piston theory is principally used for oscillating airfoils. It entails analyzing individual "slabs" of air distributed across the surface. The translation of the airfoils displaces the gas in the "slab", seen as the displacement of a piston at one end of a container of gas, which produces compression and expansion waves along the slab.

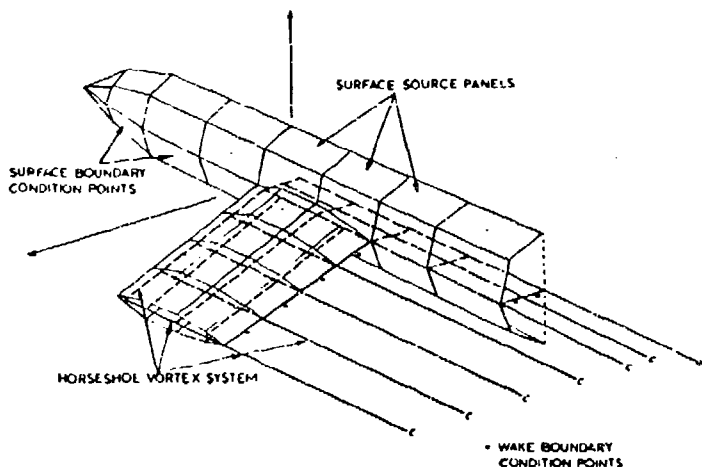


Figure 2.10 Example of Aerodynamic Paneling of an Aircraft

### **2.3 BASIC FLIGHT MECHANICS**

Flight mechanics is a broad field that encompasses the basic aerodynamic properties that allow an aircraft to fly, stability considerations, and control techniques. This section is presented to give the uninitiate reader a foundation for the understanding of aerodynamic flight and some of the principles of stability and control that have become so important in the development of advanced combat aircraft and which can impact structural stability. This background will prove important in communicating with controls engineers and test pilots in dealing with aeroelastic problems (discussed in Chapter 8.0).

### **2.3.1 REFERENCE SYSTEM**

In order to systematically study the dynamics of an aircraft, a reference system has been devised to separate motions into three mutually perpendicular axes forming a coordinate system that conforms to the right-hand rule. These axes are shown in Figure 2.11 and are the **longitudinal**, **lateral**, and **yaw or directional axes** along which the aircraft can translate or rotate. Rotation about the longitudinal axis is termed **roll** (L), about the lateral axis **pitch** (M), and about the vertical axis **yaw** (N). Along with translation along the three axes, there are then six degrees of freedom for an aircraft in flight. It is often necessary to rotate these axes to a new orientation other than that coincident with the geometric symmetry of the aircraft, such as aligning the longitudinal axes with the incident airflow (the **relative wind**) to account for an **angle of attack** ( $\alpha$ , the angle between the longitudinal axis of the plane and the relative wind in the vertical plane) and **sideslip angle** or  $\beta$  (yawed attitude, or the angle between the longitudinal axis and the relative wind in the lateral plane). These new axes are called the **stability axes** and are just one of a number of possible transformations of axes done to simplify mathematical models or more clearly define aircraft motion.

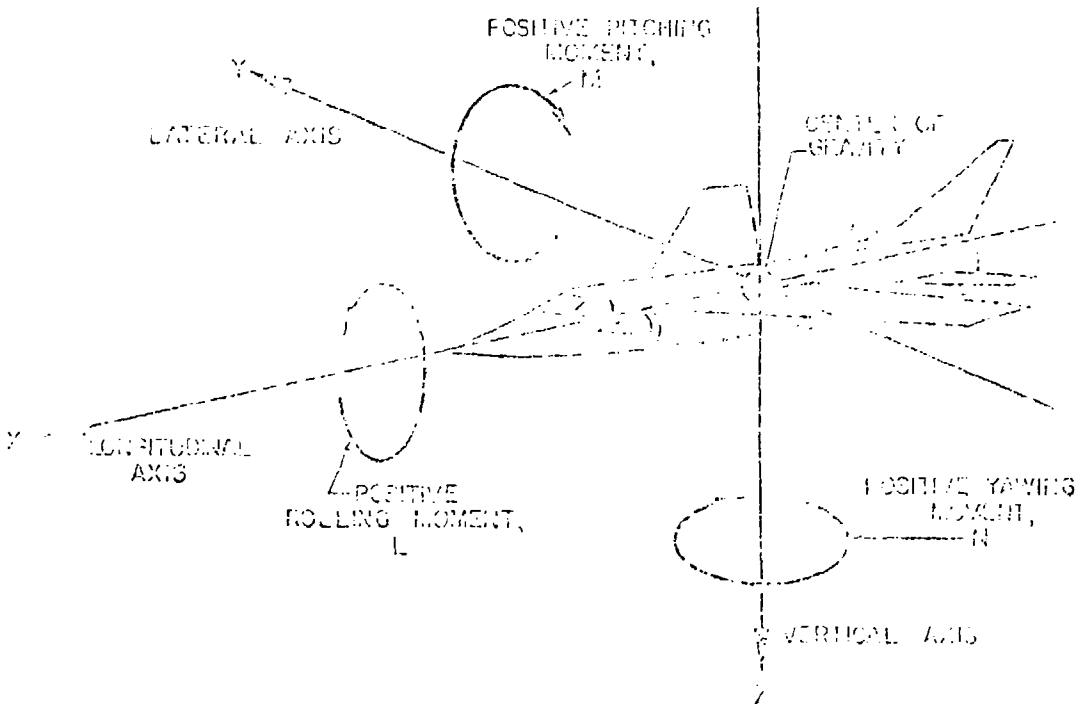


Figure 2.11 Basic Aircraft Referencing System

### **2.3.2 WEIGHT AND BALANCE**

All axes are usually fixed (called **body fixed axes**) to the **center of gravity (cg)** of the aircraft. This is the point about which the mass of the plane is equally distributed in any direction and is typically referred to in terms of percent **mean aerodynamic chord (% MAC)** of the wing.

airfoil section representing a mean of all the chords across the half-span (see Figure 1.1) or in inches aft of some convenient datum. In other words, if suspended from this point the plane would be perfectly balanced and so all aircraft moments act about this point in flight. This point can be determined mathematically by keeping track of every item on the airplane in terms of mass and its distance from some common reference point or datum. Prior to flight testing, the cg is usually checked directly by weighing the plane on scales at an **empty weight** and determining the cg position using the weight at each landing gear and the distance between them.

This issue of cg position is termed **Weight and Balance** and is important from the point of view of maximum takeoff gross weight and pitch control authority (explained later). The cg will move about as fuel is transferred or burned, stores are added or dropped, equipment is added or removed, or as wings are swept forward or aft (as on the B-1 bomber), and this empty weight cg is necessary as a constant reference. Weight will also change and is referenced to the fixed empty weight. Naturally, the thrust and lifting capability of an airplane (and thus the takeoff distance) limits the maximum weight at which an aircraft can operate.

### 2.3.3 STATIC STABILITY

The **longitudinal stability** of an aircraft is related to the position of the plane's aerodynamic center and the cg. The a.c. is the point at which all changes in lift of the entire aircraft take place, as explained earlier for the airfoil alone. Thus, the distance between the cg and a.c. constitute a moment arm. The relationship between the cg and a.c. is illustrated in Figure 2.12. The lift must overcome the weight or gravity vector concentrated at the cg. For a statically stable aircraft in flight but undisturbed, the cg is ahead of the a.c. and thus a lift vector at the a.c. produces a nose down pitching moment about the cg for a level flight attitude if the change in lift is up. For level flight this moment must be countered by an equal but opposite moment produced by the tail of the aircraft. This means that the overall lift vector of the tail must be down to bring the nose up since it is behind the cg. This down load is produced by a trailing edge up deflection of the elevator or a trailing edge up rotation of a stabilator. These effects are shown in Figure 2.12. If a canard is used (see Section 1.2.2) then it can be up-loaded to bring the nose up since it is ahead of the cg and thus contribute to the overall lift of the plane.

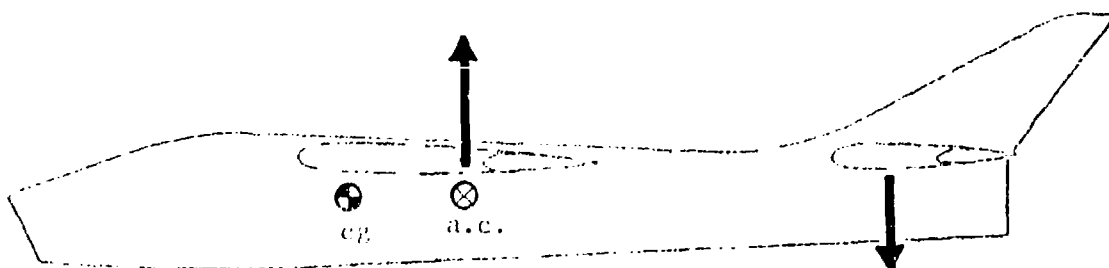


Figure 2.12 Statistically Stable Airplane cg and a.c. Relationship and Tail Load

If the cg is very close to the a.c. because of weight distribution then the moment arm is reduced and a change in the restoring moment produced by the tail load is necessary to level the aircraft. The same principle applies for a far forward cg position where a great deal of tail download is required at relatively low airspeeds to rotate the nose up to a takeoff attitude during the takeoff roll. Therefore, there are practical limits to the travel of the cg dictated by the size

and pitching moments the tail can produce. These same principles apply to the control power in the lateral and directional axes. It should be apparent at this point that an aircraft with the cg aft of the a.c. will be inherently unstable and uncontrollable in the conventional sense (though it will be discussed later about how it is possible to fly such a plane).

Roll is usually commanded by deflection of ailerons. For airplanes with stabilators (Section 1.2.2), differential rotation of the stabs will also produce a rolling moment. For example, a right roll input by the pilot would produce a right aileron trailing edge up deflection and an opposite deflection of the left aileron. This produces a higher lift on the left wing than the right wing or a rolling moment that makes the right wing drop and the left wing rise. The plane will continue to roll until the pilot checks the rolling moment with a slight left roll input and then neutral aileron command. The aircraft will remain in a wing-low attitude until corrected by the pilot. The roll attitude reorients the lift vector away from the vertical and tends to pull the plane into a turn toward the low wing. As the plane rolls, the down-going wing will experience a higher angle of attack than the up-going wing. This produces a change in the orientation of each wing's lift vector that produces a yaw tending to pull the nose toward the outside of the turn. This motion is termed **adverse yaw** and must be countered with rudder for a coordinated, efficient turn. At high speeds, rolls may be executed by using differential stabilator deflection.

Yaw motion is produced directly by use of the rudder. Deflection of the rudder is analogous to deflecting a wing trailing edge control device. For example, moving the rudder trailing edge right will produce a low pressure on the left face of the vertical tail and will produce a nose-right moment about the cg in the vertical axis. Intentional yaw is used to compensate for cross-winds on landing and the rudder is used to counter undesirable yaw motion. A yaw will change the apparent angle of attack on the wings (even when wings-level) and produce a rolling moment (like adverse yaw) that must be countered with aileron if a constant heading is to be maintained. This yawed, wing-low attitude is called a **steady-heading sideslip** and is used to increase the drag of the airplane for slowing down, point the nose for gun firing, or to produce sideloads during flight tests (see Chapter 5.0).

By the use of trim tabs or other trimming systems that bias the entire primary surface or hold the control surface at a deflected angle without pilot effort, it is possible for the pilot to produce just the right balance of forces and moments to maintain flight in either a straight and level attitude or some other orientation (within the limits of control effectiveness at the flight speed). When the aircraft is disturbed by a wind gust or a pilot input from this trimmed condition its geometry and inherent aerodynamics tend to return it to its initial state. A sudden yaw will produce an angle of attack on the vertical tail which will create a countering yawing moment. An adverse yaw motion will be reacted as explained above and raise the low wing to return the ship to wings level. A sudden pitch up will increase the AOA on the wing and horizontal tail. The increased upload on the tail and the drop in airspeed (reorientation of the thrust vector and increase in drag) will tend to cause the plane to pitch back down. These effects are examples of what makes an airplane **statically stable**.

The preceding paragraphs have described very simplistically how an airplane flies and how it is controlled in flight. The ease with which the pilot controls the airplane is directly related to its stability and is termed handling or flying qualities. Many of the most modern aircraft designs are only marginally stable or unstable in one or more axes and the cg may be coincident or aft of the a.c. Such an airplane is made controllable by computers that automatically monitor the airplane dynamics and compensate for undesirable motion. This is called "**artificial**" stability and increases the importance of aeroservoelastic effects (see Chapter 8.0). The advantages of this approach is that the flight characteristics of such a machine can be "programmed" into the

flight control computer. Also, smaller aerodynamic surfaces, meaning less control effort and drag, are typical of this type of design.

#### **2.3.4 DYNAMIC STABILITY**

Dynamic stability refers to the oscillatory motion of the aircraft after being disturbed from its trimmed state. The static stability will tend to return the aircraft to the trimmed condition but inertia and other factors may cause the ship to overshoot this trimmed attitude. An oscillation may be set up in one or more axes of the aircraft which will eventually **damp** out (decreasing amplitude of the oscillations over time) until the steady trimmed condition is regained. The amount of damping in the system (the aircraft and its aerodynamics) are important from a handling qualities and mission capability aspect. An **undamped** or neutrally damped oscillation (neither increasing nor decreasing in amplitude with time) is undesirable and an undamped or **divergent response** (increasing in amplitude) is unacceptable as it may lead to dangerous flight attitudes and structural loads that can cause the loss of the ship and crew. **Stick fixed** (held by the pilot) and **stick free** (released by the pilot) dynamics may vary because of the dynamics of the stick and the pilot's body.

Airplanes have certain dynamics that are common to all aircraft by the nature of their basic design. They are called **rigid body modes** because they are aerodynamic in nature and are not dependent upon structural dynamics (fuselage bending, wing torsion, etc.). The most fundamental of these are aircraft pitch, roll and yaw frequencies independent of control surface motion. When disturbed in one of these axes by an outside influence (a wind gust for example) the plane will oscillate at the characteristic rigid body frequency for that aircraft.

There are more complex rigid body dynamics that the structures flight test engineer should be aware of. In the longitudinal axes these are the phugoid and the short period modes. The **phugoid** is a long period (20 to 100 seconds per cycle) mode in which the pitch attitude changes very slowly with an attendant slow and small change in altitude and airspeed. Because the phugoid period is so long, it is likely that the pilot or autopilot will make some corrective input in the time it takes the mode to diverge significantly and so the mode seldom has time to develop. Thus, some instability in this mode is often tolerated. The **short period** mode has a much higher frequency than the phugoid, 0.5 to 5 second period, but is a constant velocity pitching motion with a constant AOA. A poorly damped short period is seldom tolerated because in attempting to control it manually the pilot may inadvertently exacerbate the motion due to the time lag between when the input is made and when its effect is apparent. This inadvertent feeding of the motion is called **Pilot Induced Oscillation** or **PIO**. The frequency of the short period mode can also cause it to couple with structural modes and create an aeroservoelastic problem (see Chapter 8.0).

Directional axes modes include the **spin**, a low speed condition in which one wing is stalled and thus a combination roll and yaw spinning motion is set up. Airframe loads created by a spin, an asymmetrical power (for a multi-engine aircraft) situation or a sideslip condition are often of interest in a loads test (see Chapter 5.0).

There are two lateral modes that are important; the Dutch Roll and the Spiral. The **Dutch Roll** is a combination of roll and yaw (thus often referred to as a lateral-directional mode) in which the wing tip of the plane will describe an ellipse or circle in the air. The Dutch Roll is usually on the order of less than two cycles per second. The **Spiral mode** involves the very slow rolling and gradual nose drop that eventually leads to a spiraling dive. This mode usually has a frequency of less than one Hertz.

Many aircraft have a feature of the autopilot, flight computer, or a dedicated system that damps out undesired dynamics that can otherwise lead to one of these modes developing. A **yaw damper** is a typical example of this. A system applies corrective rudder automatically in response to any yawing moment sensed through an accelerometer or gyro. All of the aircraft's motions can be modeled mathematically in equations of motion. These equations are the basis of autopilots and other automatic flight control systems. The coefficients in these equations can become very cumbersome and they are replaced with quantities called **stability derivatives** since they typically involve partial derivatives. An example of this is  $C_{l\beta}$ , which is the change in rolling moment coefficient with sideslip angle ( $\beta$ ), or

$$C_{l\beta} = \partial C_l / \partial \beta \quad (2.14)$$

By themselves the stability derivatives give easily visualized insight into the airplane's dynamics stability.

### **2.3.5 AEROELASTIC EFFECTS ON STABILITY AND CONTROL**

The elastic behavior of an air vehicle can affect its stability and control by deforming lifting surfaces or altering their incidence. The principle results are a change in trim requirements which may result in maximum trim authority being reached earlier than predicted, change in lift distribution and pitching moment, and reduction in control surface effectiveness. One example of this effect is control reversal, discussed in Section 6.4.5. Other examples of such phenomena are wing torsion producing a **washout** or reduction in angle of attack at the outboard portion of the wing, fuselage bending altering tailplane incidence, and elevator distortion (sometimes called **rollup**). Wing, fuselage and aileron distortion tends to be destabilizing while tailplane, elevator and general control surface distortion is usually stabilizing. The aeroelasticians may be able to assist their stability and controls counterparts in identifying such effects when difficulties arise.

### **NOMENCLATURE**

AOA	angle of attack
a	speed of sound
a.c.	aerodynamic center
C	Centigrade or Celsius
CAS	calibrated airspeed
CFD	computational fluid dynamics
$C_D$	drag coefficient
$C_L$	lift coefficient
$C_I$	rolling moment coefficient
cg	center of gravity
c.p.	center of pressure
D	drag
EAS	equivalent airspeed
IAS	indicated airspeed
in.	inches
Hg	mercury
KCAS	knots calibrated airspeed
KEAS	knots equivalent airspeed
KIAS	knots indicated airspeed
L	rolling moment
M	flight or freestream Mach number, pitching moment
MAC	mean aerodynamic chord

N	yawing moment
P	pressure
PIO	pilot induced oscillation
psi	pounds per square inch
q	dynamic pressure
R	gas constant, Rankine
S	wing area
TAS	true airspeed
t	absolute temperature
V	velocity
VG	vortex generator
X	longitudinal axis
Y	lateral axis
Z	altitude, vertical axis
$\alpha$	angle of attack
$\beta$	sideslip angle
$\rho$	air density
$\theta$	temperature ratio
$\sigma$	density ratio
$\delta$	pressure ratio
$\partial$	partive derivative
Subscripts	
e	equivalent condition
s	standard day condition
T	total
t	true condition

## REFERENCES

1. Herrington, Russel M., Major, USAF, et al, *Flight Test Engineering Handbook*, AF Technical Report No. 6273, AFFTC, Edwards AFB, California, January 1966.
2. Hurt, H.H., Jr., *Aerodynamics for Naval Aviators*, NAVWEPS 00-80T-80, US Navy, January 1965.
3. Kuethe, A.M. and Chow, C., *Foundation of Aerodynamics: Bases of Aerodynamic Design*, John Wiley & Sons, New York, New York, 1976.
4. Hess, Johnson and Rubbert, *Panel Methods*, AIAA Professional Study Series, AIAA, Washington D.C.
5. Roskam, Jan, *Airplane Flight Dynamics and Automatic Flight Controls*, Roskam Aviation and Engineering Corp., Lawrence, Kansas, 1979.
6. Etkin, Bernard, *Dynamics of Flight, Stability and Control*, John Wiley and Sons, New York, New York, 1965.
7. Ground School Notes Book "C", *Stability and Control*, Empire Test Pilot School, Farnborough, 1961.

# CHAPTER 3.0

## MATERIALS

### 3.1 INTRODUCTION

The structures engineer is occasionally called upon to provide expertise in the area of materials. The load bearing capability and dynamics of a structure are closely tied to the materials that compose the item. Because of this, it is important that the structures flight test engineer have a sound understanding of materials and their behavior. Composites and plastics are now firmly established as aircraft materials and must not be ignored. This chapter will attempt to provide a basic foundation upon which the engineer can build with additional reading. Familiarity with the applicable military specifications is also advised.

### 3.2 CHARACTERISTICS

#### 3.2.1 STRESS

A material may be subjected to a variety of external loads including **tension** (pulling), **compression** (pressing), **shear** (slicing), **torsion** (twisting), **bending** and combinations of these (see Figure 3.1). The resistance of the material to the applied load is termed **stress** and is expressed for the simple axial case as

$$\sigma = P/A \quad (3.1)$$

or load over the area in units such as pounds per square inch (psi). There can therefore be **tension stress**, **compression stress** and **shear stress**. The nature of the force application and the shape of the article may produce a combination of lesser stresses throughout the body, or component stresses. Sharp changes in geometry can create **stress concentrations**. Solving for the magnitudes and orientations of these stresses can become very complex.

The maximum stress and its orientation defines the **principle stress** for a plane. Three mutually perpendicular principle stresses are defined by orientation with the most significant of the principle stresses that can be resolved in the infinite orientations within an article. For example, the maximum axial stresses in a landing gear strut is the most significant of all stress directions that can be defined for that component and serves as the basis for the two other axes, the associated stresses of which now become the principle stresses in those axes.

Not all stresses are from external sources. Another source is the **residual stresses** from fabrication and assembly, rubbing of mated surfaces, weld joints, etc. There are many maintenance practices that are intended to avoid producing additional internal stresses.

#### 3.2.2 STRAIN

Strain is deformation in the article caused by the stress divided by the original dimension, or

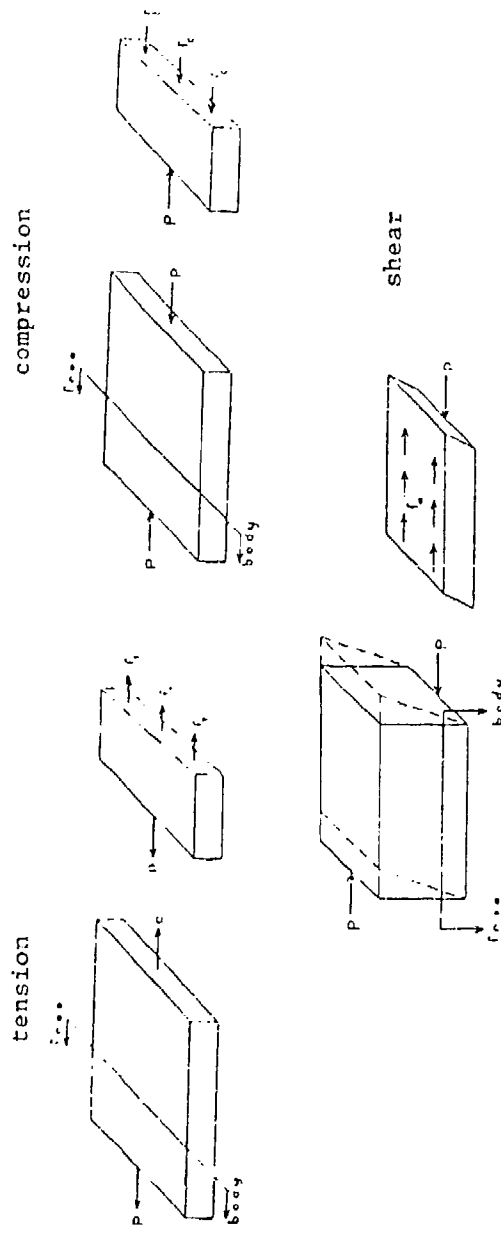


Figure 3.1 Basic Loading and Stresses

$$e_l = \Delta L/L \quad (3.2)$$

A tension load will produce some material stretching in the axis of the load (see Figure 3.2). The deformations should be measured in this axis. Conversely, compression will squeeze the material to a shorter length and the deformations should be measured in the axis of this force. Note that a tension load produces a reduction in the width of the sample as shown in Figure 3.2. A relationship between the two strains is termed **Poisson's Ratio** and is expressed as

$$\mu = -e_w/e_l \quad (3.3)$$

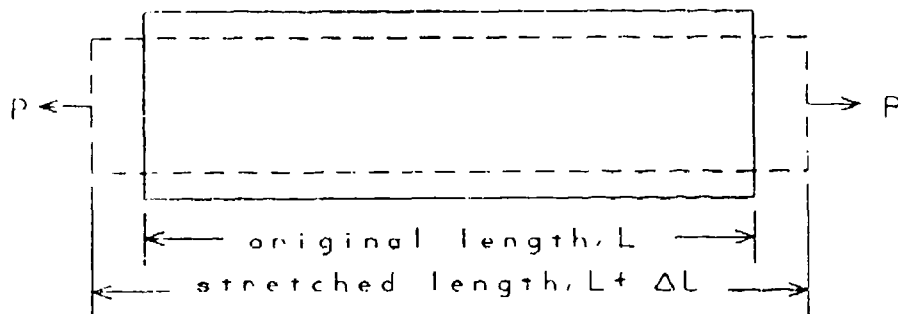


Figure 3.2 Material Deformation Under Load

Shear strain is measured as shown in Figure 3.3 and is expressed as

$$\gamma = \Delta L/L \quad (3.4)$$

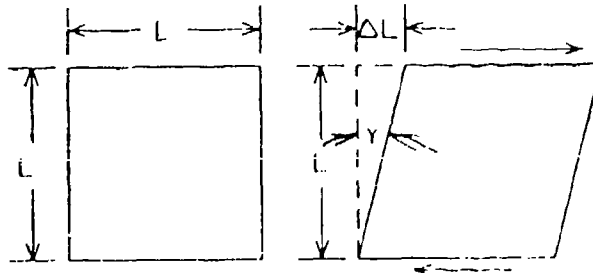


Figure 3.3 Shear Strain Illustration

The principle stresses have associated **principle strains** (see Section 3.2.1). The stress-strain properties of a material are linear for a large percentage of load that can be applied before the material fails. This is expressed by **Hooke's Law** and defines the **modulus of elasticity (Young's Modulus)**

$$E = \sigma/\epsilon \quad (3.5)$$

Typical values of E are 30,000,000 psi for steel and 10,000,000 psi for aluminum. For shear loads the modulus of elasticity is known as the **Shear Modulus** or

$$G = \sigma/\gamma \quad (3.6)$$

Multiple loads in multiple axes applied to a complex shape can produce deformations that require rigorous analysis to predict.

All of this behavior can be expressed in a stress-strain curve like that shown in Figure 3.4. The linear portion of the curve up to the limit stress corresponds to Hooke's Law. At or slightly beyond this point is the **yield** or **elastic limit**. Beyond this stress the material will not return to its initial shape even after the load is removed. In most applications this is considered to be a material failure, but in other situations only a fracture is considered failure. Considerable deformation under load will continue beyond this load up to the **ultimate stress** without loss of load bearing capability. Beyond ultimate the load cannot be sustained and cracking or actual breakage will eventually occur.

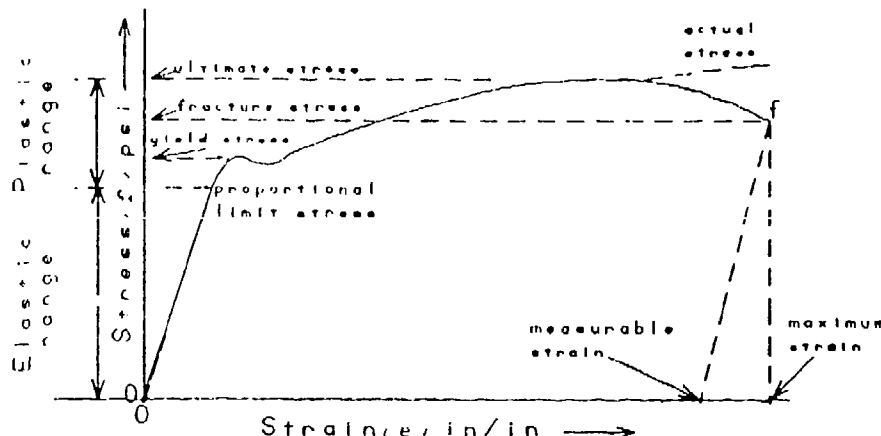


Figure 3.4 Example Stress-Strain Curve

### 3.2.3 STRESS ANALYSIS

The prediction of the stresses and strains produced by different loading configurations is the field of stress analysis. The principle objective of stress analysis is to ensure that the structure has a reasonable **factor of safety** on the actual failure stress. For aircraft applications, the failure stress of a component must be greater than 1.5 times the stress produced at the maximum load expected to be experienced in normal operation (the **design limit load** or **DLL**). Therefore, 1.5DLL is referred to as the **ultimate load**. It is important to notice that permanent deformation may occur within the factor of safety. In most cases this is considered unacceptable as this provides a "get home" capability after which overstressed components can be replaced once the airplane is safely back on the ground. A load bearing capability beyond the ultimate load is defined as the **margin of safety**. This is expressed as

$$\frac{\text{failure load as factor of DLL}}{1.5\text{DLL}} - 1 \quad (3.7)$$

A structure that completely fails at 1.76 DLL would have a margin of safety of 17%.

Stress analysis of the entire aircraft to verify the factor of safety involves complex modeling of the structure's components, their elastic behavior, load paths between the components (the redistribution of loads throughout the structure as the load condition changes). The analysis may be refined using laboratory and flight test loads data. This analysis is essential before aircraft components are actually subjected to flight loads and are extensively referenced during loads flight tests (see Chapter 5.0).

Most stress analyses today is done using **finite element modeling (FEM)**. This is a computer technique in which a structure is represented mathematically as a collection of interconnected beams, plates, solid members, etc., with the dimensions of the overall array identical to the real article. The behavior of these simple elements can be easily represented by low order, linear equations. The material properties of the actual structure is modeled by assigning such quantities as Young's moduli to each element. It is important that applicable boundary conditions be defined. Since aircraft are already truss-like structures, the elements may represent actual physical structural members (see Figure 3.5), but this is not mandatory. Distributed loads applied to the structure must be concentrated at the nodes of the model. For aerodynamic loads, the aero model discussed in section 2.2.7 may become part of the program. The equations defining the stress, strains and dynamic motion of each element can be combined in matrix form with all the elements. The solution of the matrix equations with an applied load or loads (static or dynamic) allow the resulting stresses, deformations, and dynamic response at each **node** (junction of the elements) to be resolved. The model can be refined to reflect ground and flight test data as it becomes available to improve the faithfulness of the prediction. The original and still widely used FEM computer code is NASTRAN.

### **3.2.4 THERMAL EFFECTS**

Flight through the atmosphere involves a certain amount of **kinetic heating** due to friction between the air molecules and the surface of the aircraft. Up to a certain point convective cooling from the heat conductivity of the air will play a significant role in cooling the surface, but at high mach numbers (see Section 6.4.10) the kinetic heating will become dominant. The heating will be greatest at stagnation points of the air flow on the surface (see Section 2.2.3). This heating results in both an **thermal expansion** of the material (strain), resulting **thermal stresses** particularly at interfaces and fasteners, and a drop in E. The latter effect tends to reduce the load bearing capability of the structure. These effects are considered during the design and material selection process to allow thermal expansion without detrimental stresses. The aircraft skin is directly heated by the friction and the internal structure is heated in turn by conductance. The rate of temperature rise of the internal structure is a function of the material and the duration of the heat soak. The surface of the space shuttle has already been significantly cooled by convection and radiation upon landing while the internal structure is still heating up.

### **3.3 COMPOSITES**

Metals are typically **isotropic**, that is the material properties are the same in any direction within the material. Modern composite materials are **orthotropic** with the properties different in three mutually perpendicular planes of symmetry and a function of the orientation at a point in the body. Man-made composite materials offer the opportunity to tailor the material properties in any axis to meet the expected loading configuration as economically as possible.

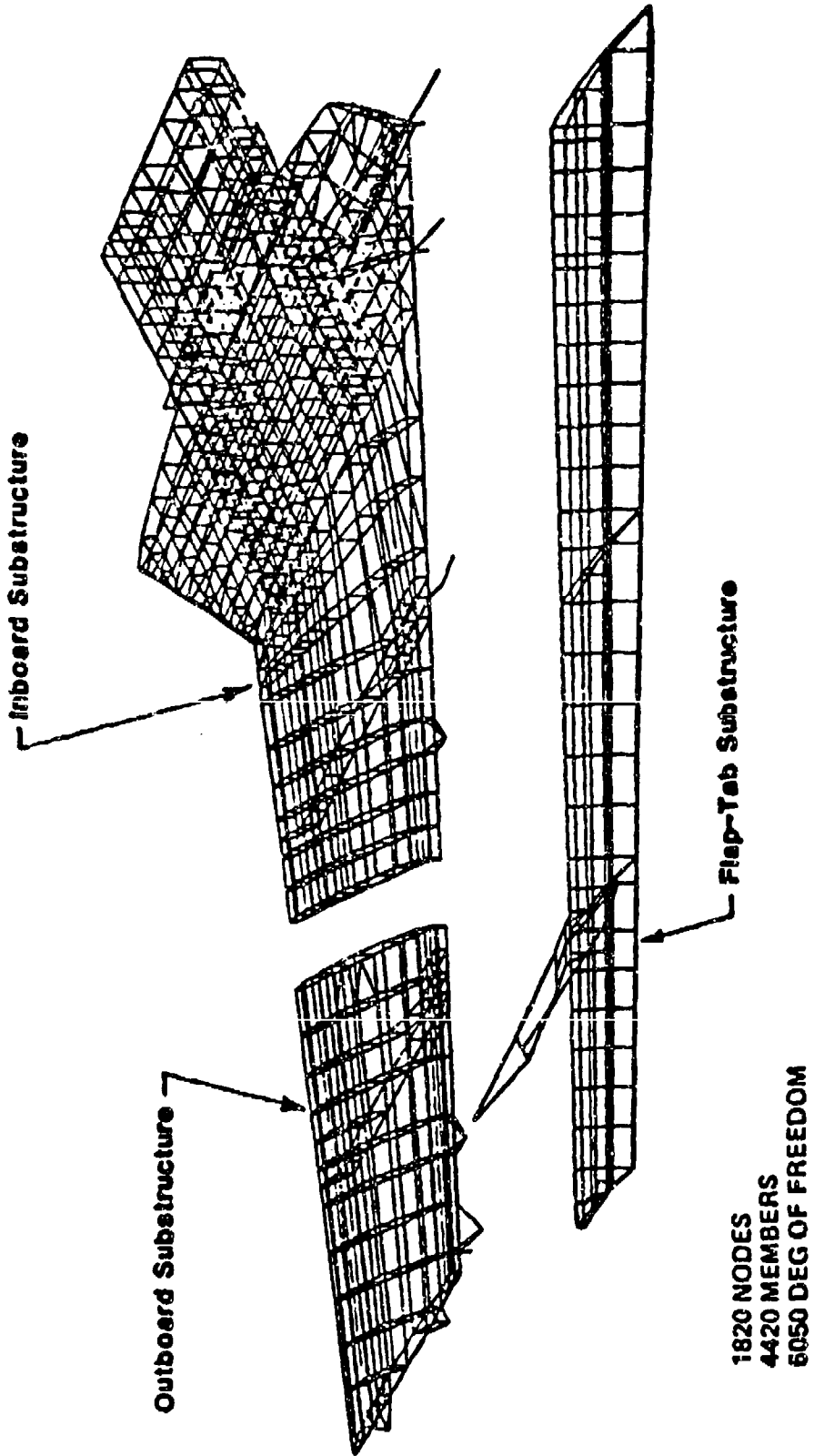


Figure 3.5 Example Finite Model - X-29A Wing Structure

Instead of being composed of one homogenous substance, composites are **in-homogeneous** or a combination of two or more substances. The type of composites most often used as structural components in aircraft are those made of long, thin glass or carbon fibers suspended in an epoxy matrix. These fibers by themselves have remarkably high tensile stress capabilities but very little compression capabilities, such as for a rope. A component made from such composites which load the fibers strictly in tension could be significantly lighter than a metal component designed to sustain the same load, while at the same time providing reduced radar reflectivity in a combat scenario.

Composites are most often produced as layered laminates, each layer consisting of a sheet of unidirectional fibers. The orientation of each layer may be varied to give the desired properties in each axis (see Figure 3.6). Some composites (particularly the glass fiber variety) come in weaves for ease of handling or to produce a particular material property.

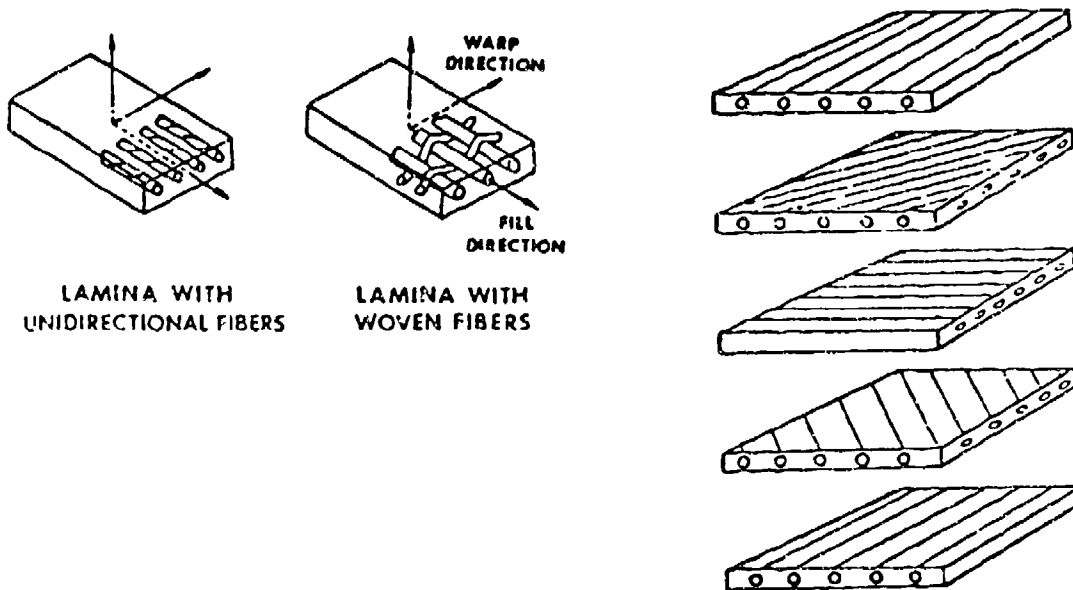


Figure 3.6 Examples of Composites

### 3.4 FAILURE MODES

This section will touch on the various mechanisms that can produce a loss of structural strength or a material failure in an aircraft structure. Most aircraft are designed for a "life" of several thousand flight hours at a typical load spectrum mission profile. Analysis and laboratory testing is necessary to ensure that none of these failure modes will result in problems before the expiration of this life time. Reskinning of the lower wing skin on the KC-135 and replacement of the C-5A and A-6 wings are just a few examples of costly rework during service when early structural problems needed correction.

### **3.4.1 CREEP**

A material subjected to a constant load over a long period will begin to deform beyond its initial loaded shape. This is known as creep and will continue slowly until failure occurs if the load is not relieved. Repeated thermal expansion and contraction can also produce creep. Elevated temperatures can accelerate the creep process. Creep is a critical consideration in the service life prediction of a component, particularly with the tight tolerances to which engine and airframe components are being manufactured today.

### **3.4.2 WORK-HARDENING**

Also known as **strain-hardening** and **cold-working**, work-hardening refers to the loading of a material beyond its yield stress but less than its ultimate stress producing a permanent set or deformation. The stress-strain characteristics of the specimen is changed with the principle result that ductility is reduced (see Section 3.6).

### **3.4.3 DELAMINATION**

Materials which are bonded together or composed of laminates bonded together may experience a failure of this bond called delamination. Common causes of delamination are the expansion of air or frozen water trapped between the laminates, the presence of a void or material defect, over-stress of the component, loading in an undesirable direction (compression leading to buckling in composites) or improper manufacturing. Delamination is most common in plastics and composites (see Section 3.3). The F-111 aircraft has suffered numerous stabilator delaminations above Mach 2.0 resulting in large sections of the outer surface and inner honeycomb material separating from the aircraft in flight.

### **3.4.4 CRACKING**

A metal component will usually display cracks as the first evidence of overstress. These cracks will typically originate at areas of stress concentrations such as rivet holes and may not be visible to the naked eye. Once found, a common technique is to "stop-drill" the crack by drilling a small hole at the end of the crack (if it can be found). A patch riveted or welded over the damaged area may be necessary.

### **3.4.5 FATIGUE**

Many materials will eventually fail in one manner or another if subjected to repeated loads less than the ultimate sustainable load. This effect is presented in an **S-N diagram** (see Figure 3.7) where S is the stress and N is the number of loading cycles to which the item is subjected. Cyclical thermal stresses can also lead to fatigue. The plot shows the number of cycles the component can withstand at a given stress before failure is likely. Predicting the fatigue life of a component as a function of operational loading cycles is an essential part of establishing the service life of an aircraft.

### **3.4.6 CORROSION**

Corrosion is the disintegration of a metal through interaction with the environment and may be influenced by factors such as stress, fatigue, moisture, and temperature. Corrosion transforms

the metal into a substance that has little of the strength of the original material. The two basic types of corrosion are chemical and electrochemical corrosion.

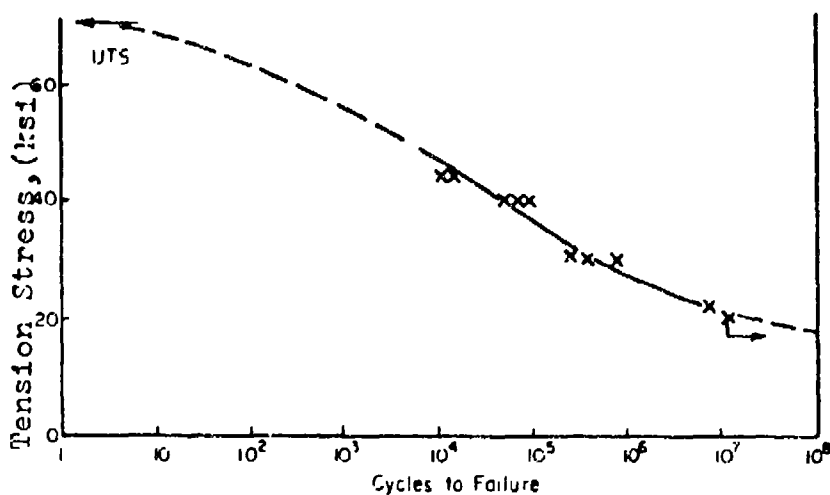


Figure 3.7 Example S-N Diagram

Corrosion may be localized or uniform over the surface. Apart from the rust and oxidation with which we are most familiar, there are many other types of corrosion modes. Pale, flaking type corrosion is common. **Exfoliation** corrosion can be identified by the lifting away of the metal in thin layers. Abrasion by rubbing (fretting) of two butted surfaces or some external source can remove protective films and thus allow corrosion to begin. The placement of two dissimilar metals together will promote **electrochemical corrosion**. Corrosion may be accompanied by **pitting** which may penetrate deeply and provide an origin for cracks.

Certain electrochemical treatments and coatings (apart from simple paint) help to prevent corrosion. Periodic inspections are mandated to search for corrosion. Many types of corrosion can be removed by simply sanding and polishing provided too much of the material is not removed (typically less than 15% of the original thickness). A patch riveted over an effected area or complete replacement of the component area may be necessary if the strength of the item is in doubt.

### 3.5 INSPECTIONS

Many methods of **non-destructive inspection (NDI)** exist. The engineer should be familiar with these as they are commonly used to determine the presence or extent of damage that may have been caused in development flight testing.

Additionally, the aircraft repair depots maintain a data base of stresses measured at a few specific locations on each aircraft in the fleet and correlated with flight events (cruise, landing, etc.). These data are recorded automatically by a **flight data recorder** on a tape which is routinely down-loaded every few flights. The data base permits the tracking of load cycles according to how the aircraft is being utilized and early prediction of life expectancy and failures.

### **3.5.1 STRESS VISUALIZATION**

Components may be coated with a resin-like paint that becomes brittle when dry. Under load this coating will crack in a pattern which can be interpreted to indicate principle stress directions and stress concentrations. A photo-elastic technique uses a clear plastic model of the component. By viewing the loaded model through polarized light, lines or "fringes" become visible that also indicate the direction of the stresses and stress concentrations. Certain coatings will discolor in a manner that will later allow a determination of the maximum temperature to which the surface has been subjected if detrimentally high temperatures are suspected.

### **3.5.2 DYE PENETRATION**

A cleaned surface (paint must be removed) is treated with a fluorescent liquid that will penetrate cracks or discontinuities and make them visible under a black light. The whole process requires some skill and time to do properly and then will only display surface flaws. However, the results are immediate and the technique is highly portable.

### **3.5.3 MAGNETIC PARTICLES**

Also known by the brand name "Magnaflux", this technique requires the cleaned part to be treated with magnetic particles while it is magnetized. After further treatment, the flaws will be visible either under normal light or black light depending upon the particles used. Surface or near-surface flaws can be seen by this means but requires some equipment that can become bulky depending upon the size of the component to be inspected.

### **3.5.4 X-RAY**

Deep voids and flaws can be found in virtually any material through this process. Considerable skill and expensive equipment is required to produce and interpret the "shadow" photograph.

### **3.5.5 ULTRASONICS**

By passing a high frequency sound wave through a component the thickness can be measured by the return time of the sound wave as it bounces off of the far side of the part. Any flaw present within the part will also reflect the waves and produce a shorter return time. A flaw at any depth can be found very quickly but requires expensive equipment and a skilled operator.

### **3.5.6 EDDY CURRENT**

This method is restricted to metals and involves inducing an electrical current in the material. A flaw will disturb the current and this can be detected on a meter. Any part of the aircraft can be inspected if accessible but only a small area at a time. The method is highly portable and the equipment is inexpensive but some skill is required to perform the inspection properly.

## **3.6 DEFINITIONS**

**Brittleness** - measure of a material's lack of ductility.

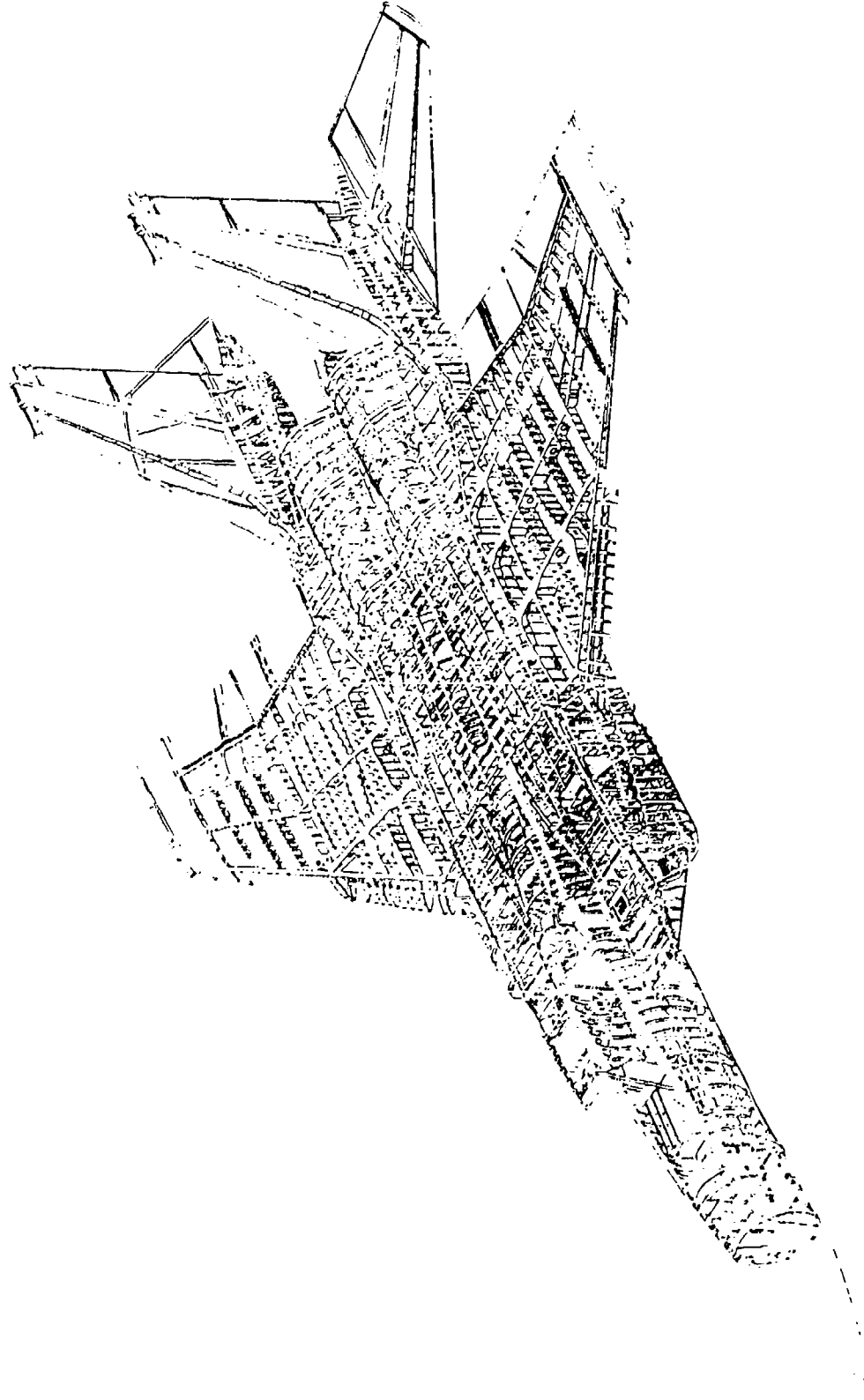
- Ductility** - ability of a material to deform without breaking.
- Durability** - ability to resist cracking, corrosion, thermal degradation, delamination, wear, and the effects of foreign object damage over time.
- Elasticity** - ability of a material to return to its undeformed shape after all loads have been removed.
- Plasticity** - deformation characteristics of a material beyond its elastic limit.
- Resilience** - a measure of the amount of energy a material can absorb elastically in a unit volume of the material.
- Strength** - ability to withstand external loads without failure.
- Toughness** - total energy absorbed before failure occurs.

## NOMENCLATURE

A	cross-sectional area
DLL	design limit load
E	Young's Modulus
e	strain
FEM	finite element modeling
G	Shear Modulus
L	length
N	number of loading cycles
NDI	non-destructive inspection
P	loads
S	applied stress
UTS	ultimate tensile strength
$\Delta$	increment of change
$\mu$	Poisson's Ratio
$\sigma$	stress
$\gamma$	shear strain
<sub>i</sub>	Subscripts
<sub>t</sub>	tension
<sub>w</sub>	compression

## REFERENCES

1. Dole, Charles E., *Fundamentals of Aircraft Material Factors*, University of Southern California, Los Angeles, California, 1987.
2. Military Specification Airplane Strength and Rigidity Reliability Requirements, Repeated Loads and Fatigue, MIL-A-00886B.
3. Military Specification Airplane Damage Tolerance Requirements, MIL-A-83444.
4. Military Specification Airplane Strength and Rigidity, Sonic Fatigue, MIL-A-008893.
5. *Aeroelasticity*, Chapter 12, Flying Qualities Theory and Flight Test Techniques, USAF Test Pilot School, Edwards AFB, California.



McDonnell-Douglas F-15A Structure

# CHAPTER 4.0

## BASIC STRUCTURAL DYNAMICS

### 4.1 INTRODUCTION

A real mechanical system, such an aircraft structure, can deform in practically infinite directions (called **degrees of freedom**), are constructed of nonhomogenous materials, are nonuniform in mass and material properties, and are acted upon (forced) by a wide spectrum of inputs of which many are random. To study and use the most dominant of the structure's dynamic properties and responses it is necessary to reduce the numerous uncertainties presented by these factors by neglecting the less significant of them and modeling the remainder in some empirical and tractable manner.

This chapter will provide you with basic knowledge to examine a structures problem in its most elemental form and yet still draw some useful engineering conclusions without man-months of costly and time-consuming computer analysis. It emphasizes concepts routinely used in structures flight testing and assumes an understanding of undergraduate dynamics.

### 4.2 BASIC SYSTEM ELEMENTS

Any structural material will have some elastic properties, including **stiffness**. This resistance to deformation does not mean that the material will not deform, even if not visibly. The stiffness, which can be thought of as a restoring force counteracting the applied force and seeking to return the structure to its original undeformed configuration, can be modeled as the force produced by a stretched spring. This is shown in Figure 4.1 and can be expressed as

$$F_s = k(x_2 - x_1) \quad (4.1)$$

where  $k$  is the **spring constant** and the  $x$ 's are the displacements shown. This equation is valid only for a material deforming within its linear **elastic range**, that is the range at which it will return to its undeformed shape after the load is discontinued (see Section 3.2.2).

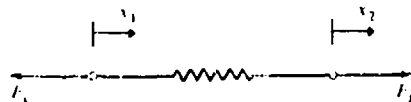


Figure 4.1 Basic Spring Element

The modeling element relating forces to velocities is the viscous damper like that shown in Figure 4.2 and expressed in the equation

$$F_d = c(\dot{x}_2 - \dot{x}_1) \quad (4.2)$$

where  $c$  is the coefficient of viscous damping. This equation is also only valid for a linear relationship. The damper can be thought of as a property that extracts energy from the system and resists an increase in displacement velocity and actually reduces it, eventually completely to zero in the unforced case. As the equation suggests, this **viscous damping** is proportional to velocity. Another type of damping, termed **proportional damping**, is a function of the mass and stiffness of the system. **Structural damping** (sometimes called **hysteretic damping**) is the result of internal friction and strain and is proportional to the displacement amplitude squared. Finally, **coulomb damping** is simply the friction that resists the motion of two bodies moving against each other, such as internal components of a structure. Only the viscous damping component this is modeled linearly and dealt with in this chapter.

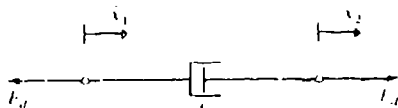


Figure 4.2 Basic Damper Element

Finally, elements of the structure can be modeled with "lump" or **point mass** (Figure 4.3). **Newton's Second Law of Motion** provides an expression for the inertial properties of this discrete mass, relating forces to accelerations

$$F_m = m\ddot{x} \quad (4.3)$$

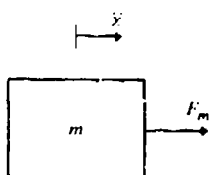


Figure 4.3 Basic Mass Element

For a simple bending case, the stiffness can be expressed as

$$EI = \text{constant} \quad (4.4)$$

where  $E$  is **Young's modulus** (Section 3.2.2) and  $I$  is the cross-sectional area moment of inertia. The equivalent spring constant can be derived in terms of these properties by starting from the basic relationship

$$k_{eq} = P/\delta \quad (4.5)$$

where  $P$  is the transverse load applied and  $\delta$  is the deflection of the object at the point of load application. For a simple torsion case, the stiffness can be expressed as

$$GJ = \text{constant} \quad (4.6)$$

where  $G$  is the **shear modulus** and  $J$  is the polar moment of inertia of the cross-section. An equivalent spring constant can be derived using these terms from the relationship

$$k_{eq} = M/\theta \quad (4.7)$$

where  $M$  is the applied torque and  $\theta$  is the angular displacement. These relationships are introduced because they reoccur repeatedly in structural analysis.

All of these discrete elements, except the point mass, are considered massless, and linear for small displacements. They can be combined in parallel and series with associated reduced equation forms such as those shown in Figure 4.4 (see Reference 3). These then are our most basic building blocks for modeling a structure.

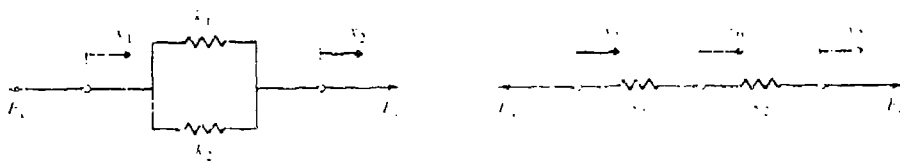


Figure 4.4 Example of Combined Basic Elements

### 4.3 SIMPLE SYSTEM MODELS

Consider the case of a mass free to move in one direction (a **single degree of freedom** or SDOF) but with some stiffness and damping. Such a system can be modeled as shown in Figure 4.5 with a force applied as well as gravity acting on the mass. A free body diagram of this problem (Figure 4.6) shows that a sum of forces written in their equivalent elemental model form would be

$$F = m\ddot{x} + c\dot{x} + kx + mg \quad (4.8)$$

where  $g$  is the acceleration of gravity. If the analysis is started from the equilibrium or static condition (the  $x_{eq}$  displacement shown in Figure 4.5) then a  $-kx$  term will exactly cancel the  $mg$  term. Therefore, if the displacement of the mass is consistently measured from the static equilibrium position, the system can be expressed as shown in equation 4.9, here given as a function of time

$$F(t) = m\ddot{x}(t) + c\dot{x}(t) + kx(t) \quad (4.9)$$

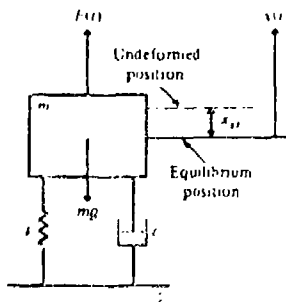


Figure 4.5 Example Structural Model

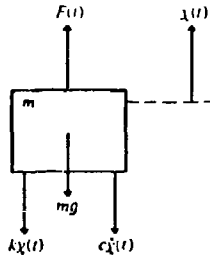


Figure 4.6 Free-Body Diagram of Figure 4.5

### 4.3.1 FREE RESPONSE CASE

For the unforced case, and after dividing 4.9 through by  $m$ ,

$$0 = \ddot{x} + ax + bx \quad (4.10)$$

This is a second order, linear, homogeneous differential equation of motion of the mass, called a **spring-mass-damper system**. One can easily see that if the mass is disturbed and then allowed to respond freely, it will oscillate about its equilibrium position due to the action of the spring. The oscillation will be at one frequency typical of that system, which we call the **damped natural frequency** ( $\omega_d$ ). This motion will eventually reduce to zero as a result of the damper action.

It can be observed that the amplitude of the motion damps out exponentially. Therefore, for small displacements, the displacement can be assumed to be of the form

$$x(t) = Ae^{st} \quad (4.11)$$

where  $A$  is some amplitude and  $s$  is the Laplace variable. Substituting this term into the general equation (4.10), the characteristic equation for the system is arrived at, or

$$0 = s^2 + as + b \quad (4.12)$$

and  $s$  now represents the roots of this equation. It is convenient to define some useful parameters.

$$\omega_n^2 = k/m \quad (4.13)$$

called the **undamped natural frequency**, or the oscillatory frequency for the same system without damping. The damped natural frequency is related to this by

$$\omega_d = \omega_n \sqrt{1 - \zeta^2} \quad (4.14)$$

where

$$\zeta = \frac{c}{2m\omega_n} \quad (4.15)$$

and is called the **viscous damping factor**. This can also be expressed as a ratio (**the damping ratio**)

$$\zeta = \frac{c}{c_r} \quad (4.16)$$

where  $c$  is the damping present in the system and  $c_r$  is the **critical damping coefficient**, or the highest damping that will still produce oscillatory motion. Also,

$$\tau = \frac{c}{k} \quad (4.17)$$

is termed the **time constant** and defines the speed of return of the system to equilibrium.

Applying equations 4.13 and 4.15 to equation 4.12, it now becomes

$$0 = s^2 + 2\zeta\omega_n s + \omega_n^2 \quad (4.18)$$

This equation has two roots

$$s_1, s_2 = \omega_n (-\zeta \pm \sqrt{\zeta^2 - 1}) \quad (4.19)$$

If the damping factor ( $\zeta$ ) is greater than 1 the roots will be real and the system is termed **overdamped**. This means that once disturbed and allowed to respond freely, the system will return to equilibrium quickly without overshoots or oscillation, as shown in Figure 4.7. This is also called a **deadbeat response**. If the damping factor is between 0 and 1 then the roots will be imaginary and the system will be **underdamped**. This means that the system will oscillate about the equilibrium condition, with the motion slowly decaying to zero (see Figure 4.8). For  $\zeta = 0$ , the **undamped** or neutrally damped case is obtained in which the system will continue to oscillate indefinitely at the same amplitude without decaying (Figure 4.9). For  $\zeta$  less than 0 an unstable system with oscillations increasing in amplitude with time, called **divergence** (Figure 4.10), is created. Naturally, the amplitude will quickly reach magnitudes that exceed the elastic restoring ability of the structure's material and structural failure will result.

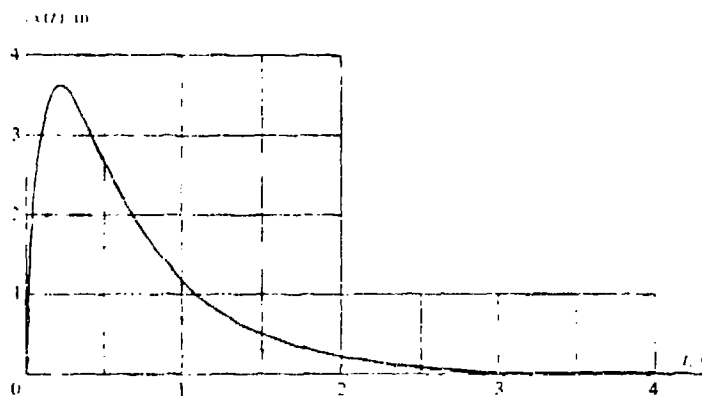


Figure 4.7 Example of an Over-Damped Displacement Response

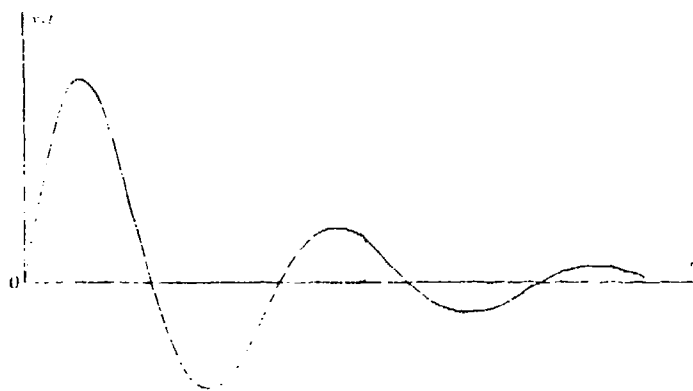


Figure 4.8 Example of an Under-Damped Displacement Response

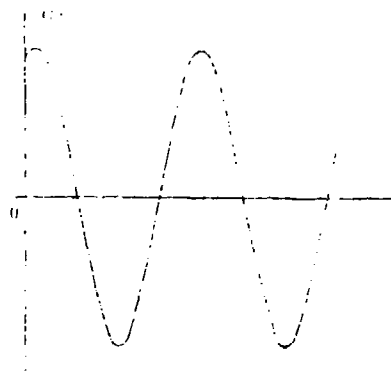


Figure 4.9 Example of an Undamped Displacement Response

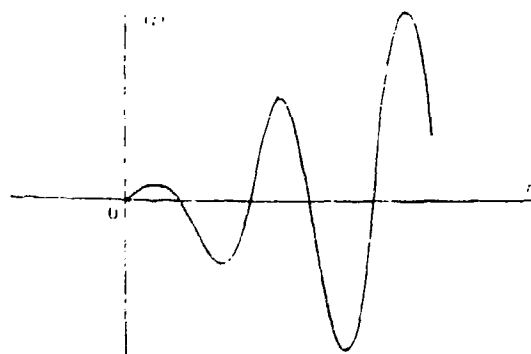


Figure 4.10 Example of a Divergent Displacement Response

### 4.3.2 FORCED RESPONSE CASE

A forced system is a system disturbed by some external excitation. The disturbance can be in the form of some initial displacement or velocity, or as an applied force. Since idealized linear systems modeled as differential equations have been assumed, the response to initial conditions (**transient response** or the homogenous solution) and the forced response (**steady-state case** or the particular solution) can be solved separately and combined through superposition for an expression of the total motion.

For the forced motion case equation 4.9 is returned to and the same substitutions made for equation 4.18 are inserted. At the same time, a **harmonic excitation** can be assumed of the form

$$F(t) = \omega_n^2 m A \cos(\omega t) \quad (4.20)$$

where  $\omega$  is the frequency of the input. The reason that the harmonic forcing function is of importance is the possibility of this oscillatory input occurring at the natural frequency of the system. The importance of this will be explained shortly. The nonhomogeneous equation has now been developed of the form

$$\omega_n^2 A \cos(\omega t) = \ddot{x}(t) + 2\zeta\omega_n \dot{x}(t) + \omega_n^2 x(t) \quad (4.21)$$

If we also assume that the steady-state or harmonic response solution will have the form

$$x(t) = C_1 \sin(\omega t) + C_2 \cos(\omega t) \quad (4.22)$$

or, after substitution and manipulation (see Reference 3)

$$x(t) = X(\omega) \cos(\omega t - \phi) \quad (4.23)$$

where

$$X(\omega) = \frac{A}{\sqrt{[1 - (\omega/\omega_n)^2]^2 + (2\zeta\omega/\omega_n)^2}} \quad (4.24)$$

and the **phase angle** is

$$\phi = \tan^{-1} \left\{ \frac{2\zeta\omega/\omega_n}{1 - (\omega/\omega_n)^2} \right\} \quad (4.25)$$

The steady-state response can also be expressed in the complex exponential form as

$$x(t) = X(i\omega) e^{i\omega t} \quad (4.26)$$

However, the formulation in 4.23 will be retained.

All the tools needed to examine the important system responses to a harmonic excitation are now in hand. Figure 4.11 shows how the system amplitude (expressed as  $X(\omega)/A$  or transmissibility) will react as the excitation frequency approaches the natural frequency of the system. It can be seen that the amplitude of the response increases as the two frequencies approach each other. When they are identical the amplitude is the greatest and, with no damping present, the motion will sustain itself indefinitely. This is the undamped case discussed in the previous

section. The coalescence of the natural frequency and the excitation frequency is called the **resonance case**. A structure will have an infinite number of such resonant frequencies or **modes**, although only the first few are usually of importance. The equation of motion is no longer valid at resonance, but this is seldom of interest in real applications. Suffice it to say that the magnitude of the response will grow without bound. The peak responses at all other conditions will occur at

$$\omega = \omega_n \sqrt{1 - 2\zeta^2} \quad (4.27)$$

At frequencies less than the resonance the response is governed by stiffness or restoring forces. At the resonance all of the restoring forces result from damping only. At frequencies above the resonance the motion is dominated by the inertia or mass.

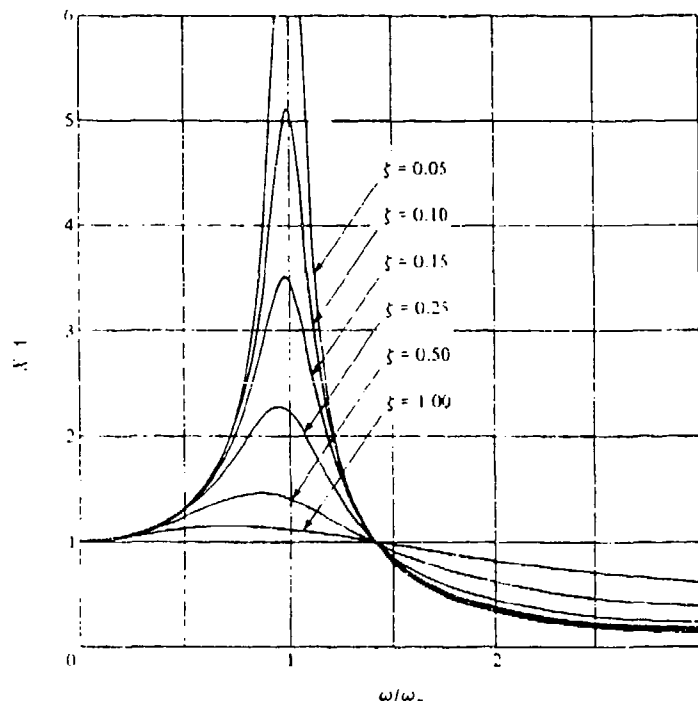


Figure 4.11 Typical Magnitude Response Showing Effect of Resonance and Damping

The phase angle is an expression of the difference between the peaks of the force and the response, as shown in Figure 4.12 where both have the same frequency. The **period** of the oscillation ( $T$ ) is defined as

$$T = \frac{2\pi}{\omega_n} \quad (4.28)$$

( $\omega_n$  in rad/sec) and is the time to complete one cycle of the motion such as positive peak to positive peak. The reciprocal of equation 4.28 is just the natural frequency in cycles per second (Hertz or Hz) rather than radians per second. Figure 4.13 shows that at resonance the phase angle is always 90 degrees (said to be out of phase 90 deg., or  $\pi/2$ ). At 0 phase angle the two waveforms are exactly in phase and are moving in the same direction. At 180 deg, they are exactly out of phase and are moving in different directions, that is, the maximum positive peak of one wave occurs at the same time as the maximum negative peak of the other.

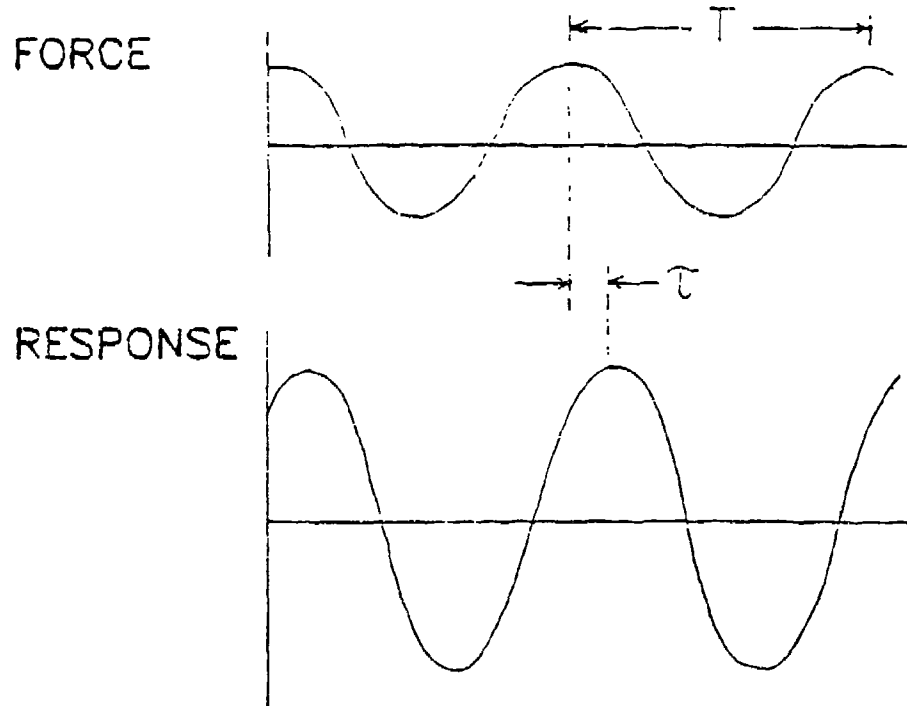


Figure 4.12 Definition of Phase Angle

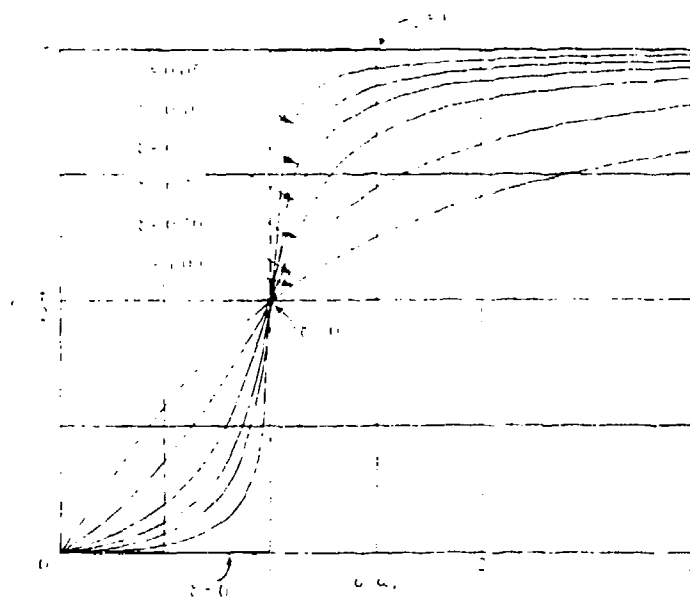


Figure 4.13 Typical Phase Angle Response Showing Effect of Resonance and Damping

This section has focused on a single degree of freedom system only and used only one analysis method with one type of forcing function so that basic concepts could be easily illustrated. In fact, **multiple degree of freedom system (MDOF)** is the norm and will be dealt with later in the chapter. There are certain energy approaches to mechanical systems analysis, particularly using **Hamilton's Principle** and the **Lagrangian**. The **Fourier Series** and **Laplace** methods are also popular ways of analyzing these structures. The response to a unit step function or a random input (analyzed with a convolution integral) are also very useful. Readers are encouraged to follow-up on these areas to round out their understanding of structural dynamics.

## 4.4 SUPPLEMENTAL CONCEPTS

### 4.4.1 RESPONSE RELATIONSHIPS

It is important for you to understand the relationship between the different system responses. So far only displacement has been discussed, but velocity and acceleration can be addressed as well.

Recall that velocity is just the time derivative of displacement, and acceleration is the time derivative of velocity. In the last section, an expression for the displacement of the spring-mass-damper system that was a function of cosine (equation 4.23) was developed. Differentiating this once will produce a sine function with the amplitude increased because of the product of the original amplitude and the frequency of the input function. This velocity expression can be differentiated again with similar results but with the function once again becoming a cosine but now with a sign change. The result of these operations are illustrated in Figure 4.14.

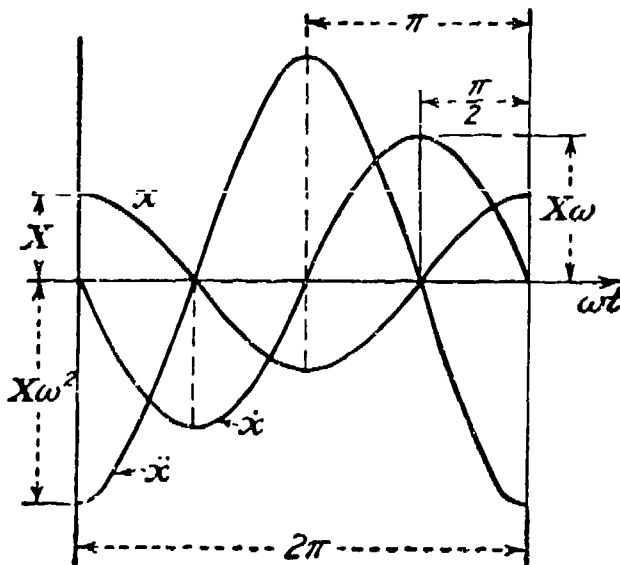


Figure 4.14 Relationship of Displacement, Velocity, and Acceleration

If the first peak of each of the waveforms is allowed in Figure 4.14, it can be seen that from displacement to velocity there was a 90 degree phase shift, and from velocity to acceleration yet another 90 degree shift as well as the sign change (or 180 degrees from displacement). In the case of the resonance condition discussed at the end of the last section, the displacement is 90 deg out of phase with the forcing function but the velocity is exactly in phase (phase angle of 0). This is the condition of maximum response of the oscillating system.

Several specific force/response relationships have been established and may be encountered on occasion.

$$\text{Accelerance or Inertance} = \text{Acceleration}/\text{force} \quad (4.29)$$

$$\text{Effective or Apparent Mass} = 1/\text{Accelerance} \quad (4.30)$$

$$\text{Mobility} = \text{Velocity}/\text{Force} \quad (4.31)$$

$$\text{Impedance} = 1/\text{Mobility} \quad (4.32)$$

$$\text{Dynamic Compliance} = \text{Displacement}/\text{Force} \quad (4.33)$$

$$\text{Dynamic or Apparent Stiffness} = 1/\text{Dynamic Compliance} \quad (4.34)$$

For a pure, undamped sinusoidal motion it is possible to derive peak (versus peak-to-peak) velocity and displacement from acceleration and frequency alone without an equation of motion. This is really just a unit conversion and can be shown graphically in Figure 4.15 or stated mathematically,

$$x_p (\text{inches}) = 9.780 \frac{\ddot{x}}{\omega^2} \quad (4.35)$$

$$\dot{x}_p (\text{inches/sec}) = 61.42 \frac{\ddot{x}}{\omega} \quad (4.36)$$

where the acceleration is in g's, frequency is in Hz, and the subscript P indicates peak response. The value of this in flight testing is that it allows the determination of maximum displacement and velocity at an accelerometer response location if it appears to be excited by a single-degree-of-freedom undamped sinusoid. A case in point may be a vertical tail vibrating from side to side as the result of a vortex impinging on it during high angle-of-attack flight. The response of an accelerometer mounted at the tip of the surface would probably show a nearly repeatable peak acceleration at one dominant frequency. If the load (i.e. stress) in the tail is of concern but it has not been instrumented to provide this data, deriving the peak displacement will provide at least one indicator of how great a load is acting on the structure.

#### 4.4.2 COMPLEX MODES

The discussion so far has assumed only proportional damping is playing a role and modeled it as viscous damping. This also implies that the phase at any point is either zero or 180 degrees. The result is a "real mode" in which the shape is that of a standing wave. In truth, other damping and nonlinearities produce more of a traveling wave in which the phase can be other than 0 or 180 deg, and all points do not reach maximum deflection at the same time. This is termed a **complex mode**. Where the damping is light, as in aircraft structures, the proportional damping

180 deg, and all points do not reach maximum deflection at the same time. This is termed a **complex mode**. Where the damping is light, as in aircraft structures, the proportional damping assumption will generally yield adequate approximations to the modal parameters for practical purposes.

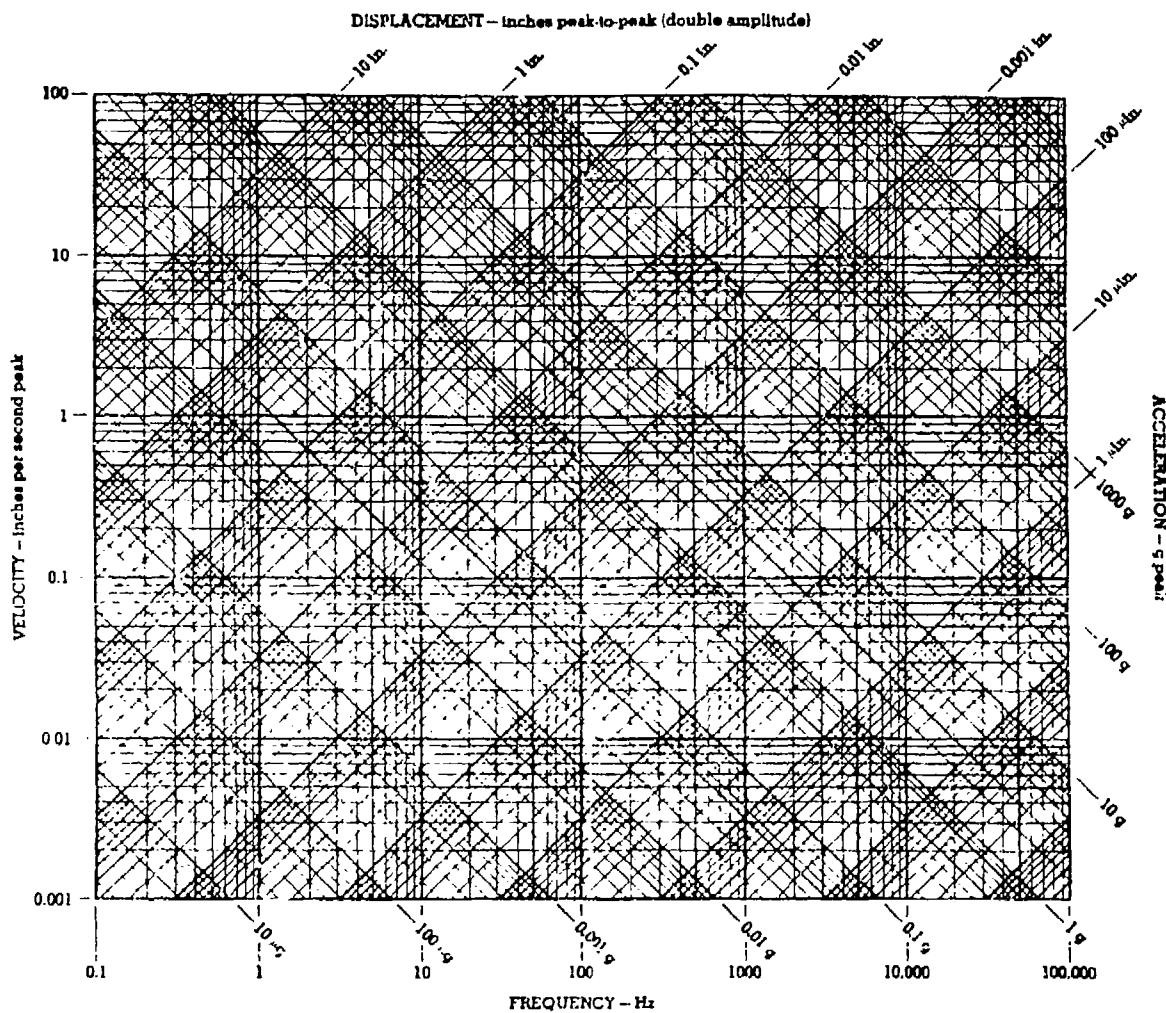


Figure 4.15 Vibration Nomograph for Sinusoidal Motion

#### 4.4.3 BEATING

When two waveforms with nearly identical frequencies are summed, a result like that shown in Figure 4.16 occurs. This effect becomes difficult to perceive if the lower frequency is less than about 85 percent of the higher frequency. In real mechanical systems this "beating" may even be audible as a warbling tone. This effect is important to understand because it indicates an approaching resonance condition with the large amplitudes that result. The frequency of the beat response shown by the dotted line in the figure (indicated by the period shown) is just the difference of the two original waveform frequencies.

#### **4.4.4 HARMONICS**

Often encountered are frequencies which are an integer multiples of some initial frequency (the fundamental). These integer multiples are called harmonics or overtones. The fundamental is the first harmonic, the first integral multiple the second harmonic, and so on. When a structure is observed to respond at fixed frequency intervals, twice some fundamental, three times, four times, and so on, harmonics should be suspected.

#### **4.4.5 JUMP PHENOMENA**

Figure 4.17 illustrates a curious effect that, while rare, is not unknown in the real world of nonlinear, damped systems. The figure shows that it is possible for the system to have more than one response amplitude at the same frequency.

As the frequency is increased, the amplitude approaches point 1 and "jumps" to point 2 for higher frequencies. If this effect were observed in a laboratory setup then there would be a sudden drop in displacement amplitude (for example) with little change in frequency. When decreasing frequency to point 3, the response would suddenly jump up to the point 4 amplitude. The area between point 1 and 3 is never traversed and is considered unstable. This phenomenon is very important in ground vibration tests and is the basis of nonlinearity checks (see Section 7.9).

### **4.5 MODAL ANALYSIS**

#### **4.5.1 MULTI-DEGREE OF FREEDOM SYSTEMS**

A real structure with many parts can be modeled with each part represented by a single mass attached to adjoining masses with springs and dampers. Even a simple beam with distributed mass and material properties can be broken down into such discrete elements. Each of these elemental masses can move relative to all the others but not without influencing the others. The motion of the masses are then said to be **coupled**. This relative motion requires a degree of freedom for each mass if the motion of the entire system is to be expressed mathematically. An example of such a multi-degree of freedom system is shown in Figure 4.18. As before, the system is still being simplified considerably to keep the mathematics from getting out of hand.

An equation of motion can be written for each of the masses in Figure 4.18 using the approach outlined in Sections 4.2 and 4.3. For the three masses, each excited by a separate force, the following series of equations can be formulated .

$$\begin{aligned} Q_1 &= m_1 \ddot{q}_1 + (c_1 + c_2) \dot{q}_1 - c_2 \dot{q}_2 + (k_1 + k_2) q_1 - k_2 q_2 \\ Q_2 &= m_2 \ddot{q}_2 - c_2 q_1 + (c_2 + c_3) \dot{q}_2 - c_3 \dot{q}_3 - k_2 q_1 + (k_2 + k_3) q_2 - k_3 q_3 \\ Q_3 &= m_3 \ddot{q}_3 - c_3 \dot{q}_2 + c_3 \dot{q}_3 - k_3 q_2 + k_3 q_3 \end{aligned} \quad (4.37)$$

where  $Q$  is the applied force and  $q$  the coordinate of the model component related to the real structure. The coefficients of this equation can be collected into three matrices; the **inertia or mass matrix** [ $\mathbf{m}$ ], the **damping matrix** [ $\mathbf{c}$ ], and the **stiffness matrix** [ $\mathbf{k}$ ], as shown below in equations 4.38 through 4.40.

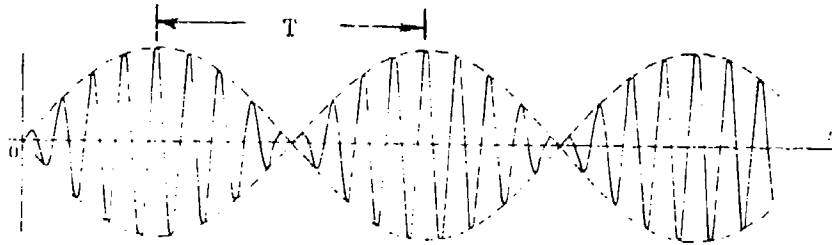


Figure 4.16 The Beating Phenomena

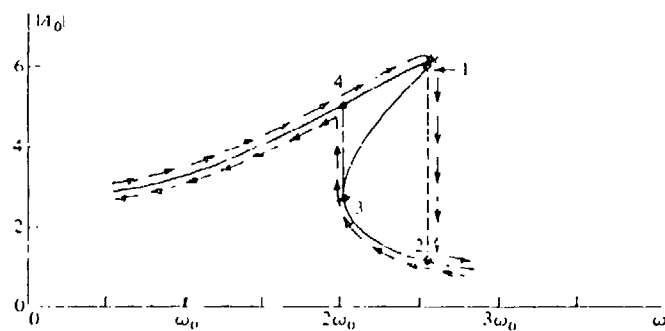


Figure 4.17 The Jump Phenomena

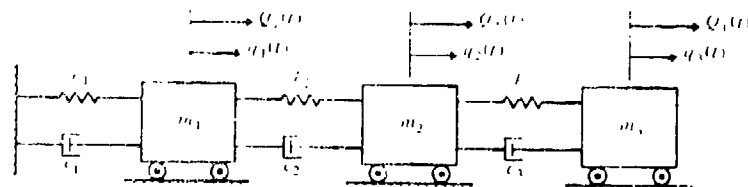


Figure 4.18 Example Multidegree of Freedom System

$$[m] = \begin{bmatrix} m_1 & 0 & 0 \\ 0 & m_2 & 0 \\ 0 & 0 & m_3 \end{bmatrix} \quad (4.38)$$

$$[c] = \begin{bmatrix} c_1 + c_2 & -c_2 & 0 \\ -c_2 & c_2 + c_3 & -c_3 \\ 0 & -c_3 & c_3 \end{bmatrix} \quad (4.39)$$

$$[K] = \begin{bmatrix} k_1 + k_2 & -k_2 & 0 \\ -k_2 & k_2 + k_3 & -k_3 \\ 0 & -k_3 & k_3 \end{bmatrix} \quad (4.40)$$

The system's equation of motion can now be written as

$$\{Q(t)\} = [m]\{\ddot{q}(t)\} + [c]\{\dot{q}(t)\} + [k]\{q(t)\} \quad (4.41)$$

where the **generalized coordinate array**  $\{q(t)\}$  and the force array  $\{Q(t)\}$  are

$$\{q(t)\} = \begin{Bmatrix} q_1(t) \\ q_2(t) \\ q_3(t) \end{Bmatrix} \quad (4.42)$$

$$\{Q(t)\} = \begin{Bmatrix} Q_1(t) \\ Q_2(t) \\ Q_3(t) \end{Bmatrix} \quad (4.43)$$

The stiffness matrix can be considered as an **influence coefficient matrix**. That is, any element  $k_{ij}$  expresses the force needed at coordinate  $q_i$  for a unit displacement at  $q_j$ , with all other displacements equal to zero. The inverse of the stiffness matrix is called the **flexibility matrix**

$$[a] = [k]^{-1} \quad (4.44)$$

Any  $a_{ij}$  expresses the displacement needed at coordinate  $q_i$  for a unit force at  $q_j$ .

#### **4.5.2 COORDINATE TRANSFORMATION AND SOLUTION**

If an expression that provides only the motion of one mode of the coupled system (one of the natural frequencies) is sought, it will be necessary to decouple the equations. This is done by changing the coordinates to another in which equation 4.41 will be naturally decoupled, with each of the coefficient matrices diagonalized. The coordinates can be transformed to the new coordinates,  $\eta_j(t)$  by use of a square transformation matrix  $[u]$ .

$$\{q(t)\} = [u]\{\eta(t)\} \quad (4.45)$$

with derivatives

$$\{\dot{q}(t)\} = [u]\{\dot{\eta}(t)\} \quad (4.46)$$

$$\{\ddot{q}(t)\} = [u]\{\ddot{\eta}(t)\} \quad (4.47)$$

When these equations are applied to the equation of motion, the coefficient matrices will be post-multiplied by the transformation matrix. Both sides of the equation can also be multiplied by the transpose of the transformation matrix at the same time without loss of generality. This is equivalent to pre-multiplying the coefficient matrices, or

$$[M] = [u]^T [m] [u] \quad (4.48)$$

and likewise for the damping and stiffness matrices. Also

$$\{N(t)\} = [u]^T \{Q(t)\} \quad (4.49)$$

is the generalized forces associated with the new generalized coordinates. The transformation matrix that makes the coefficient matrices diagonal (decoupled) is termed the **modal matrix** and the coordinates  $\eta_j(t)$  are called the **natural or principal coordinates**. Such a transformation matrix is said to be **orthogonal**. The resulting coefficient matrices are now **modal mass ( $M$ )**, **modal stiffness ( $K$ )**, and **modal damping ( $C$ )** matrices.

If the transformation matrix had the effect of reducing the mass matrix to the identity matrix, that is

$$[U]^T [m] [U] = [I] = \begin{bmatrix} 1 & 0 & 0 \\ 0 & 1 & 0 \\ 0 & 0 & 1 \end{bmatrix} \quad (4.50)$$

then the transformation is termed **orthogonal**. It is this relationship that is used to solve for the actual values of the elements of the transformation matrix. For such a transformation the final matrix equation of motion has the form

$$\{N\} = [I]\{\ddot{\eta}\} + [C]\{\dot{\eta}\} + [K]\{\eta\} \quad (4.51)$$

or, since the equations are now decoupled and the matrices are diagonalized, only one equation at a time need be referenced. The equations would have the general form of

$$N_r = \ddot{\eta}_r + 2\zeta_r \omega_r \dot{\eta}_r + \omega_r^2 \eta_r \quad (4.52)$$

where  $r = 1, 2, 3, \dots$ , for each mode or resonant frequency, one equation for each. This implies that the elements on the main diagonal of the orthogonal modal damping matrix are of the form  $2\zeta_r \omega_r$  and the elements on the diagonal of the orthogonal stiffness matrix are  $\omega_r^2$ . The natural frequencies and damping coefficient of each mode can now be easily derive. But what modes are they? Examine the modal matrix again.

The modal matrix has some important properties. The columns of the matrix are the mode shapes of the system. An example of a mode shape for a five degree of freedom system is

$$\begin{Bmatrix} 0.02 \\ 0.12 \\ 0.79 \\ 1.33 \\ 2.67 \end{Bmatrix}$$

The values in the column are not unique, only their amplitude relative to each other, or between columns. Therefore, the vector can be presenting it in a normalized form.

$$\begin{pmatrix} 0.01 \\ 0.04 \\ 0.30 \\ 0.50 \\ 1.00 \end{pmatrix}$$

For a simple cantilever beam, each of these numbers correspond to a point on the beam at which an imaginary concentrated mass was centered for the purpose of the analysis. The numbers give the magnitude of the displacement at each of the masses as shown in Figure 4.19 for the resonant frequency or mode. The first mode shown in the figure is called first bending. Other cantilever beam modes are also shown. Each will have its own unique resonant frequency. Such mode shapes or normal modes (natural modes or characteristic modes) are typically displayed in an exaggerated form so that the shape can easily be identified. Where the displaced shape crosses the undisturbed centerline indicating zero displacement (although rotation occurs there) is termed a node or antiresonance, and where the shape is at a maximum displacement is termed an antinode or resonance point. Note that the number of nodes corresponds to the order of the mode, that is third bending has three nodes (including the fixed end).

This development has been necessarily abbreviated and simplified for the purpose of illustration. A more complete development would normally include a discussion of the undamped and unforced case which is solved as an eigenvalue problem, with the eigenvalues supplying the natural frequencies and the eigenvectors the mode shapes. There are other techniques in which the analyst makes a careful guess at the mode shape and then solves for the associated frequency. The method may involve an iteration process for convergence to the correct solution. These are the Matrix Iteration and Raleigh Quotient methods. The methods may use the dynamical matrix, defined as

$$[D] = [m]/[k] = [m][a] \quad (4.53)$$

Energy methods can also be applied to multi-degree of freedom systems. Modal analysis today is commonly done with finite element analysis, as described in Section 3.2.3.

## NOMENCLATURE

A	amplitude
a	constant, flexibility matrix
b	constant
c	constant, coefficient of viscous damping
c <sub>r</sub>	critical damping coefficient
D	dynamical matrix
DOF	degree of freedom
deg	degrees
E	Young's Modulus
e	exponential constant
F	force
G	shear modulus
g	acceleration due to gravity
Hz	Hertz
I	cross-sectional area moment of inertia, identity

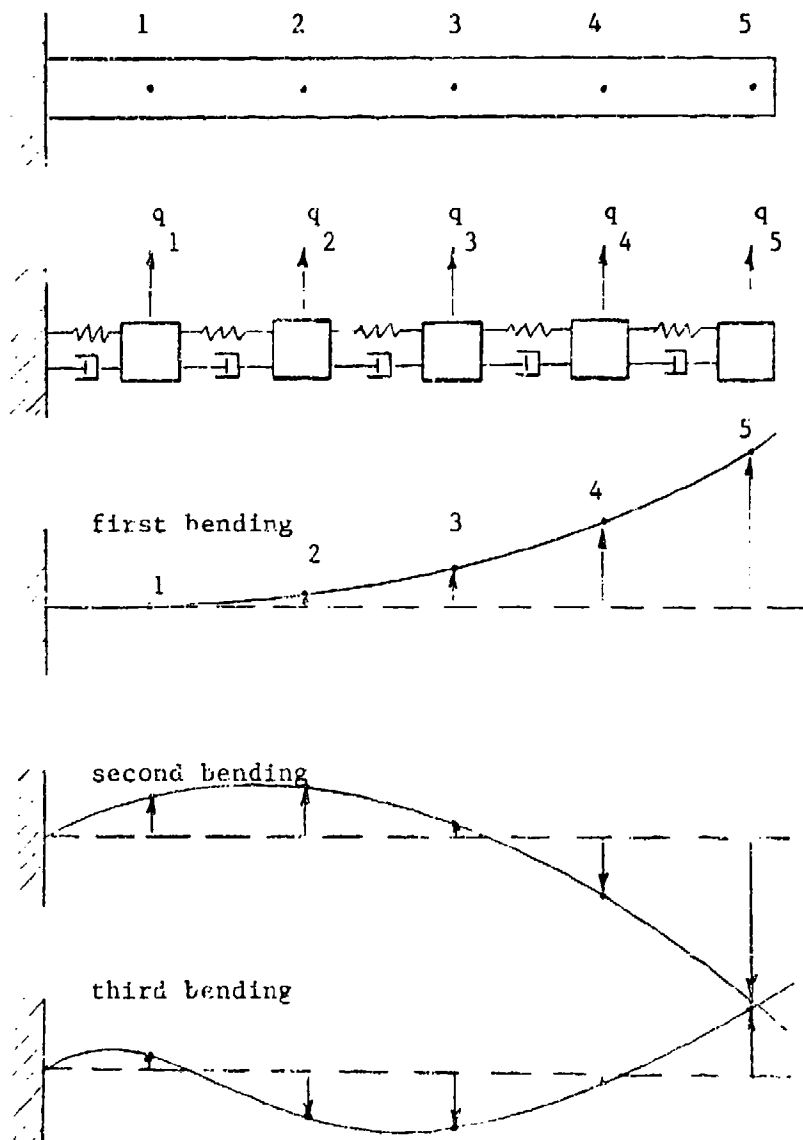


Figure 4.19 Beam Bending Problem with Mode Shapes

i	imaginary number
J	cross-sectional polar moment of inertia
k	spring constant
M	applied torque, generalized mass
MDOF	multiple degree of freedom
m	mass
N	generalized force
P	load
Q	force
q	coordinate
rad	radians
s	roots
sec	seconds
T	period of oscillation
t	time
u	transformation matrix
x	displacement
$\delta$	deflection at point of application
$\zeta$	viscous damping factor
$\eta$	transformed coordinate
$\theta$	angular placement
$\omega$	frequency
$\phi$	phase angle
$\tau$	time constant
K	modal stiffness
M	modal mass
C	modal damping
$\pi$	pi
	Subscripts
d	damper, damped
eq	equivalent
i	matrix column counter
j	matrix row counter
m	mass
n	natural
p	peak
r	mode or DOF counter
s	spring
st	static
	Superscripts
.	first derivative
..	second derivative

## REFERENCES

1. Hartog, J.P. Den, *Mechanical Vibrations*, Dover Publications, New York, New York, 1984.
2. Jacobsen, Ludik S. and Ayre, Robert S., *Engineering Vibrations*, McGraw-Hill Book Company, New York, New York, 1958.
3. Meirovitch, Leonard, *Elements of Vibration Analysis*, McGraw-Hill Book Company, New York, New York, 1986.

4. Meirovitch, Leonard, *Analytical Methods in Vibrations*, Macmillan Publishing Company, New York, New York, 1967.
5. Myklestad, N.O., *Vibration Analysis*, McGraw-Hill Book Company, New York, New York, 1944.
6. Lang, George F., *Understanding Vibration Measurements*, Application Note 9, Rockland Scientific Corporation, Rockleigh, New Jersey, December 1978.
7. *The Fundamentals of Modal Testing*, Application Note 243-3, Hewlett-Packard Company, Palo Alto, California, 1986.

# CHAPTER 5.0

## LOADS

### 5.1 INTRODUCTION

Aircraft are carefully designed for light weight but great strength. Its structure is subjected to an almost infinite variety of forces or loads distributed throughout it. These include:

- |                            |  |
|----------------------------|--|
| <b>Airloads</b>            | - external pressure gradients created by passage through the air.  |
| <b>Inertia Loads</b>       | - the dead weight of structural and non-structural mass (fuel, payload, engines) which can increase with acceleration. |
| <b>Reaction Loads</b>      | - static loads such as from resting on landing gear, towing, jacking and hoisting.                                     |
| <b>Live Loads</b>          | - thrust, arrestment, store separation, gun fire, etc.   |
| <b>Environmental Loads</b> | - cabin pressurization, thermal gradients, etc.  |

The loads can be further categorized as:

- |                       |   |
|-----------------------|---|
| <b>External Loads</b> | - requiring prediction of the aerodynamic forces, landing impact, taxi reactions, etc.  |
| <b>Internal Loads</b> | - requiring evaluation of load paths and stresses within the structure from external loads, and reactions from such things as thrust transmitted to the airframe. |

The magnitude of these loads can be surprisingly high. Such loads the design process particularly challenging and requires flight testing to verify that the aircraft can perform its assigned tasks without structural failure.

The principle objective of flight loads testing is to validate the mathematical model used in the design of the aircraft by checking the loads or strains at several vital points on the machine. It also provides a controlled and safe buildup to the **flight operating limits (FOL)** of the machine and its components to verify that they can withstand the conditions without failure and provide a safe margin on the design limit loads. These might include such things as bending and torsion loads at a couple of locations in the wing and vertical tail, stabilator pivot loads, gear compression and drag loads, mid fuselage bending moment, etc. It is impractical to verify the strength of every component of the plane and, from a safety point of view, is unnecessary. Less critical components are suitably checked during ground loads testing and routine inspections. Flight loads test data may also be compared with analytical results to validate fatigue trends and service life predictions.

The advent of the fly-by-wire aircraft (see Section 2.3.3) has added a new twist to flight loads testing. Critical loads distributions and load protection may be closely tied to the flight

control system (FCS). Thus, changes to the FCS and the resulting maneuver load changes may require further flight testing to evaluate the structural impact.

## 5.2 MANEUVER LOADS

Flight maneuvers can produce structural loads in any of the three aircraft axes (see Section 2.3.1). The vertical (normal) axis is the most common for maneuvering. The load in this axis, termed the **normal load**, is produced by lift force and inertia (vertical accelerations). An example of normal load is shown in Figure 5.1 for an aircraft in a level (constant altitude) turn. The **normal load factor ( $n_z$ )** is defined as the lift force ( $L$ ) divided by the gross weight ( $W$ ) of the aircraft, and can be related to the bank angle ( $\phi$ ) shown in Figure 5.1.

$$n_z = 1/\cos \phi = L/W \quad (5.1)$$

The maximum load factor achievable at any airspeed and weight would occur at the maximum lift for that speed. This would be, using the equation 2.12

$$L_{\max} = C_{L\max} q S \quad (5.2)$$

A similar equation can be written for lift equal to the gross weight except that the airspeed would be at the stall speed. Combining such an equation with 5.2 gives an expression for the maximum load factor in terms of airspeeds, or

$$n_{\max} = (V/V_s)^2 \quad (5.3)$$

The maximum or **limit load factor** is generally driven by mission requirements. Fighter, attack, and trainer aircraft generally require -3.0 to 7.33 or 9.0 g's normal acceleration while large transport or long-range patrol aircraft require only about -1.0 to +3.0 g's. **Asymmetric normal loads** are produced by aircraft roll or asymmetric store configurations and can be important for the loads at the wing attachment, the fuselage structure, the vertical tail(s) as well as store pylons and attachments.

It is important to understand that maximum normal load factor is not directly analogous to structural **limit load** (see Section 3.2.3). Also, a maximum acceleration turn will not likely produce the maximum vertical tail load or any number of other critical loads. Load factor is used because it is so easily measured and displayed to pilots and because it has immediate meaning to them because they feel this load directly. Some aircraft have an **Overload Warning System (OWS)** that automatically warns the pilot when the aircraft is near its normal load limit (a cockpit tone or verbal message), and even a g-limiter system that prevents the pilot from commanding more load than is recommended. **Side loads** generated in yaw maneuvers (see Figure 5.2) are generally limited by control deflection limitations (full rudder deflection) to avoid over-loads to the vertical tail, gear doors, etc. All of these limits vary as a function of aircraft external configuration and weight.

Because of the criticality of normal load factor, flight manuals normally contain a **V-n** (or **V-g**) **diagram** like that shown in Figure 5.3. The point labeled as A in the figure is referred to as the "corner" point or **maneuver speed** and represents the speed at which the pilot may command the tightest turn (highest load factor and smallest radius). Figure 5.4 shows how some of the maximum load conditions relate to the V-n ( $N_z$  for the figure) for one particular aircraft. Often more than one such diagram is given, one for each aircraft configuration such as heavy weight (fuel and stores), landing configuration (gear and flaps extended), various altitudes, etc.

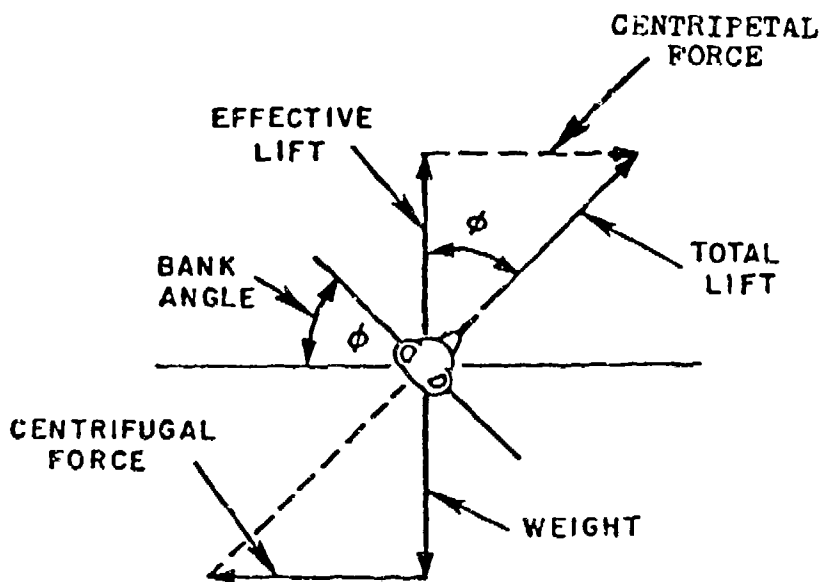


Figure 5.1 Forces Acting on an Aircraft in a Level Turn

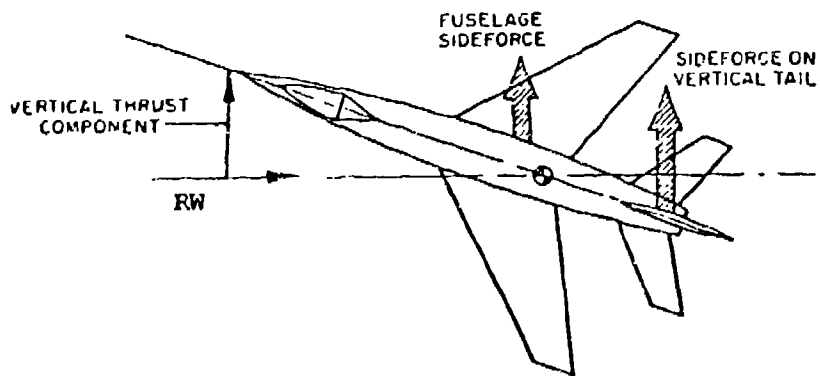


Figure 5.2 Forces Acting in a 90° Roll Attitude

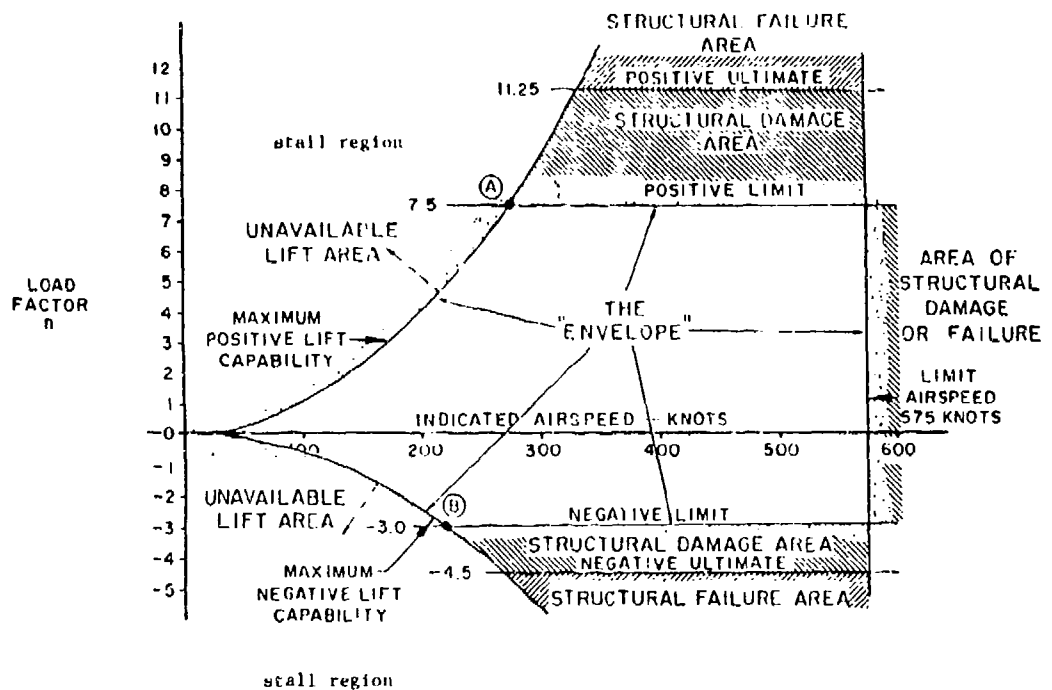


Figure 5.3 Significance of the V-n Diagram

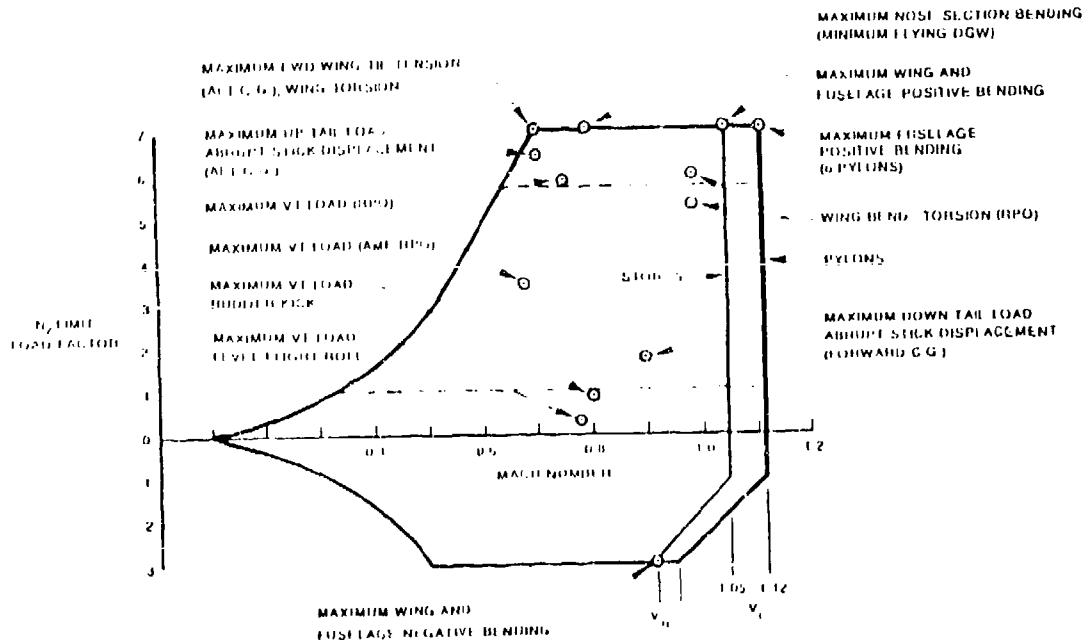


Figure 5.4 Example Maximum Loads Related to V-n Plot

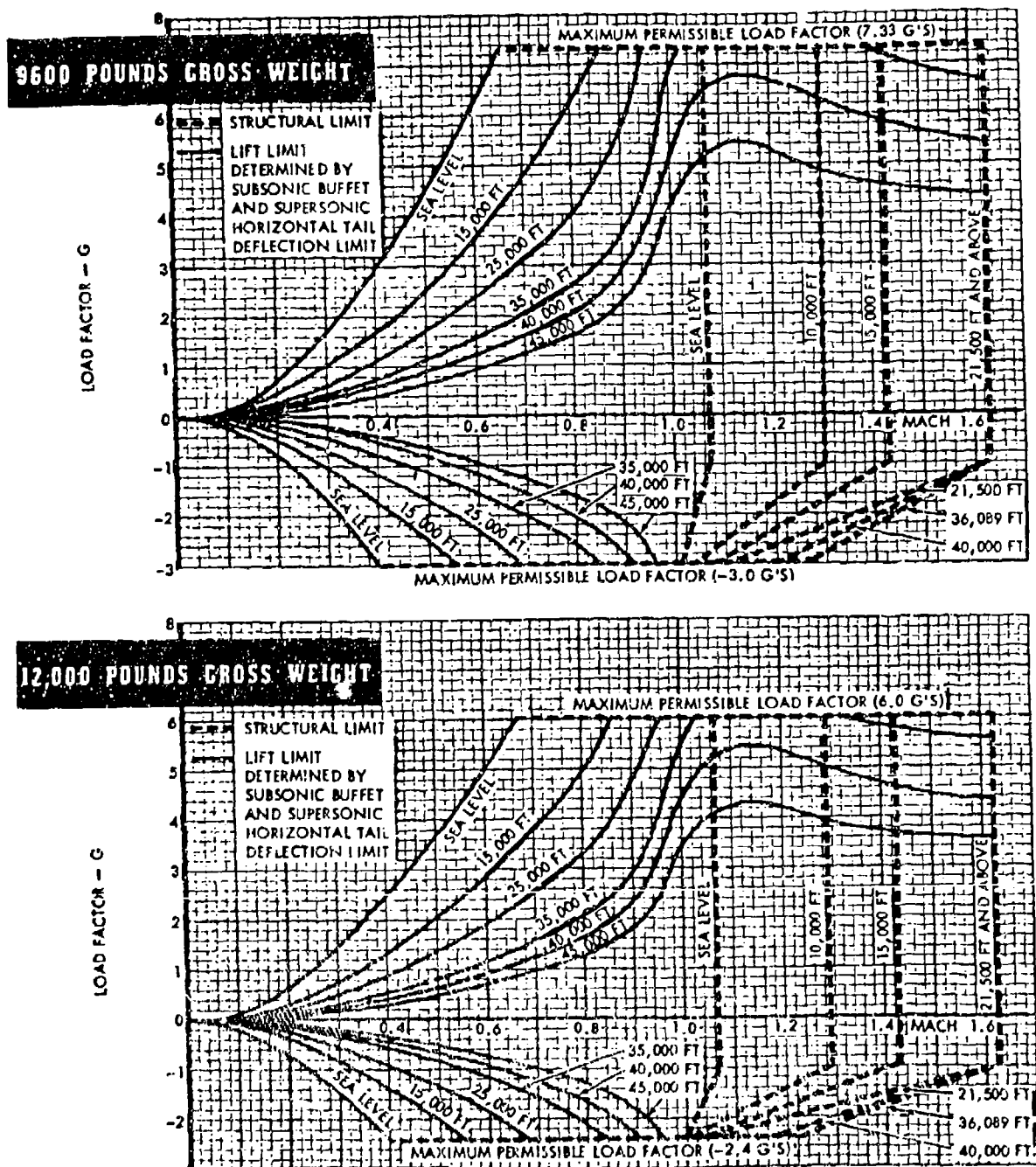
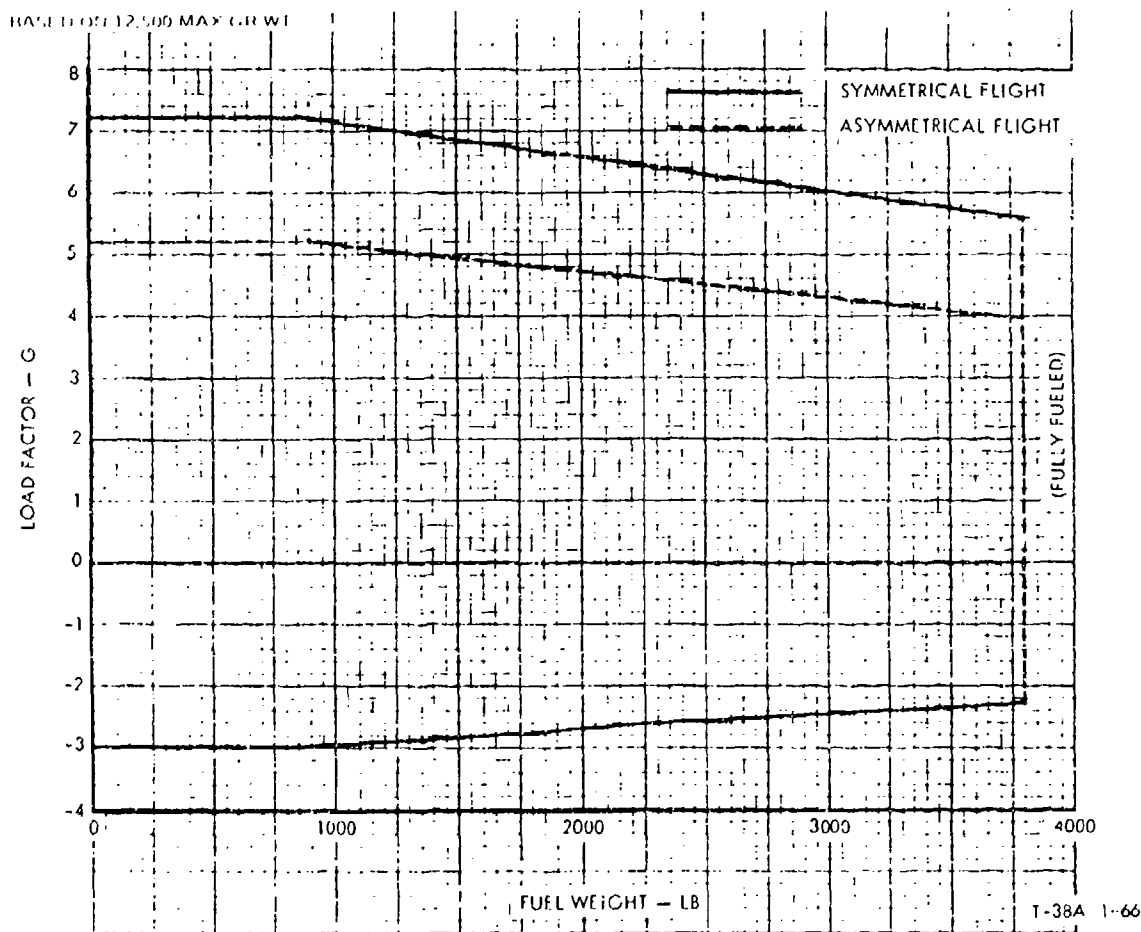


Figure 5.5 Example V-g Diagrams - T-38A (Symmetric)



### LOAD FACTOR LIMITATIONS.

Do not exceed the following

#### SYMMETRICAL FLIGHT.

Load Factor (G's)	Weight of Fuel Remaining (Pounds)
-2.3 to +5.6	3800
2.6 to +6.4	2300
3.6 to +7.33	900 or less

#### ASYMMETRICAL FLIGHT.

Load Factor (G's)	Weight of Fuel Remaining (Pounds)
0 to +4.0	3800
0 to +4.6	2300
0 to +5.22	900 or less

Figure 5.6 Example Load Factor Limits Chart - T-38A

(see Figure 5.5). The maximum loads for an asymmetric maneuver are typically 80 percent of those for a symmetric maneuver (see Figure 5.6), and lower still with stores.

Pilots sense maneuver loads as inertia forces acting on their bodies. However, for the aircraft structure, the concern is for the actual loads to which it is subjected. The loads to keep a 20,000-lb airplane in straight and level flight are much greater than those required to keep the same airplane weighing 10,000-lb at the same condition, all else remaining the same. If the pilots of these aircraft both perform a maneuver with a 4.0 g load factor the heavier plane is still being subjected to a greater overall load although the pilot of both machines feel only the 4.0 g normal load factor. Thus, the maximum load factor is proportionally lower as gross weight increases (Figure 5.6). Because of this, flight manual limit load factors and flight test conditions are frequently given as  $n_{\text{L}}W$ . Another important measure of this is **wing loading** or  $W/S$  (weight over wing area). An airplane with high wing loading is generally much less maneuverable (to avoid over-g of the structure) than an airplane with lower wing loading. Asymmetric loads are frequently the most critical conditions.

The distributed airload on a control surface can be observed as a **hinge moment**. The force produced by the actuator(s), or the pilot's muscles for reversible control systems, must be capable of overcoming this moment in order to move the surface. The measurement of hinge moments is then important in determining whether the loads analysis for the control surfaces has been performed correctly and the proper actuators chosen.

### **5.2.1 LOADS GROUND TESTS**

A static loads test is conducted on an aircraft and separate components during the development stage of the project, prior to flight. The static loads test is performed to ensure that the aircraft is structurally adequate to withstand the anticipated stresses along with a 50 percent **factor of safety** (see Section 3.2.3). Because of this, the test structure must be as close to the final production configuration as possible. The characteristics of the structure (moduli, stress-strain relationship, fatigue, etc.) can also be explored. In these tests the structure is subjected to up to 150 percent the maximum anticipated operational loads (**design limit load, DLL**) for the aircraft, and occasionally to failure. Any capability to carry load beyond the **ultimate load** (1.5DLL) is referred to as the **margin or safety** as defined in equation 3.7.

Static tests to 100 percent of design limit load ("proof" test) are required prior to first flight. The aircraft is then limited to 80 percent of the limit load for the initial flight testing. Static tests to 150 percent are necessary for flight to the limit load conditions. These ultimate load ground tests may be waived for some portions of the airframe if structural adequacy can be demonstrated by comparison to similar structures or a substantial margin has been demonstrated by major subassembly tests. Mathematical models are then improved by incorporating the results of these ground tests.

The aircraft is usually mounted in a rigid test jig and the loads applied with hydraulic rams. Similar tests using cyclically applied loads may be conducted to verify **fatigue life** predictions. Such tests may run through typical mission loading profiles on an accelerated schedule over months or years. For a pressurized structure, static pressure tests are also required. Tests to 133 percent of the maximum pressurization level must be demonstrated prior to the first flight with pressurization. **Durability** tests to twice the airframe life, fatigue and **damage tolerance** tests (the structure should be able to carry essential loads through several paths to provide redundancy in the event of battle damage) are also routinely performed with detailed post-test inspections.

### **5.2.2 LOADS FLIGHT TESTS**

Loads flight tests can be done to measure loads for comparison with the predictions used to design the vehicle or to measure the stresses in critical components under load to ensure that a safe margin exists on the elastic limits. The former method is the generally preferred approach, although examining stresses alone is valuable if nothing else is available or the strain gages have not been calibrated (see Section 10.2.3). The tests are normally performed in two steps; to 80 percent of DLL (following acceptance of the design loads analysis) and then to 100 percent DLL. Tests at 100 percent may not be as thorough as those to 80 percent, although the build-up should be thorough, and are sometimes called "demonstrations" because of this. It may not even be possible to produce 100 percent limit loads in some structural components within the normal flight envelope and maneuver restrictions.

Both the 80 percent and 100 percent steps involve considerable buildup in airspeed, altitude, gross weight, center of gravity (Section 2.3.2), control deflection and load factor. Reasonable tolerances on all of these parameters should be defined for safety and data correlation purposes. Progression along constant dynamic pressure ( $q$ ) lines rather than a constant altitude is a common practice. The loads measured on critical or primary structure must be monitored realtime during the test flight. Loads can then be extrapolated as the buildup progresses in order to clear the pilot to the next test point. Frequent comparisons with predicted load trends are also done in an effort to anticipate potential overload conditions. A poor match to predictions during the 80 percent buildup may require changes to the math model to more closely match test results and new predictions for 100 percent run before flight testing is allowed to proceed.

Different external configurations will also be tested because of the changes in load distribution that they produce. Buffet can also induce serious loading states that may require testing at high angles of attack (AOA) or other conditions to produce separation and vortex impingement. As with the ground tests, the aircraft must be as close to the final production configuration as possible.

It is widely accepted that a component which has been over-designed to 187 percent DLL may fly to 100 percent DLL without loads instrumentation on the component and without ground loads tests. Otherwise, flight to 100 percent DLL is normally permitted only with proper instrumentation. This criteria is generally reserved for modifications to existing air vehicles which have already undergone considerable loads testing.

#### **5.2.2.1 INSTRUMENTATION**

A totally new aircraft will be heavily instrumented and may have hundreds of loads parameters that require examination as the buildup is underway. Accelerometers, force transducers and pressure taps (pressure survey to determine airload distribution) are occasionally used in loads tests. However, the most common transducer used is the strain gage. The nature of the load the gage will measure (torsion, bending, shear, etc.) will determine the orientation and calibration of the gages (see Section 10.2). Often more than one gage is used to determine a load measurement so that an equation is required to derive the result. Instrumentation is arranged to measure the bending, torsion and shear loads in the primary load bearing structure, plus secondary members as necessary. It is occasionally possible to use the same strain gage installation for flight tests that was used for ground loads tests provided that the test aircraft was also the ground test aircraft. This provides a significant time and cost savings in terms of installation and calibration. A typical instrumentation arrangement is shown in Figure 5.7.

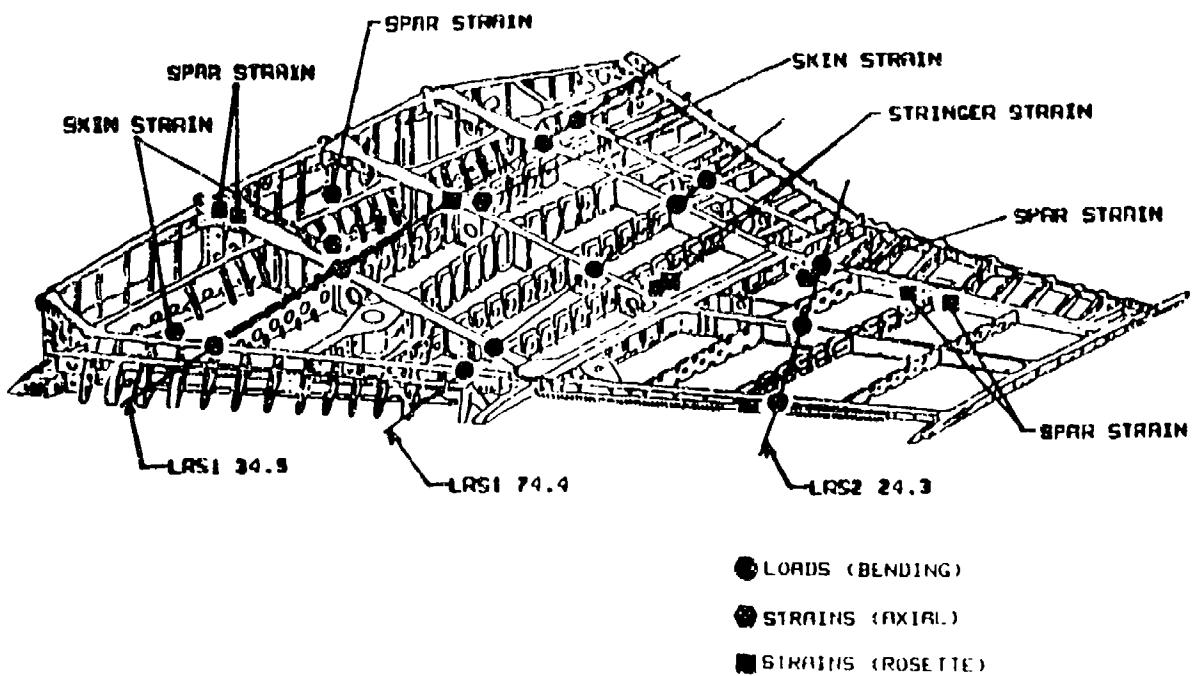


Figure 5.7 Example Loads Strain Gage Installation - F-15 Wing

MIL-A-8871 specifies the minimum strain gage installation for flight tests:

"Wing load distribution measurements by the strain gage method (one wing) shall include at least four stations for spanwise bending moment, shear, and torsion to cover the wing root, two midspan, and wingtip region(s) on small-to-medium-size airplanes (semispan along quarter-chord line, 50 feet or less); and at least six stations for spanwise bending moment, shear, and torsion measurements to cover the wing root, four midspan, and wingtip region(s) on medium-to-large-size airplanes (semispan along quarter-chord line greater than 50 feet). Unless otherwise agreed, spanwise distribution shall be obtained on the right wing. In such instances, however, instrumentation shall be provided for obtaining at least the total loads (bending moment, shear, and torsion) on the opposite wing to facilitate the determination of unsymmetrical loads. Tail loads measurement by the strain gage method shall include at least the total loads (bending moment, shear, and torsion) at the root of each vertical and horizontal surface. Vertical and side bending moments and shears shall be measured for at least one forward fuselage station and one aft fuselage station ... For certain aircraft, additional strain gages may be required as agreed upon between the contractor and procuring activity."

A data sample rate of about 50 samples per second (sps) is normally adequate for flight loads testing. An exception may be made for things like gear dynamic loads and gust loads test where 200 to 400 sps may be necessary. The sign convention for the forces and moments can change between projects and contractor, so this must be specifically noted.

### **5.2.2.2 MANEUVERS**

Some basic relationships of flight conditions with critical loads are helpful in planning a flight loads test. Maximum wing shear and bending moments are usually experienced at a light wing condition (no internal fuel or external stores) and maximum load factors. The highest torsion will likely be seen during large leading or trailing edge control surface deflections. The addition of stores, particularly those at the wing tip, and large fuselage protuberances can greatly alter the wing loads. The maximum fuselage shears and bending moments are typically found during maneuvers in each axes, such as vertical maneuvers and sideslips. Elevated aft fuselage torsion is most often experienced during rolling maneuvers. Large horizontal tail load will occur during maximum stab or elevator deflections, usually at high airspeeds. Torsion loads are particularly critical in the tail. Rolling maneuvers with heavy wing stores can produce particularly high tail load. Rolling and yawing maneuvers with large sideslip angles create very high vertical tail loads. Maximum torsion in the vertical tail will be seen with large rudder deflections.

The following maneuvers are typically used to produce the loads during a loads flight test.

#### **Symmetric Maneuvers**

- a. Steady and abrupt **push-overs** to negative load factor with and without abrupt checking.
- b. Steady and abrupt **pull-ups** to positive load factor with and without abrupt checking. This maneuver is very susceptible to pilot technique and has the potential for producing increased hazards from unusual high nose-up or nose-down attitudes. The target normal load factor can only be maintained for a fraction of a second.
- c. **Windup turn** to positive load factor (turning maneuver of increasing normal load). This permits a gradual buildup in normal load and sustained target normal load factor without unusual attitudes. A descent may be necessary to maintain the target airspeed and for this reason is often called a **winddown turn**.

#### **Asymmetric Maneuvers**

- a. Uncoordinated 180 and 360 deg (or more) aileron rolls.
- b. Abrupt and normal coordinated and uncoordinated **rolling pull-outs (RPO or elevated-g roll)** with and without abrupt checking or roll reversals.
- c. Steady and abrupt (dynamic) **sideslips (yaws)**.
- d. **Rudder kicks and abrupt rudder reversals.**

Any special missions such as aerial refueling, jinking, or missile breaks may also need to be tested. Stalls and spins can produce special load conditions (particularly buffet) that may require testing.

Aircraft trim is generally set to zero for these maneuvers. References 4 and 8 describe each maneuver in detail and gives the minimum number of test conditions for each. These documents plus past test plans and reports should be consulted when formulating the tests for individual projects.

### **5.2.2.3 ANALYSIS**

Critical outputs are displayed realtime during the test to permit the engineer to demand termination of a maneuver if limit loads are approached or exceeded. If an over-g occurs then a post-flight inspection of critical areas or the entire vehicle may be necessary before another flight. The percentage of the over load will dictate the extent of the inspection.

Loads flight test data analysis consists mostly of plotting the flight loads against the analytical load envelopes at 80 percent and 100 percent of design limit, normally as a cross-plots of two loads (Figure 5.8). The plot may show how the load varied during the maneuver (as shown in the figure) or as a discrete point for the peak load experienced during the maneuver. The loads could be gear door side loads, vertical tail torsion, wing bending loads, or just about any load condition on the test vehicle.

When using the normal load factor in solutions or plots, it is common practice to correct it to some standard or design gross weight. This is done as shown in the following equation.

$$\text{corrected } n_z = (\text{test } n_z)(W_0/W_s) \quad (5.4)$$

Watch the sign convention!

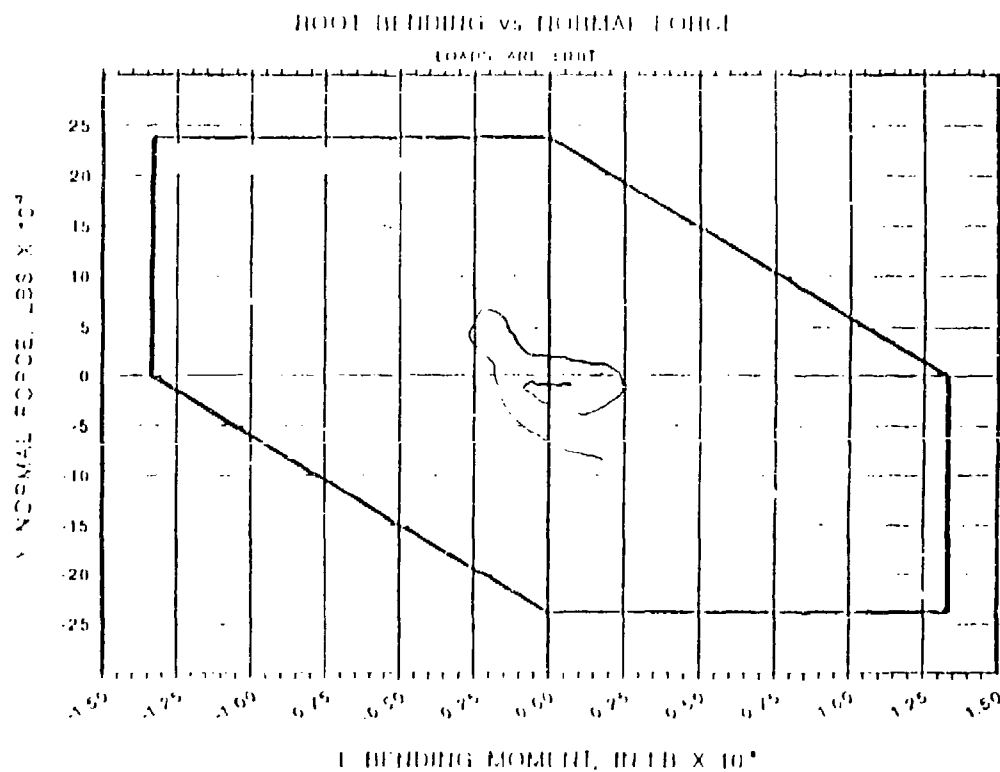


Figure 5.8 Example Loads Cross-Plot

## 5.3 GUST LOADS

Clear air turbulence, thermals, and wake turbulence can impose both vertical and horizontal air loads on an aircraft flying through them. These loads are typically brief and possibly periodic in nature and are referred to as gusts. Vertical loads from gusts are the most common and produce the largest increase in loads on a structure in flight. They increase the effective AOA of the wing, increasing the lift on the wing and the overall wing load. Aircraft frequently have an associated thunderstorm or turbulence penetration speed to protect against overloads due to gusts.

The increase in load factor (using nomenclature from Chapter 2.0) is

$$\Delta n = 0.115m \sqrt{\sigma} V_e(KU)/(W/S) \quad (5.5)$$

where  $\Delta n$  is increase in load factor due to a vertical gust,  $m$  is slope of  $C_L$  versus angle of attack curve,  $\sigma$  is density ratio at flight altitude,  $V_e$  is equivalent airspeed (knots),  $KU$  is effective gust velocity (fps) and  $W/S$  is wing loading (psf).

The aircraft is never subjected to the entire gust velocity ( $U$ ) instantaneously. The actual gust velocity is multiplied by a gust alleviation factor,  $K$  (see Reference 4 for values of  $K$ ). A typical value of  $K$  is 0.6 except for very sharp gusts. The maximum value of  $U$  that is likely to be experienced at sea level in a storm-free weather system is 30 fps. Gusts up to 50 fps may be expected in a thunderstorm penetration situation. Gusts can also be characterized with a wave length, the maximum amplitude of the wave being the maximum velocity of the gust. An aircraft traversing the wave very quickly will feel a sharper gust than an aircraft of the same weight which traverses the same gust at a slower velocity.

A heavy aircraft will experience a relatively small increase in load factor and the pilot will not feel the turbulence as well as the pilot of a lighter aircraft. However, recall that the limit load factor is reduced as weight is increased. In fact, the limit load factor goes down faster than the gust imposed load factor (see Figure 5.9). Therefore, heavily loaded aircraft can be more easily damaged by gust loads causing the limit load factor to be exceeded without high g loadings being experienced by the pilot. Reference 4 provides detailed design criteria for gusts.

### 5.3.1 GUST LOADS FLIGHT TESTS

There are two approaches to the flight testing of aircraft for gust loads. The first is to fly the aircraft at as low a gross weight as possible so that there is very small structural inertia. The gusts will produce the greatest possible structural deformation and facilitate measurement. The loads measured are then added to those expected or measured for the greatest loading conditions to ensure that the limit loads will not be exceeded. The second method is to fly the aircraft at heavy weight conditions, perhaps at those predicted as the worst case loadings, and actually demonstrate that the loads with gusts have not exceeded limits. A combination of the two approaches is probably best.

Gusts can be simulated by use of a structural mode excitation system (see section 6.6.1) using a rapid "kick" or simulated waveform. Real gusts of significant velocity may be difficult to find at high altitudes and are most likely to occur at low altitudes above ridges or mountains, particularly in strong surface winds. Horizontal gusts are difficult to find except with this latter method. However, safety of flight considerations may effect how low an aircraft can be flown over turbulence-producing terrain.

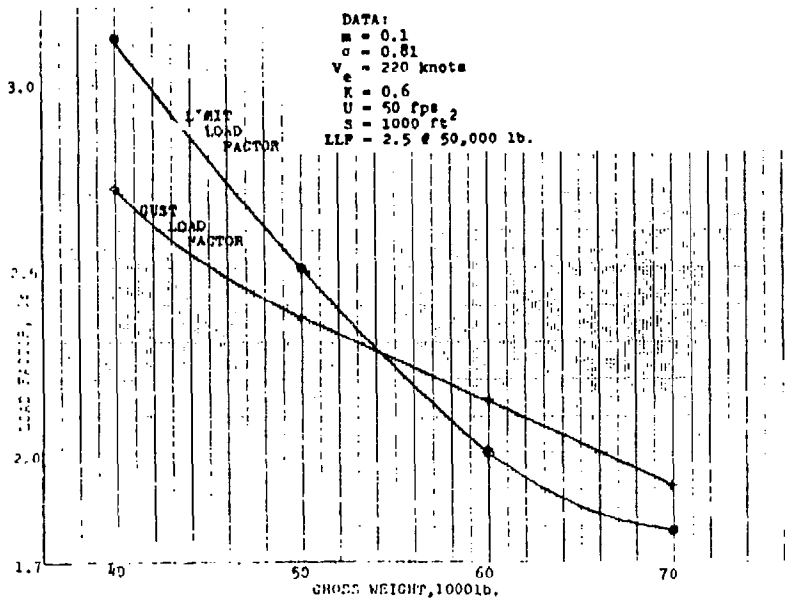


Figure 5.9 Comparison of DLL and Gust Load Factor with Weight

The velocity of the gust in its various components can be measured with static ports on the aircraft or on a static pressure "gust probe" ahead of the nose. Using the root mean squared (RMS) value of the accelerations at the cg of the aircraft, integrated for velocities, can also be used as a measure of the gust velocity. Military specifications require that the frequency content of the gust be measured. This generally means that the bending of a gust probe and the elastic behavior of the airframe must be subtracted out of gust measurements by analytical means. The velocity of a gust is normally determined as an RMS value of a series of gusts encountered in a region of turbulent air. A true gust velocity of 2 fpm is generally considered to be necessary to produce measurable loads on transport aircraft with one to three minutes of data required to be averaged for power spectral density (PSD, see Section 11.3.3) analysis. However, any gust level that produces sufficient measurable response is acceptable, unless specific frequencies are necessary.

Each aircraft may have unique critical load conditions or areas susceptible to gust loads. Examples are: engine pylons in lateral shear (transports); vertical stabilizers and fuselages in lateral shear, bending, and torsion; and wings in vertical bending and vertical shear. These structures would be instrumented in the same manner as that for other loads tests.

#### 5.4 LOAD ALLEVIATION SYSTEMS

The advent of inexpensive and reliable electrical control systems has permitted the introduction of **Active Control Systems (ACS)** into flight vehicles (see Chapter 8.0). This has in turn allowed the incorporation of autonatic load alleviation systems into aircraft, particularly large transport and bomber types. The payoff in such systems are weight savings, an increase in the fatigue life of the structure, increased aerodynamic efficiency, and improved ride quality.

The result may be a structure that can withstand loads that it would otherwise not be able to without an expensive and heavy "beef-up."

The principles of load alleviation systems are to change the aerodynamic load distribution on the structure by use of the available control surfaces. This can be done to reduce maneuver loads (**Maneuver Load Control** or **MLC**) or to reduce gust loads. The L-1011 airliner incorporates the later system. Gusts loads are sensed by instrumentation and the MLC is triggered when the loads exceed a preset level. The ailerons are then automatically biased to move the center of lift on the wing inboard, thus lessening the wing bending loads (see Figure 5.10).

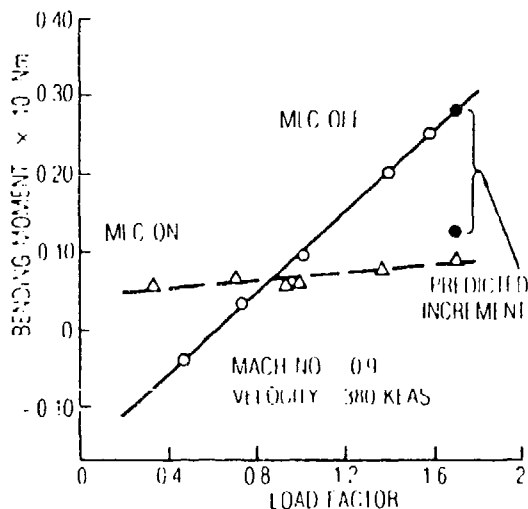


Figure 5.10 MLC Results for L-1011 (71% of Semispan)

## 5.5 LANDING GEAR

### 5.5.1 GEAR LOADS

The landing vertical load factor is

$$N_{LG} = N_S X_S \left[ V_S^2 / (2g) - N_T K_T X_T^2 / (2W) + (1 - L/W)(X_T + X_S) \right] \quad (5.6)$$

where  $N_S$  is strut efficiency,  $X_S$  is the strut stroke (ft),  $V_S$  is the sink rate (ft/sec),  $N_T$  is the nonlinear tire deflection factor,  $K_T$  is tire spring constant (lbs/ft),  $X_T$  is the tire deflection under load (ft),  $W$  is the gross weight,  $L$  is the wing lift (lbs), and  $g$  is the acceleration due to gravity (ft/sec<sup>2</sup>). The last two terms and the strut efficiency can be neglected for quick formulations. In addition to this, loads produced by hard landings (high rate of descent), high touchdown ground speed, gear side loads (landing in a crab), gear spring back, wheel spin up, and rough fields may also require testing.

During the aircraft development phase the gear will be tested to the design maximum sink rate impact either separately or mounted on the aircraft. This can be done by dropping the entire aircraft from an appropriate height, or the gear alone may be mounted in a rig and subjected to different loads varying in frequency, force level, and waveform. This data is then used along with an analytical model to develop load envelopes for each component of the gear. Examples of gear loads of interest are axial load, side load, drag load, brake loads, drag moment, drag brace load, spin-up and spring-back loads. The latter two develop during the landing impact itself.

Landing and taxi tests are necessary to verify that the gear has been adequately designed to meet service requirements without exceeding the design limit loads. This testing takes the form of landings at different sink rates and attitudes, and taxi tests over various surfaces. Two point and three point attitude braking roll, unsymmetrical braking, and reverse braking (backing condition with reverse thrust) are specifically required to be demonstrated. The taxi tests can become quite complex and will be covered in greater detail.

Strain gages are the preferred form of instrumentation for gear loads. Reference 8 states that "... the landing gear and backup structure shall be sufficiently instrumented with strain gages to measure vertical, drag, side, and torsion loads." Gear structure can vary greatly between aircraft types, but the resolution of vertical, side, and drag (longitudinal) loads are still the common results sought regardless of the design.

For the taxi tests, the aircraft may be taxied over surfaces of various roughnesses. This roughness can be simulated on a runway by securing elevated articles (2"x4" wood) or by creating uniform "ruts" or spalls in the surface. Tests over various configurations of 1-cosine function bumps and dips (Figure 5.11) as well as 1" or 2" steps are also mandated. In the past these functions have been simulated by AM-2 runway repair mats or stacked plywood. A specific series of these concrete 1-cosine and step functions are in place in the Edwards AFB lakebed for such tests. The results of such tests are compared with the analytical model as well as ensuring that measured loads are within the design limits. The height and wave length of the 1-cosine function may be selected to create the worst case excitation of rigid and flexible modes at selected taxi velocities, or a number of more benign configurations tested to verify the analysis. If the match is adequate then the model will be accepted to clear the worst case condition if it predicts loads within limits. Miscellaneous loading conditions produced during towing, turning, pivoting, and braking the wheels in flight during retraction may also need to be tested.

Soft surfaces will create higher gear drag loads than a hard, concrete or asphalt surface. For aircraft intended to be operated on soft fields, gear testing at various surface densities and roughness is necessary. **California Bearing Ratio (CBR)** is the accepted measure of surface density. A CBR of about 32 is equivalent to concrete, with softer surfaces having progressively lower values.

These tests may be done at gross weights, taxi speeds and braking forces up to the maximum. Various center of gravity positions may be run to place the aircraft at different ground attitudes and static gear load states. Tire heating generated by brake rotor radiant heat and simple friction with the ground surface can create the hazard of tire bursting. A hydraulic leak can result in this inflammable fluid contacting the hot surfaces and igniting. These dangers require that brake and tire temperatures be monitored during these tests as well as taxi distance. These measurements are cross-referenced against flight manual brake energy and taxi distance charts. Most wheels incorporate "fuse plugs." These are metal plugs that melt down to relieve tire pressure when they reach a specified temperature. A flat tire is much easier and safer to deal with than a burst tire. Most modern aircraft brakes also incorporate an anti-skid system which automatically

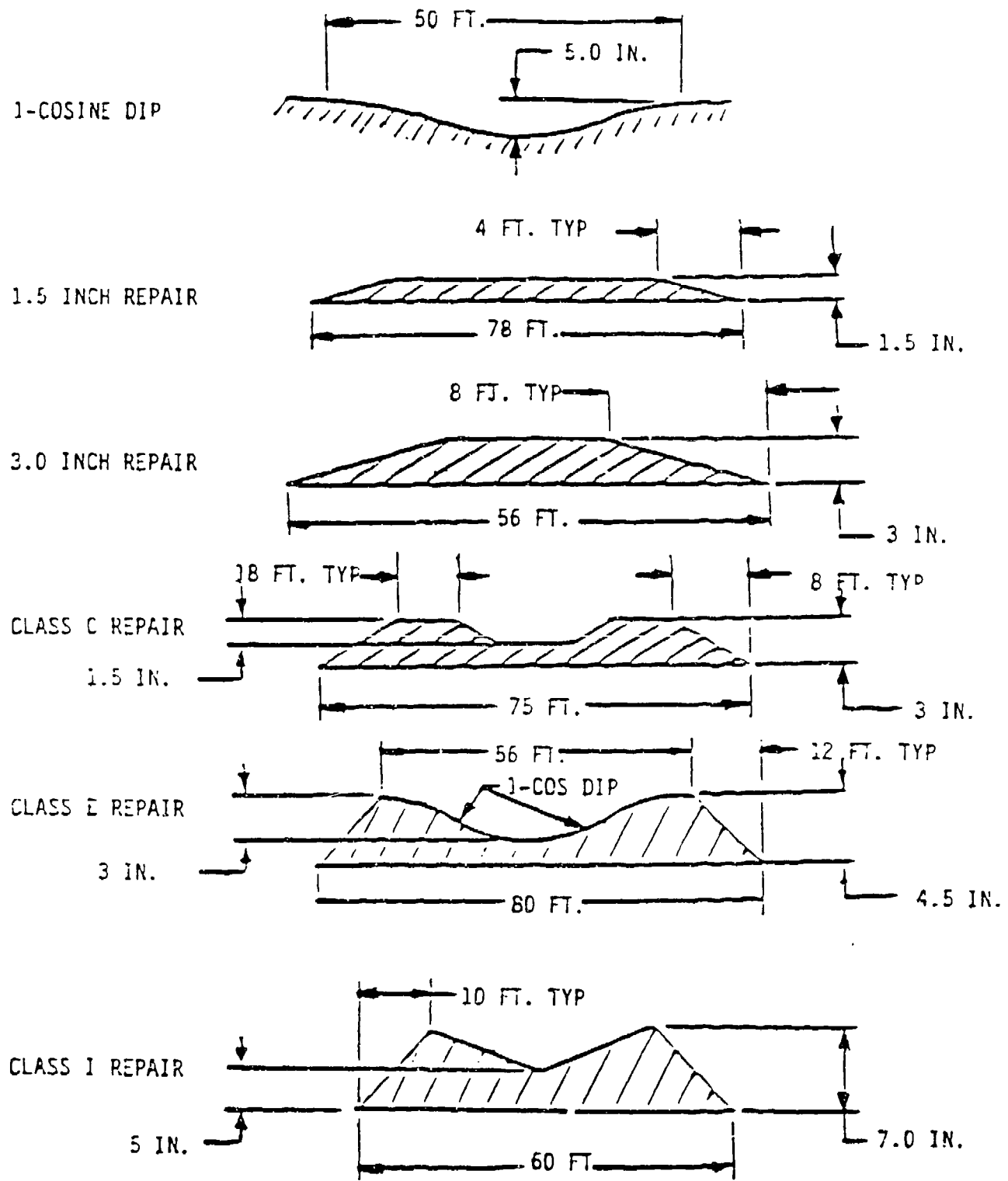


Figure 5.11 Typical Runway Repair Landing Gear Testing Profiles

relieves brake pressure if a sudden drop in wheel speed, indicative of a potential skid, is sensed. A skidding tire abrades rapidly and a rupture is likely.

**Arrestment or barrier tests** are also routinely performed for those aircraft with tailhooks to ensure that it and associated structure has been adequately designed.

### **5.5.2 GEAR SHIMMY**

Landing gear shimmy, normally experienced in the nose gear, is an oscillatory instability excited by lateral force on the wheel and induced by a sharp steering command or an obstruction on the taxi surface. The motion is a rapid rotation of the wheel/axle assembly about its pivot point. The oscillations can produce severe vibration in the aircraft and result in overload failures in the gear assembly or other parts of the aircraft subjected to high inertia loads. Factors which play into the problem are the tire elastic characteristics, the rotational inertia of the wheel, the distance of the wheel rotational center from the pivot point (the "trail"), the steering angle, and lateral strut deflection, and the airframe motion.

Shimmy or gear dynamics tests are performed by taxiing the aircraft over discrete obstructions, such as a 2"x4" piece of wood, typically oriented at 45 degrees to the path of the machine. Tests are performed at ever increasing speeds. Testing on an unobstructed surface may be acceptable for aircraft with no off-field operation (landing on dirt). Rudder pedal and brake pulses should be used in this case. If shimmy is excited then an immediate deceleration is necessary. The simplest solution to shimmy is the addition of a damper to the system which has been tailored to the shimmy frequency. Variation to the factors introduced in the previous paragraph may be necessary if the design cannot abide the additional volume or weight of a damper.

### **NOMENCLATURE**

ACS	active control system
AOA	angle of attack
CBR	California Bearing Ratio
$C_L$	lift coefficient
DLL	design limit load
FCS	flight control system
FOL	flight operating limit
fps	feet per second
g	acceleration due to gravity
K	gust alleviation factor
L	lift force
MLC	maneuver load control
m	slope of $C_L$ versus AOA curve
N	vertical load factor, efficiency, factor
$n_z$ or $n$	normal load factor
OWS	Overload Warning System
q	dynamic pressure
RMS	root mean squared
RPO	rolling pull-out
RW	relative wind
S	wing area
s	landing gear stroke
sps	samples per second
U	gust velocity

V	velocity
W	gross weight
X	deflection
$\Delta$	increment of change
$\sigma$	density ratio
$\phi$	bank angle
Subscript	
H	maximum for maneuvering
L	limit
LG	landing gear
max	maximum
S	stall condition, sink, strut
s	standard condition
T	tire
t	test condition

## REFERENCES

1. Dole, C.E., *Fundamentals of Aircraft Material Factors*, University of Southern California, Los Angeles, California, 1987.
2. Hurt, H.H., Jr., *Aerodynamics for Naval Aviators*, NAVWEPS 00-80T-80, US Navy, January 1965.
3. Military Specification Airplane Strength and Rigidity - General Specification, MIL-A-8860.
4. Military Specification Airplane Strength and Rigidity - Flight Loads, MIL-A-8861A.
5. Military Specification Airplane Strength and Rigidity - Landplane Landing and Ground Handling Loads, MIL-A- 8862.
6. Military Specification Airplane Strength and Rigidity - Miscellaneous Loads, MIL-A-8865.
7. Military Specification Airplane Strength and Rigidity Ground Tests, MIL-A-8867.
8. Military Specification Airplane Strength and Rigidity - Flight and Ground Operations Tests, MIL-A-8871A.
9. Moreland, William J., "The Story of Shimmy," in *Journal of the Aeronautical Sciences*, Vol 21, No. 21, December 1954.

# CHAPTER 6.0

## FLUTTER

### **6.1 INTRODUCTION**

New engineers are encouraged to read some of the theoretical flutter material contained in the text books found in the reference section. A little theoretical knowledge will help in interfacing with contractor flutter engineers, many of whom have a solid analytical background as well as test experience in the subject.

It is important to understand that flutter prediction is far from an exact science. The mechanisms responsible for structural damping are still not entirely understood or fully predictable. There are many means of flight testing for flutter and interpretation of the results. Flutter is never entirely eliminated, simply delayed to airspeeds beyond the normal flight envelope of the aircraft. The pilot(s) and program management must understand that flutter testing cannot be done "seat of the pants" but requires careful buildup with concurrent analysis. Flutter is little understood except by a small number of analysts and flight test engineers. This tends to produce frustration and incaution by management and pilots.

### **6.2 DESCRIPTION**

Flutter is the complex interaction of unsteady aerodynamics, structural elasticity and inertia producing an unstable, usually divergent oscillation of an aircraft structure or component. Therefore, flutter is a phenomenon seen only by those structures subjected to an unsteady fluid stream and treated as a non-rigid body, thus differing from the traditional treatment of aircraft dynamics. Flutter susceptibility generally increases with airspeed and is aggravated by thin, very flexible structures. It is apparent that with the ever lighter, complex, less stiff structures and higher speeds of modern aircraft, flutter continues to be a matter of great concern. Many problems would be nonexistent if aircraft were built to the highest rigidity that materials and construction techniques could allow, but the weight penalty would be prohibitive.

The effects of unstable oscillation in an aircraft structure is seen as a "flutter mechanism"; a complex interaction of forces and moments, structural dampings and stiffnesses. The change in the intensity and the distribution of airloads with associated structural deformation and restoring motion results in a cyclic phenomena. Small perturbations about the steady-state flight attitude and small elastic structural deformations create the unsteady flow. Load factor, angle of attack, and the nonlinear lift curve slope (see Section 2.2.5) have also contributed to flutter mechanisms. As flutter begins, it is an oscillation of increasing amplitude with each succeeding cycle. If the oscillation is allowed to persist, the flutter will continue until some structural restraint is reached or until catastrophic structural failure occurs. Figure 6.1 shows how all the forces affecting a flight vehicle interact to form the aeroelastic and aeroservoelastic (see Chapter 8.0) problem. Each effect will be dealt with to some degree in this handbook.

In the case of a multiple degree of freedom (DOF) system, the flutter mechanism is a coalescence of two or more natural vibration modes of the structure (see Chapter 4.0). The phase angles and frequencies of the individual modes shift in a manner that allows the coupling; a change from no net work of the system to positive net work. A coalescence of two modes is

called **binary flutter**. If three degrees of freedom contribute to a flutter state then it is termed **ternary flutter**. Four and five modes coupling are called **quaternary** and **quinary flutter**, respectively. Flutter of more than two DOF is rare. Flutter resulting from the coupling of a structural mode and an aircraft rigid body mode (aircraft pitch, roll, yaw, and plunge or vertical translation) is termed **body freedom flutter**. Assuming that the inertia and stiffness of the structure does not change in flight (neglecting heating effects and short term fuel burn), the overall system damping will change with a change in the magnitude and frequency of the aerodynamic forces. The natural frequency of all modes will change as the aerodynamic forces change (increased flow velocity, for example) with the frequencies contributing to the flutter mechanism approaching each other and the phase shifting toward an unstable state. The damping of one of the modes move towards zero. When the two modes finally coalesce to form the "flutter mode" the resulting mode shape will be a combination of both individual modes. The energy from each mode will now contribute to an increase in the net work done by the system.

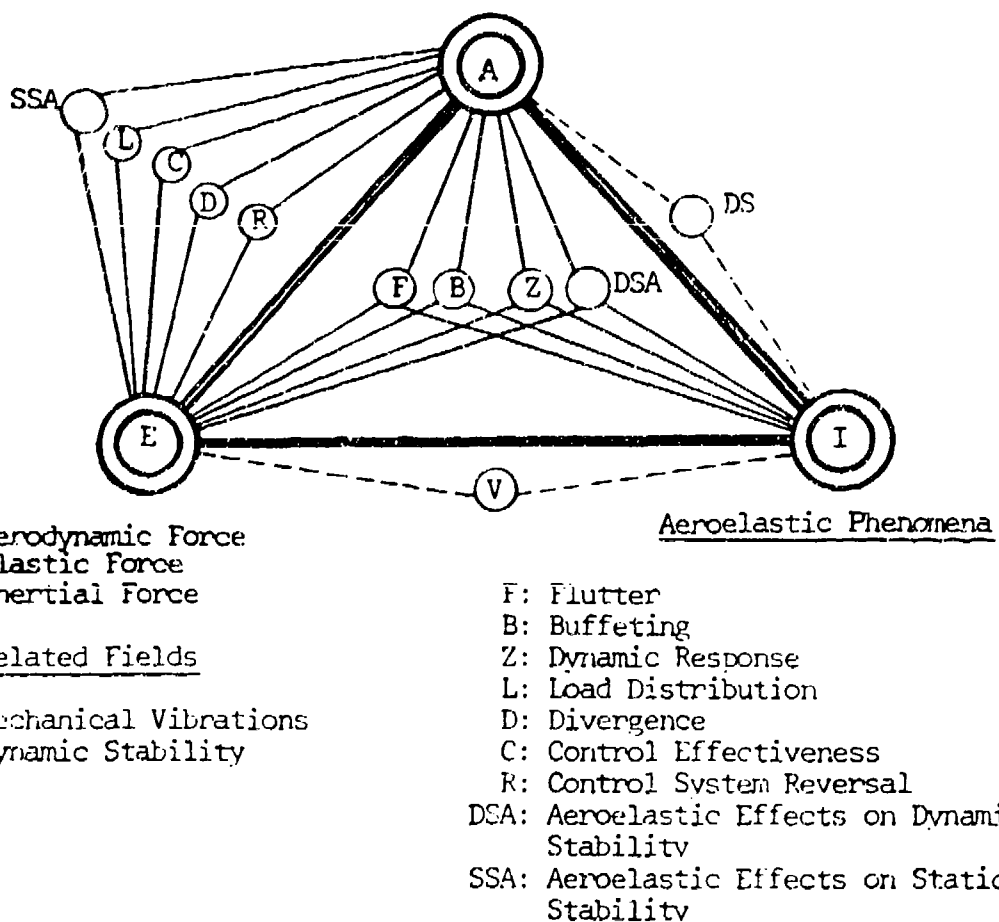


Figure 6.1 Collar's Aeroelastic Triangle of Forces

Normal aluminum aircraft structures have about 2 percent of inherent structural damping (G, see Chapter 4.0). Composite aircraft structures have about 1 percent inherent damping. Just the mass of the air and the "centering tendency" of a high velocity air stream will tend to damp aircraft structural oscillations. This is known as **aerodynamic damping**. The frequency content of unsteady aerodynamics will result in an oscillatory forcing function which may act positively (i.e., add to the system damping) or negatively (subtract from the damping). The net value of structural damping and aerodynamic damping is called the "aeroelastic" or **total (system) damping**. Total system damping generally tends to increase with an increase in airspeed until damping in a "critical mode", or the mode with the lowest flutter speed, begins to decrease rapidly. At the **flutter speed** the damping of the mode is zero and the oscillation is just able to sustain itself without divergence. Just a small addition of energy to the system by an increase in speed and a small disturbance can trigger the divergent oscillation that is very likely to damage the structure, possibly within only two to three cycles. Once it starts, the motion is self-sustaining and requires no further external forces.

When a flutter mechanism is active in a structure overall system damping is negative. The aerodynamic damping has completely negated the structural damping and begins to add energy to the system. The amplitude of the cycles begins to increase over time rather than decrease as in the case of positive damping. This situation is termed "**divergent flutter**" and will eventually cause the structural limits of the component experiencing the flutter to be exceeded.

Because control surfaces are specifically designed to rotate, they can be easily excited by aerodynamic forces or other structural motion. This makes them very important components to consider in flutter analysis and during flight testing. The rotation frequency of the control surface is of paramount concern. For surfaces moved by actuators, the rotation frequency is primarily contributed by the stiffness of this equipment. For surfaces moved by cables or push rods, the mass distribution of the surface will determine the rotation frequency. This can be altered as necessary by changing the balance weight. This a concentrated mass placed ahead of the hinge line. **Mass balancing** is necessary every time there is a change to the surface, such as repairs or repainting. Balance weights are almost universally used even on surfaces driven by actuators, to ensure against flutter should the actuator pressure decay due to a hydraulic failure.

Military standards (see Reference 12) require analysis to demonstrate, and flight test to verify as much as possible, that the flight vehicle is free of flutter or other aeroelastic instabilities to  $1.15V_L$ , or a 15 percent margin on the design limit flight speed ( $V_L$ ). This provides a safety buffer on the normal aircraft red line in the event of overspeed. The damping (G) of any critical flutter mode or other significant dynamic response must be at least 0.03 throughout the envelope. Some configurations may require a reduced flight envelope for flutter-free operation.

### **6.2.1 FLUTTER EXAMPLES**

A few examples of flutter mechanisms are useful to illustrate real flutter events and to assist in identifying mechanisms that may be encountered during future tests.

#### **EXAMPLE 1**

A good example of binary flutter is the coupling between wing bending (also called **flexure**) and wing torsion; the classical **bending-torsion flutter**. If wing bending and torsion are in phase, that is, the surface reaches the maximum upward bending at the same time that it reaches the maximum leading edge down twist, and visa versa for downward deflection and leading edge up twist, there is no net work done by the system and it is stable. Seen another way, an upward

translation of the wing produces a reduction in the effective angle of attack as does the nose down twisting. These effects will naturally reduce further bending and torsion because of the loss in the lift force producing the deformation. However, if torsion lags the bending by 90 deg, an unstable situation prevails. Now, an upward bending is accompanied by a positive increment in angle of attack due to twist which will increase the lift force and thus drive the wing to further deformation and yet further lift. The location of the wing center of gravity and its elastic axis have an important influence upon the likelihood of this flutter. Such a wing bending-torsion flutter occurred on the T-33 during testing with wing tip fuel tanks after the pilot took it upon himself to add some higher speed test points that were not planned. He managed to jettison the tanks and land but the aircraft was damaged beyond repair.

### EXAMPLE 2

An often quoted example is the experience of the Handley-Page 0/400 bomber of World War I. In this case, a fuselage torsion mode coupled with asymmetric elevator rotation. This resulted in twisting of the aft fuselage and tail up to 15 deg as the left and right elevator flapped dramatically about their hinge lines in opposing phases. The solution was to increase the elevator asymmetrical rotation frequency by joining the surfaces with a single torque tube (now a common practice for aircraft without differential stabilizers). The increase in rotation frequency effectively eliminated the possibility of coupling with the fuselage mode within the normal flight envelope.

### EXAMPLE 3

Another classical inertia coupling flutter case is that of aileron rotation/wing bending. The mechanism is not much different from Example 1. If the center of gravity (cg) of the aileron is aft of the axis of rotation or hinge line then an upward motion of the wing will tend to produce a trailing edge down deflection of the aileron. Should the rotation frequency occur at the same frequency as wing bending an unstable condition is established and the wing or aileron may be driven to divergent oscillations. Trailing edge down rotation of an aileron produces an increase in lift on the wing for an upward bending moment on the wing. The opposite deflection occurs for downward bending of the wing but the effect is still unstable, tending to sustain or amplify the wing bending. The initial aileron rotation may be induced by rhythmic separation and reattachment of flow on the aft portion of the wing, producing an alternating high and low pressure on the control surface, but this is not required for the flutter mechanism. This is an example of how inertia effects can interact with unsteady airloads. This effect can also be seen in tab surfaces.

The most common solution to this problem is to increase the control surface rotational frequency by increasing the actuator stiffness or, by placing a mass ahead of the axis of rotation (mass balancing) to move the cg forward of the hinge line. Control surface free-play (compliance), backlash, and general rigging can also play an important role in this flutter mechanism. An example of this sort of flutter was seen during the T-46 flight testing when an aileron re-balance caused the rotation frequency to couple with wing bending to produce flutter that was non-catastrophic only because the limited rotation of the aileron could not drive the wing to great enough bending deformation. Such high frequency, large amplitude control surface motion in a reversible control system will result in violent stick motion that can harm the pilot. A dynamic balance to alleviate flutter may create objectionable static unbalance, requiring excessively large forces to displace the control. The use of mechanical dampers on the control surface may be dictated in such a case.

#### **EXAMPLE 4**

The pitch or yaw of an engine or the motion of the wing on which the engine is mounted can excite a gyroscopic motion of the spinning propeller. This motion can diverge to produce **propeller whirl flutter** or the propeller motion can drive the wing to a flutter state. A variation of this was seen in the Lockheed Electra and led to many deaths until the cause was isolated. The main landing gear and engine mount assemblies were interconnected and landing impacts produced a weakening of the engine mount structure. This weakening changed the mount stiffness and permitted gyroscopic propeller motion which drove the wing to flutter.

#### **EXAMPLE 5**

During initial flight testing of a small Israeli tactical transport called the Arava, a maintenance crewman failed to adequately torque the bolt holding the external strut to the wing. This had the effect of rendering the wing less stiff than it had been designed and cleared for. In flight the wing fluttered and failed, with several persons being killed.

#### **EXAMPLE 6**

During initial flutter testing of the KC-135 a limited amplitude flutter was encountered in the vertical tail. In an effort to slow the aircraft, the pilot deployed the wing spoilers. However, the oscillations grew in intensity. The peak-to-peak displacement of the vertical tail was 24 to 36 inches and was sustained for 46 seconds before the aircraft was finally slowed below the flutter speed. After considerable wind tunnel and flight testing with extensive analysis, a fix was finally arrived at. It included rudder and rudder tab dampers, increased thickness of the front and rear spar caps, increased skin thickness in the two top panels between the front and rear spars, and increased rudder control cable tension.

#### **EXAMPLE 7**

During early deployment of the KC-135 tanker the refueling boom began oscillating while in the trail position and separated from the aircraft. Fixes included a strengthening of the boom yoke and replacement of the cable stowing mechanism with a hydraulic system.

#### **EXAMPLE 8**

During flutter testing of the transport version of the KC-135, a horizontal tail and elevator instability was encountered. The fix was simply to install the commercial 707 tail on the aircraft. However, later testing for autopilot compatibility resulting in a reoccurrence of the event.

#### **EXAMPLE 9**

In 1988, a Navy derivative of the Boeing 707-320, the E-6A TACAMO, experienced severe flutter in the vertical tail resulting in loss of the upper half of the fin and rudder. The next flight in 1989 resulted in nearly identical damage. At the time of writing the flutter mechanism and a fix has yet to be identified.

## **EXAMPLE 10**

The frequent changes in the equipment contained in the large wing pods of the TR-1 and U-2R (the "super pod"), often with antisymmetric loading, has resulted in occasional flutter events. These are associated with wing first torsion and sometimes in combination with aileron rotation. Such factors as speedbrake vibration, increased angle of attack, increased lift coefficient, increased normal load factor, transonic effects, aileron buzz (see Section 6.4.2) and the normal biasing of the ailerons from the faired position to relieve gust loads also contributed to the problem. The flutter produced violent control surface motion up to 75 percent of full deflection which displaced the cockpit control yoke with such force that the pilot could not hold on to it. Considerable wing bending and torsion accompanied these oscillations with up to 18 g's experienced and some structural damage. Resolutions of the problem has included a limit to the speed envelope, load factor restrictions, and additional mass balancing of the ailerons. A 15 percent flutter margin does not exist at all points of the operating envelope for this aircraft.

### **6.2.2 FLUTTER SUPPRESSION**

The great advances in automatic flight controls has made possible flight in aircraft that are otherwise unflyable. In recent years this technology has also been used to alleviate gust loads, reduce fatigue, and also reduce troublesome vibrations by creating equal but opposite excitations. An example of this are the small movable vanes on the nose of the B-1 bomber. They serve to suppress a 3 Hz oscillation in the forward fuselage during low altitude operations that interact with the natural modes of the pilot's body and considerably reduce pilot tolerance and efficiency. Research has also been progressing in using active controls to suppress structural modes that might contribute to flutter or divergence (see Section 6.4.4). The concept has been proven in wind tunnel and development flight tests. The closest thing to a production application of this concept is active suppression of an objectionable 5 to 6 Hz heavy wing oscillation at low altitude for the F/A-18 with certain store loadings using the ailerons.

The easiest means of flutter suppression, if effective, is steady state or oscillatory control deflections to counter sensed structural harmonics. A less practical but potentially more effective means is rapid mass redistribution within the structure. This has been used during flutter testing of an F-4 in Germany with masses on arms that swung out from the underwing fuel tanks. Research is also underway into structures that actually change their stiffnesses upon demand by use of hydromechanical or electromechanical rams.

### **6.3 FLUTTER PREDICTION**

The prediction of aircraft flutter is based upon well-developed structural and aerodynamic modeling methods combined with eigensolution matrix techniques. However, each component incorporates many simplifying assumptions (such as the small deflection assumption) in reduction of the myriad nonlinearities to make the solution more tractable. The study of unsteady aerodynamics and oscillating airfoils are still in its infancy and this also effects the validity of the predictions. The modeling of transonic aerodynamics is particularly limited and this presents a major stumbling block because of the large number of flutter mechanisms that occur in this regime. The prediction of separated flow characteristics is currently not possible. Static structural tests, ground vibration tests (GVT), wind tunnel results, and even flight test data are of help in refining the model to reflect the real vehicle. But, flutter analysis remains something of a "black art" in which engineering judgment and experience is more highly regarded than stacks of computer printout. Many flutter analysis codes exist (NASTRAN, FACES, UFAPS, to name a few), have their own assumptions and solution techniques. The common assumptions

are linear structures, small displacements, and a finite number of degrees of freedom (the semi-rigid case). Results are approximations only and generally cannot be counted on by themselves to clear a new or highly modified aircraft without a safe envelope expansion flutter flight test.

Reference 11 provides some guidelines for the flutter analysis. One of the first steps is to perform an "in-vacuo" analysis, that is one in which the airflow is completely neglected. This is a static (zero airspeed) state with which GVT results may be compared (see Chapter 7.0). The mass of the static air is not considered since this is negligible. The more important analysis is done with the airflow effects included to act as an external forcing function. Supersonic and subsonic analysis are done separately because of the profound differences in modeling these flows. Transonic flow can be modeled by using some compressible flow assumptions with the subsonic analysis. The mathematical aerodynamics and structural models used in these analysis are later verified through wind tunnel and flight testing. Analysis including the effects of discrete failures such as a broken hinge, low actuator pressure, etc., should also be done.

The analysis of the entire aircraft or at least a substantial portion thereof will be dealt with here. The basic two-degree of freedom wing analysis has little real value for accurate flutter prediction. Because of the incredible increase in computer running time and cost as the number of degrees of freedom are increased, components of the aircraft may be modeled separately with appropriate boundary conditions, but with the model for that component greatly simplified when the entire aircraft model is simulated. Figure 6.2 shows a flutter structural model for the F/A-18 wing while the model for just one side of the F-15 STOL (Figure 6.3) has the wing shown as just a series of beams along the span and the control surfaces.

The very basic flutter equation upon which all analysis is based is that defining the relationship with stiffness, mass and aerodynamics. In operator form this is

$$\{M\} - \{A\} + \{K\} = Q \quad (6.1)$$

where  $\{M\}$  is the **mass operator** including inertia of the structure,  $\{A\}$  is the **aerodynamics force operator**,  $\{K\}$  is the **stiffness operator**, and  $Q$  is the **generalized forcing function**. The forcing function may act through one or more of the operators. The mass of the air may or may not (the in-vacuo case) be included in the inertia operator. Creating appropriate forms of the operators can become very complex. A generalized modal matrix form (see Section 4.5.2) this would be

$$[M]\{\ddot{q}\} - [A]\{\dot{q}\} + [K]\{q\} = Q \quad (6.2)$$

where  $\{q\}$  is the **generalized coordinate vector**. Care must of course be taken to ensure that the matrices are compatible. The aerodynamic matrix defines the aerodynamic influences, the derivation of which is too complex to present in this handbook. It includes complex terms since it involves unsteady effects. The stiffness and mass matrices are usually produced by finite element modeling (see Section 3.2.3).

The solution as a matrix equation is typically accomplished by forming the **flutter determinant** and solving the resulting characteristic equation. That is, using the non-modal stiffness, mass, and aero matrices

$$|[k] - [m] - [a]| = 0 \quad (6.3)$$

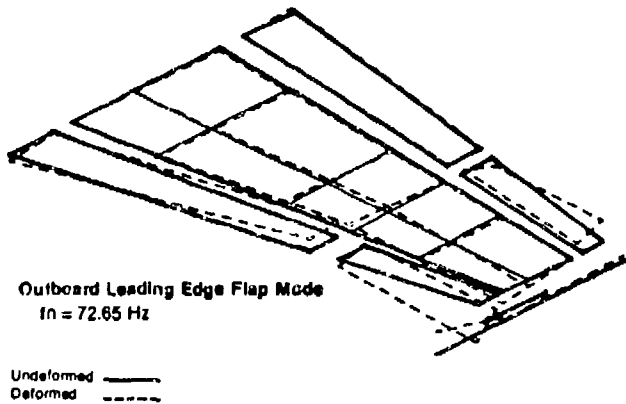


Figure 6.2 Example Wing Flutter Model - F/A-18

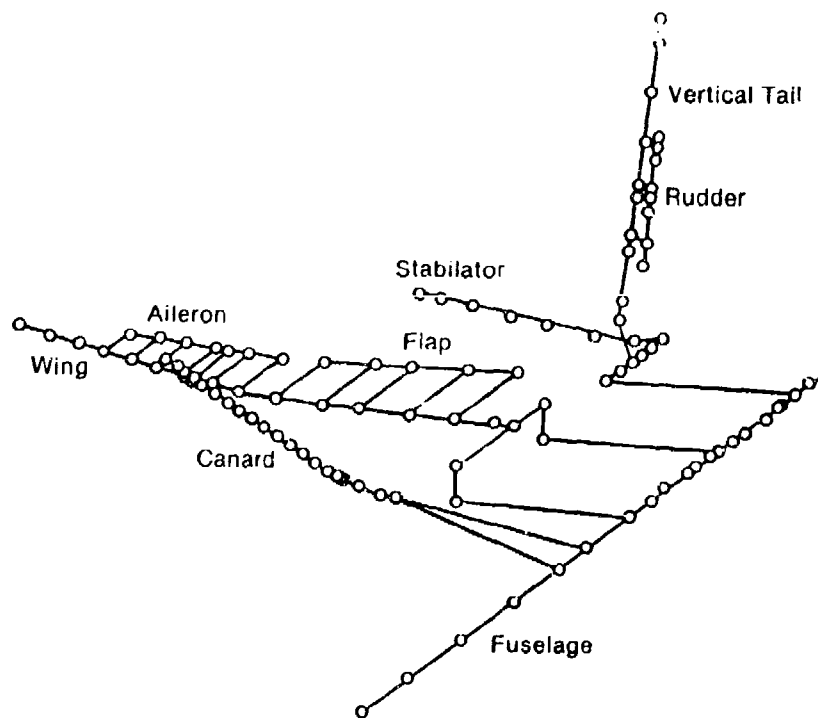


Figure 6.3 Example Aircraft Flutter Model - F-15 STOL

Since the aero matrix is formulated for a single airspeed only, the solution is only valid at that airspeed. The eigenvalues of the flutter determinant will be complex, each representing a mode of deformation as defined by the eigenvectors. The real part of the eigenvalue will indicate whether the mode it represents is stable or unstable (see Section 4.3.1). A negative real part is stable, with the magnitude of the value indicating the amount of damping present. Conversely, a positive real part represents an instability and implies flutter. A zero real part implies a neutrally stable condition for which a zero imaginary part represents divergence and a non-zero represents flutter.

### 6.3.1 K-METHOD

For the “K-method” (sometimes known as the **American method** because it was created by the Air Material Command in 1942 when the only other such method was a British approach) the assumption of undamped, simple harmonic motion oscillations is made. In this case it is necessary to introduce an unknown **hysteretic damping** term,  $G$  (twice the damping factor introduced in Section 4.3.1 and based upon assumptions discussed in Section 11.3.4), to balance the imaginary aerodynamic damping terms and bring the system into neutral stability as the method demands. The damping term applied to the stiffness matrix is

$$1 + iG \quad (6.4)$$

For sinusoidal motion, the generalized coordinates may be written as

$$\{q\} = \{\bar{q}\} e^{i\Omega t} \quad (6.5)$$

where the  $\Omega$  may contain damping. If  $\omega$  is the frequency of the undamped oscillations, then

$$\Omega = i\omega \quad (6.6)$$

and equation 6.2 can now be cast in its most familiar form

$$[-\omega^2 [M] + [K] - [A]] \{\bar{q}\} = 0 \quad (6.7)$$

The aerodynamics matrix often uses a term known as **reduced frequency**, or

$$k = \omega b/U \quad (6.8)$$

where  $b$  is a reference semi-chord of the wing and  $U$  is the freestream velocity. **Reduced velocity** is the inverse of reduced frequency.

The equation to be solved in the K-method becomes

$$\left[ \frac{(1 + iG)}{\omega^2} [K] - [M] - \frac{\rho b^2}{2k^2} [A] \right] \{\bar{q}\} = 0 \quad (6.9)$$

where the multiplicative term on the stiffness matrix is taken as the eigenvalue,  $\lambda$ , to be solved for. A value of reduced frequency,  $\rho$  (defining the altitude), and airspeed must be assumed for the calculation to proceed. The important results are then obtained from the relationships

$$\omega = 1/\operatorname{Re}(\lambda) \quad (6.10)$$

$$G = \omega^2 \operatorname{Im}(\lambda) \quad (6.11)$$

and the corresponding velocity to produce the unstable state is derived from equation 6.8 using the reduced frequency from the aerodynamic computation and the derived  $\omega$ . It is important to note that the sign of  $G$ , the total system damping, in this analysis is opposite to what one expects. A positive  $G$  will correspond to an unstable condition.

Because of the assumption of zero damping, the prediction is only valid at the point of neutral stability. If the flutter velocity does not match that used in the aerodynamic calculations then iterations must be performed until they do match. This is called a **match point analysis** and may not always be done due to the large amount of computer time required. However, even when the flutter speed and analysis speed match, the rest of the frequencies and damping for all non-flutter modes are not true values but only guides to them. The predicted flutter speed should still only be used as a guide to the true speed. The number of eigenvalues produced depends upon the number of degrees of freedom modeled. Tracking the individual modes requires prior knowledge of corresponding frequencies (GVT results) or an examination of eigenvectors for mode shapes. Some programs include sophisticated algorithms that are able to track the modes automatically but may be confused when unrelated modes "cross" at similar frequencies.

Typically, a velocity versus frequency (**V-f**) and velocity versus damping (**V-G**) or dynamic pressure ( $q$ ) versus  $G$  plots are produced as a result of the flutter analysis (see Figure 6.4 and 6.5). Where two frequencies come together at an instability (crossing of the 0.0G line in the V-G plot) the two modes are said to be coupling to produce the flutter. Recall that the K-method assumed that there was no system damping at all. Since the structure has some inherent damping, a 0.02 to 0.03 G crossing is usually taken as the flutter point. The velocity corresponding to such a crossing is used with the V-G and V-f plots to determine the flutter speed and frequency. The lowest such velocity, if several crossings exist, is the **critical flutter velocity**. The difference between this speed and the red line airspeed of the aircraft (assuming the former is higher than the latter) defines the **flutter margin**.

The slope of the crossing is also important. A very steep crossing implies **explosive flutter** or that which happens extremely quickly and with little warning because the damping drops very rapidly as the flutter speed is approached. A shallow crossing would provide more warning and may be recoverable once it begins. The airspeeds at which such shallow crossings occur should not be taken as precise. Small errors in the analysis that may raise or lower the modal line will result in relatively large changes in the flutter speed associated with the mode. Modes that cross shallowly and then recross to the stable side of the plot are called "**hump**" or "**dome**" modes (see Figure 6.4) and may produce **Limit Cycle Oscillation** (see section 6.4.6) but is unlikely to produce explosive flutter. Hump modes are most common in store flutter and may be aggravated by elevated acceleration ( $g$ ) loads.

### **6.3.2 PK-METHOD**

The PK-method was created at the Royal Aircraft Establishment and is thus occasionally referred to as the **British method**. It assumes a response of the form  $e^{pt}$  prior to flutter where  $p$  can be either a real or a complex number

$$p = \sigma + i\omega \quad (6.12)$$

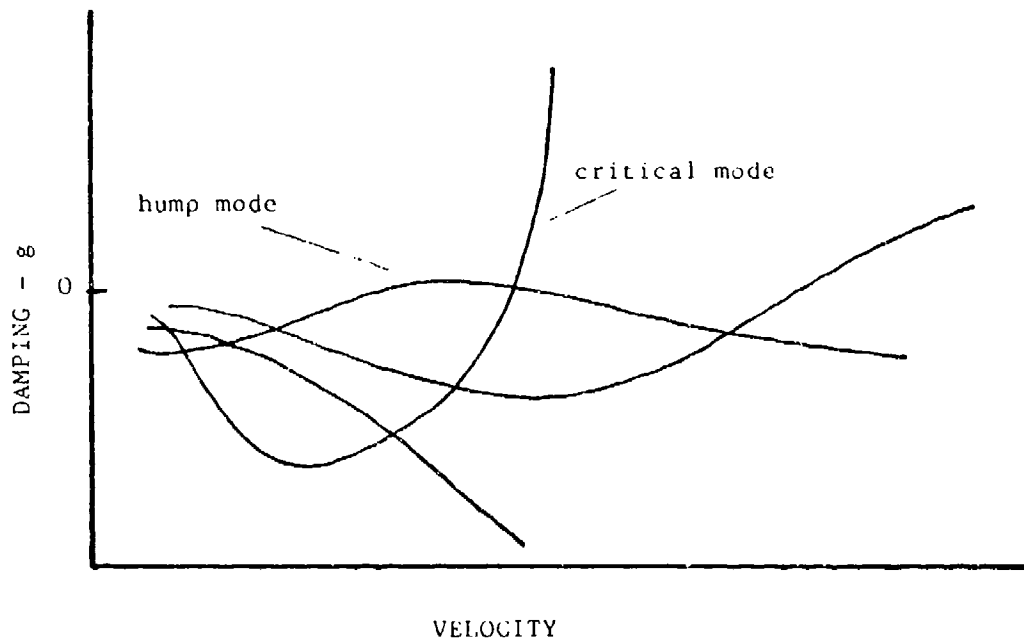


Figure 6.4 Example V-G Diagram

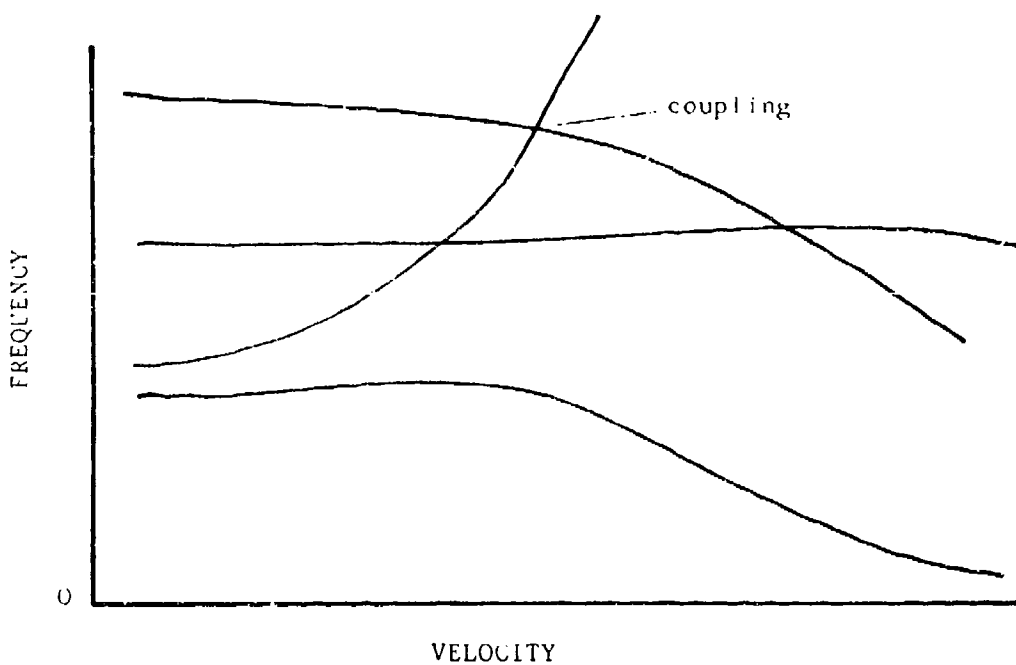


Figure 6.5 Example V-f Diagram

The  $-\omega^2$  of equation 6.7 is replaced by  $p^2$ . The assumption that  $p/(i\omega) = 1$  allows the imaginary part of the aerodynamic matrix to be multiplied by this ratio without effect and is called the aerodynamic damping. It may then be combined with the equivalent viscous structural damping to create the real **damping matrix [B]**. The real part of the aerodynamic matrix, termed the **aerodynamic stiffness**, is then combined with the structural stiffness matrix to form a **[C]** matrix. The resulting formulation is

$$[ p^2[M] + p[B] + [C] ] = 0 \quad (6.13)$$

The equation is solved for the eigenvalue  $p$  which will be of the complex form

$$p = \omega(\gamma \pm i) \quad (6.14)$$

For small damping the artificial structural damping will be equal to

$$G = 2\omega\gamma = 2\sigma \quad (6.15)$$

in rad/sec where  $\sigma$  is the estimated aerodynamic damping in the system.

### **6.3.3 P-METHOD**

The "P-method," an American modification of the PK-method, gives better subcritical trends for the heavier damped modes by assuming damped harmonic functions for the generalized coordinates. For this approach, the  $\Omega$  in equation 6.5 becomes

$$\Omega = \omega(v + i) \quad (6.16)$$

where the  $v$  is the viscous damping coefficient. Using the reduced frequency

$$\Omega = U k(v + i)/b \quad (6.17)$$

where the  $k(v + i)$  term is called  $p$ . The equation to be solved for this method is now

$$[(U^2/b)^2[M] + [K] - (\rho U^2/2)[A]](\bar{q}) = 0 \quad (6.18)$$

The solution procedure is much the same as in the K-method except for the relationships

$$\omega = (U/b)\text{Im}(p) \quad (6.19)$$

$$v = U\text{Re}(p)/(b\omega) \quad (6.20)$$

### **6.3.4 OTHER METHODS**

A variation of the K-method is the **KE-method** which neglects viscous damping and eliminates eigenvectors from the output. While much more limited than the standard K-method, it allows many more modes to be followed much more carefully without increasing the computer resources required.

Another flutter prediction method is to assume a mode shape that the structure may take on and use this in an energy analysis to arrive at the associated modal frequencies. This approach tends to be very involved and is still limited at this time.

In an effort to simplify the aerodynamic loads model, a quasi-steady or quasi-static assumption is made. This is generally only considered valid when the reduced frequency is much less than 1.0 ( $k \ll 1$ ). That is, the airfoil is not in motion and the surrounding flow is in static equilibrium. Such an assumption generally produces large errors subsonically but may be acceptable at supersonic and particularly hypersonic airspeeds.

Aerodynamic and stiffness formulations are many and varied. The general dynamic equation formulation also show some variations dependent upon application and the individual desires of the user. A great number of mathematical tricks are common to simplify the matrix operations, such as converting the mass matrix to an identity matrix or diagonalizing other matrices. Some eigensolution techniques require the flutter mode to be assumed first. The degree of accuracy is also very broad and the results are very much subject to interpretation and the experience of the analyst. This presentation is, therefore, a general overview only of a field which is still growing. Detailed examples of flutter analysis can be found in some of the references provided at the end of the chapter.

## **6.4 OTHER AEROELASTIC PHENOMENA**

There are a number of other structural dynamic effects that must be dealt with, often in ways similar to flutter. Aeroservoelasticity and acoustics are dealt with separately in Chapters 8.0 and 9.0, respectively.

### **6.4.1 PANEL FLUTTER**

An unsteady airload on the exterior skin of an aircraft can cause a periodic expansion and contraction of the membrane between supporting or stiffening members to produce a traveling or standing wave in the material. This single degree of freedom flutter phenomena is most often seen on the forward fuselage. The B-1 bomber experienced annoying panel oscillations in this part of the structure. Frequencies on the order of 300 Hz are normally associated with panel flutter. Very high speed aircraft can experience destructive panel flutter. It can be eliminated by increasing the stiffness of the surface by substitution of a thicker material or one with a higher modulus, or by addition of another stiffener inside the panel. The RF-4C experienced a vibration that began at exactly a certain supersonic Mach number. It was isolated to a fuselage door that was "oil canning" because a stiffener had somehow been left out in manufacturing. The fix was obvious.

### **6.4.2 BUZZ**

Flutter can occur as a single degree of freedom mode. This type of flutter is called "buzz" and can involve only small amplitude oscillations without the potential for destructive flutter or very large and dangerous motion. It is caused by phase lags associated with boundary layer or shock wave effects and interactions which result in the loss of aerodynamic damping. Separated flow over the control surface, perhaps caused by a shock, or the position of the shock on the surface itself are common causes. Inlet buzz in supersonic aircraft is caused by the oscillation of a shock wave within the inlet. Panel flutter can be considered a special case of buzz but limited

to membranes between supporting structure. Even if of limited amplitude, buzz is undesirable because of its tendency to distract the pilot and the potential for structural fatigue or over-stress.

There are a number of solutions to the buzz problem that do not require serious redesign. One approach is to change the flow over the surface. Delay of flow separation by use of vortex generators (see Section 2.2.5) are common. Mass balance has little or no effect. However, increasing the elastic hinge stiffness (often objectionable to the pilot and controls people) and decreasing the surface inertia have helped to increase the buzz onset speed. Rate dampers (damping only high velocity motion) have also been used.

#### **6.4.3 STALL FLUTTER**

Another rare single DOF flutter phenomena (typically wing torsion) is that induced by cyclical flow separation and reattachment on the wing at stall. A large change in lift forces occur in such a situation and create a powerful oscillating forcing function.

#### **6.4.4 DIVERGENCE**

Divergence of an aerodynamic surface is a non-oscillatory instability in which high velocity and deformation of the structure create aerodynamic forces which tend to increase the deformation. While aerodynamic forces increase with airspeed, structural restoring forces are constant. Therefore, a speed may exist in which the two forces are in balance. Beyond this speed divergence is possible and will likely produce catastrophic failure of the structure. This speed is referred to as the divergence speed. The extremely light structures found in World War I aeroplanes, (the Fokker D-8, as an example), and the very thin wings on early supersonic aircraft were particularly susceptible to this phenomenon and failure of wings in operation was not unknown.

The swept wing is characterized by a coupling between structural bending and twisting. The upward bending of an aft swept wing results in a reduction in angle of attack in the streamwise direction producing a negative increment of lift. This negative lift effectively opposes further nose up twist of the structure. Divergence of an aft swept wing is, therefore, unlikely because of the stabilizing influence of the wing torsion. The opposite is true for forward swept wings wherein nose up twisting occurs with bending; a destabilizing effect. Only moderate amounts of aft sweep are sufficient to raise the divergence speed to the extent that divergence becomes practically impossible. Forward sweep of even small amounts can produce divergence at relatively low airspeeds. Divergence is not eliminated, only delayed by design to speeds beyond the craft's airspeed envelope. The X-29's forward-swept wing would diverge if the aircraft is just 15 percent beyond its design limit speed. Even this could only be achieved by careful tailoring of the bending and torsion response of the wing by use of composite laminate construction (see Section 3.3).

If inertia effects in equation 6.3 are disregarded then a determinant suitable for divergence speed calculations results. For this steady formulation the unsteady aerodynamic operator may be used with evaluation at a frequency of zero. The solution of the characteristic equation then yields a series of eigenvalues, the largest of which corresponds to the inverse of the divergence dynamic pressure. Divergence, a static phenomenon, can be considered as flutter at zero frequency.

#### **6.4.5 CONTROL REVERSAL**

Lateral control reversal refers to an aeroelastic phenomena whereby wing deformation reduces the effectiveness of a roll control device to zero. The trailing edge down deflection of an aft mounted aileron or flaperon produces a leading edge down twisting moment due to an aft shift of the center of pressure on the wing. This causes a reduction in the effective AOA of the wing-aileron combination and reduces the rolling moment normally expected of a rigid wing. This twisting moment increases with airspeed until reversal speed is reached where rolling moment from the control deflection is reduced to zero. Beyond this speed aileron deflection will produce rolling moments opposite to the normal control sense. Reversal is aggravated by wing sweep which normally produces torsional structural deformation under load. Early models of the B-52 suffered degraded aileron effectiveness at high speeds because of this effect, which led to the addition of spoilers on later model of the aircraft. The term used to evaluate the control reversal effect is  $P_b/2V$  (roll rate times wing mean semi-chord divided by twice the velocity) called the **helix angle** or **roll effectiveness**. When this term becomes negative roll reversal occurs.

#### **6.4.6 LIMIT CYCLE OSCILLATION**

Another flutter phenomena occurs when the aerodynamic damping exactly cancels the structural damping. This is called limit cycle oscillations (LCO) and is characterized by sustained sinusoidal structural oscillations that neither increase nor decrease in amplitude over time (see Reference 14). LCO has also been called **Limit Cycle Flutter** or **LCF** in some sources, but is not flutter by a strict definition. So far LCO has defied accurate prediction and wind tunnel study due to nonlinearities. Leading edge control devices and increasing load factor or AOA have been associated with LCO. The amplitude of the oscillation will generally increase with airspeed. Where a control surface rotation is involved the constraints on divergence may be simply the rotation angle stops of the surface. Limit cycle oscillations will continue indefinitely until a change in airspeed, altitude, or some disturbance initiates a change in aerodynamic damping. Since the change in flight conditions required to go from a slightly positively damped vibration to a negatively damped one are very small, limit cycle oscillation is not observed during most aircraft testing. LCO has most often been observed during carriage of heavy underwing stores, most notably on the F-16, F-111, and the F/A-18 and so has been also called **Heavy Store Oscillation (HSO)**.

LCO has been both resistant to a divergent response and highly susceptible to it. In any case, and as with any neutrally stable condition, it should not be taken lightly. At the very least, the oscillation can promote fatigue (particularly if control surface rotation is involved), will be uncomfortable to the aircrew, and probably effect the efficiency of onboard weapons. During flight testing, a "knock it off" condition during LCO has been a certain structural deflection limit (such as wing tip displacement) that could lead to an overload state. Since such deflection is seldom measured directly, the LCO frequency and peak acceleration is used as a measure of the displacement (see Section 4.4.1). A limit on peak acceleration for a given frequency ensures that excessive deformation does not occur.

#### **6.4.7 BUFFET**

Buffet is the transient vibration of structural components induced by flow separation from components upstream of it, another aircraft ahead, or random air turbulence. As these impulses are generally random, the gust loads effects are the usual concern. An example of this is horizontal tail buffet from wing flow separation at angles of attack approaching stall. Such

empennage buffet was experienced during the initial flight testing of a Douglas dive bomber of World War II when the large dive flaps ahead of the tail on the wings were deployed. The buffet produced severe structural deformation and was cured by perforating the flaps with a pattern of large holes. An example of this is a 300g low amplitude response at the tip of the F-18 stabilators resulting from impingement of vortices shed from the aircraft's leading edge extensions (LEXs) at high angles of attack. This response produced cracks in the honeycomb core of the stabs and even leading edge balance weight separation. The solution was the substitution of a stronger core and the addition of more composite plies to stiffen the structure and permit the removal of the balance weight altogether. Similarly, cracking in the vertical tails of the F-15 was caused by impingement of vortices shed off of the forebody during high angle of attack maneuvering.

#### **6.4.8 MECHANICAL VIBRATION**

This vibration is induced by internal sources, most commonly the engines. High frequency engine dynamics can couple with airframe modes to produce annoying vibrations or, over long exposure, metal fatigue. An example of this are the engine vibrations that occurred during the early flights of the British TSR-2 prototype. A low-pressure compressor shaft failure induced by a cooling airflow instability had the unfortunate tendency to cause the engine to explode above 97 percent power. This mandated that the pilots maintain this setting or lower. An out-of-tolerance reheat fuel pump also caused high amplitude vibrations. At 87 to 96 percent power this vibration was near to the resonant frequency of the pilots' eye balls and caused their vision to wash-out.

#### **6.4.9 DYNAMIC RESPONSE**

This area is concerned principally with the loads induced by transient response of a structure due to such inputs as gusts, landing impacts, or taxi operations. An example occurred during the testing of the F-16XL when a flaperon torque spindle failed while the surface was under load. As the flaperon oscillated, seeking freestream deflection, it set up an vibration in the wing that was amplified at the tip. The rapid, high g deflections at the wing tip caused the tip missile and launcher to separate from the plane.

#### **6.4.10 AEROTHERMOELASTICITY**

As a metal is heated its modulus of elasticity (see Section 3.2.2) decreases. The magnitude of this decrease increases the higher the temperature becomes. The friction of the air upon the outer surface of an aircraft can produce extremely high temperatures at high Mach numbers (see Figure 6.6). In this regime the reduction in the stiffness due to aerodynamic heating can significantly reduce the natural frequencies of the structure and lower its resistance to static and inertia loads associated with vibration (see Reference 4). These factors may act to allow a modal coupling that would otherwise not have appeared. Such an event was found during development of the X-15 hypersonic rocket aircraft. In a certain load and heating state the torsional rigidity of the stabilators were reduced to the point of permitting serious buckling problems. Changes to cure the problem resulted in a 21 percent weight increase in the surfaces.

### **6.5 PRELIMINARY GROUND TESTS**

Because mathematical modeling of the aerodynamics and structural properties of an aircraft are so subject to uncertainties, many ground tests are done with models and the full scale article prior to the beginning of flight testing. The results of such tests are used to improve the computer

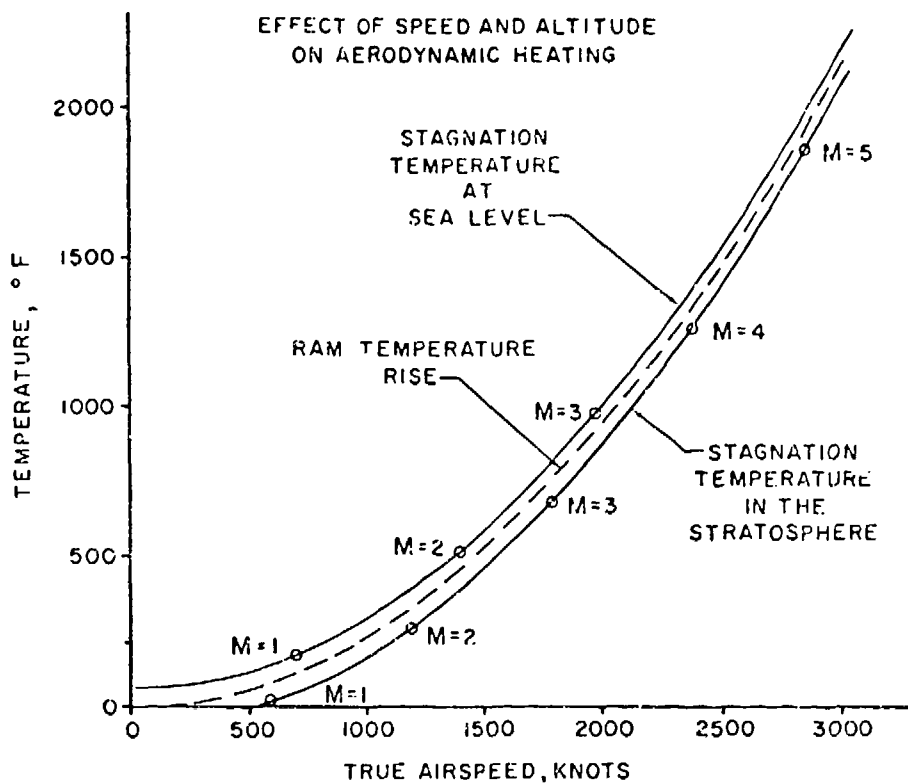


Figure 6.6 Stagnation Temperatures

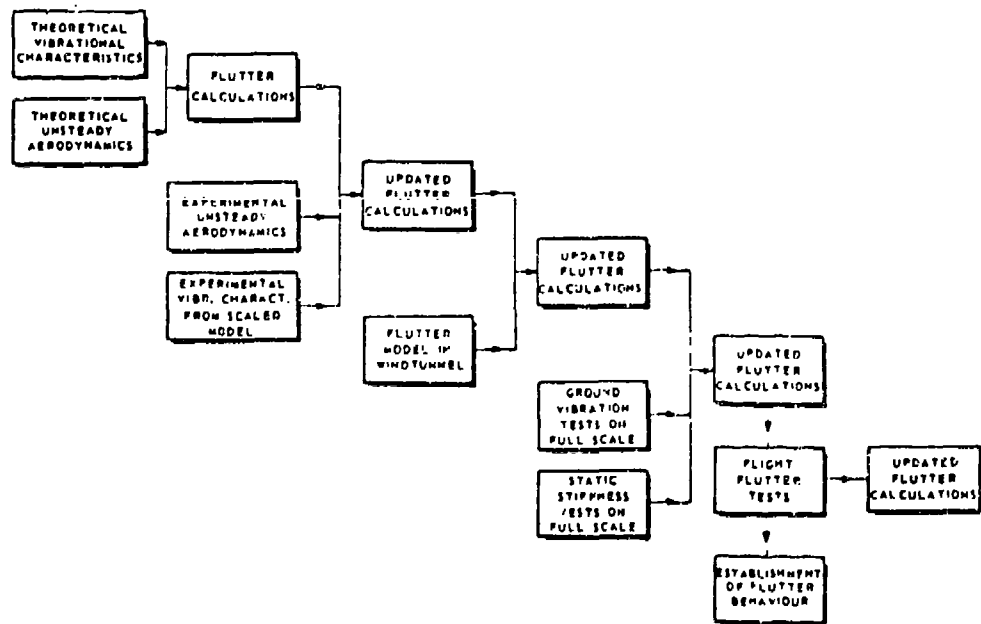


Figure 6.7 Diagram of Flutter Investigation During Development

models and refine the estimates used in planning the flight test. The entire development flow is shown in Figure 6.7.

### **6.5.1 WIND TUNNEL TESTS**

One preliminary test conducted prior to flutter flight test of an aircraft is a wind tunnel flutter test. An elastically and mass distribution-scaled model of the aircraft is subjected to an airstream that has also been scaled to the same dimension (i.e. reduced frequency number) as the aircraft. Only a partial model (tail surfaces removed, for example) may be used in an effort to isolated effects. The scale model of the entire aircraft may be "flown" either free or on bungees at speeds corresponding to the envelope of the real aircraft, and the flutter mechanisms are verified as much as possible. It is common for the scale airspeed (occasionally produced with a gas other than air) to be taken beyond the normal envelope to verify the flutter margin. Definitely checking for the critical mode by observing the flutter (hopefully without destroying the model) is also done. Testing and data reduction methods are much the same as for full scale flight tests. General tunnel turbulence, upwind oscillating vanes, and external inputs (tapping the surface with a rod) are common excitation means. Mass, stiffness and shape changes can be made relatively easily and the effects tested on the model before being incorporated in the actual design. The wind tunnel data is always subject to errors involved in accurately modeling the aircraft and the airflow. Corrections to the wind tunnel data for tunnel effects and compressibility are typically performed, to include **blockage effects** (velocity errors).

### **6.5.2 GROUND VIBRATION TEST**

One of the typical essential preliminary tests conducted on an aircraft is the **ground vibration test** (GVT). This test may be performed at an early stage on the wind tunnel model discusses in the previous section to ensure that it adequately replicates the desired stiffnesses. A full scale GVT is mandatory for new designs and for any substantial changes to an existing aircraft. This test is used to verify and update the flutter model as well as provide a means for identifying modes from frequencies found in flight test data. Details of the GVT are contained in the next chapter.

## **6.6 FLUTTER FLIGHT TESTS**

Flutter flight tests of aircraft are performed to verify the existence of the flutter margin of safety estimated by analysis. Flight near the estimated flutter speed entails a risk of accidentally encountering the flutter sooner than anticipated with the potential for a catastrophic structural failure. For this reason, the flight envelope is cleared for flutter in an incremental fashion from a considerably lower airspeed by measuring the frequency and damping of the vehicle's response to an excitation at successively increasing increments of airspeed. The frequencies permit an identification of the modes of the response by comparison with ground test and analytical data. If sufficient instrumentation is installed, actual mode shapes can be determined to supplement the frequencies in modal identification. The damping provides a quantitative measure of how near to flutter each airspeed point is.

### **6.6.1 EXCITATION**

Several methods have been used to excite the aircraft structure to permit the individual response modes to be observed and their frequencies and dampings obtained. Some methods are more suitable than others for certain frequency ranges, nature of the modes sought to be

excited, and amplitude or amount of energy to be put into the modes. Experience will also help in selection of the proper system to use. Whatever the method used it is important that the excitation be applied as close to the surface of interest as possible. An impulse at the tip of the wing may not have much chance of sufficiently exciting a high frequency horizontal tail mode for adequate analysis. The position of the excitation source relative to the node lines of the significant modes is also critical. Applying an impulse directly to the wing elastic axis has no chance of producing any torsional displacement. But, an impulse off of the elastic axis will produce both torsional and bending excitations. An impulse close to the node line will not produce as much displacement as the same amplitude of impulse farther from the node line by virtue of the longer moment arm.

#### **6.6.1.1 PULSE**

Pulse or raps are sudden control impulses to produce sudden control surface movements that can excite up to 10 Hz modes very well, occasionally to 30 Hz not so well. The objective is to produce an input that most closely approximates a "step" input since such an input contains the highest frequency content possible. Therefore, the sharper the input the better the data. Longitudinal stick raps, lateral stick raps, and rudder kicks are the most common pulses used. The choice of pulse direction depends upon the modes sought to be excited.

For pulse excitation the pilot will stabilize the aircraft on condition and make the rap. The stick pulse can be made by striking the stick with the palm of the hand or with a mallet. Aircraft with automatic flight controls can be programmed to make these pulses without pilot intervention. Sometimes a rapid stick movement with the stick held in the usual manner, a "singlet," is sufficient. More energy may be generated by a "doublet" which are two such inputs in rapid succession in opposite directions. But, the singlet and doublet can only be done at a low frequency compatible with human limitations, about 4 Hz for stick inputs and less for rudder pedal inputs. A **control oscillation** is a variation of the doublet but with some specified time between the two inputs. An example may be a one inch aft stick deflection, hold for three seconds, and a return to neutral. A time to produce the control input, a "ramp-up" time such as one second for the one inch stick deflection, may be specified. The oscillation is tailored to excite a specific mode, such as a 3 Hz fuselage first vertical bending mode for the maneuver just described. The pilot may deflect the control surface and then fly "hands-off" to allow the aircraft oscillations to naturally damp out ("stick-free" pulse) or he may arrest the stick as it returns to the neutral position ("stick-fixed" pulse), depending upon which technique yields the best response from the aircraft. A variation is to hold the stick as the rap is made. For a large aircraft a rap may not produce enough control deflection for sufficient excitation. In this case a rapid, full-deflection displacement of the control followed by a release is useful.

It may be desirable to make several raps and to average either the time histories or fast Fourier transformations (FFTs see Section 11.3.1) of the raps together to remove noise and other corrupting influences. The principle deficiencies of the pulse technique is the non-selectivity of the frequencies to be excited and the generally poor energy content above about 15 Hz.

#### **6.6.1.2 SWEEP**

This is the most attractive and preferred excitation means but is also one of the most complex and expensive to implement. Sweep data and burst data (next section) requires the use of an excitation system to "shake" the aircraft or individual surfaces in flight. Frequencies as high as 65 Hz can be excited by this method. The frequency response characteristics of the exciter system or control surface actuators will determine the frequencies that the system can excite in the

aircraft. Hydraulic or electric actuators generally show an attenuation of response amplitude beyond 30 Hz, but the excitation in this part of the spectrum can lead to responses at high frequencies. This method of excitation requires some time and thus may be unsuitable if the test condition can only be obtained in a dive. Several different types of sweep excitors have been used.

B-1 flight testing included use of a "wand" at the wing and tail extremities (see Figure 6.8). The wand consists of a mass placed at the end of a pivoted arm attached to the tip of the structure. The oscillation of the mass about the pivot point produces a periodic structural response by virtue of the inertial displacement of the mass on the arm. Other such inertia excitors use out-of-balance rotating masses. One drawback to this technique is the disturbance in the airflow if the wand extends beyond the surface of the aircraft. Another disadvantage is that larger masses are needed to excite lower frequencies and the overall system weight may become prohibitive.

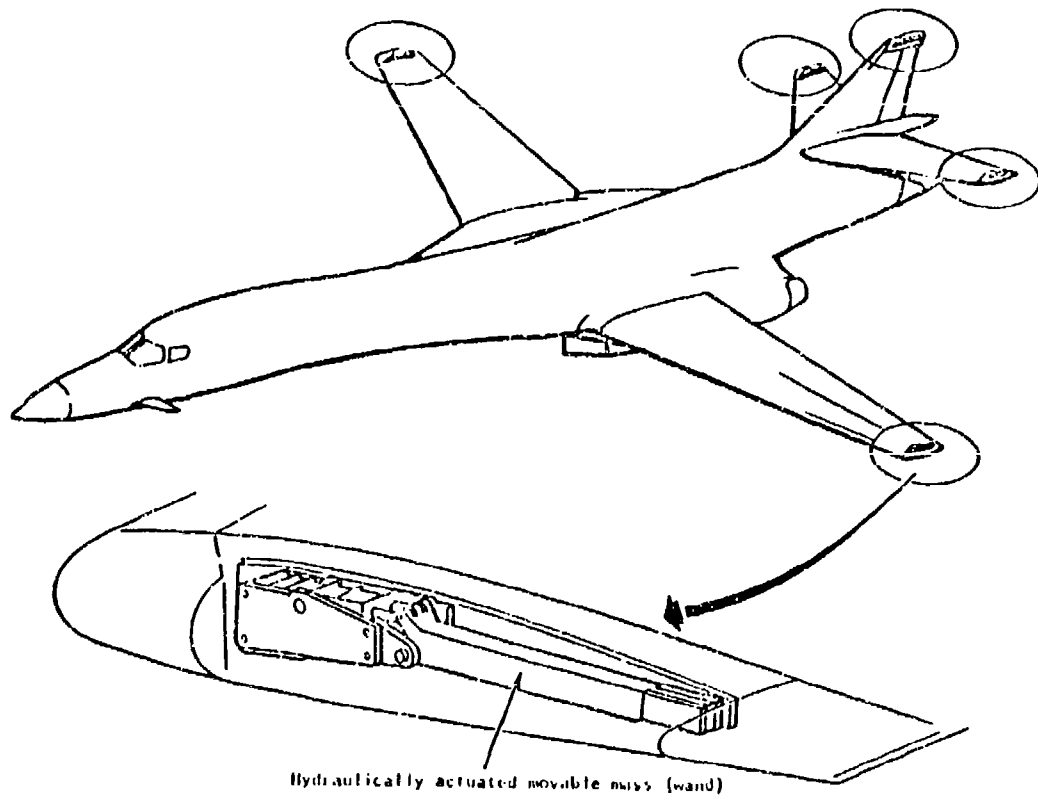


Figure 6.8 Wand Flutter Exciter System

The French have done quite a bit of work with electrodynamic excitors. Akin to electrodynamic shakers used in GVTs (see Section 7.6), a mass is suspended within the structure by springs. The mass incorporates coils that are in close proximity to coils attached to the structure (see Figure 6.9). By sending an alternating current through the coils the mass can be made to move within the electromagnetic field. The frequency of the movement is proportional to the electrical signal. Although successfully used on many European projects such as the Transall and Concorde, the advantages and disadvantages are much the same as those for the other systems here discussed with the added difficulty of access once the units are enclosed within the aircraft structure.

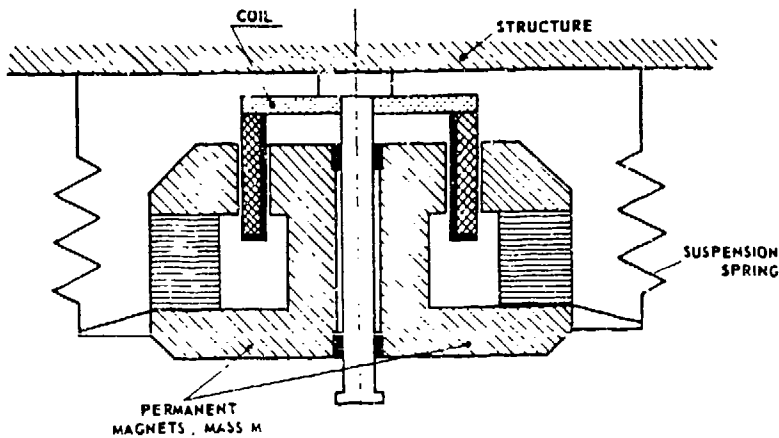


Figure 6.9 Electrodynamic Exciter

Oscillating vanes or "flutterons" mounted on wings and tails have been used many times, namely the T-46 and A-10 test programs (see Figure 6.10) as well as several recent airliner tests. The vanes create a varying aerodynamic force as well as an inertia input that acts on the aircraft structure. Several sizes and masses of the vanes may need to be available as the speed and dynamic pressure at different points in the envelope alter the effectiveness of the inputs. The great advantage of this system is that it can easily excite low frequency modes and higher frequencies are only limited by the frequency response of the vane actuator. Below 3 Hz the input may not be sufficient to adequately excite the structure under test. A disadvantage is the change to the mass distribution of the surface which it is attached and the disturbance to the normal airflow that its presence and operation produces.

For "fly-by-wire" aircraft, using the flight control system as an excitation means has the attraction of requiring no additional hardware to the basic aircraft. The oscillatory signal to the control surface actuator(s) are produced by a special function of the flight control computer. The pilot is generally provided the means of varying the sweep rate, end frequencies, and amplitudes of the inputs. Random inputs by this means is also possible. There is difficulty in exciting high frequency modes because the attenuation or rate limiting characteristics of the actuator will limit the displacement or level of excitation in this part of the spectrum. This method has been used with great success on the various F-16 test programs.

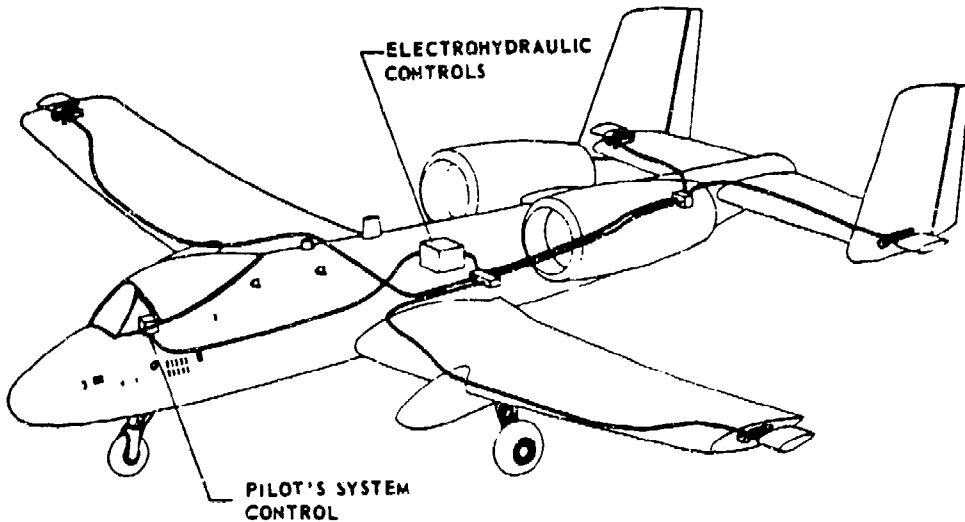


Figure 6.10 Vane or Flutteron Exciter

When SWCCP data is collected, the excitation system is run through one or more frequency sweeps at a predetermined rate. Common rates are linear, such as 1 decade/sec, or logarithmic variation. The proximity of modes and the potential for noise problems may effect the selection of sweep rate. Sweep data is normally analyzed on the computer to determine frequencies to use for a burst-and-decay method or to stand on its own. This method is analogous to conducting a GVT in flight. Its greatest advantage is to directly apply energy into modes that may otherwise be very difficult to excite with sufficient energy by other means.

As with GVT excitation (see Section 7.8.3.i), sweeps have a tendency to increase the noise from local nonlinearities. A sweep performed too quickly will also tend to make the modes appear to have a slightly greater frequency and damping value than they really do.

#### **6.6.1.3 BURST-AND-DECAY**

Burst-and-decay data is collected by running the excitation system at a certain frequency and then shutting it off to allow the structure of the airplane to damp itself out. This is typically done at the frequency that will excite the critical mode(s) to specifically check the damping there. Generally only a few cycles are necessary before stopping to allow the decay. For a mechanical excitation system, the wind-down characteristics, that is its ability to cease movement when commanded without overshoots, becomes important to how clean and faithful the resulting decay data is.

#### **6.6.1.4 PYROTECHNIC**

The so called "bonker" is a very small pyrotechnic charge that is typically placed externally near the trailing edge of a control surface and detonated electrically. The tiny explosion produces a sharp pulse excitation that comes very close to simulating the ideal step input. A series of such

charges may be placed along the trailing edge so that many such impulses may be produced on a single flight. The disadvantage of the method is the limited number of excitations that can be produced in a flight and the disturbance of the normal airflow that the presence of the charges and their wiring create. The bonker has seen wide use in Europe on such programs as the Airbus, Jaguar and Tornado.

#### **6.6.1.5 AIR TURBULENCE**

Random air turbulence can be used as a source of excitation. Even if not felt by the pilot, there is always some energy content to an air mass. Generally, low altitudes have a greater magnitude of this excitation. The area around Edwards AFB is ideal for this technique in that deserts have many rising columns of air and high winds that, when flowing over mountains, produce a good deal of energy in the air. Weather fronts also produce turbulent air. This technique, while attractive from a cost standpoint, must be used with prudence. There is generally very little energy to be obtained in the spectrum above about 20 to 30 Hz and some structures will not respond to turbulence as well as others because of differences in wing loading (see Reference 14).

The normal procedure is to have the aircraft stabilize on condition and collect response data for some pre-determined time period, as much as two minutes. The resulting data (the response of the aircraft to the random inputs) is collected on the computer and analyzed to determine the frequencies and dampings of the observed modes. A "near real-time" computer analysis is required for point-to-point clearance if dampings and frequencies are to be tracked. The approach to an instability may sometimes be seen by a "burst", a brief period of lowly damped, higher amplitude response, or by Lissajous figure indications (See Section 11.2.6). This is referred to as incipient flutter.

Another approach using turbulence is to measure the gusts with a "gust probe", or very sensitive alpha (angle of attack) and beta (sideslip) vanes on a nose boom for measuring vertical and lateral gust components. An accelerometer or strain gage may be mounted on the boom to allow rigid body aircraft and boom dynamics to be removed. The result is a measure of the input forcing function with the resultant aircraft structural dynamics measured in the usual way. Knowing the input and output allows a transfer function (see Section 11.3.5) to be formed. This provides a powerful means of predicting modal response at other points in the flight envelope.

Deployment of a speedbrake, landing gear, flaps or other device on the aircraft that will produce a great deal of buffet vibration, and even flying in the wake of another aircraft, have been also used for turbulence excitation. These techniques are likely to introduce a dominant response representing the primary vibration frequency of the device (vortex shedding rate off of the speedbrake, for example) which may mask true structural responses.

#### **6.6.2 PROCEDURES**

In the normal conduct of a flutter test, a buildup procedure is used whereby less critical points are flown prior to more critical ones. This technique allows the engineers to determine damping trends as dynamic pressure and Mach number increases. These two parameters are normally treated separately. Because high Mach numbers are generally only possible at high altitude and high  $q$ 's are obtained at low altitudes, there is usually a considerable altitude difference between the two test conditions. If the critical mode(s) are suspected to be altitude critical then a build-up in altitude may be necessary. In any event, a minimum safe altitude for the testing should be established. If  $q$  is determined to be more critical than Mach (as is

commonly the case), the Mach points may be flown first, although jumping between the two conditions in the course of the testing to for the purposes of a concurrent build-up in both parameters is not unknown (see Figure 6.11 and Reference 9). Testing across the transonic range is important because of the significant aerodynamic changes that occur there. Having the pilot maintain precise airspeed control and using corrected airspeed readings (calibrated airspeed to match a target equivalent airspeed, see Section 2.2.2) is essential to avoid overspeeding a test point and creating a potentially hazardous situation. A careful airspeed calibration must precede or be conducted concurrent with the flutter program.

Generally, the buildup will consist of points of ever-increasing airspeed. The airspeed increments between points will depend upon the proximity to the predicted flutter boundary and the confidence in the flutter analysis. Smaller steps are required when close to a flutter condition or where a rapid decrease in damping is seen. Naturally, some practical airspeed must be selected to begin the buildup since the aircraft must takeoff and climb to the test altitude. The choice of this airspeed must be based upon conservative review of the predicted flutter modes and flutter margin. A reasonable tolerance on airspeed and altitude must be established and published in the test plan. Naturally, no overspeed at the aircraft maximum airspeed is permitted. The test conductor must remain flexible and be prepared to take smaller airspeed steps than the test cards dictate if low damping is observed. This decision can be facilitated by real-time analysis of the data, either on the stripchart, computer, or both, prior to each test point. The aircraft is restricted to the envelope that has been cleared by flutter testing. This is necessarily much less than the ultimate flight envelope of the aircraft but will slowly be expanded to this objective as testing proceeds.

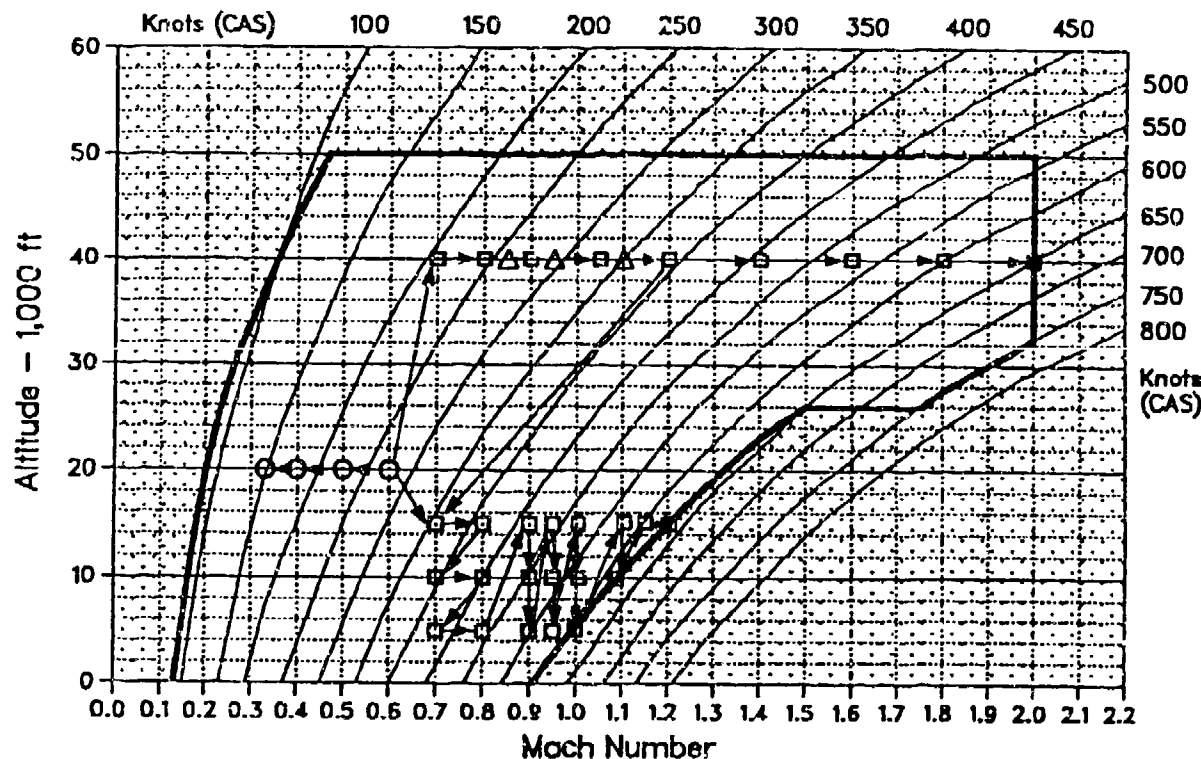


Figure 6.11 Flutter Expansion Example

The maneuvers used in flutter testing depend upon the type of data to be collected. If sweep, burst-and-decay, or random data is acquired, the aircraft will stabilize on condition (i.e., fly a constant airspeed and altitude) for the time required. Sometimes, when dive test points have to be flown, the aircraft will reach a target airspeed, and the random, burst, or sweep data will be taken between a band of altitudes to prevent significant changes in the air density, i.e. dynamic pressure. In some test programs an airspeed schedule is flown to ensure that the aircraft flies along a given flight profile and does not overshoot its target airspeed,  $q$  or Mach. This is usually done when the test conductor wishes to verify flutter free flight along the redline airspeed curve after clearing to this speed at discrete altitudes. Instead of flying many stabilized points at many different altitudes, the plane is dived along this "line" and brief excitations made to verify that no lowly damped responses are seen. The whole line can be cleared in one test maneuver. This technique is good for demonstration purposes but is not advised if useful damping values are sought. It should only be done after the test team is reasonably confident that flutter will not occur along the line because the dive does not allow as quick a recovery from a flutter event as a straight and level condition.

If personnel at the ground telemetry station or the pilot(s) sees flutter beginning then immediate action must be taken to save the aircraft and possibly the aircrew. The command "Terminate, Terminate, Terminate," or similar words like "Abort" and "Stop" are transmitted to the pilot(s). A flutter engineer monitoring the aircraft response should have a direct radio link to the aircraft to reduce the reaction time needed to have someone else communicate a termination command. The immediate cockpit action must be to pull the engine power back to slow the aircraft from the critical speed as quickly as possible. Deploying speedbrakes (airbrake) or similar devices may also be advisable, but caution is advised since some speedbrake locations may aggravate flutter. Assuming a slight nose high attitude will also assist in slowing the aircraft. This last maneuver is not advised when store loadings are involved since g-loads may aggravate store flutter. If a loaded maneuver is in progress, unloading and returning to straight and level flight is required. Mechanical excitation systems should be immediately arrested if in action. It is important that the pilot have direct means of stopping the exciter, usually with a switch on the control column or throttle. The structural oscillations may not immediately die out when backing off the test condition as a chance input may have triggered the response beyond a lower possible onset speed.

A safety chase aircraft is almost always mandatory for flutter testing (see Chapter 13.0). Because flutter testing is typically labeled as at least Medium Risk, only minimum flight crew is used. The airspeed system should have been calibrated so that a confidence of 2 to 3 kts in the airspeed readings exists. The aircrew should be cautioned against overspeeding the test points. Such testing is normally conducted in clear air without turbulence (unless used as an excitation source) since it may corrupt the data and add to analysis difficulties. Since the fuel mass in wing and fuselage tanks can significantly effect modal responses, analyzing and testing the aircraft at various fuel states may be advisable. Since the impulse caused by the sudden release of stores may also excite flutter, apart from the loads aspect, this should also be considered in analysis and perhaps flight tested. It is also usually advisable to perform flutter testing with any control augmentation system in both the ON and OFF states in the event that these systems are adding damping which is hiding a potential flutter response.

Consistent and proper servicing of the aircraft is important to avoid shifts in modal frequencies and dampings. The torquing of bolts holding major components on airframe, such as external stores, can be an important factor in stiffnesses. Wear of such components as hinges and bearings can change rotational frequencies. The X-29 had a rubber-like fairing to fill the gap between each canard and the fuselage. During the course of flutter testing this fairing slowly abraded and caused an increase in the canard rotational frequency.

## **6.7 DATA REDUCTION**

The methods used to analyze flutter test data are discussed in Chapter 11.0. The results of data analysis are typically airspeed ( $V$ ,  $M$ , or  $q$ ) versus frequency ( $V-f$ ) and airspeed versus damping ( $V-G$ ) showing the modes being tracked. Clearly, some prior knowledge of modal frequencies are required to identify modes from the flight test data unless sufficient instrumentation has been installed to allow actual mode shapes to be determined, which is rarely the case. If some measure of the structural input is available then more detailed systems analysis is possible using transfer functions (see Section 11.3.6). This data is used to establish a safe flight envelope for the aircraft based upon extrapolation of the damping trends to the case of zero damping (onset of flutter) and application of the 15 percent safety margin in airspeed below the predicted "flutter airspeed". Usually, the aircraft is not tested at damping values less than 2 percent damping or 0.02 G (though 0.03G is specified by MIL-A- 0008&70). During stores testing of the F-16, damping as low as 0.01G was permitted because of a frequently encountered LCO (0.0G), see Section 6.4.6.

The extent of the analysis of real-time data is at the discretion of the flutter test director. In some cases an experienced test director may be able to determine the damping by "eye-ball" the stripchart traces without extensive analysis. Some aircraft or modes are more easily excited than others and stripchart traces alone may be adequate for a point-to-point clearance. In other cases, particularly where more than one mode is present, more detailed analysis, perhaps involving computers, is required. Real-time analysis or even display of every flutter parameter may not be technically or practically feasible. The flutter engineer must apply his or her best judgment as to the most critical parameters. If stripchart traces show damping of 0.05G or less, or when more than one mode is present, then more detailed frequency domain analysis is advisable. If there is no transient response evident following termination of the excitation the response is termed "deadbeat."

If it is important to track damping of critical modes (both predicted and those found to have decreasing damping) for point-to-point flight clearance then a "real-time" analysis will be required before clearing the pilot to accelerate to the next test condition. The dominant mode appearing in the data is not necessarily the most important mode to watch. A mode that is not easily excited or seen may still have low damping and is waiting to make life interesting. Typically, only one of the two participating modes will show the rapid drop in damping as flutter is approached so it is important that the frequency shifts and damping of both components of the suspected flutter mechanism be tracked. Detailed analysis between flights should always be done using all available data to track frequency and damping of significant modes with the best precision available in an effort to predict flutter onset from the trends.

Modal frequencies and dampings can be extracted from the data using any number of the methods discussed in Chapter 11.0. By using an exciter system, it is possible to obtain an input function for transfer function and particularly coherence plots (Section 11.3.7). However, it is important to remember that the exciter signal or output is not the true or even the only forcing function acting on the aircraft. The changes to the airflow on the aircraft or the impulsive inertia change is the true structural input. Turbulence, general aerodynamics, and miscellaneous pilot and systems inputs will still be present as uncorrelated signals. These will impact the quality of the plots and may lead to erroneous conclusions.

In recent years a method for extrapolation of flutter test data by employing a two degree of freedom math model to predict the flutter onset (see Reference 11) has been developed. This has the advantage of using actual test data to provide a measure of the flutter margin from the

last test condition flown. While employing many limiting assumptions, these flutter margin calculations provide the flight test engineer with another tool for safe flutter clearance.

## **6.8 STORE FLUTTER TESTING**

The addition of external stores on the aircraft and the many download variations have a tendency to reduce flutter speeds. The modes that participate in a store flutter event are generally low order wing modes. Stores testing is generally restricted to the subsonic range due to aircraft limitations. Flutter speed tends to increase with asymmetric loads and modes become more difficult to excite. When doing a symmetric stores loading test it is important that the loads are as truly symmetric as possible, that is that everything on one side of the airplane weighs the same as everything on the other side. This should be verified by careful mass properties tracking. Fuel distribution should also be watched carefully. The aircraft to pylon, pylon to rack/launcher, and rack/launcher to store interfaces greatly increase the nonlinearities that can create analysis difficulties. Care should be taken to reduce these "rattles" as much as possible. It is critical that such attachment fittings as rack sway brace bolts be torqued down similarly and to maintenance specifications. Since the flutter speed of external store loading configurations are occasionally influenced by acceleration loads, such maneuvers as "windup turns" (see Section 5.7) may be used to produce these accelerations while some source used is to produce structural excitations.

Exciters have been incorporated directly into the stores or pylon/racks/launchers. This helps to ensure that the store is adequately excited without having to be concerned with amplitude or frequency attenuation through the intervening structure between the exciter and the store. A vertical and lateral accelerometer at the tip of the store, perhaps at the front and rear, and maybe on the pylon are very common instrumentation installations (see Figure 6.12).

Serious store oscillation or flutter problems can be remedied in whole or in part by the addition of isolators between the various components, or between the airplane and the store components. These usually take the form of dashpots to change critical frequencies, such as missile launcher pitch, and reduce the potential for adverse coupling. Slight changes in the store location can produce beneficial redistribution or move the store out of an adverse flow field.

## **6.9 RULES OF THUMB**

Certain facts derived from practical experience in the last 80 years of flutter flight testing are worth recording.

- a. Elevated AOA seldom aggravates flutter except where vortex shedding may act as an unsteady forcing function.
- b. An increase in distributed structural mass will tend to decrease natural frequencies while an increase in stiffness will tend to increase natural frequencies. Adding mass ahead of a surface's center of gravity will tend to lower torsional or rotational frequencies while added mass at the tip will tend to lower bending frequencies.
- c. In manned aircraft, modal frequencies up to 60 Hz, but occasionally as high as 100 Hz, are of concern depending upon the design. Damping values on the order of 0.01 to 0.30 G are to be expected.
- d. Control surface flutter modes may be altitude dependent, but few other types of flutter have displayed such a tendency.

e. As the number of control surfaces increase the higher the order of the modes that may participate in a flutter event. Generally, only a few modes above the fundamental modes are important as these lower order modes are more efficient at extracting energy from the airflow. For the F/A-18, with two leading edge and two trailing edge control surfaces, modes as high as the 25th in ascension of frequency needed to be considered in the analysis.

f. In general for wings, when torsional rigidity alone is increased, flutter speed also increases. However, when bending rigidity alone is varied, only a small difference in the flutter speed is seen. The minimum flutter speed will usually occur when the flexural rigidity becomes so large that the frequency of the uncoupled oscillation is equal to that of the uncoupled torsional oscillation. Further increase in this rigidity increases the flutter velocity.

g. Control surface backlash or free-play should be kept to less than 0.25 degree to assist in avoiding buzz (see Reference 6).

h. Most structural modes can be expected to show an increase in frequency as airspeed is increased because of aerodynamic "stiffening."

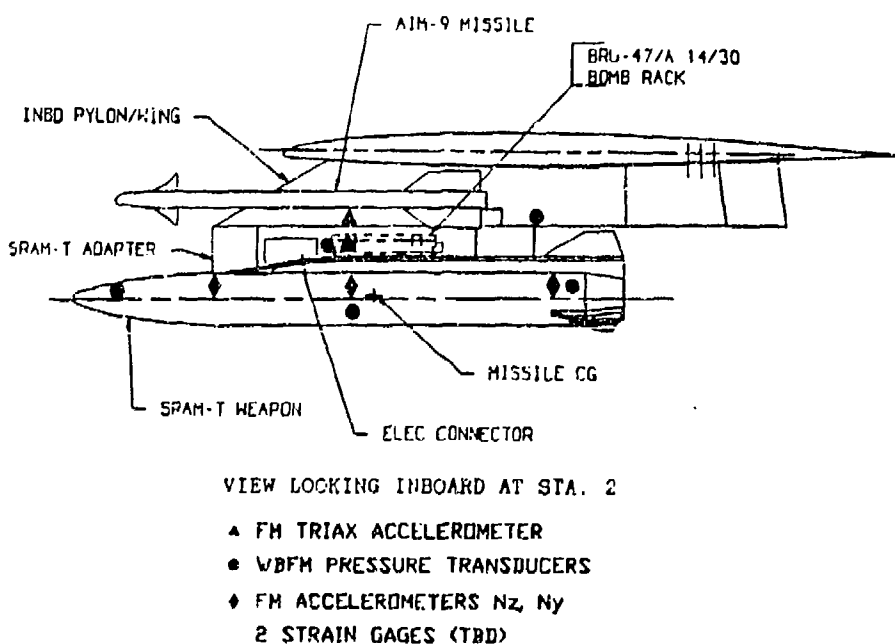


Figure 6.12 Example Store Flutter Instrumentation Installation

## NOMENCLATURE

A	aerodynamic operator
AOA	angle of attack
a	non-modal aerodynamics
B	damping matrix
b	reference semi-chord
C	stiffness matrix
DOF	degree of freedom
e	exponential constant
f	frequency
G	total system damping, hysteretic damping
GVT	ground vibration test
g	acceleration due to gravity
HSO	heavy store oscillation
Hz	Hertz
Im	imaginary part
i	complex number
K	stiffness operator
k	non-modal stiffness, reduced frequency
LEX	leading edge extension
LCF	Limit Cycle Flutter
LCO	Limit Cycle Oscillation
M	mass operator
m	non-modal mass
P	roll rate
p	complex operator
Q	generalized forcing function
q	dynamic pressure, generalized coordinate
Re	real part
rad	radian
t	time
sec	second
U	freestream velocity
V	velocity
$\gamma$	operator
$\nu$	viscous damping coefficient
$\lambda$	eigenvalue
$\rho$	air density
$\sigma$	operator, aerodynamic damping
$\Omega$	operator
$\omega$	frequency
L	Superscript
-	limit condition
	generalized coordinate, harmonic motion

## REFERENCES

1. Bisplinghoff, R.L., Ashley, H. and Halfman, R.L., *Aeroelasticity*, Addison-Wesley Publishing Company, Menlo Park, California, 1955.
2. Bisplinghoff, R.L. and Ashley, H., *Principles of Aeroelasticity*, Dover Publications, New York, New York, 1975.

3. Fung, Y.C., *An Introduction to the Theory of Elasticity*, Dover Publications, New York, New York, 1969.
4. Garrick, I.E., A Survey of Aerothermoelasticity, *Aerospace Engineering*, AIAA, Washington D.C., Vol. 22, No. 1, January 1963, pp. 140-147.
5. Jones, W.P., ed., *Manual on Aeroelasticity*, AGARD Vol. V, London, England, 1960.
6. Rodden, W.P. and Harder, R.L., *Aeroelastic Addition to NASTRAN*, NASA Contractor Report 3094, 1979.
7. Sanford, M.C., Irving, A. and Gary, D.L., *Development and Demonstration of a Flutter-Suppression System Using Active Controls*, NASA TR R-450, December 1975.
8. Van Nunen, J.W.G. and Piazzoli, G., *Aeroelastic Flight Test Techniques and Instrumentation*, AGARD-AG-160, Vol. 9, AGARD, London, England, February 1979.
9. Weisshaar, T.A., *Aeroelastic Tailoring of Aircraft Subject to Body Freedom Flutter*, AFWAL-TR-83-3123, AFWAL, Wright-Patterson AFB, Ohio, November 1983.
10. Zimmerman, Norman H., Prediction of Flutter Onset Speed Based On Flight Testing at Sub-Critical Speeds, in *AIAA/AFFTC/NASA-FRC Conference on Testing of Manned Flight Systems*, 4-6 December 1963.
11. Military Standard Airplane Strength and Rigidity, Flutter, Divergence and Other Aeroelastic Instabilities, MIL-A-008870.
12. *Aeroelasticity*, Chapter 12, Flying Qualities Theory and Flight Test Techniques, USAF Test Pilot School, Edwards AFB, California.
13. Norton, William J., Captain, USAF, Random Air Turbulence as a Flutter Test Excitation Source, *Society of Flight Test Engineers 20th Annual Symposium Proceedings*, September 1989.
14. Norton, William J., Captain, USAF, Limit Cycle Oscillation and Flight Flutter Testing, *Society of Flight Test Engineers 21st Annual Symposium Proceedings*, August 1990.
15. Scanlan, R.H. and Rosenbaum, R., *Introduction to the Study of Aircraft Vibration and Flutter*, Dover Publications, New York, New York, 1968.

# CHAPTER 7.0

## GROUND VIBRATION TESTS

### 7.1 INTRODUCTION

The concept of the ground vibration test (GVT, sometimes referred to as a **ground vibration survey**) was first introduced in Section 6.5.2 as a critical ground test preceding a flight flutter test. The purpose is to determine the true frequency, mode shapes and zero-velocity damping of the most important structural modes of vibration. The results can then be used to update mathematical models which are used to predict the flutter susceptibility of the aircraft and assist in identifying the modes in flight test data. The GVT is very complex with many factors that can effect the validity of the resulting data. The reader will need to refer to Chapters 4.0, 11.0 and 12.0 for explanations of dynamics terms, data presentation formats and signal processing techniques while reading this chapter. Because a GVT is so complex, it is difficult to fully explain all aspects of it in a short chapter. You are strongly encouraged to observe or participate in one when possible. Reading GVT reports can also provide useful insights.

### 7.2 OVERVIEW

A basic illustration of the typical GVT is in order before delving into details. The aircraft or aircraft component should be as close structurally to the final production configuration as is practical. The **rigid body responses** of the airplane (that is, those obeying Newton's laws of motion) must be isolated and their frequencies reduced below the lowest structural mode so that they do not obscure the elastic response which is sought. These six rigid body modes are roll, pitch, yaw, and translation of the three axes (see Section 2.3.3). In most cases the GVT will be conducted with the aircraft on its landing gear, and the plane will have unique rigid body reactions in this condition. Special measures can be taken to "suspend" the plane to reduce the rigid body frequencies. The idea is to reduce the influence of boundary conditions to simulate the in flight **free-free condition**.

Structural responses are most often sensed with accelerometers (see Section 10.3) attached to the surface of the airplane. Usually, only one or two axes of motion are of interest at any location, but tri-axial accelerometers are still frequently used. The tips of aero surfaces (wings, horizontal and vertical tails, control surfaces), fuselage extremities, engine nacelles, and pylon or stores are the typical positions for the accelerometers. The test may involve dozens of transducers and associated wires which require careful organization to avoid confusion. When the excitation to the test article has begun, it is important to allow time for the transient portion of the forced response (see Section 4.3.2) to die away to the steady-state condition before taking data. The structural response over a broad frequency band is usually followed by a **survey** at a single frequency. The survey entails moving a "**roving**" **accelerometer** to pre-selected positions on the structure so that responses at positions other than the few fixed accelerometer locations can be obtained and the entire mode shape clearly seen and positively identified. Animated mode shapes can be displayed on a computer screen for this purpose. There are some mathematical analysis techniques that do not require a survey.

The excitation of the aircraft structure is most often produced by **electrodynamic shakers**. These are essentially electric motors which cause a center armature to translate up and down

as a function of the applied current. The armature of the shaker is attached to the structure of the aircraft by a **sting**. The surface on which the shaker is placed will respond to the shaker dynamics and can produce rigid body shaker motion that will produce confusing results. Therefore, measures to suspend the shaker may need to be taken to reduce or increase its rigid body frequencies so that they are not within the frequency band of the test subject which are of interest. There are many types of shaker inputs that can be used for different results and more than one shaker may be used at the same time.

### **7.3 UNDERLYING ASSUMPTIONS**

The GVT rests on three basic assumptions; stationarity, linearity, and reciprocity. The first of these assumptions is that the responses will not change over time. This principle of **stationarity** means that, all else remaining the same, the test can be done at any time of the day and on any day of the week and the results will be the same. Since wind can rock and buffet the airplane during the test, causing extraneous and unaccounted inputs, the test should be done indoors. Since temperature changes can alter the structural response through thermal expansion, the temperature at the test location should be regulated to within a range of about ten degrees Fahrenheit. Fuel leaks, hydraulic leaks, people climbing on the machine, and other such controllable factors can also affect the results by violating the stationarity assumption.

For consistent results, it is important that the structural response is not appreciably nonlinear with input force. **Linearity** demands that the test be conducted in the force region in which the response is linear with increasing force levels. However, by its nature, an aircraft structure is nonlinear because of the thousands of fasteners, and numerous joints.

Even if the excitation is made at only a single point, the structural response will typically be recorded from several other locations simultaneously. This is permitted by the principle of **structural reciprocity**. **Maxwell's Reciprocity Theorem** states that, for real structures, the motion at one point in the structure due to a force at another point is equal to the motion at the second point due to the same force applied at the first point. Thus, a certain symmetry is to be expected. Outputs and inputs can be swapped with the same results, meaning that the associated frequency response functions (FRFs, see Section 11.3) would be identical. Reciprocity can be checked by comparing FRF plots from two stations with the excitation applied at each point in turn. Significant differences such as frequency and phase shifts for the same modes, poor modal resolution, or missing modes indicate that non-linearities and non-stationarity are adversely affecting the data.

Another essential assumption is that a normal mode can be excited at any point in the structure (except where the mode shape has zero displacement, the node described in Section 4.5.2). The modal parameters are global and can be estimated from FRFs taken anywhere on the structure. It is still wise to take redundant measurements to ensure that the various experimental errors that can crop up are not adversely influencing the results.

### **7.4 PREPARATION**

A GVT is one of the most complex and expensive aircraft ground tests that can be performed. It is also one in which the data is most subject to undesirable influences and subjective interpretation. There are any number of problems which can render the test results useless. It is essential that the test be done properly the first time. Careful test preparation will help to keep irate supervisors and analysts at bay. A detailed test plan is essential if wasted time, high costs, and questionable results are to be avoided. The GVT is typically proceeded by a detailed

mathematical analysis of the test subject. This will provide insight into the frequencies of the most significant modes of vibration. This helps in focusing the GVT team's attention on the most important modes and in identifying the modes that are found. It is possible to do a GVT without this analysis, but it will likely take much longer than would otherwise be the case.

#### **7.4.1 CONFIGURATION**

As mentioned earlier, the test article should be as close to the final production configuration as possible. Incidental components like certain instruments, avionics boxes, electrical lines, antennas, etc., need not be in place for the GVT if they do not significantly affect structural response or the inertia of the test item. In fact, many such components will respond at their own resonant frequencies which are of little interest to the structural dynamicist. These responses may be detected by the test sensors and show up as noise or misleading signals in the data. Such noise is referred to as **nonlinearities**. Tests of individual components (control surfaces, for example) can be done separately as a matter of convenience. This allows their responses to be accounted for more readily during the complete aircraft test where high modal density can make mode separation and identification difficult.

The objective is to get the aircraft into as close to a flight configuration as practical. Physically, this means access doors, canopies, and panels should be closed. Systems-wise this means that at the aircraft hydraulics (or at least the hydraulic system controlling the control surfaces) should be powered. The hydraulic or electrical control surface actuators must be powered to provide representative inflight reaction stiffnesses, although unpowered controls may be tested as a check of failure conditions. A problem here is that hydraulic power ground carts may not be able to supply the required flow rate without fluctuation required to represent inflight conditions (actuator stiffness). Electronic flight controls are seldom required for the GVT but are used in the similar ground resonance test (GRT; see Section 8.4). Controls should be properly rigged with the proper balance weights. Powering some of the electronic systems may also be necessary. It may be necessary to temporarily defeat some fail-safe devices to achieve this simulated flight condition.

If the aircraft is capable of carrying external tanks and stores, it is advisable to test the response of the structure and these external components as well as the "clean" configuration. Fuel distribution within the aircraft may significantly affect the modal characteristics and so should be considered when selecting the test configuration. It may be wise to test at several fuel loading configurations. The associated hazard of having a fueled aircraft within a hanger or other shelter may require the substitution of some inert fluid (as long as the density is nearly the same as fuel) or moving the test to an outside location.

Engine vendors often require that the engines aboard the test aircraft be rotated periodically in the course of the test to prevent flat spots from developing in the bearings. The rotation can be done with compressed air blown through the engine or by some other means.

#### **7.4.2 REDUCING NONLINEARITIES**

The problem of nonlinearity noise was introduced in the last section. Reducing these nonlinearities will help to ensure clean and representative frequency response data. When attempting to curve fit a linear math model to the data from a necessarily nonlinear structure, reducing the nonlinearities is critical for a faithful match and good approximations to the modal characteristics extracted from that model. It may be desired to evaluate the amount of non-

linearity in a structure. In this case reducing nonlinearities, particularly by some of the excitation or analysis techniques discussed later, is not necessarily desirable.

The easiest means of reducing such nonlinearities is to remove the component causing the rattle, however this is not always desirable or practical. The distributed mass of such articles on an airplane structure can make up a significant mass of the structure and removing them can change the modal response. Normal maintenance servicing (tightening nuts, adding washers) may eliminate the source of the problem. Unimportant components such as gear doors, spoilers, etc., can be pinned or tied off against one end of its freeplay band as long as it doesn't artificially increase stiffness elsewhere in the structure which will affect the validity of the GVT results.

#### **7.4.2.1 PRELOADS**

Freeplay in the flight controls or other movable aircraft components can produce the annoying nonlinearities that corrupt response data. Attempting to remove this freeplay by normal rigging and maintenance efforts is not always adequate. An additional method to remove the freeplay is to preload the surface. This may consist of nothing more than taping the component off to keep it from rattling. Large components such as a control surface may require such measures as hanging a mass from the trailing edge to artificially increase the inertia of the component and hold it against one end of the freeplay displacement range. A soft spring must be placed between the hanging mass and the structure to reduce the dynamics associated with the preload. Sometimes a bungee of a suitable spring constant is simply connected to the control surface and a floor, a wall, or whatever is stiff and convenient. The amount of mass used depends upon how effective the preload is in reducing the problem. Of course, preloads on control surfaces cannot be used when the surface rotation frequency is being sought. In general, preloads should be avoided when possible because of the change in stiffness and mass distribution that they introduce to the structure. Another method of preload in combination with the shaker is discussed in Section 7.6.3

Another sort of preload that can be helpful are those used to reduce the influence of structural members in order to isolate some other component. An example may be to pre-load a wing so that shaking on the aileron will excite only aileron modes within the frequency range of interest. This can be done by placing heavy bags of shot on top of the wing, placing jacks under the wing pressing against the bottom surface, placing a sling under the wing and pulled from above, or a combination of these. These will artificially stiffen the wing and greatly increase its resonant frequencies beyond those of the aileron we are interested in exploring.

### **7.5 AIRCRAFT SUSPENSION**

In most cases the GVT will have to be conducted with the aircraft resting on its landing gear. If the gear is attached at the fuselage this is generally acceptable as long as fuselage modes are not critical. However, if the gear is attached at the wing, the modal responses measured on the gear may be so dissimilar to an inflight condition that an on-gear GVT would be unacceptable.

A form of soft suspension can be placed beneath the tires. The suspension system will have resonance conditions that are of no interest and the gear struts and tires will have similar reactions that we wish to reduce or eliminate. The plane will also have the usual rigid body pitch, roll, yaw, and translation modes while on its gear or suspended which must also be recognized or reduced so that they are not confused with actual structural dynamics. The landing gear modes are easier to reduce to this level than a series of jacks holding the aircraft up so that the gear can be retracted. For this reason, conducting a GVT with the plane on jacks is seldom practical. It

may be possible for the smallest planes to be hung via **bungees** so that the gear can be raised. For this method, the cantilever response of the crane holding the aircraft up must be considered as well as that of the bungee. In any case, the undesired rigid body responses must be accounted for and reduced to about a third of the first aircraft flexible mode frequency. The first step in a GVT should be to actually check the aircraft rigid body frequencies to ensure that they are low enough not to influence the data you're really after.

For the on-gear condition, the struts can be depressurized and the tires partially deflating. Placing the plane on specially prepared pads with adjustable reaction frequencies (usually a pneumatic flotation system) is the most desirable solution. Another method has been to place the strut axles in bungee slings. Bungees can be obtained with various stiffnesses and even combined for the desired characteristics. The length of the bungees and the mass of the airplane will determine the pendulum frequency of the suspension. **Slip plates** riding on a film of oil placed beneath the tires have also been used successfully to reduce the lateral rigid body mode.

If only a component of an aircraft is being tested then it must be supported in a fixture with rigid body modes that will not affect the reading of true structural dynamics of the test subject. The fixture is usually very rigid by nature, so the easiest means of ensuring that its dynamics do not influence the test results is to make sure that it is stiff enough to have its lowest flexible frequency above the highest frequency of interest for the test subject. The frequencies of the fixture must be checked the same way those of the entire airplane are checked. For control surfaces, actuator and hinge stiffnesses, either real or simulated, must be provided.

## **7.6 ELECTRODYNAMIC SHAKERS**

Structures such as satellites may be excited as a unit by placing it on a **vibration table** for a **base excitation**. This approach may also be employed in laboratory tests of such items as ejection seats, avionics boxes, etc. This, however, is seldom practical for an aircraft or major aircraft structural components, and the venerable shaker is most commonly used.

### **7.6.1 CHARACTERISTICS**

The size or weight of the shaker is a direct function of the frequency range in which it can respond and the mass of structure it can effectively displace or excite. They vary in size from units that fit in the palm of the hand, to monsters weighing hundreds of pounds used to shake buildings. Apart from the mass, there are many other characteristics that are important to consider when choosing a shaker for a test. An essential piece of equipment used with the shaker which is not discussed is the power amplifier that boosts the excitation signal to the level necessary to produce the desired force amplitude and then powers the shaker. A schematic of a typical GVT equipment arrangement is provided in Figure 7.1.

#### **7.6.1.1 PHYSICAL FEATURES**

The electrodynamic shaker is essentially an electric motor with the center armature translating axially instead of rotating. Hydraulic shakers have been used for very large structures, but they are seldom used for aircraft GVTs. The frequency and amplitude of armature displacement is a function of the input current to the shaker. The mass of the armature will then determine the actual magnitude of the force produced. The applied current and motion of the armature can create fraticidal heat that typically requires a **blower** to be attached to the unit for cooling.

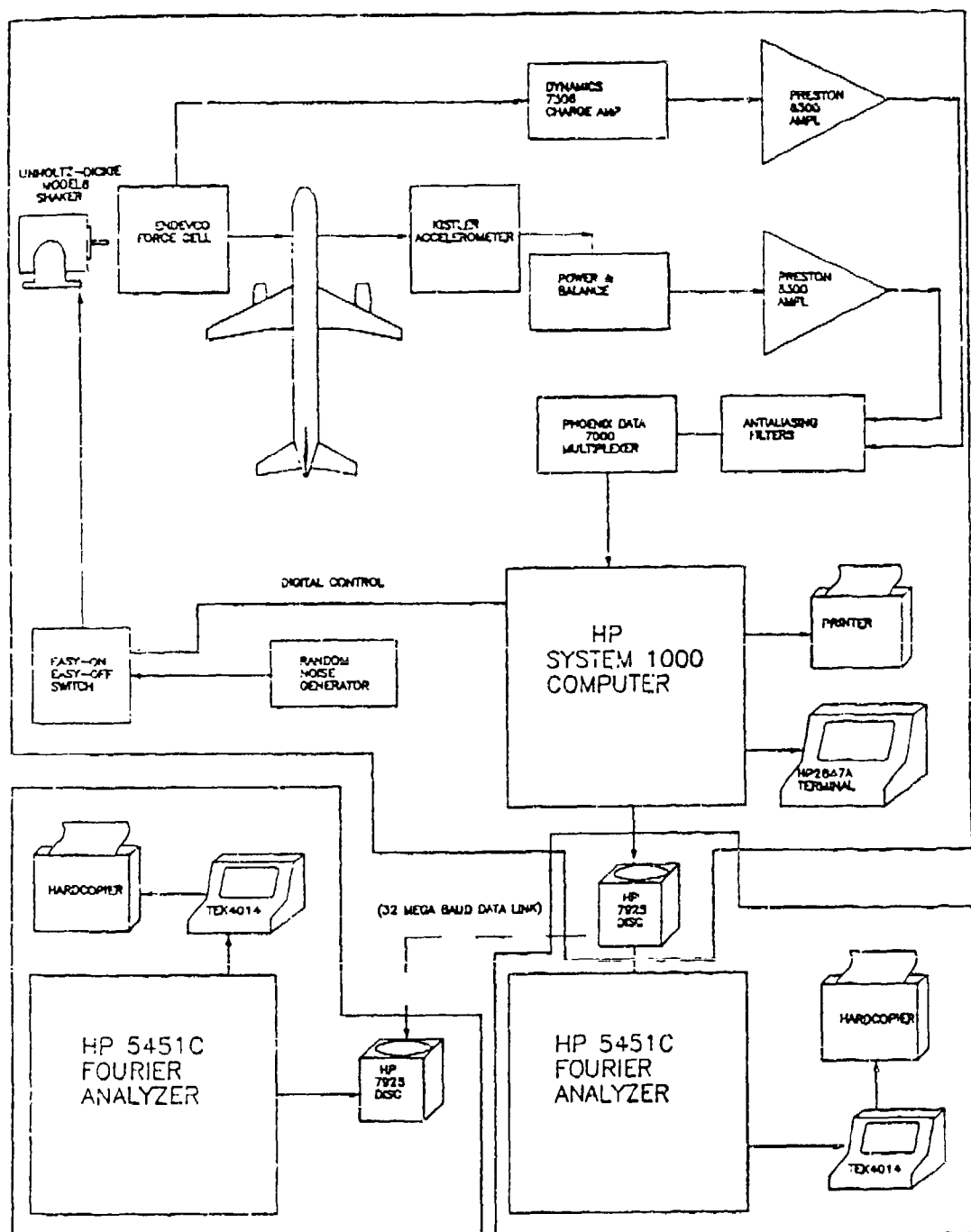


Figure 7.1 Schematic of GVT Equipment Arrangement

### **7.6.1.2 SELECTION**

A reasonable requirement in shaker selection is that the output force actually displace the structure it is attached to. If the structural inertia is greater than the force, then the shaker may simply displace itself instead of the test subject, or the armature will simple resist displacement. Another vital limitation is that the armature mass be a small fraction of the structural mass. With the armature/sting attached to the structure it essentially becomes part of the structure and contributes its mass. This is referred to as **effective mass** and will unavoidably alter the response characteristics which are sought. One method for getting a handle on this effect is to add mass to the armature, twice the armature/sting mass, and observe amount of the shift in frequencies that result.

If you wish to stop the shaker abruptly in order to allow the structure to damp out naturally, the ability of the armature to stop with few overshoots, akin to a spring response, will be an important consideration. Actually, this spring characteristic is always present when the shaker is operating. Because of the inertia and spring characteristics of the armature, the output of a load cell placed between the shaker attachment and the test subject should be used when the input force is needed (in a transfer function, for example), not the signal sent to the shaker. Another consideration, although one that is seldom a problem, is the stroke of the armature while attached to the structure. Large displacements could produce significant rigid body motion that will feed into other shakers that may be operating simultaneously, or the structure may even be overloaded.

Shakers are most often rated by their electrical load, weight, and maximum force displacement. Actually, these are all related in ways far too complicated to elaborate on here. Suffice it to say that a fifty pound shaker can produce a larger force than a 20 pound shaker. The 50 pound shaker will give much better low frequency inputs by virtue of its armature mass, but will be unable to produce appreciable displacements at high frequency for the same reason. It is sometimes possible to add weights to the top of the armature to increase its mass. For low frequency inputs, relatively large strokes are necessary to get measurable excitations, so checking the maximum stroke capability of the unit is recommended. At higher frequencies, large strokes are less likely and eventually become impossible anyway due to the inability of the shaker to respond fast enough (**attenuation**). A typical 50 pound shaker used in aircraft GVTs will usually be good to around 2000 Hz.

### **7.6.2 SUSPENSION**

As with the reduction of the aircraft rigid body modes, the reaction of the shaker and whatever surface the shaker is placed on must be considered and adjusted when necessary to beyond the frequency range to be investigated. At least the rigid body dynamics of the shaker will then be effectively decoupled from those of the test article. Placing the shaker directly on a concrete floor is best because such a floor can be considered to have infinite stiffness when compared with an aircraft structure. So, the response of the floor transmitted to the structure through the shaker case and armature will be of such high frequencies and low amplitudes that it will not influence the structure to any appreciable degree. However, it is often necessary to place a shaker on a stand to get it close to a portion of the aircraft, such as a vertical tail. In this case the reaction of a comparatively flimsy maintenance stand can produce dynamics which will feed into the aircraft structure the same as pure armature displacement. For this reason, shaker stands tend to be very heavy steel constructs. A careful choice of stand, recognizing the frequencies in which the stand influence will be felt (a minor GVT of the stand may be necessary)

can all help to reduce this problem. A special suspension system can be used for the shaker the same as for the aircraft.

Occasionally, it is necessary to hang the shaker from a crane in order to excite a particularly inaccessible part of the plane. The shaker should be attached to the crane by a bungee or other damping system to reduce the vertical displacement frequency that is a characteristic of the crane arm bending and suspension cable stretching. Pendulum motion, however, is a frequent problem. This frequency should be identified by calculation or by running the shaker through a frequency sweep and observing where the pendulum motion occurs. The pendulum frequency can be reduced simply by altering the cable length between the crane arm to the shaker or by adding mass to the shaker unit. The latter method will also help to assure that the structure is displaced by the armature and not the shaker case.

### **7.6.3 ATTACHMENT TO THE STRUCTURE**

It is theoretically possible to extract all of the necessary modes from an aircraft using a single exciter location, a wing tip for example. In practice though, a structure as complex as an aircraft requires several locations to be used to get enough energy into the modes to clearly distinguish them and to obtain useful modal parameters. For example, a shaker input on one wing tip may be inadequate in exciting the opposite wing through the carry-through structure to give suitable resolution to all the modes of interest. Such locations as the wing tips, horizontal tail tip, vertical tail tip, control surface trailing edge, pylons, engine nacelles, and external stores are most common. It will be obvious whether a vertical, lateral or longitudinal excitation is best, especially when mathematical analysis has already provided you with an idea of what the modes of interest are. Multishaker techniques would use similar input locations, just several simultaneously.

If the modes are not being excited adequately, the attachment point may be near the **elastic axes or node line** of the motion (imaginary line about which deformation takes place). Moving the input point a few inches may cure this problem. At a wing tip, for example, the shaker input should be made near the leading or trailing edge to ensure that both bending and torsion modes are excited.

The shaker armature is typically attached to the structure through a sting (also known as a **quill or thruster**). This is typically a steel or aluminum shaft of appropriate length which has a fairly high compression and tension stiffness to ensure that its natural frequencies are of no concern. The sting will incorporate a thin steel rod. The rod acts as a **structural or mechanical fuse** such that it will fail at a specified tension or off-axial load during input to the structure. This is a safety measure to ensure against damage to the article under test or shakers which cannot abide off-axis loads. The thin member also allows some needed lateral flexibility since the structural displacements are usually more of a rotation than a pure translation. Another technique of attachment requires an armature with a hole that passes directly through its center. A piano wire attached to the structure passes through this hole. The free end of the wire is attached to a bungee or some other elastic anchor that permits the test item to be preloaded (see Section 7.4.2.1). The armature and wire are then attached together so that when the shaker is activated they will move together. This approach allows a preload without additional equipment, reduces effective mass, and incorporates the functions of a structural fuse without additional components.

The sting should be aligned with the axis of motion to be excited, but need not be aligned with more than "eyeball" precision. Slight misalignments will only mean that some of the input force is going into more than one axes of motion. Having some input energy expended in bending

of the thruster is also undesirable. It is sometimes practical to maintain a preload in tension on the thruster to ensure against these bending moment errors.

A load cell is typically placed between the shaker and the thruster to permit monitoring of the input force. This is done both to ensure against overloading the test subject and for linearity measurements, as explained later. It is important that the load cell input axis be precisely aligned with the armature axis for a valid input function to be measured if transfer functions using this signal are planned. Placing an accelerometer at this same point (often called the **reference accelerometer**, as is any other fixed accelerometer) permits a **driving point measurement** to be taken. Other measurements are termed **cross point measurements**. The distinctions between the two are shown in Figure 7.2 and 7.3. In the imaginary plot of the driving point response, all of the resonant peaks fall on the same side of the zero axes. Response data taken at the driving point will have distinct **antiresonances or nodes** between every resonance, minimum value valleys, when plotted with a logarithmic amplitude scale. The phase is also seen to lead as the magnitude enters an antiresonance and then lags through a resonance. All of the modes are necessarily in phase with each other and the imaginary resonant peaks need not all lie on one side of the zero axes. This is not necessarily true at the cross points, as shown in 7.3. Clear antiresonances will not appear between two modes that are not in phase.

The end of the sting can be attached to the structure by means similar to the attachment of the accelerometers and the Section 10.3.4 discussion for accelerometer attachment is generally applicable to thruster attachment. Attachment can be by screwing into an existing screw hole in the structure or a specially prepared hole, gluing, or attachment to a pad held on by bees wax. A vacuum pad have also been used to hold the sting to the structure. This allows easy moving of the attachment, but a vacuum source must be available, and the air hoses add additional complexity to an already cumbersome experimental setup.

#### **7.6.4 IMPEDANCE MISMATCH**

The shaker amplifier and the electrodynamic shaker do not pass an electrical signal completely unaltered. Both will have their own individual capacitance, resistance, and inductance. This **electrical impedance** between the two units should be matched or the excitation signal sent via a cable to a shaker will not be seen by the structure exactly as produced by the signal generator. The electrical impedance of the shaker is a function of the amplitude of the armature displacement. The force level throughout the bandwidth of the signal will be altered. It is possible that the excitation at a critical frequency will be changed to such a low input level that the structure will not be adequately excited. This problem may go completely unnoticed with the misleading results having series consequences during later flutter analysis and flight testing.

The mass and spring-like characteristics of the shaker are a form of **mechanical impedance** that can alter the test results in ways that may be difficult to define quantitatively. The shaker force tends to drop off at resonance because the the structure is resisting less and allows the force measurement to be susceptible to noise.

If an impedance mismatch problem is suspected during the course of the test then a trial and error substitution of cables, amplifiers and shakers is the usual remedy. Simply moving the shaker to a location where the mechanical impedance has less effect can also improve the situation. A more rational approach is to characterize the impedance of the the system before testing to avoid a mismatch. Changes to the setup can then be made or the input signal can be tailored to ensure that the structure is forced as desired.

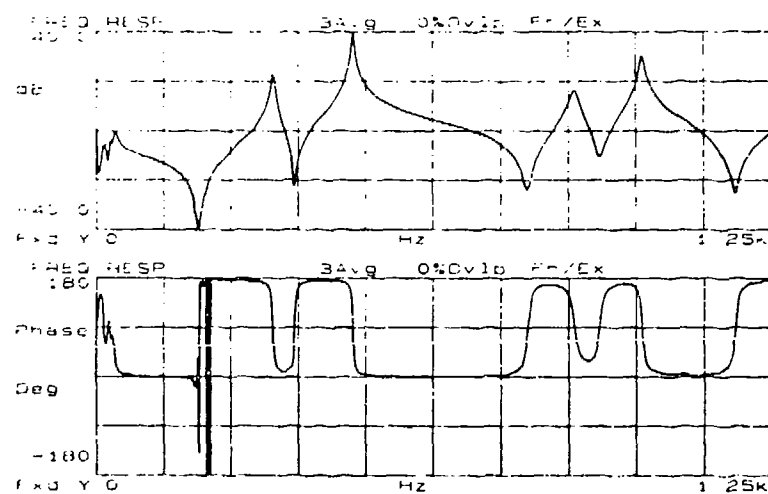
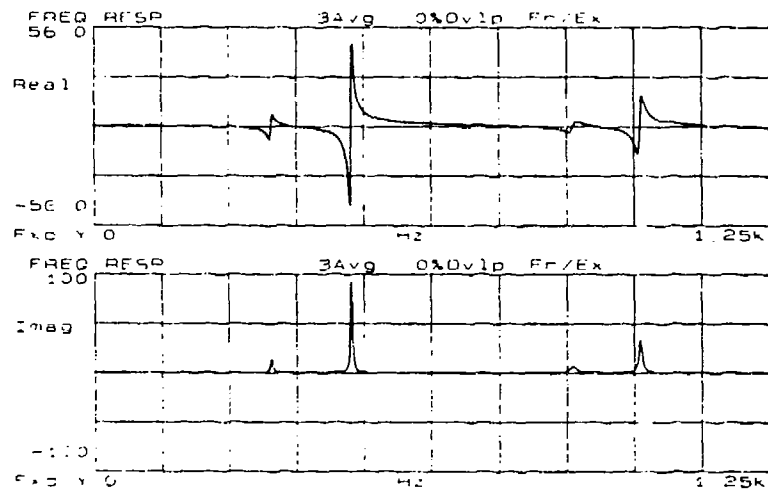


Figure 7.2 Characteristics of a Driving Point Measurement

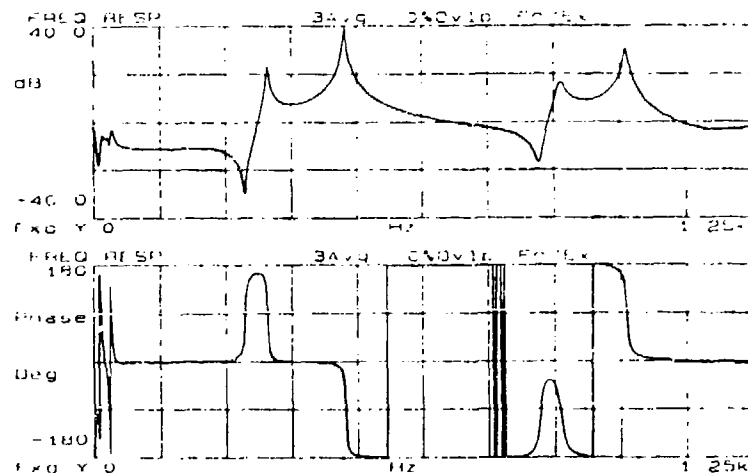
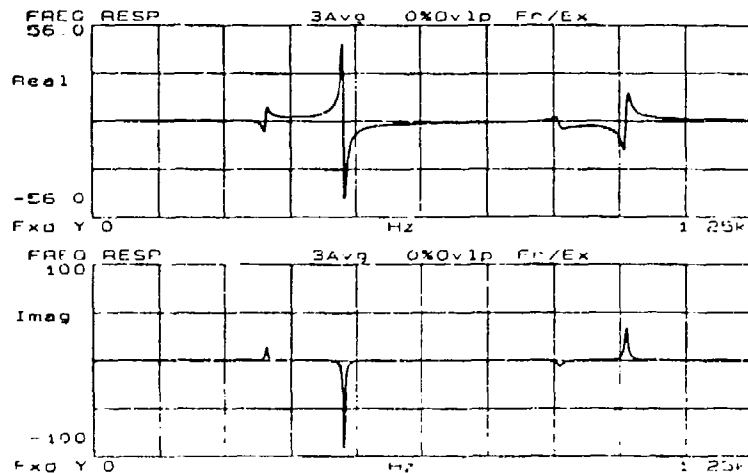


Figure 7.3 Characteristics of a Cross Point Measurement

## **7.7 TRANSDUCER INSTALLATION**

The actual mechanics of accelerometer installation is covered in Section 10.3.4. The selection of accelerometer location is very important for accurate data that can be readily correlated with an analytical model. The reference accelerometers used should be placed in so called "hot spots" where a large response for all expected modes is expected. This would certainly include where the force is being applied. Placing an accelerometer at the root of the wing would be of very limited value because of the very small motion that actually occurs there. A location at the mid chord of the wing may be very close to the elastic axis where little motion also occurs. The sensors should be aligned with some structural axes of the test subject. For an entire plane, this would probably be either parallel to or perpendicular to the floor, and parallel to and perpendicular to the aircraft centerline. To achieve this on curved surfaces, the sensors will need to be placed on specially formed blocks fastened to the surface which transitions from the curve to a flat, aligned area. The alignment should be done with care, but location marking using a yard stick referenced to normal panel lines of the plane will be adequate.

Sensor locations relative to the modes of interest are important. For example, to positively identify a wing torsion mode with reference accelerometers alone or without referring to analysis results, it is necessary to place a transducer at the leading edge and another near at the trailing edge of the surface. Determination of whether a mode is antisymmetric or symmetric will require transducers on both sides of the aircraft centerline. Accelerometer responses from one side of the plane can be added or subtracted from the response at the mirror image location on the opposite side of the plane, or from the leading and trailing edges of a surface, to positively differentiate symmetric and antisymmetric and bending or torsion modes.

One important precaution is to ensure that transducer cables are not free to flap about excessively or strike the structure during excitation as this can produce distorted signals. It may be necessary to tie the cables off to a stand placed next to the plane to reduce flapping.

## **7.8 EXCITATION TECHNIQUES**

While the electrodynamic shaker is the most commonly used excitation source for aircraft GVTs, there are many signal forms available to drive the shaker. The driving signals should be selected after considering the nature of the structure and the desired data resolution. Certain inputs may fall out of favor occasionally or particular equipment may not be able to produce some of the forms discussed here. However, no single method of excitation or data/signal processing is superior in every application. Pros and cons of the various methods are summarized in Table 7.1. It is important for the engineer to have some familiarity with the typical inputs that have been used over the last 25 years. Keep them all in mind as alternatives when unique problems crop up.

### **7.8.1 OPERATING INPUTS**

It is occasionally possible to use the aircraft itself or its ambient environment to excite the structure. These operating or self-operating inputs might include programming the automatic flight control system to command rudder motion, the inertia of which will excite modes in the vertical tail and aft fuselage. A manual input is seldom controlled enough to provide the force levels and frequency content necessary. Simply running the engine(s) might provide sufficient excitation for usable modal data. This approach is typically more trouble than it's worth, and has found few adherents. The force levels tend to be very small and produce poor data. But, for some test articles this is the only practical excitation.

**Table 7.1**  
**Comparison of GVT Excitation Forms**

	Size Steady State	True Random	Periodic*		Transient In Analyzer Window			
			Pseudo Random	Random	Fast Sine	Impact	Burst Sine	Burst Random
Minimize Leakage	NO	NO	YES	YES	YES	YES	YES	YES
Signal to Noise Ratio	VERY HIGH	FAIR	FAIR	FAIR	HIGH	LOW	HIGH	FAIR
RMS to Peak Ratio	HIGH	FAIR	FAIR	FAIR	HIGH	LOW	HIGH	FAIR
Test Measurement Time	VERY LONG	GOOD	VERY GOOD	FAIR	FAIR	VERY GOOD	VERY GOOD	VERY GOOD
Controlled Frequency Content	YES	YES	YES	YES	YES	NO	YES	YES
Controlled Amplitude Content	YES	NO	YES	NO	YES	NO	YES	NO
Removes Distortion	NO	YES	NO	YES	NO	NO	NO	YES
Characterize Nonlinearity	YES	NO	NO	NO	YES	NO	YES	NO

\* REQUIRES ADDITIONAL EQUIPMENT OR SPECIAL HARDWARE

### **7.8.2 TRANSIENT**

Also known as impulse testing, this method of excitation is based upon producing individual transient responses of the structure by a sharp, almost step input which has high frequency content. It can then be repeated as necessary. The major disadvantage of the method is the difficulty in precisely controlling the content of the input.

#### **7.8.2.1 IMPACT**

This approach consists of striking the structure, generally with a hammer, to produce the transient excitation. The method gives a fairly constant force over a broad band of frequencies. This allows many excitations to be made over the test article in a very short time allowing a modal survey (explained later) to be completed very quickly without shakers. Very large hammers are available for large structures but these are impractical for aircraft use because of potential damage to the plane. The hammer typically has a force transducer or load cell at the head to measure the impulse. The hammer and transducer must be calibrated as a unit.

The frequency content of the impact is inversely proportional to the width of the pulse and the weight of the hammer and directly proportional to the hardness of the tip. Several types of impact head weights and materials (rubber, phenolic, steel) are available to provide some control over the impact form and duration. A harder head will excite higher frequency modes whereas a softer head will more effectively excite low frequency modes (see Figure 7.4). The technique would require a very soft head if frequencies below 20 Hz are sought. In general, a wider force impulse will excite lower frequency modes. The force of the impact is dependent upon the

velocity and weight of the hammer (Figure 7.5). Most hammers have additional weights that can be added. However, if the weight of the hammer becomes too great, it will be difficult to avoid multiple impacts for a single blow which will produce poor data.

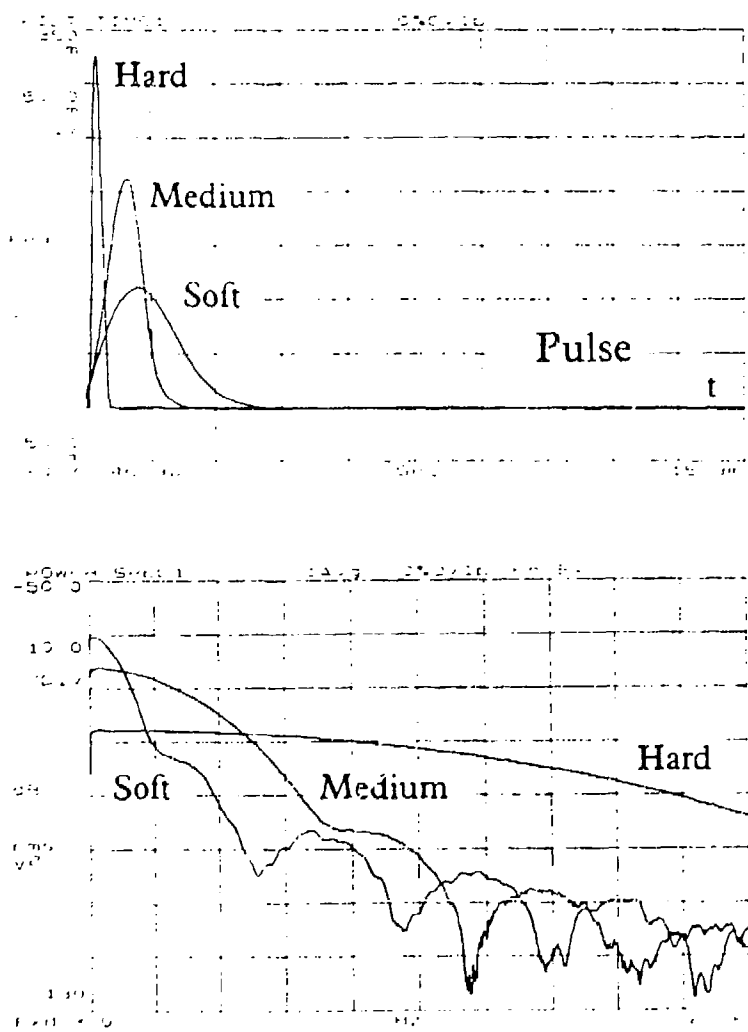


Figure 7.4 Influence of Impact Hammer Tips

Since most data acquisition systems require sensitivity gain to be set to the anticipated level of the input and response signals, success is therefore very much dependent upon the technique of the person handling the hammer. It sometimes takes several tries to achieve the right impact without overloads. Hitting too hard also excites nonlinearities. Trial data should be taken in an effort to set the sensitivities properly.

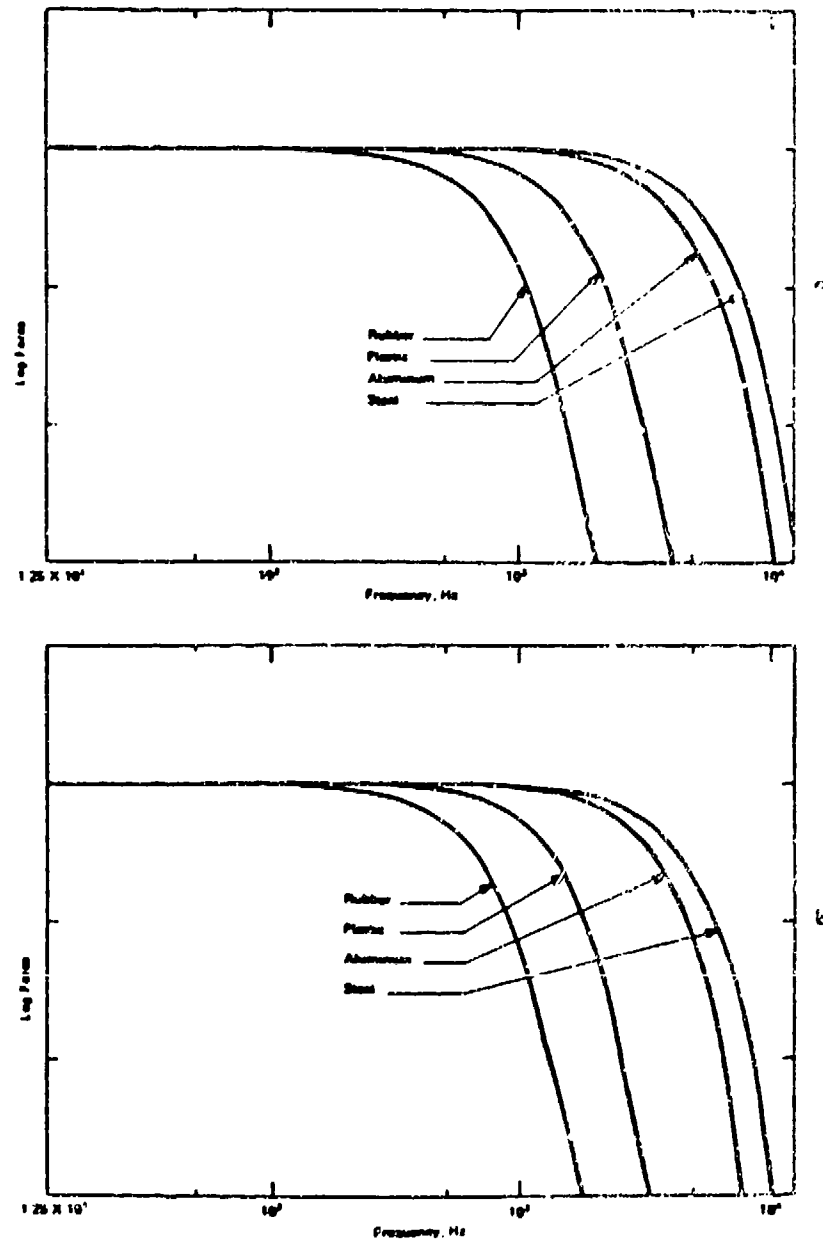


Figure 7.5 Influence of Impact Hammer Weight and Force, Hammer b With More Weight Than Hammer a

The impact technique offers a particularly easy way of extracting the mode shapes. The response at each selected point on the structure is recorded for an impact at each of these points. The magnitude of the imaginary component of the inertance (acceleration/force, see Section 4.4.1) for each response at each resonant frequency is then determined. For a cantilever beam with four impact/response points (point 1 near the free end, point 4 near the fixed end), the results might look like

Impact Point	Mode			
	1	2	3	4
1	7.93	15.10	19.50	17.00
2	6.25	-7.31	-28.60	-45.00
3	3.68	-17.50	5.81	32.40
4	1.37	-16.00	32.50	-20.10

where each successive mode has a higher frequency. Each of the columns are then the mode shape for the mode whose frequency is obtained as described in Section 11.3.5. The columns are typically normalized by dividing through by the largest value in the column. By examining the results, it can be seen that mode 1 is the first cantilever beam bending mode, the second mode the second bending, and so on.

The method is applicable only for very light structures and, since the impact excites many nonlinearities, it is only suitable for relatively linear structures. Checking the coherence of the data (see Section 11.3.7) will assist in determining the quality of the results. The method has a low signal-to-noise ratio (S/N) (see Section 12.3.4) and so should only be used in a low noise environment and with equipment possessing a large measurement dynamic range. At best, the FRFs are "noisy" and require the averaging of the results of several raps to be useful. Also, since the response of a lightly damped structure may not decay to zero within the sample window, leakage problems are possible (see Section 12.3.3). Another principle drawback of impact testing is that the input form is largely unpredictable. The result is the excitation of undesirable nonlinearities. It is also difficult to get enough energy into complex structures to excite all of the important modes.

### 7.8.2.2 STEP RELAXATION

Another form of transient testing, the step relaxation method entails preloading the structure to the desired force level with a high tension, lightweight cable or wire. A step input is produced when the cable is suddenly severed or released to allow the structure to relax to its unloaded state. Because of the sound caused by releasing the restraint, this method is often referred to as a "twang" test. This step input produces the transient response. This method is capable of putting considerable energy into the low frequency end of the spectrum but is a slow method and a complex test to set up.

### 7.8.3 SINE WAVEFORMS

The sine waveforms as a GVT excitation is the oldest and still widely used form. Its principle points of praise are the very good signal-to-noise ratio, less influence from nonlinearities, the ability to visually see the resonances, the good resolution at high frequencies, and the ease of understanding and implementing the method. Its primary problem is the length of time the test takes when compared with the random techniques.

### 7.8.3.1 SINE SWEEP

The sine sweep is often the first part of a GVT and followed by sine dwells at the frequencies identified from the results of the sweep. The sweep involves exciting the structure with a single sine waveform that increases in frequency from a set lower limit to a set upper limit which include the frequency range of interest for the structure under test. The sweep can be done linearly, exponentially, or any other sweep rate method the user can dream up. The sweep is usually logarithmic, increasing in rate with frequency because enough cycles must occur in the vicinity of a frequency for sufficient energy to be transmitted to the structure. Obviously, more cycles occur in a brief time at high frequencies than at low frequencies. As the input frequency coincides with the normal modes of the test subject, a large amplitude response will result. At least theoretically, all of the modes can be identified from the resulting frequency response function.

As mentioned, the problem with this method is that the sweep must be conducted very slowly to meet the assumption of quasi steady-state conditions. Such a sweep over 50 Hertz could require as much as 15 to 20 minutes. If the sweep is conducted too quickly, shifts in resonant peaks and erroneous damping and amplitude data will result (see Figure 7.6). Even when the sweep is done slowly, the data may only be useful as a guide for a sine dwell test, or other methods. A common practice is to conduct a sweep with increasing frequency and then repeat it with decreasing frequency. The former will tend to shift resonances to higher frequencies and the latter to lower frequencies. By examining the two resulting FRFs, a more precise estimate of the true resonant frequency will generally lie between the two slightly separated peaks for each resonance from the two plots. Time averaging of sweeps (see Section 12.4.2) can also help in eliminating the shift problem. Transfer function type FRFs do not suffer from the shift at all.

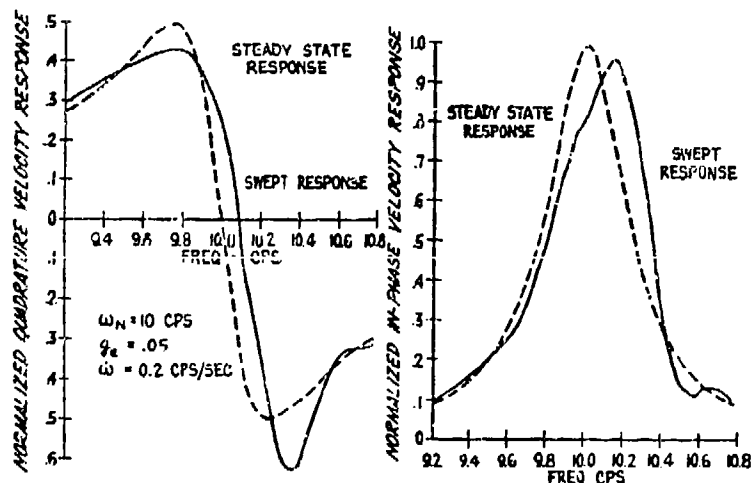


Figure 7.6 Effect of Sine Sweep Rate on Data

Multiple input tests using a swept sine signal is not uncommon. For example, exciting wing modes with a shaker on each wing using a symmetric or an antisymmetric excitation will provide a much more easily analyzed response than for a single shaker on one wing. It may in fact be the only way to get data clean enough to correlate with mathematical analysis results.

### **7.8.3.2 SINE DWELL**

The ability to apply a steady sinusoidal input to a structure at a constant frequency can permit a careful analytical and visual study of the resulting motion. If the mode is properly "tuned", the motion at various points throughout the structure will be either in phase or out of phase. This tuning operation consists of slight frequency adjustments, and changes to the input force until the response meets the criteria for a normal mode (acceleration 90 deg out of phase with the force, no beating in the decay, etc.). Lissajous figures (see Section 11.2.6) and/or CO/QUAD displays (see Section 11.3.8) are used to judge when the mode has been tuned or the quality of the best tuning that can be achieved. Another criteria that might be used is that the measured shaker force drops at resonance because the structure is not resisting the motion as much.

Shakers may have to be repositioned if difficulty is encountered in the tuning. If a mode is not truly symmetric or antisymmetric but shows a disproportionate displacement from one side to another (the wing tip on one side displacing twice as much as the other tip while still in phase, for example) then equal shaker force from two symmetrically placed shakers will not produce a perfectly in phase response. This type of response is termed an **asymmetric mode** and this method of tuning is called the **proportional force method** of shaker excitation. The force amplitudes are tailored proportional to the displacement of the mode shape at the shaker input location. Single input sine dwell mode tuning might be used during a random test where there are very close modes or where nonlinearities complicate the analysis, but multishaker setups are common.

### **7.8.3.3 CHIRP**

The chirp or fast sine sweep is a brief logarithmic sweep which begins and ends within the sampling window to reduce leakage effects. The sweep can be repeated as many times as necessary and averaged. A series of small bandwidth chirps can be performed to cover the entire spectrum desired. The result is a reduction in excitation time compared to a slow sweep. As with other sine methods it is not possible to eliminate all nonlinear distortions. A similar method is the stepped sine technique which utilizes brief, discrete sine sweeps at many frequencies necessary to cover the desired spectrum.

## **7.8.4 RANDOM**

The use of random signals as GVT excitation sources has become very popular in recent years because digital revolution and the great reduction in testing time it often allows. However, there are many cautions in the following paragraphs that must be considered when using this approach. Also, because random methods can tend to obscure the nonlinear behavior, a nonconservative overestimation of damping is likely.

### **7.8.4.1 PURE RANDOM**

The pure random signal is not periodic in any manner so it never repeats (see Figure 7.7). A signal generator is typically set up to concentrate the energy of the signal within a bandwidth of interest with a flat spectrum (same level throughout the band). Because of the nature of the pure random signal, there is no chance that the input or the response will be periodic within the sampling window and so a weighting function must be used to reduce the possibility of leakage (see Sections 12.3.3 and 12.4.1). The greatest advantage of pure random is that each succeeding sample of data can be ensemble averaged together to remove noise and nonlinearities (see

Section 12.4.2) and this is frequently essential to produce useful data. The signal also produces the best linear approximation of a nonlinear system for curve fitting purposes. If the signal is produced by an analog signal generator, often the case for pure random, it may not be possible to tailor the signal to the impedance mismatch of the system. This can prove a major disadvantage of this excitation input.

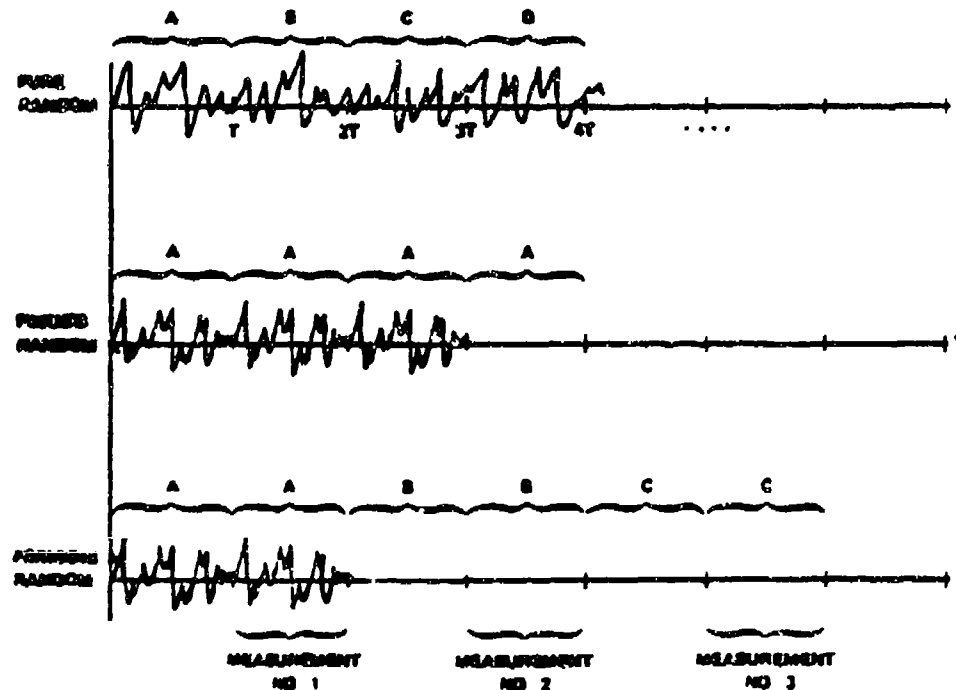


Figure 7.7 Characteristics of Various Random Signal Types

#### **7.8.4.2 PSEUDO-RANDOM**

The pseudorandom signal has equal, repeated periods of the same random signal and thus leakage effects are reduced if the period of the signal is the same as the sample period. A reasonably good measurement can be obtained with just one sample. Because all desired frequencies are being excited during each signal period, the energy input at any one frequency is fairly small. This produces a comparatively low S/N. Unlike the pure random, ensemble averaging will not remove structural nonlinearities and distortions, appearing as spikes in the plots, since these will be exactly repeated during each period of the excitation. This constitutes a major disadvantage of using the pseudo-random signal.

#### **7.8.4.3 PERIODIC RANDOM**

This waveform combines the best features of the pure and pseudo-random signals without the disadvantages. A certain random signal is repeated a few times and then another random signal is repeated for a few periods, and so on (see Figure 7.7). For each signal, the transient response of the signal is allowed to die out before the structural response is sampled. Ensemble

averaging can then be done as with pure random and the signals will be periodic within the sample window as with pseudo-random. It is also a good input for modeling a nonlinear system in curve fitting approaches. The disadvantage is that a test by this method will generally take two to three times as long as with the other random inputs.

#### **7.8.4.4 BURST RANDOM**

This signal uses one of the random forms discussed previously, but provides the input in a burst that begins and ends within the sample window to reduce leakage effects. The time between the end of the input and the end of data sampling permits time for the transient structural response to die out, or to be artificially set to zero, in the data sample. The input is then repeated at discrete intervals. The approach is claimed to provide better modal resolution and S/N.

### **7.9 LINEARITY CHECK**

The concept of structural linearity was presented in Section 7.3. For the purposes of the GVT, we are only concerned with the extent of nonlinearity that would produce shifts in modal frequencies at progressively higher force levels. At a certain input force level, slippage in joints and other events that can produce changes in frequency response can occur and cause a change in modal response. It is then necessary to test below this force level. Of course, at very high force levels the structure may be damaged and cause a considerable change in response.

The linearity check is performed by simply measuring the response of each transducer at each frequency dwell. The measurement is taken at a series of ever-increasing force levels to the highest level anticipated to be used in the test. A comparison of responses at each level for each transducer will reveal any nonlinearity effects. Generally, the highest practical force within the linear region is used to ensure adequate excitation of all modes. The influence of nonlinearities on damping can also be checked in the same manner.

### **7.10 SURVEYS**

If the testing involves a dwell on a tuned mode (discrete sine dwell), it is possible to verify the modal identification or mode shape by conducting a survey across the surface. The mode tuning process itself will help to separate true normal modes from "local" or false modes (a rattle, a substructure mode, etc.) and other misleading signal analysis errors. This entails moving an accelerometer around to different locations on the test article and recording the amplitude and phase of the signal. A sketch or computer generated diagram of the amplitude vectors with the appropriate phases on a drawing on the test subject will provide a visualization of the mode shape. Node lines can be quickly located in this manner if data is simply examined on an oscilloscope or other device and not recorded. Otherwise, the node line is interpolated from the resulting mode shape display or printout. Many points will have to be surveyed before the entire mode shape can be defined. By making the survey at pre-selected points on the surface, generally a grid pattern (see Figure 7.8), it is possible to locate nodes by interpolating to a zero response or sign change by using the trends identified in the survey.

During the survey, the roving accelerometer can be temporarily attached to the surface (double-sided tape, bee's wax, etc.) or placed against the surface using a "wand." The wand is a handle (sometimes quite long if it has to reach to the top of a vertical stabilizer) with the transducer mounted near the end. The end must have a soft spring to which the transducer mounts to isolate the wand modes from the response. For this to happen, the spring, often just a light

aluminum band screwed to the wand, must have a natural frequency much lower than that of the dwell frequency.

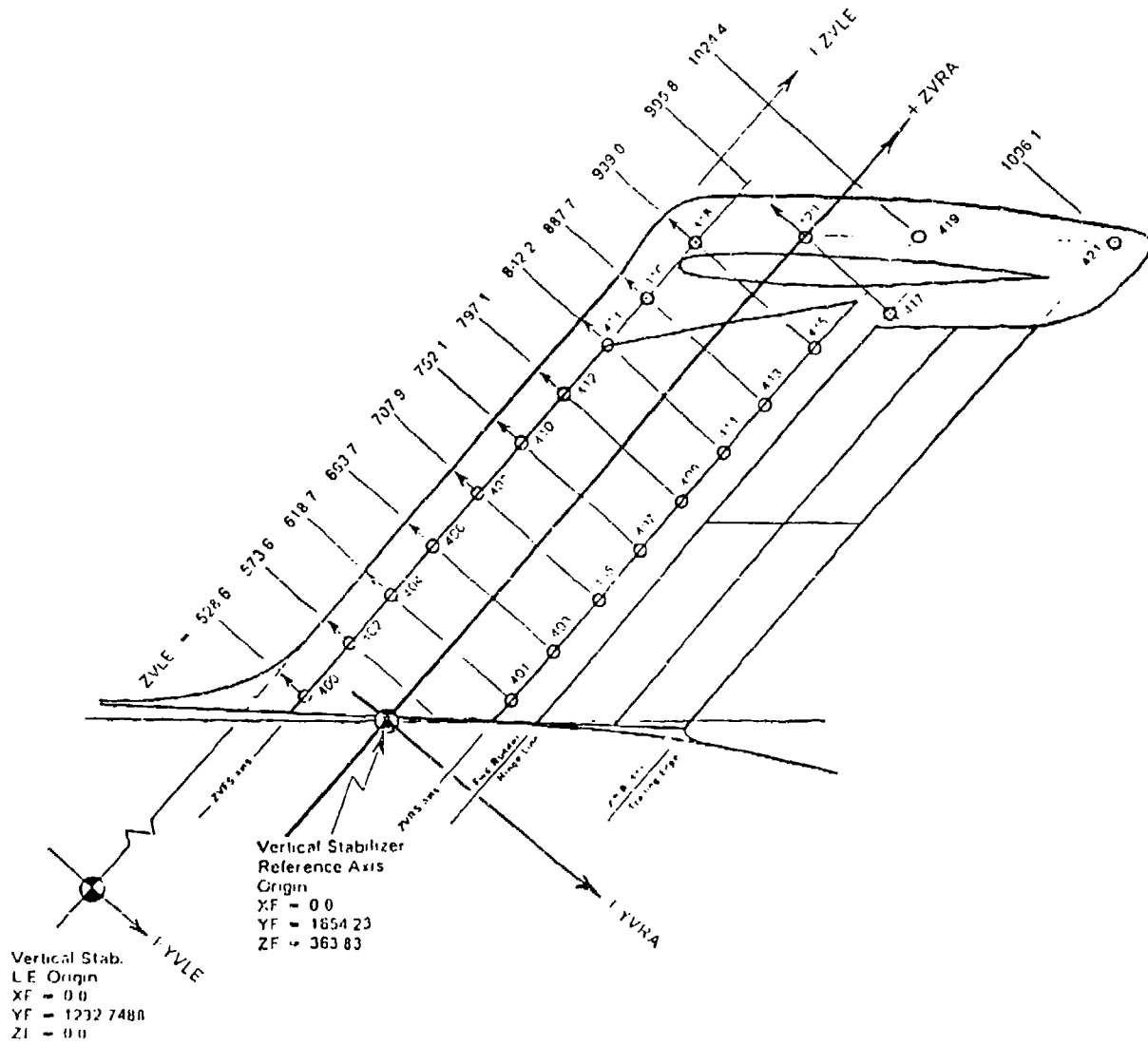


Figure 7.8 Example of a GVT Survey Grid

Tests such as multipoint random does not allow a survey such as is done with sine dwell. Instead, transducers must be placed at each of the points that would otherwise have been surveyed, and all of the responses are collected at once. This can amount to well over a hundred accelerometers for an entire airplane test, and provides a challenging organization problem. The wires from each of the transducers must be carefully coordinated, and the floor quickly becomes

a sea of "spaghetti." While the price of accelerometers have decreased markedly in the last few years, this may still be an expensive undertaking. A large number of signal conditioners, filters and analog-to-digital converters (see Chapter 10) may also be required with their attendant expense. However, if successfully done, a great savings in time (also associated with test cost) can be realized.

## 7.11 MODAL RESULTS

### 7.11.1 MULTIPONT DATA

Digital test equipment and mathematical techniques now allow us to use several excitors operating simultaneously and with the response of many sensors on the structure being recorded at once. Multipoint excitation analysis can be highly dependent on computer curve fitting methods to extract the modal data. To check that the inputs are not correlated at any frequency (not sharing identical inputs), forming a **partial coherence** (see Section 11.3.7) between each pair of inputs will help in evaluating this. Low coherence would indicate little correlation. **Multiple coherence** between an output and some or all of the inputs would help in gaining confidence in the modes shown in the FRFs and to see how much nonlinearity and leakage effects are present. Values close to unity are considered reliable data.

Knowing each input signal from the load cells at the shakers, and each response from the accelerometers placed on the surface, it is possible to form input auto power spectrums of all of the inputs in the matrix  $[G_{xx}]$  and the cross power spectrums between all inputs and all outputs,  $[G_{xy}]$  (see Section 11.3.3). A transfer function between one and the other,  $[H]$ , or

$$[G_{xy}] = [H] [G_{xx}] \quad (7.1)$$

will provide the frequency response functions needed to obtain the required modal parameters. This matrix can be solved for by the expression

$$[H] = [G_{xy}] [G_{xx}]^{-1} \quad (7.2)$$

Of course, some important matrix properties are necessary to ensure that the auto spectrum matrix can be inverted. Most of these rest on the requirement that the inputs be uncorrelated at any frequency. There are other mathematical means of solving equation 7.1 without an inversion, however.

The FRF matrix will look like

$$[H] = \begin{bmatrix} H_{11} & H_{12} & H_{13} & \dots & H_{1n} \\ H_{21} & H_{22} & H_{23} & \dots & \dots \\ H_{31} & H_{32} & H_{33} & \dots & \dots \\ \vdots & \vdots & \vdots & \ddots & \vdots \\ \vdots & \vdots & \vdots & \ddots & \vdots \\ H_{n1} & \dots & \dots & \dots & H_{nn} \end{bmatrix} \quad (7.3)$$

Reciprocity has already dictated that

$$H_{ij} = H_{ji} \quad (7.4)$$

so there is some redundancy in the off-diagonal measurements. The diagonal terms (driving point measurements) are unique and so essential. Any single row or column contains sufficient information to derive a complete set of modal parameters for all of the modes, at least theoretically.

The curve fitting (also called **parameter extraction**, **estimation**, or **identification**) routines for modal parameter extraction used by many of the microcomputer software packages for obtaining the modal data, sometimes combining time domain and frequency domain analysis such as **Poly Reference** or **Ibrahim Time Domain**, involve theories and mathematics far too lengthy and complicated to delve into here. The vast majority of the methods are based on linear models, so nonlinearities will only increase the error in the results. Highly damped or closely spaced modes may not be suitably modeled, if at all. The reader is referred to some of the modal analysis texts shown at the end of this chapter for detailed presentations. Most analysis methods, particularly those that employ minicomputers, cannot deal with nonlinear results and so a best estimate curve fit is used. So, results cannot be considered to be absolutely faithful.

Adding frequency response functions from symmetric locations on the aircraft will enhance symmetric modes and assist in differentiating them from antisymmetric ones. The subtraction of the FRFs would conversely enhance antisymmetric modes. This approach is particularly valid for dual-input excitations, for example on opposite wings. However, it is necessary that the responses be measured simultaneously.

### **7.11.2 MODE VISUALIZATION**

As a modal survey is conducted, the response at each survey point (velocity and phase, for example) can be read off of a voltmeter, oscilloscope, or other device. This data can then be manually plotted for a visualization of the mode shape. Current data analysis systems will often have the means of extracting the mode shapes from the modal data. The success of the calculations depend directly upon the number of response transducers placed across the test subject. For example, deriving third wing bending with any measure of certainty with only a tip accelerometer is unlikely. At least fore and aft vertical accelerometers locations at the tip and two inboard wing stations will probably be required if such data is desired. The computer may then be able to display the shapes graphically, either statically or as an animated model. The analysis techniques involve considerable smoothing and curve fitting, so the results are not going to be precise.

One very old but still useful method for visualizing mode shapes is by spreading a thin layer of sand on the object under test (if this is practical). During the excitation the **sand pattern** particles will migrate to the node lines as these areas are moving the least. The resulting pattern will permit a relatively easy determination of the node lines and thus the actual mode. The drawback is the fury of the aircraft maintenance people who find sand in the workings of their machine.

Figure 7.9 shows typical mode shape results. Tables 7.2 through 7.4 give frequency data obtained from a wide variety of aircraft types. These should be used as a guide for planning future GVTs.

### **7.11.3 ORTHOGONALITY CHECK**

Another confidence check of the applicability of the data is the orthogonality check. If measured mode shapes are going to be associated with a finite element model of the structure

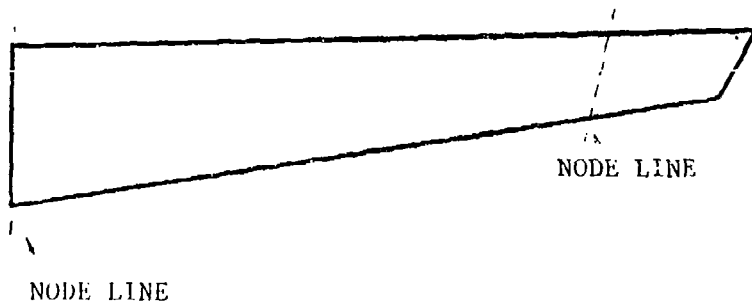
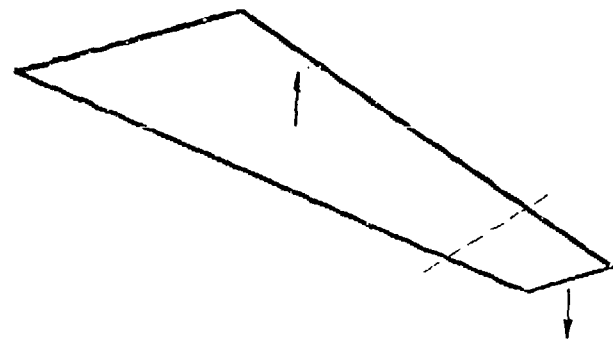


Figure 7.9 Example Wing Second Bending Mode Shape Presentations

(see Section 3.2.5), it will probably need to be adjusted to match the lumped mass modeling of the analysis. Unless the GVT survey points exactly matched the lumped mass model locations, the mode shape will have to be adjusted to match the modeled points while still providing essentially the same shape. After this has been done, the following operation is performed

Table 7.2  
Example C-17A Modes

<u>Type</u>	<u>Frequency</u> <u>(Hz)</u>	<u>Mode Identification</u>
Symmetric	1.70	Inboard Engine Nacelle Yaw
	2.17	Wing First Bending
	2.56	Inboard Engine Nacelle Pitch
	3.72	Vertical Tail Pitch
	4.51	Inboard Engine Nacelle Roll
	5.62	Horizontal Tail Bending
	6.18	Wing Second Bending
	6.93	Wing Fore/Aft Bending
	9.45	Fuselage Vertical Bending
	10.16	Wing Torsion
Antisymmetric	1.64	Vertical Tail Lateral Bending
	1.77	Inboard Engine Nacelle Yaw
	2.23	Vertical Tail Torsion
	3.13	Inboard Engine Pitch
	3.67	Aft Fuselgae Lateral Bending
	4.19	Horizontal Tail Bending
	4.51	Inboard Engine Nacelle Roll
	4.84	Wing Second Bending
	7.94	Wing Third Bending
	8.44	Wing Fore/Aft Bending
	9.99	Wing Torsion

(for illustration purposes only)

Table 7.3  
Example AFFI F-111 Modes

<u>Type</u>	<u>Frequency</u> <u>(Hz)</u>	<u>Mode Identification</u>
Symmetric	3.79	Wing First Bending
	5.13	Wing Chordwise Deformation
	13.29	Stabilizer Bending
	14.09	Wing Tip Torsion
	15.63	Stabilizer Pitch
	26.64	Wing Second Torsion
	5.13	Wing Chordwise Deformation
	6.81	Wing First Bending
	15.06	Stabilizer Bending

Fuselage	26.97	Wing Second Torsion
	7.91	First Vertical Bending
	9.33	Lateral Bending
	17.02	Torsion
	21.77	Second Vertical Bending
Vertical Tail	12.38	Left Wing Torsion

(for illustration purposes only)

Table 7.4

Example T-46 Modes

Type	Frequency (Hz)	Mode Identification
Rigid Body	2.12	Yaw
	4.43	Pitch
	5.31	Roll
	6.35	Plunge
	8.33	Wing First Bending
Symmetric	9.80	Horizontal Tail Bending
	21.86	Rudder Rotation
	26.17	Vertical Fin Lateral Bending
	26.77	Vertical Fin Fore/Aft Bending
	30.33	Wing Second Torsion
	44.27	Wing Torsion
	12.59	Horizontal Tail Torsion
Antisymmetric	14.59	Wing First Bending
	20.76	Vertical Fin Lateral Bending
	23.82	Rudder Rotation
	44.63	Wing First Torsion
	7.42	Aft Torsion
Fuselage	19.71	Lateral Bending
	27.27	First Vertical Bending
	31.94	Vertical Bending/Torsion
Misc.	48.99	Aileron Tab Rotation

(for illustration purposes only)

$$[\Phi]^T [M] [\Phi] \quad (7.5)$$

Where  $[\Phi]$  is the adjusted mode shape matrix in which columns are the eigenvectors and  $[M]$  is the modal mass matrix (see Section 4.5.1). The result is near diagonalization of the resulting matrix with values close to 1 on the diagonal and values close to zero in the off-diagonal terms. Perfect orthogonality would have exactly ones or zeros. Experimental reality dictates that the data will not produce exact unity or null values, so 10 percent of these targets are accepted as good orthogonality and the data can be confidently correlated with the finite element model. Poor orthogonality might indicate that some of the inputs were correlated, the modes were not mapped with fine enough resolution (insufficient survey points), or "false" modes are included in the eigenvector matrix. A cross-orthogonality can be performed where the GVT eigenvector matrix is augmented with the eigenvector matrix from a previous test of from analysis.

## NOMENCLATURE

FRF	frequency response function
$G_{xx}$	input auto power spectrum
$G_{xy}$	cross power spectrum
GRT	ground resonance test
GVT	ground vibration test
H	transfer function
Hz	Hertz
M	modal mass
MISD	multi-input sine dwell
MPR	multipoint random
S/N	signal-to-noise ratio
$\Phi$	mode shape
	Subscripts
i	matrix row counter
j	matrix column counter

## REFERENCES

1. Ewins, D.J., *Modal Testing: Theory and Practice*, John Wiley & Sons, New York, New York, 1984.
2. Lang, George F., *Understanding Vibration Measurements*, Application Note 9, Rockland Scientific Corporation, Rockleigh, New Jersey, December 1978.
3. Stroud, Richard C., "Excitation, Measurement, and Analysis Methods for Modal Testing," in *Sound and Vibration*, August 1987.
4. *The Fundamentals of Modal Testing*, Application Note 243-3, Hewlett-Packard Company, Palo Alto, California, 1986.
5. Lenzi, David C. and Cogburn, Lowell T., *AFTI/F-111 Mission Adaptive Wing Ground Vibration Test*, AFFTC-TR-85-1, AFFTC, Edwards AFB, California, February 1985.
6. Ramsey, Kenneth A., "Effective Measurements for Structural Dynamics Testing," in *Sound and Vibration*, November, 1975, pp. 24-35.
7. Halvorsen, William G. and Brown, David L., "Impulse Technique for Structural Frequency Response Testing," in *Sound and Vibration*, November, 1977, pp. 8-21.
8. Brown, D., Carbon, G and Ramsey, K., Survey of Excitation Techniques Applicable to the Testing of Automobile Structures, in *International Automobile Engineering Congress and Exposition*, held by Society of Automotive Engineers, Detroit, Michigan, February 28 to March 4, 1977.
9. Lally, Robert W., Testing the Behavior of Structures, in *Test*, August/September, 1978.
10. Allemand, R.J., Rost, R.W. and Brown D.L., *Multiple Input Estimation of Frequency Response Functions: Excitation Considerations*, 83-DET-73, The American Society of Mechanical Engineers.

11. Stahle, Clyde V., Modal Test Methods and Applications, in *The Journal of Environmental Sciences*, January/February, 1978.

# CHAPTER 8.0

## AEROSERVOELASTICITY

### 8.1 INTRODUCTION

The aircraft motion sensors (normal and lateral accelerations, pitch, roll and yaw rate, etc.) are mounted in the aircraft to measure flight parameters. Since the aircraft structure is not infinitely stiff, these sensors will also measure acceleration and angular velocities caused by structural deformation such as fuselage bending and torsion. Control surface rotation and elastic modes will also be picked up via surface position sensors. General structural motion can cause what are perceived as uncommanded control surface deflections. The signals produced by the sensors will then be fed into the flight control system (FCS) computer, which will in turn command control surface deflections to counter what it takes to be aircraft rigid body motion or erroneous control surface positions. If the phase lag from the sensor to the control surface is 180 degrees and the system gain is high enough, a sustained surface motion can result. These sorts of feedback are called **structural feedback** or **structural coupling**. It is possible for structural feedback to produce large neutrally damped or even divergent oscillations of the control surfaces, resulting in overall system instability and the possibility of structural failure. Even if control surface motion is not divergent, the response can be at a frequency and amplitude that promotes general aeroelastic flutter. This sort of problem is addressed in the field of aeroservoelasticity or ASE.

High loop gain (explained later) is a principle factor in ASE difficulties. Design features that lead to such high gains are high dynamic pressure, relaxed static stability (see Section 2.3), leading edge control devices, forward swept wings. In general any condition where high control system gain is matched with low structural frequencies can aggravate ASE instabilities.

An example of structural coupling occurred during ground tests of the F-15 STOL aircraft. With the control system engaged and the angle of attack (AOA) probes sitting above 15 deg, a divergent asymmetric rotation of the stabilators (stabs) was observed. At high AOA, the system was designed to move the stabs asymmetrically to counter high yaw rates that tend to develop due to asymmetric vortex shedding off of the nose. This stab motion excited a first asymmetric stab bending mode that was felt through the structure at the yaw rate sensor. This response was fed back through the system and resulted in additional stab rotation to counter what the system interpreted as an oscillatory yaw motion of the aircraft. The larger stab motions only enforced the bending response thus leading to the divergent rotations. The fix was a digital filter to attenuate feedback signal at the bending frequency to the point that it no longer adversely affected the control system.

The effects of structural coupling of the kind just described can be reduced by placing the sensors at ideal locations or "sweet spots" within the structure. These are generally locations with the least motion overall, but may also be where particular structural modes are least likely to create feedback problems. Figure 8.1 shows how a fuselage second longitudinal bending mode has two points of least angular motion and one practical point of least linear motion. The point of least angular motion (the anti-node of the motion) is ideal for a gyro sensor, and the point of least linear motion (at the node) is ideal for an accelerometer. Low order modes generally contain the most energy, and sensors are usually placed to minimize influence from them. Figure 8.2 shows how the best location was found for the F-15 STOL using this criteria but also

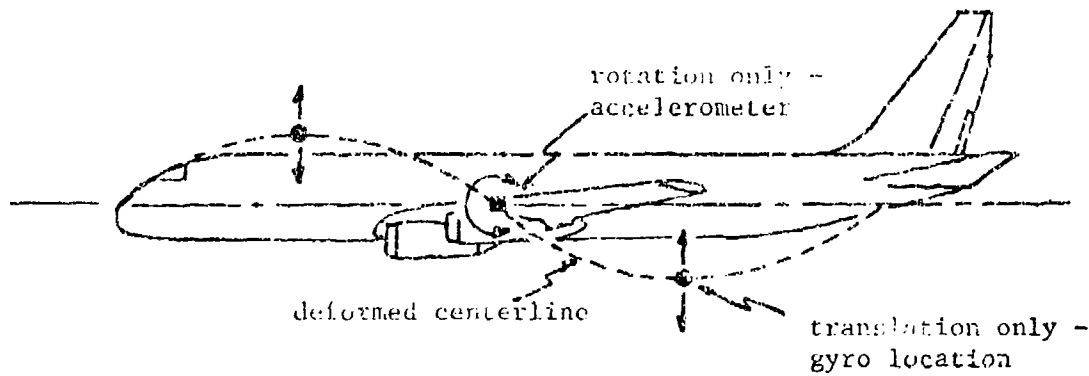


Figure 8.1 Example Sensor Placement Considerations  
Fuselage Second Vertical Bending

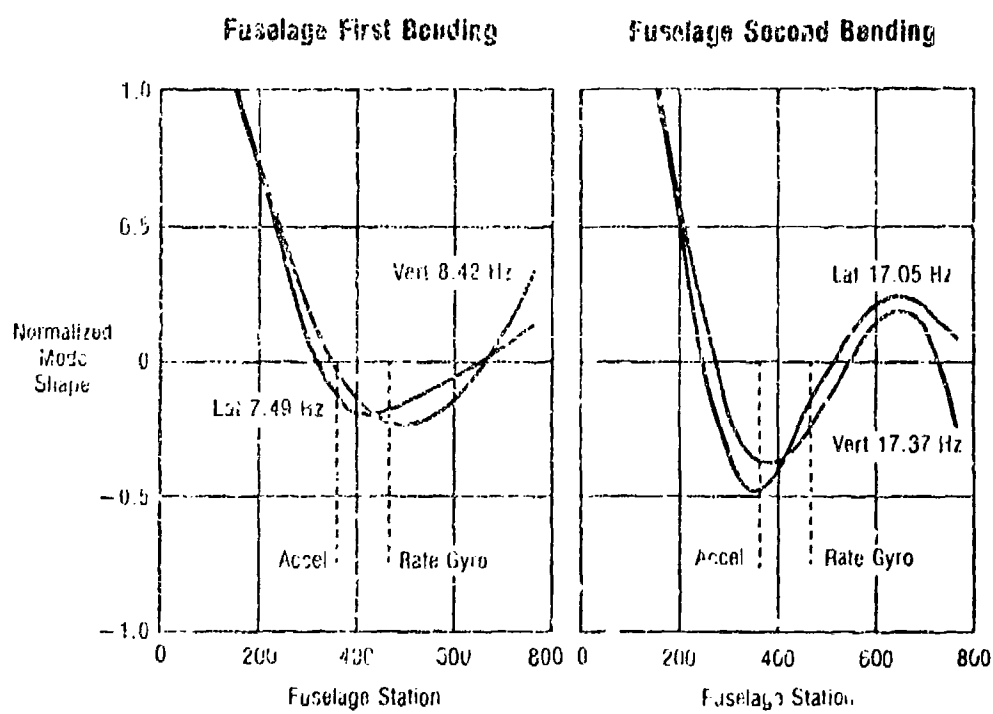


Figure 8.2 Example Determination of Sensor Locations

accounting for practical limitations on the placement. All of this was accounted for during the design of the X-29 aircraft but problems were encountered when an "oil can" effect (panel oscillation) of the bulkhead to which the sensor package was mounted produced adverse feedback.

More typical today, the structural signal is simply filtered at the frequency of concern. Because of the bandwidth of flight control sensors and the low energy of high frequency structural modes, structural coupling will usually involve fundamental or other low frequency modes. Analysis and testing therefore concentrates on these modes. However, it is difficult to filter out low frequency responses like fuselage first and second bending while maintaining adequate gain and phase margins (see Section 8.2.3.2).

Another example of elastic structures causing control problems is the oscillations of heavy stores on the wings of the F-111 fighter-bomber. An antisymmetric store pitching occurs near the edge of the envelope which, due to the high inertia of the stores, actually causes the airplane to roll. The motion is at a low enough frequency for the pilot to "get in the loop" or accentuate the motion when trying to stop it. Even when the pilot tries to hold the stick centered the rolling accelerations causes his body to sway from side to side and lateral stick inputs are still made. Releasing the stick is no good because the pendulum mode of the stick is nearly the same as the rolling motion and the stick just ends up oscillating stop to stop. The only way to recover is to slow down.

## 8.2 CONTROL THEORY

The structures engineer must have a background in the basics of control theory to understand the stability and control engineers' language and their diagrams. This section is taken principally from Reference 1 which may be a good starting point for more detailed information. A course in linear control theory is the best way to go. The reference section lists some worthy texts that may provide answers to questions and explanations of advanced analysis techniques.

### 8.2.1 BASIC CONCEPTS

A system can be described as a series of operations working together to perform a specific function. A simple block diagram of this is shown in Figure 8.3. This is termed an **open-loop** system as opposed to a closed-loop system. The **closed-loop** system modifies the response of the system by feedback of one or more responses of the system (Figure 8.4), making the ultimate control action dependent upon the output. Open-loop system control action is independent of the output. **Multiple-input, multiple-output (MIMO)** systems will be of primary concern here versus **single-input, single-output (SISO)** systems. An example of a MIMO system and a simplified aircraft lateral-directional control system is shown in Figure 8.5.

The arrows in Figures 8.3 and 8.4 indicate the direction of flow of the indicated signal. Signals may be added or subtracted at a summing point (as shown). Other points are simple sampling points where a signal goes to two or more different points in the system. Boxes may indicate a **plant** or parts of the system that use or modify the incoming signals. Plants can also be considered a transfer function (see section 11.3.6) and are normally modeled as mathematical equations. Other boxes are system elements that may represent a transducer that transforms the signal to an appropriate form. The disturbance is some undesirable input signal such as electrical system noise or atmospheric turbulence. System diagrams can be reduced with block diagram algebra as shown in Figure 8.6.

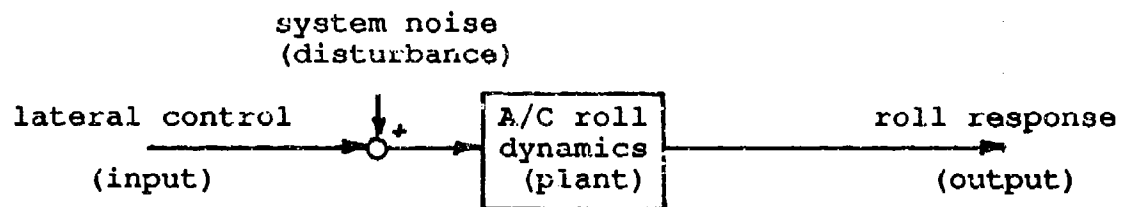


Figure 8.3 Open-Loop System Diagram

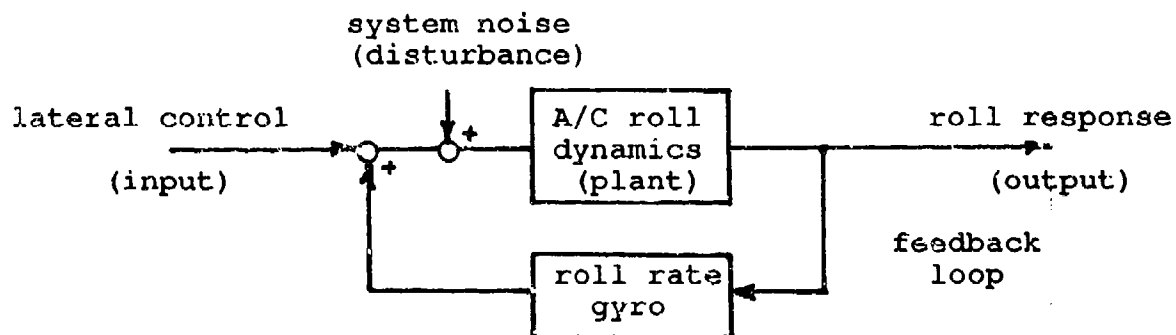


Figure 8.4 Closed-Loop System Diagram

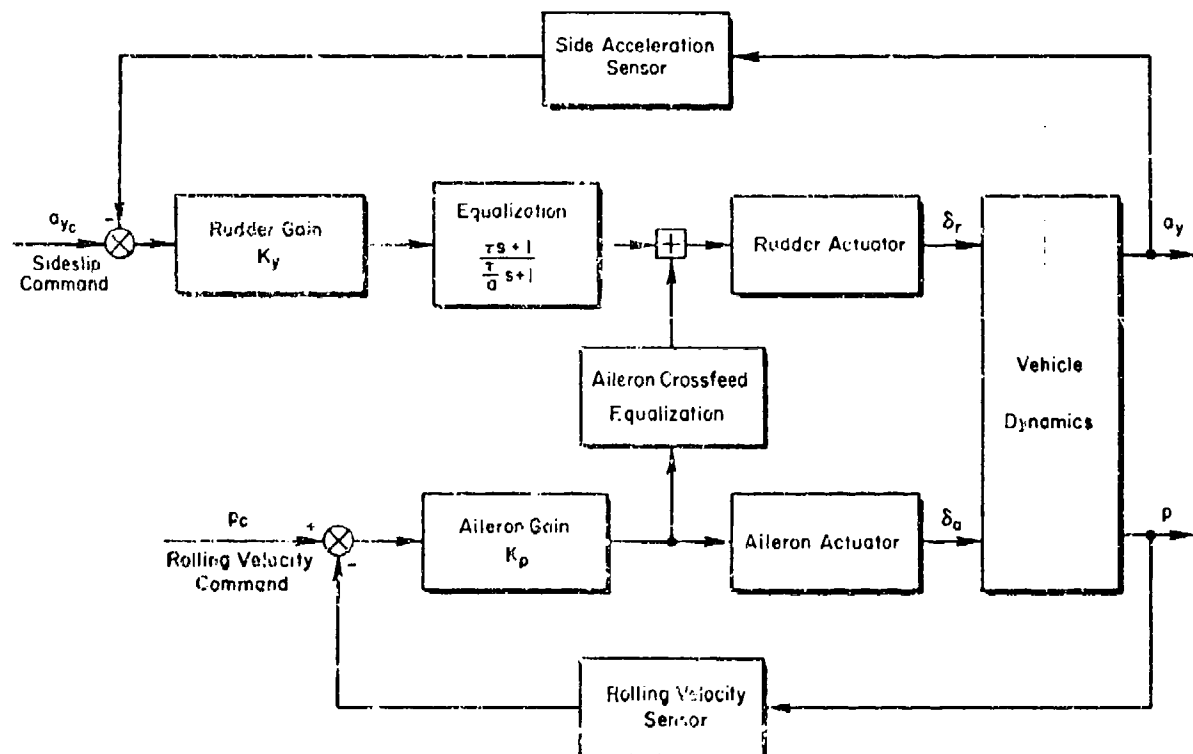


Figure 8.5 Example MIMO System - Aircraft Lateral-Directional Control System

It is generally oscillatory structural responses that are a primary ASE concern with time-variant systems being more susceptible than time-invariant systems. The former is of primary concern here. The range of frequencies over which the system will satisfactorily respond is termed the **bandwidth**. An **unstable system** is one that will tend toward an output of ever-increasing amplitude at a certain input condition.

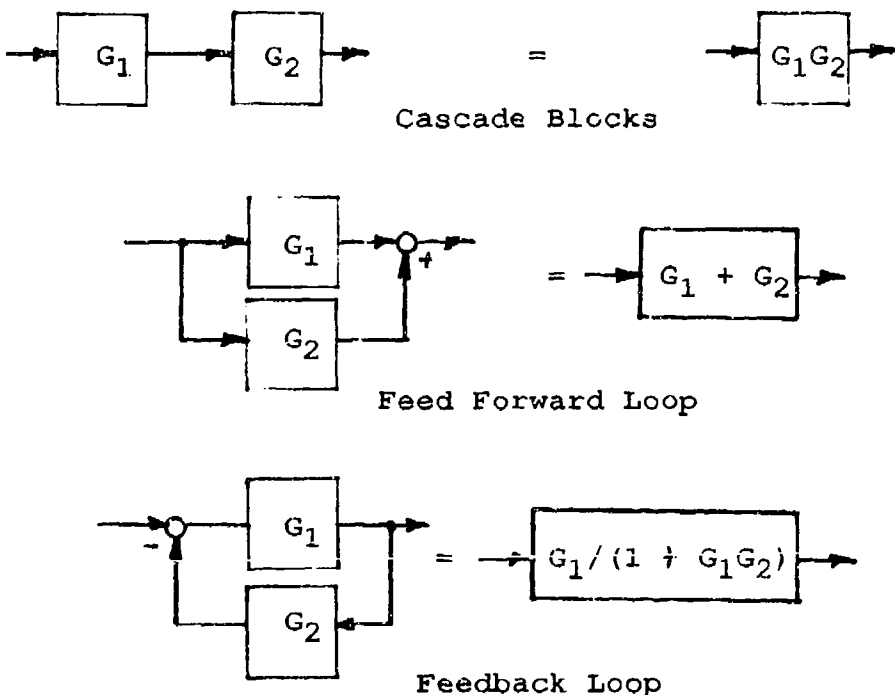


Figure 8.6 Block Diagram Algebra

Initial system conditions often play a significant role in system performance and must be accounted for. Certain definitions with regard to the system response to a **step input (indicial response)** may come up. A **time (transport) delay** is the time between when the input is made and when the system begins to respond. The time for the system to reach 67 percent of its final value (excluding any time delay) is termed **rise time** and the time to arrive within 2 to 5 percent of the final value is **settling time**. These terms have importance for real systems that do not respond to indicial inputs ideally; that is, the response must reach a steady-state value in a finite time and then return to its initial state in some finite time after the input is terminated. System **error** refers to the difference between the desired output and the actual output. One of the principle purposes of feedback is to minimize this error and to stabilize the system. The sensitivity of the system to the disturbances or other inputs may also need to be considered.

Most systems, particularly aircraft systems, are nonlinear and the mathematical modeling equations may be complex, of high order, and involve differentials and integrals in order to adequately describe the system linearly. The rapid solution of these equations, often by specialized methods, are very computer intensive and constitute a significant area of controls theory.

System gain is the weighting given to an individual feedback or input to the system. Changing of gains is a simple means of modifying system performance. For example, using Figure 8.4, the output of the roll rate gyro may be boosted to increase its weighting with respect to the pilot's lateral control input. The system may also include filtering elements so that only certain parts of the signal are passed. For example, a filter downstream of the roll rate gyro in Figure 8.3 may pass only low frequency output so that higher frequency structural responses (structural filtering) is not passed.

### **8.2.2 COMPENSATION**

The FCS may be programmed to change the basic control laws at different flight conditions to provide suitable flying qualities as the dynamics and aerodynamics change throughout the flight envelope. This is known as compensation. The simplest compensation is variation of basic gains, but this is not always successful. The response of a system can also be modified by introducing basic control elements into either the forward or feedback loops, or both. This is known as compensation or dynamic compensation. Three types of compensation will be introduced; lead, lag, and lag-lead compensation. The effects of compensation will be shown graphically in Section 8.2.3. In a block diagram it would be represented by a mathematical formulation in an element block.

**Lead** takes its name from its phase-lead characteristic. It results in a greater bandwidth of the system. It also permits an increase in system gain without adversely affecting transient performance (unforced response following termination of the input). Depending upon how it is implemented, lead compensation may provide better performance (smaller system error).

The phase-lag characteristic of a lag compensator attenuates high frequency response resulting in a reduction in bandwidth and slowing down of system response. System error may tend to increase with lag compensation. Lag-lead incorporates many of the advantages of the two previous compensations without excessive bandwidth change.

### **8.2.3 REPRESENTATIONS**

Four principal system response representations, root-locus, Bode, Nyquist, and polar form will be introduced along with general interpretation and how the effects of compensation can be seen when using them. They will be discussed further in Chapter 11.0 with regard to how they are used in structural dynamics analysis. The Nichols form is seldom used in ASE analysis and will not be covered in this handbook.

#### **8.2.3.1 ROOT-LOCUS**

The first requirement in producing a root-locus plot is the equation describing the system in s-plane form by use of pole-zero or fractional form and the Laplace transform. This is a transfer function, representing the system plant, with a numerator (zero) polynomial divided by the denominator or characteristic polynomial. How this is done is beyond the scope of this text, but an example of such a transfer function is provided below.

$$F(s) = \frac{2(s+1)(s-2)}{(s+3)(s^2+2s+2)} \quad (8.1)$$

where the numerator 2 is the gain and  $j$  represents an imaginary number. The second order term in the denominator must be factored for plotting. Each of the expressions in parenthesis will then yield a root of the system. The roots in the numerator are termed **zeros** (plotted with a small circle) and those in the denominator are called **poles** (plotted with a small  $x$ ). The complex roots will have the form

$$s = \sigma \pm j\omega \quad (8.2)$$

and are plotted in the s-plane in a pole-zero plot as shown in Figure 8.7 for the system of equation 8.1.

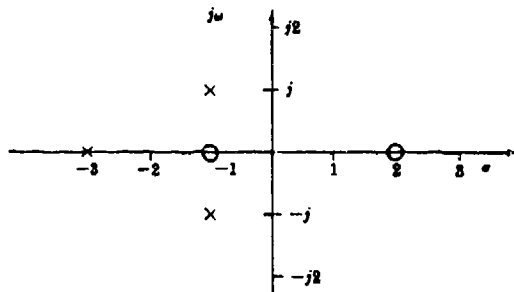


Figure 8.7 Typical Pole-Zero Plot

The stability of a system can be determined from the root-locus. The presence of a pole in the **right half-plane (RHP)** of the plot implies an instability or divergent response. A system with open-loop poles or zeros in the right half-plane is referred to as a **non-minimum phase system**. Otherwise, it is a **minimum phase system**. Compensation can correct instabilities as well as alter the dynamics of the system. If the gain(s) change then the system will have different roots. Plotting the roots as a function of varying gain will show the movement of the poles and zeros with the change in gain (or compensation) and the best gain for the desired system response can be found. An example of this is shown in Figure 8.8 for equation 8.1. Such a plot may indicate an unstable or nearly unstable condition at some gain. In general, poles will tend to converge to the zeros or go to infinity. The position of the poles and zeroes in the s-plane are significant to system characteristics. Section 11.3.9 discusses how some of these characteristics can be extracted from the root-locus.

Lead compensation will be equivalent to applying a term like that shown in equation 8.3 to the Laplace equation of the system, where  $b$  is greater than  $a$ .

$$\frac{s+a}{s+b} \quad (8.3)$$

Lag uses a term like equation 8.4, where  $b$  is again greater than  $a$ .

$$\frac{a(s+b)}{b(s+a)} \quad (8.4)$$

Lag-lead would look like

$$\frac{(s+a)(s+b)}{(s+c)(s+d)} \quad (8.5)$$

where c is greater than a and b is greater than d. The requirement for ab=cd is often imposed for mechanization considerations.

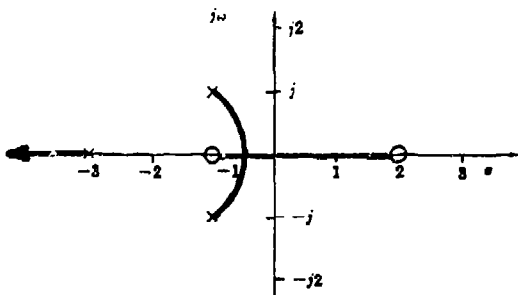


Figure 8.8 Root-Locus Plot for Figure 8.7

### 8.2.3.2 BODE

Like the root-locus, Bode plots require the transfer function to be cast in a special form, the Bode form. An example of this is shown in equation 8.6.

$$G(j\omega) = \frac{1}{j\omega} \frac{j^{0.2} + (\omega^2)^2}{(1 + j^{0.5})(1 + j^{0.4})} \quad (8.6)$$

The means of separating the magnitude and phase from this equation and the plotting of each element is beyond the scope of this handbook. Converting the magnitude to decibels (dB) is done as shown in equation 8.7

$$(\text{mag})\text{dB} = 20\log_{10}(\text{mag}) \quad (8.7)$$

The resulting plot for equation 8.6 will look like Figure 8.9, with a logarithmic frequency scale. The magnitude and phase are sometimes plotted on top of each other with the respective axes on opposite sides of the plot.

Figure 8.10 shows how the gain margin and phase margin are determined from a Bode plot of the open-loop system. These two parameters are a measure of the closed loop system stability. **Gain margin** is defined as the maximum gain which can be added to the system without producing an instability. This is the gain at the frequency where the phase angle is at the **phase crossover**, or -180 deg. The **phase margin** ( $\phi_{pm}$ ) is defined as 180 degrees plus the phase angle corresponding to a magnitude of 1.0 (unity gain) or 0 dB. For a minimum-phase system, it represents the amount of phase shift that is possible without causing instability, and which must be positive for a stable system. The larger the  $\phi_{pm}$ , the more stable the system.

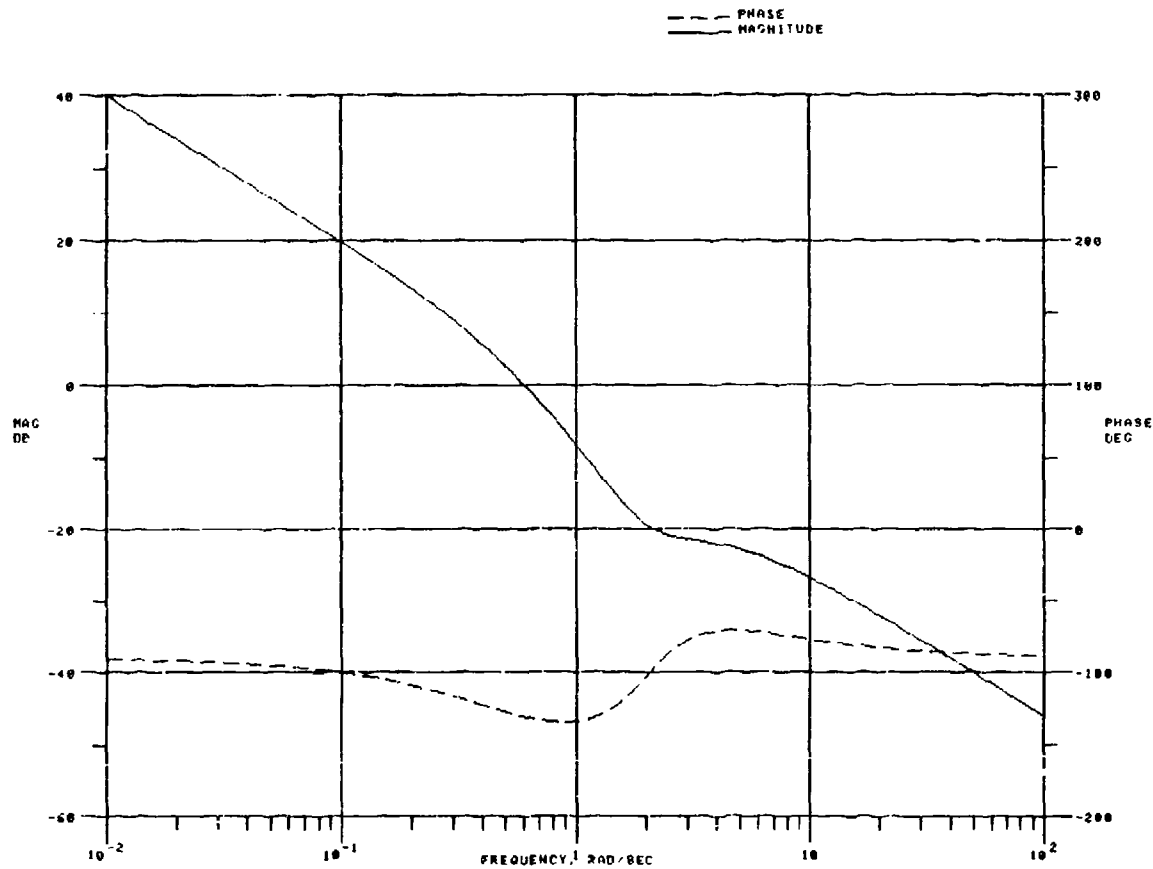


Figure 8.9 Bode Plot for Equation 8.6

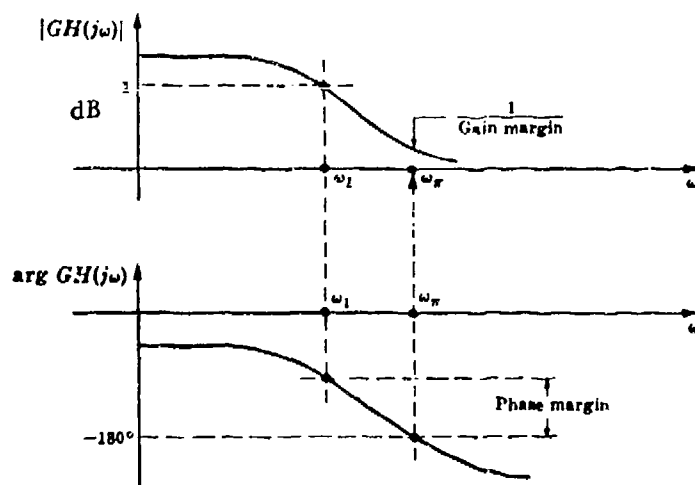


Figure 8.10 Determining Phase and Gain from a Bode Plot

Simple gain compensation will result in moving the magnitude plot up or down on the dB scale and will not effect the phase plot. Lead compensation, shown in equation 8.8, will lower the overall magnitude plot in the low frequency regime and raise the phase curve in the low to middle frequency range. In general, it has the effect of increasing the gain or phase margins, or both, or to increase the bandwidth. Lead compensation has the form

$$P(j\omega) = [(a/b)(1 + j\omega/a)]/(1 + j\omega/b) \quad (8.8)$$

where  $a$  is less than  $b$ . The lag compensator would have the form

$$P(j\omega) = (1 + j\omega/b)/(1 + j\omega/a) \quad (8.9)$$

and has the effects discussed in Section 8.2.2. The lag-lead compensator has the form

$$P(j\omega) = \frac{(1 + j\omega_a)(1 + j\omega_b)}{(1 + j\omega_c)(1 + j\omega_d)} \quad (8.10)$$

with properties also presented earlier.

### **8.2.3.3 NYQUIST AND POLAR**

The polar plot is an s-plane presentation in which  $j\omega$  is substituted for  $s$  in the expression for  $P(s)$ . The plot can be shown in three possible coordinate systems.

**Polar Coordinates:**

$$P(j\omega) = |P(j\omega)| \angle \phi(\omega) \quad (8.11)$$

**Euler Coordinates:**

$$P(j\omega) = |P(j\omega)|[\cos \phi(\omega) + j \sin \phi(\omega)] \quad (8.12)$$

**Rectangular Coordinates:**

$$P(j\omega) = \text{Re}P(j\omega) + j\text{Im}P(j\omega) \quad (8.13)$$

Gain margin is found on the polar plot as shown in Figure 8.11 (GH is the open-loop transfer function), where the crossing of the negative real axis is termed the **phase crossover frequency**. The same figure shows how the phase margin is found, where the **gain crossover frequency** is associated with the point where the unit circle intersects the curve. There is a graphical means of determining the resonant frequencies and damping from the same plot but, as this has been supplanted by much more accurate and simpler techniques, it will not be covered.

The Nyquist plot is a polar plot of the open-loop system which provides a graphical means of determining the exact stability of a closed loop system. The plot is done in the s-plane (see Section 8.2.3.1) which consists of  $\text{Re}P(s)$  and  $\text{Im}P(s)$  axes, the real and imaginary parts of  $P(s)$ , the coupled function, respectively. System stability is determined by using the **Nyquist Stability Criterion**. This states that the number of clockwise encirclements by the plot of the point  $(-1,0)$  must be less than or equal to zero (counterclockwise encirclements are taken as positive) for stability, where the direction of the encirclement is determined by increasing frequency.

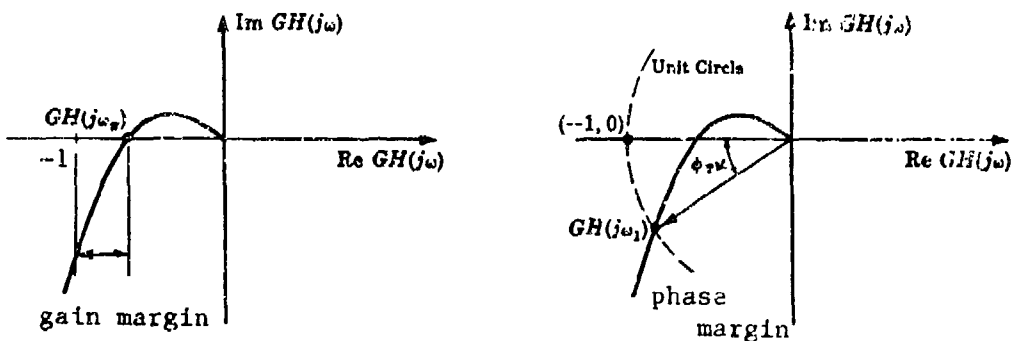


Figure 8.11 Phase and Gain Margin From a Polar Plot

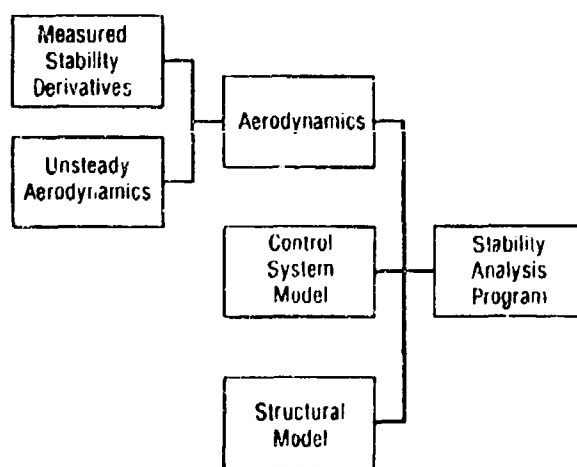


Figure 8.12 Aeroservoelastic Analysis Flow Diagram

### **8.3 ANALYSIS**

The dynamics of the aircraft (equations of motion) are modeled by control methods and run in simulations long before the aircraft ever flies. The simulations play a large role in the overall aircraft design to meet the customer requirements, particularly the flight computer software design. This aspect of the design process becomes very critical for "fly-by-wire" aircraft. An attempt is made to predict structural dynamics at this conceptual design stage so that these may be incorporated in the simulation. This is the earliest stage at which structural filters or sensor locations are considered. The analysis will follow the flow indicated in Figure 8.12. There is a much more manageable program available in Air Force Systems Command to check for aeroservoelastic stability called ADAM (Analogue and Digital Aeroservoelasticity Methods). Ground Vibration Tests (GVT), Ground Resonance Tests (see next section) and early flight results may cause changes as required to reduce detrimental structural feedback. The structures flight test engineer must be familiar with all of this work and participate to the largest extent possible to ensure that structural effects are considered in the control design, all necessary testing is completed, and potentially dangerous feedback is accounted for.

### **8.4 GROUND TESTS**

ASE ground tests should be proceeded by stability tests of the control system alone using aircraft hardware, either as a bench test or in an ironbird which has control surface actuators and representative surface masses, to ensure that there is no confusion as the source of instabilities. Reference 8 (now replaced with MIL-F-87242) states that

"Prior to first flight the following minimum testing will be performed.

- a. Gain margin tests to demonstrate the zero airspeed 6 dB stability margin requirements for feedback systems depending on aerodynamics for loop closure and to demonstrate stability margins for nonaerodynamic loops. Primary and secondary structure shall be excited, with special attention given to areas where feedback sensors are located with loop gains increased to verify the zero airspeed requirements. For redundant and multiple-loop systems, the stability requirements in degraded configurations should also be demonstrated. (These tests are performed in conjunction with structural testing. They are designed to determine if structural mode frequencies are propagating into the FCS and, if so, if there is proper compensation.)
- e. Ground vibration tests with active controls using soft suspension system to simulate free-free condition. Flight control sensor outputs and open loop frequency response data should be recorded for correlation with analytical results in predicting servoelastic and aeroservoelastic stability.
- f. Taxi tests with increasing speed and all feedback loops closed to examine servoelastic stability above zero airspeed. Flight control sensor outputs and control surface deflections should be recorded."

The static structural coupling ground test described above is called a **Ground Resonance Test** (GRT, also known as a **Structural Mode Interaction**, SMI, **Structural Coupling** or **Structural Resonance Test**). It is not a true ASE test since the aerodynamics are not simulated. This testing should not be confused with **Limit Cycle Tests** in which the aircraft rigid body motions simulated using the equations of motion and fed into the FCS for general system stability checks. There are two types of structural coupling tests: open-loop frequency response and

closed-loop gain margin tests. The objective of these tests are to determine the gain margin plus the sensor and overall system susceptibility to structural coupling.

In an open-loop frequency response test, each feedback loop of the system is opened separately and a signal (swept sinusoid being common) is introduced at the "downstream" side of the break. For Figure 8.5, this would be between rolling velocity (roll rate) sensor and the command input summing point, or between the side (lateral) acceleration sensor and the sideslip (lateral acceleration) command summing point. The output is monitored at the "upstream" side of the break, or the end toward the side acceleration or rolling velocity sensor in Figure 8.5. The sine sweep signals (linear or logarithmic) may be produced by a ground unit or as a special function of the flight control computer. A constant input at both large and small amplitudes should be done in case of nonlinear response behavior. The open-loop frequency response is obtained using a dynamic analyzer. Frequency response plots are made for several different input amplitudes to observe the system's input amplitude sensitivity. The amplitudes and the phase angle of the input and output signals are plotted (transfer function) as a Bode plot. The same open-loop frequency response results would be obtained using either a swept sine input or a random noise input of equivalent intensity over an equivalent frequency range for a purely linear system.

In any linear system the frequency response is not a function of input amplitude. However, in real systems numerous nonlinearities are present. These can be such factors as break-out forces, hysteresis, nonlinear response or rate limiting of actuators. An intentionally designed nonlinearity is scheduled gain changes in the control laws. The effect of these nonlinearities on system stability can be observed by obtaining the frequency response for several different input amplitudes. Most often, the greatest structural coupling has been found to occur at relatively small amplitudes. Therefore, the amplitudes chosen for use in the frequency response usually represent only a small percentage of that which is possible.

Closed-loop tests involve structural excitations to directly test for structural feedback. The FCS may be used to excite the structure through control surface rotation using the swept sine signals or similar functions described above. The signal can be sent directly to the control actuators themselves for a purely structural test. Manually induced stick raps and rudder kicks may also be used in this portion of the test. The closed-loop gain margin test is performed by inserting a variable gain at an appropriate location in the FCS. The loop gain is increased until a condition of lightly damped or undamped response occurs. The frequency and gain for this condition are recorded and their correspondence with data from the open-loop tests checked. Since military specifications require a 6 dB gain margin, or twice the nominal gain, without instabilities (see Table 8.1 for precise gain and phase margin requirements), a simple demonstration of this without actually going to instability is generally sufficient. However, it is best to find the actual gain to produce instability in the event that programmed gains are altered in the course of flight testing.

These tests should be performed in all the different control modes, including degraded modes or failure scenarios. It will probably be necessary to create the conditions of flight artificially with a pneumatic ground test unit. Hydraulic power and electrical power to the aircraft will also be required. Every effort should be made to ensure that the hydraulic flow rate is not less than that normally supplied by the aircraft pumps or the control surface responses and actuator stiffnesses will not be faithfully duplicated. The test is often performed with the aircraft in the same arrangement as for a GVT (see Chapter 7.0) such as fiction and sensors. In fact, the GVT and Ground Resonance Test are often done back-to-back since much test and analysis equipment is common to the two tests. The use of electrodynamic shakers to excite the structure is not advised because the shaker armature does not move very far and will also resist control surface

**Table 8.1**  
**Gain and Phase Margin Requirements**

Mode Frequency Hz	Airspeed Below $V_{oMIN}$	$V_{oMIN}$ To $V_{oMAX}$	At Limit Airspeed ( $V_L$ )	At $1.15 V_L$
$f_M < 0.06$	$GM = 6 \text{ DB}$ (No Phase Requirement)	$GM = \pm 4.5$ $PM = \pm 30$	$GM = \pm 3.0$ $PM = \pm 20$	$GM = 0$ $PM = 0$ (Stable at Nominal Phase and Gain)
$0.06 \leq f_M < \text{First Aero-Elastic Mode}$	$V_{oMIN}$	$GM = \pm 6.0$ $PM = \pm 45$	$GM = \pm 4.5$ $PM = \pm 30$	
$f_M > \text{First Aero-Elastic Mode}$		$GM = \pm 8.0$ $PM = \pm 60$	$GM = \pm 6.0$ $PM = \pm 45$	

where:

- $V_L$  = Limit Airspeed (MIL-A-8860).
- $V_{oMIN}$  = Minimum Operational Airspeed (MIL-F-8785).
- $V_{oMAX}$  = Maximum Operational Airspeed (MIL-F-8785).
- Mode = A characteristic aeroelastic response of the aircraft as described by an aeroelastic characteristic root of the coupled aircraft/FCS dynamic equation-of-motion.
- GM = Gain Margin = The minimum change in loop gain, at nominal phase, which results in an instability beyond that allowed as a residual oscillation.
- PM = Phase Margin = The minimum change in phase, at nominal loop gain, which results in an instability.
- $f_M$  = Mode frequency in Hz (FCS engaged).
- Nominal Phase and Gain = The contractor's best estimate or measurement of FCS and aircraft phase and gain characteristics available at the time of requirement verification.

motion commanded by the FCS. This can result in the shaker thruster being driven through the surface.

Tests at different aircraft configurations (stores, fuel, wing sweep, etc.) may be necessary. It is also important that the control laws and structure be as close to the final production form as possible for the test to be valid. If significant changes are made to these in the course of flight testing, it may be necessary to repeat portions or all of the test. It is also critical that a single emergency cut-off switch be available to open all feedbacks and kill the artificial input signal in the event of a divergent control surface oscillation that may damage the aircraft.

Prior to the first flight, the aircraft should undergo taxi tests to greater and greater speeds. This will test system responses to actual operational mechanical inputs (taxiing over the ramp tar strips, engine vibrations) and see the effect of automatic gain changes as the airspeed increases.

## **8.5 FLIGHT TESTS**

ASE flight testing is a cross between flutter (see Chapter 6.0) and basic flight controls (flying qualities) testing. Some of the instrumentation is similar to that used for flutter testing; strain gages or accelerometers for structural response and displacement transducers for control surface motion. These serve to warn the test engineers of any undesirable response due to structural feedback.

Testing should begin with the gains at half that found to produce an instability in the GRT or the nominal gain, whichever is lowest. The gain can then be incrementally increased in flight to the nominal condition. This naturally requires a means of changing the gains in flight, a feature usually only available on prototype aircraft. A means of rapidly opening the feedback loops (or at least reducing the gains if the aircraft is unstable without feedback), as in the GRT, is essential for safe recovery in the event of an instability. Transfer function plots of surface motion and other aircraft responses (rates and attitudes) can be produced point-to-point or flight-to-flight to determine phase and gain margins and for comparison with model and simulator results. These plots will assist in identifying any unusual characteristics that may contribute to or are directly attributable to structural feedback.

This flight testing is usually conducted in association with the flying qualities engineers. The reader is referred to texts on stability and control test methods such as References 2 and 7. The test engineer should watch for any sign of lightly damped control surface motion as well as any significant deviation from predicted response as seen on real-time transfer function plots or in post-flight analysis. Using a flutter exciter system, stick raps (see Section 6.6), doublets, control sweeps made by the pilot, a function of the flight control computer, or other stability and control test maneuvers are helpful in exciting the structure and generating any potential feedback. Testing in certain degraded flight control system modes (failure modes) is important because this may affect certain feedback and coupling characteristics.

### **8.5.1 NOTCH FILTER**

Should an undesirable system or aircraft response or the potential for one be uncovered, the easiest remedy without disturbing beneficial flying qualities is the application of a notch filter. Shown in Figure 8.13, this is either an analog filter or a digital algorithm which seeks to attenuate a signal (output of the roll rate gyro, for example) at a specific frequency to a level that will no longer produce the detrimental system response. The results of the use of such a filter is shown

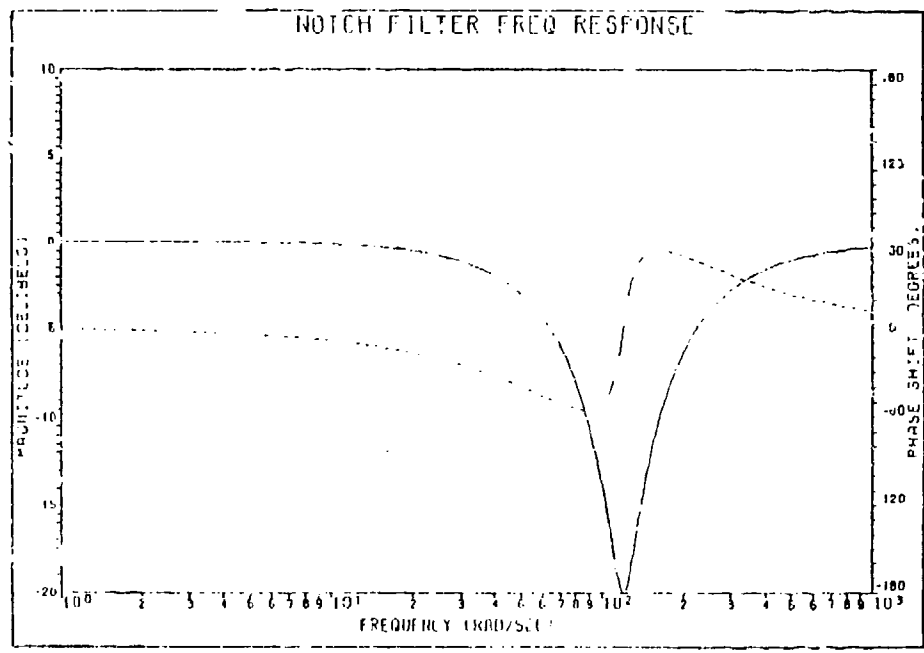
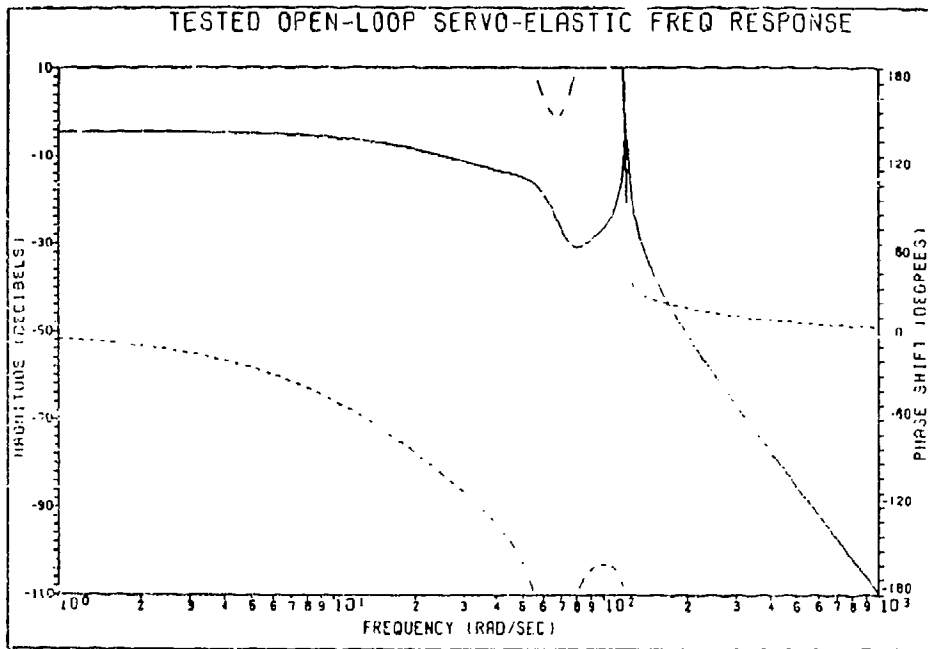
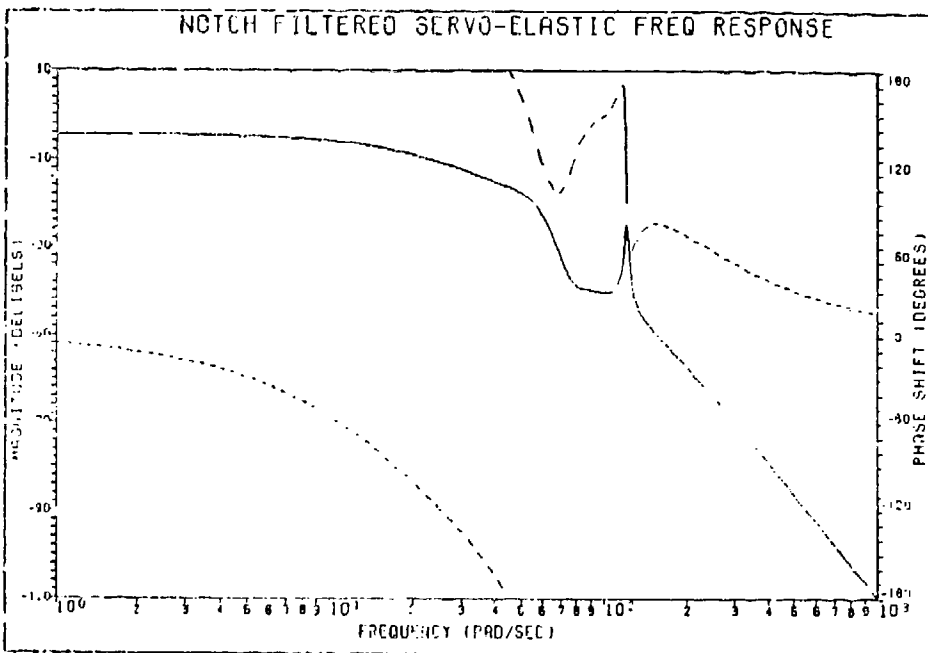


Figure 8.13 Example Notch Filter



a. Undesirable Response



b. Undesirable Response Attenuated by Notch Filter

Figure 8.14 Effects of Notch Filter

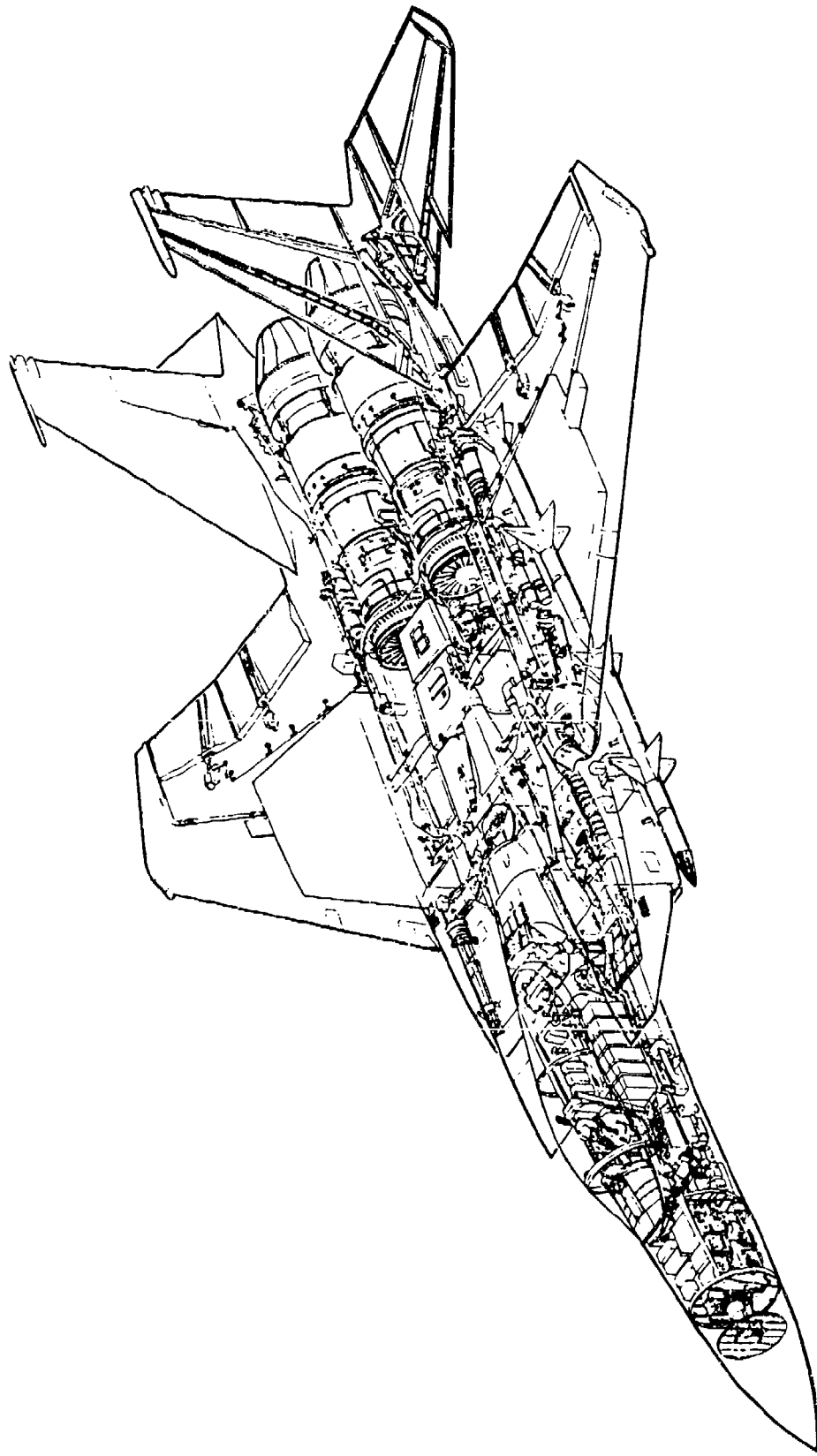
in Figure 8.14. As with any changes to the flight controls, a subsequent flight test is mandatory. The control systems should be designed with such filters from the beginning using predicted modal responses for the airframes and control surfaces. The data update rate of the FCS serves as a form of self filtering. An update rate of 30 samples per second (sps) would effectively ensure that modes above 30 Hz will not be a problem. However, aliasing (see Section 12.3.2) may cause responses within the sample range from higher frequency modes unless good anti-aliasing filters are used.

## NOMENCLATURE

a	constant
ADAM	Analogue and Digital Aerosevoelasticity Methods
AOA	angle of attack
ASE	aerosevoelasticity
b	constant
c	constant
d	constant
dB	decibel
deg	degree
F	function
FCS	flight control system
f	frequency
G	Bode form function
GH	open-loop transfer function
GRT	ground resonance test
GVF	ground vibration test
Hz	Hertz
Im	imaginary part
j	imaginary number
lat	lateral
mag	magnitude
MIMO	multiple input, multiple output
P	function
Re	real part
RHP	right half-plane
SISO	single input, single output
SMI	structural mode interaction
s	Laplace variable
sps	samples per second
V	limit airspeed
vert	vertical
$\sigma$	complex variable coefficient
$\omega$	frequency
$\phi$	phase
Subscripts	
$l$	limit
$M$	mode
$max$	maximum
$min$	minimum
$o$	operational
$pm$	phase margin

## REFERENCES

1. DiStefano, Joseph J., III, Stubberud, Allen R. and Williams, Ivan J., *Theory and Problems of Feedback and Control Systems*, Schaum's Outline Series, McGraw-Hill Book Company, New York, New York, 1967.
2. Nagy, Christopher J., *A New Method for Test and Analysis of Dynamic Stability and Control*, AFFTC-TD-75-4, Edwards AFB, California, May 1976.
3. D'Azzo, J.J. and Houpis, C.H., *Linear Control System Analysis and Design*, McGraw-Hill Book Company, New York, New York, 1981.
4. McRuer, D., Ashkenas, I. and Graham D., *Aircraft Dynamics and Automatic Control*, Princeton University Press, Princeton, New Jersey, 1973.
5. Reid, J.G., *Linear System Fundamentals, Continuous and Discrete Classic and Modern*, McGraw-Hill Book Company, New York, New York, 1983.
6. Franklin, G.F., Powell, J.D. and Emami-Naeini, A., *Feedback Control of Dynamic Systems*, Addison-Wesley Publishing Company, Menlo Park, California, 1986.
7. *Flying Qualities, Theory and Flight Test Techniques*, USAF Test Pilot School, Edwards AFB, California.
8. Flight Control System - Design, Installation and Test of Pilot Aircraft, General Specification for, MIL-F-9490D.
9. Kirsten, Paul W., Flight Control System Structural Resonance and Limit Cycle Oscillation, in AGARD Conference Proceedings No. 233, *Flight Test Techniques*.



McDonnell-Douglas F-15A Cutaway

# CHAPTER 9.0

## VIBRO-ACOUSTICS

### **9.1 INTRODUCTION**

The operation of onboard equipment and the influence of aerodynamic forces create a broad spectrum of vibration sources that can affect an airplane in many different ways. The study of a portion of these influences have been called vibro-acoustics and aero-acoustics. Nearly every flight test discipline has to concern itself with this subject to one extent or another. The vibration environment to which an avionics box is subjected is very critical to its reliability and sometimes its ability to function properly. Early KC-135 testing revealed a coupling between the fuselage vertical bending mode and the autopilot shock mount frequency that caused the autopilot to command sharp pitch oscillations so violent as to yank the control yoke from the pilot's grasp. While such a problem would not normally be within the purview of the structures engineers, their understanding of structural interactions and frequency response analysis techniques tends to draw them into these other areas of testing.

The acoustics source of the vibration problem will be given dominant attention in this chapter. Sound is but a vibration in the atmosphere or a series of traveling pressure waves. This vibration is transmitted to a structure immersed in the air. High noise levels from boundary layers, separated or turbulent flow (see Section 2.2.5), aircraft maneuvering, engine operation and other onboard equipment can excite high frequency resonances in an aircraft structure that may cause local overloads or eventually to fatigue (known as sonic fatigue) of components and the general airframe (see Section 3.4.5). A frequency range of 50 to 60 Hz is near natural airframe coupling frequencies and high amplitude excitations in this range can induce severe damage. External stores are particularly susceptible to frequencies up to 200 Hz with wakes (often oscillatory) from other stores, unstable shock waves, excessively turbulent flow, and vibrations from aircraft internal components creating an environment the weapon developers never anticipated. An example of this sort of problem is the case of a shallow weapons bay with a length-to-depth ratio of 4.5:1 (such as used for a semi-submerged store). At transonic speeds this cavity can experience pressures generated by unstable shock waves equivalent to being three feet from an F-15 in full afterburner. The problem can be relieved by changing the structure to change the natural frequencies and strength, applying a passive damping material, or by active suppression by applying an equal but opposite excitation. For acoustics applications, involving avionics and other equipment; frequencies on the order of thousands of cycles per second must be dealt with.

An example of the problems noise can cause is the severe aft fuselage skin cracks found early in the life of the KC-135A tankers. These aircraft use water injected into the turbojet engine exhaust for increased mass flow in heavy weight takeoffs. The water injection creates a tremendous amount of noise that fatigued the aircraft structure aft of the engines. The solution was to add many external metal hoop bands around the aft fuselage. Much later in its service life a proposal was made to place a thin polymer layer on the inside skin of the aft fuselage to act as a passive damper to reduce vibration levels and extend the fatigue life even further. An example of external store acoustics problems are those on the F-15. Testing of the AMRAAM missiles was greatly troubled by failures attributable to a bad vibro-acoustics environment.

The study of acoustics is largely concerned with human factors; the effects of noise on the performance and health of people. This is not subject matter for this handbook and will not be discussed. The measurement of sound intensity also constitutes a sizable portion of the acoustics field. This is the accurate measurement of the noise in an area closely surrounding the source of the sound. The intent is to determine the best means of reducing the intensity and sound level in the areas subjected to the sound. Since the noise of concern in flight testing is seldom present except during flight and for which only aerodynamic changes to the aircraft will produce sound intensity changes, intensity measurements are impractical and will be excluded from the handbook.

## **9.2 GENERAL VIBRATION**

Much of the avionics and other internal components will have undergone laboratory shock and vibration tests using shaker tables to specification limits of g's as a function of axis and duration (see Reference 7). Flight testing is still necessary because there is no certainty that these tests have adequately replicated the true inflight conditions. General shock and vibration environmental testing uses much the same instrumentation and analysis techniques as flutter testing. The specification limits to which the results are compared are presented similarly to that discussed in Section 9.5.3. The basic approach is to determine critical areas (such as for an autopilot computer mounted in an avionics compartment) and instrument each location with a tri-axial accelerometer (see Section 10.3). Data is collected at representative flight conditions (taxi, maximum power takeoff, low-level cruise, aerial refueling, etc.) with 30 seconds to a few minutes dwell on each condition. Results are typically presented as a power spectral density (PSD) or other frequency response function (see Section 11.3) with averaging used to smooth the data.

Avionics boxes and other components can be partially shielded from adverse vibration ranges and levels using isolator mounts. These normally take the form of a dashpot, spring column, or rubber pad with stiffness designed to damp a specific frequency range of response.

## **9.3 FUNDAMENTALS OF SOUND**

If sound is thought of as a pressure wave, an associated wavelength and frequency can be surmised. Wavelength can be defined as

$$\lambda = (\text{speed of sound})/\text{frequency} \quad (9.1)$$

where the speed of sound in air at 21°C is 344 m/sec. This is shown graphically in Figure 9.1. Humans can hear sounds from 20 Hertz (Hz, cycles per second) to 20,000 Hz, above which is termed **ultrasound** and below it is **infrasound**. Sounds outside this human hearing range can still adversely effect aircraft structures.

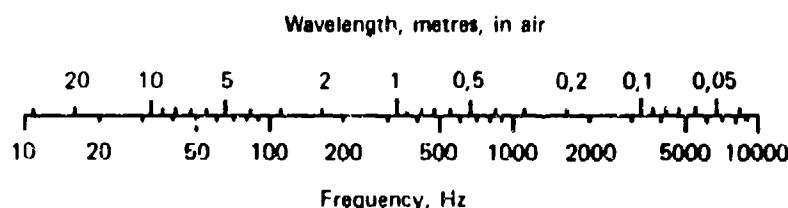


Figure 9.1 Wavelength versus Frequency of Sound in Air

For a pressure wave in the atmosphere (or any medium), it makes sense to define "sound pressure" as a dynamic variation in atmospheric pressure. This can be used to provide a definition of sound amplitude, what are called **sound pressure level (SPL)**, or

$$L_p = 20 \log \left( \frac{p}{p_0} \right) \quad \text{in decibels (dB)} \quad (9.2)$$

where  $p$  is the root mean squared (RMS) value of sound pressure in Pascals (Pa) and  $p_0$  is a reference value of pressure (for 0 dB), or 20  $\mu\text{Pa}$  for air. The RMS is used, from a set of instantaneous values, because it is directly related to the energy content of the sound. The convenience of expressing the result in units of decibels is that it compresses a wide range of amplitudes to a small set of numbers, accentuates peaks, and allows percent changes in dB to be read directly. The most significant thing to remember about decibels is that it is a logarithmic function. This means that a doubling of dB values does not correspond to a doubling of the measured pressure, but possibly much more.

It is often convenient to deal with just parts of the frequency spectrum. These can be identified as octave or decade bands. An **octave** is a band with the upper frequency exactly twice the lower frequency. It is common in acoustics to work with **third-octaves** (highest frequency 1.26 times the lower, or a ratio of  $2^{1/3}$ ). The most recognized octave bands and the center frequencies of the band are shown in Table 9.1. It can be seen that the upper bands encompass much more of the spectrum than the lower bands. A **decade** is a band in which the upper frequency is ten times the lower frequency (such as 3 to 30 Hz). Like the octave, higher decade bands contain much more of the spectrum.

Noise can be classified in three ways. **Random noise**, of most interest in the aircraft structures field, has an instantaneous amplitude that cannot be specified at any instant of time, but can only be defined statistically by an amplitude distribution function. **White noise**, often used in ground tests or simulations, is broadband noise with constant energy per unit of frequency. Finally, **pink noise** is also broadband but with an energy content which is inversely proportional to frequency (-3 dB per octave or -10 dB per decade).

#### **9.4 MEASUREMENT OF SOUND**

SPLs cannot be reliably measured close to the object emitting the sound because different parts of it may emit sounds at different amplitudes. A suitable distance (greater than the wavelength of the lowest frequency emitted or twice the greatest dimension of the object, whichever is greater) is necessary to get beyond this **near field** and into a region where the sound has assumed an even distribution. This latter region is called the **far field** (see Figure 9.2). In the far field the sound level will decrease -6 dB as the distance from the source is doubled. This is due to the inverse square law or the spherical spreading of the pressure waves and their associated dissipation of energy. Figure 9.3 shows the effects of the inverse square law and the natural sound absorption capability of air to attenuate the sound level. If the noise source is within an enclosure, the sound waves can be reflected from the walls and confuse level readings (the **semireverberant field**). For the applications addressed in this handbook, it is assumed that the measurements are always in the **free field**.

The presence of a transducer (pressure sensor or microphone), its supporting mount, and any associated recording and analysis equipment can influence the SPL reading. Depending upon the type of transducer used (see Section 10.6), its orientation may also be critical. However, for flight test applications the transducer is typically mounted within the aircraft structure flush with the external surface and all supporting equipment is inside the aircraft.

Table 9.1 Octave and Third-Octave Passbands

<b>Band No.</b>	<b>Nominal Centre Frequency</b>	<b>Third-Octave Passband</b>	<b>Octave Passband</b>
1	1.25 Hz	1.12 – 1.41 Hz	
2	1.6	1.41 – 1.78	
3	2	1.78 – 2.24	1.12 – 2.82 Hz
4	2.5	2.24 – 2.82	
5	3.15	2.82 – 3.55	
6	4	3.55 – 4.47	2.82 – 5.62
7	5	4.47 – 5.62	
8	6.3	5.62 – 7.08	
9	8	7.08 – 8.91	5.62 – 11.2
10	10	8.91 – 11.2	
11	12.5	11.2 – 14.1	
12	16	14.1 – 17.8	11.2 – 22.4
13	20	17.8 – 22.4	
14	25	22.4 – 28.2	
15	31.5	28.2 – 35.5	22.4 – 44.7
16	40	35.5 – 44.7	
17	50	44.7 – 56.2	
18	63	56.2 – 70.8	44.7 – 89.1
19	80	70.8 – 89.1	
20	100	89.1 – 112	
21	125	112 – 141	89.1 – 178
22	160	141 – 178	
23	200	178 – 224	
24	250	224 – 282	178 – 355
25	315	282 – 355	
26	400	355 – 447	
27	500	447 – 562	355 – 708
28	630	562 – 708	
29	800	708 – 891	
30	1000	891 – 1120	708 – 1410
31	1250	1120 – 1410	
32	1600	1410 – 1780	
33	2000	1780 – 2240	1410 – 2820
34	2500	2240 – 2820	
35	3150	2820 – 3550	
36	4000	3550 – 4470	2820 – 5620
37	5000	4470 – 5620	
38	6300	5620 – 7080	
39	8000	7080 – 8910	5620 – 11200
49	10K	8910 – 11200	
41	12.5K	11.2 – 14.1K	
42	16K	14.1 – 17.8K	11.2 – 22.4K
43	20K	17.8 – 22.4K	

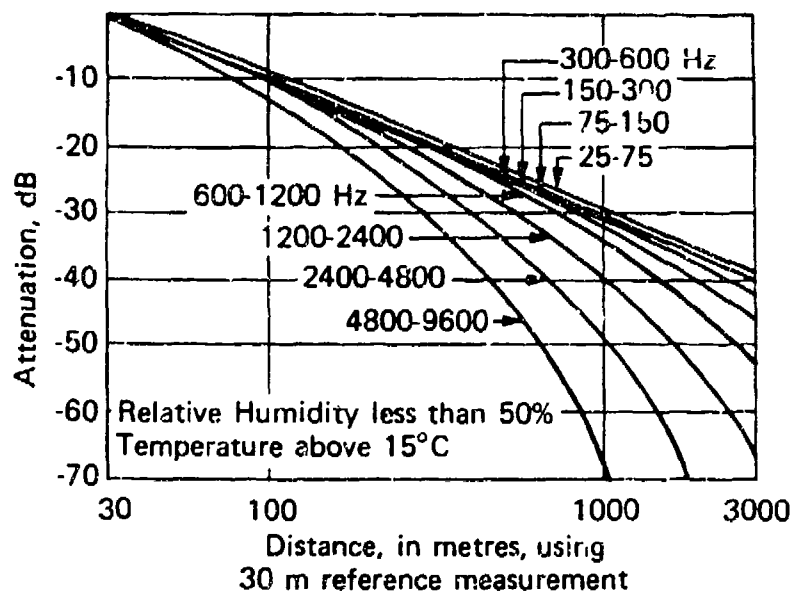


Figure 9.2 Sound Fields

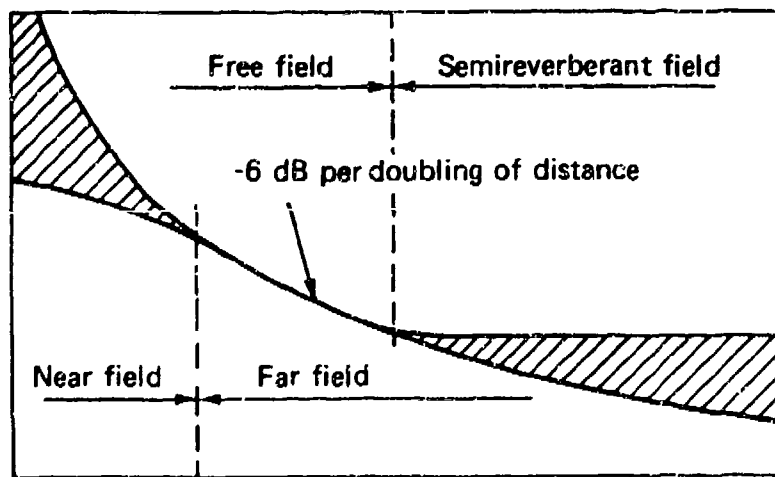


Figure 9.3 Sound Attenuation in Air

For human factors applications, the SPL measurement is often multiplied by different factors for different parts of the spectrum so that the levels can be more easily associated with the varying sensitivity of the human ear. The most popular such correction is the **A weighting**. For structures applications no weightings should be used.

When more than one sound source is present, it may be desired to know the total SPL with both emitting after making separate measurements, or to find the level of one source knowing only the level of the other source and the combined level with both emitting. It is not proper to simply add and subtract SPLs because of the logarithmic decibel scale. Instead, the two plots in Figures 9.4 and 9.5 are used. For two separate SPL readings from two sources, Figure 9.4 with the difference of the two readings should be used to get the additional level to be added to the higher of the two measurements for the combined peak level. Similarly, with the total SPL and a level for one of the two sources, using Figure 9.5 with the difference of the two readings will yield the level to be subtracted from total for the SPL of the unknown source.

Although SPL is most often measured with RMS values, it may also be given as a peak value. Only RMS values can be added and subtracted as discussed above. Because experimentally measured environmental noise, particularly that from flight testing, can vary greatly in amplitude at any given frequency over a period of time, using peak values can be very misleading. Of more interest is some average SPL that the structure will be subjected to over the long term. It is most often desirable to see the SPLs as a function of frequency but it is also occasionally necessary to obtain a single value defining a broadband level. Assuming the response of the sensing and analysis equipment is "flat" throughout the frequency range of interest, it is possible to produce this broadband result which is called the **overall sound pressure level (OASPL)**. This is a time averaged integration of the levels throughout the spectrum and is essentially an integration of all the power under the SPL curve. It represents the total power of the signal.

$$\text{OASPL} = 10 \log_{10} (\sum 10^{\text{SPL}/10}) \quad (9.3)$$

where SPL is each octave, third-octave, or individual spectral line sound pressure values, whichever is desired, composing the entire spectrum to be analyzed.

Because the sound level often varies over a time period in a random fashion, we must sample for a long enough time to be certain that the RMS value will be suitably close to the true average. This creates an element of uncertainty in the dB readings as shown in Figure 9.6. This figure indicates that at least 10 sec should be allowed for a reading, and perhaps as great as 30 sec or more in flight testing.

It is occasionally useful to determine a sound power, measured as **sound power level**, the total sound energy radiated by a source per unit of time, or

$$L_w = 10 \log (P/P_0) \quad \text{in decibels (dB)} \quad (9.4)$$

where P is the RMS of the sound power in watts (W), and  $P_0$  is a reference value of 1 pW.

Some additional terms may also present themselves from time to time. **Power spectrum level** is the level of power contained in a band 1 Hz wide, referenced to some given reference level. The **sound exposure level (SEL)** is a constant sound level acting for 1 sec with the same acoustic energy as another, non-constant level sound. The **equivalent continuous sound level ( $L_{eq}$ )** is similar to SEL but can be for any given time period.

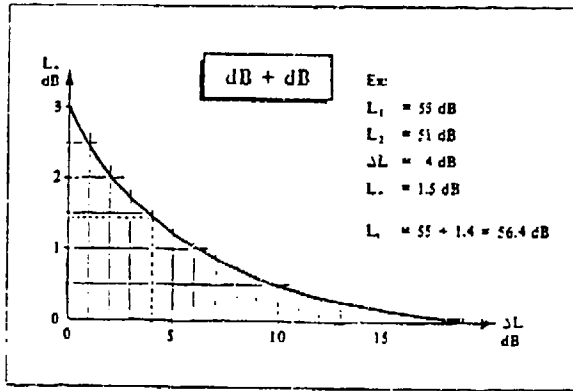


Figure 9.4 Summing Sound Pressure Levels

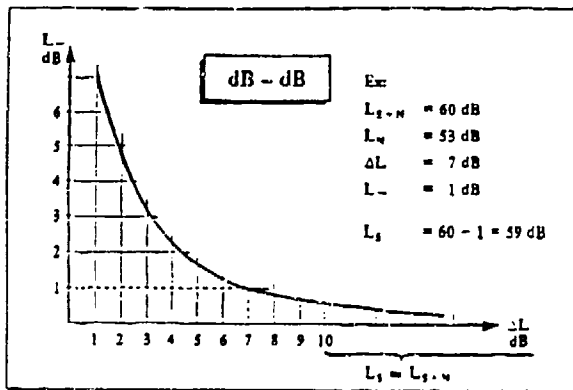


Figure 9.5 Subtracting Sound Pressure Levels

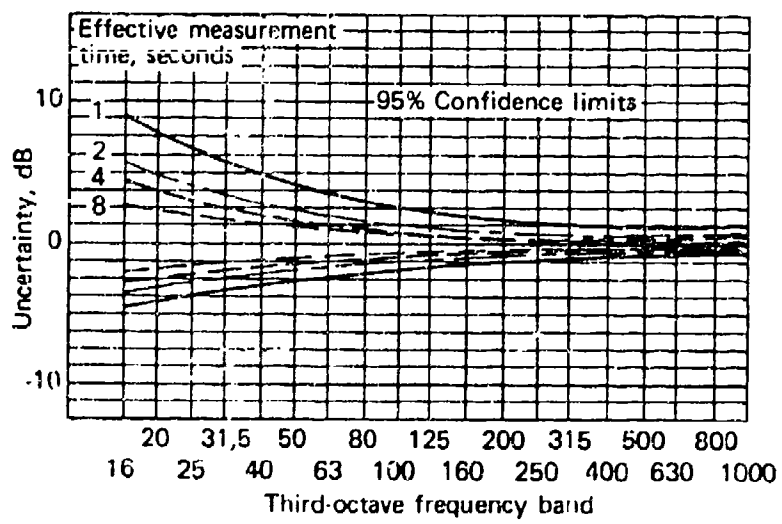


Figure 9.6 Effect of Measurement Time on SPL Results

## **9.5 FLIGHT TESTS**

A few years ago an airworthiness flight test was conducted on a heavily modified C-135 aircraft. The modification included several deep fairings added to the underside of the fuselage. These produced violent turbulence and vortex shedding that caused cracks to appear on the belly of the aircraft aft of the fairings and also broke an antenna off in flight, which subsequently impacted the plane, punching a hole. In order to determine exactly how long most of the belly skin and underlying structure could survive in this environment, it was necessary to do an acoustics flight test to find the exact pressure levels on the belly as a function of frequency and to compare this with empirical data for the fatigue life of the material.

Vibro-acoustic data is collected as a matter of course in areas of high susceptibility during the early development flight test effort. Problems like the KC-135 sonic fatigue cracking discussed in Section 9.1 is the most common reason for doing later testing. The intention is to define the environment to which a piece of equipment will be subjected and to match this against its specifications or lab test levels. Apart from simply measuring the sound levels, loads and accelerations of the test subject are typically the most important data to come out of such tests. However, it is often questionable whether the excitations are due strictly to acoustics, are transmitted by the airframe from internal components, or are just general structural dynamics. This can become important if a decision is made after these inputs instead of simply isolating the victim system.

### **9.5.1 PRELIMINARY GROUND TESTS**

It is seldom practical for an entire airframe to be tested in a sound chamber prior to flight. But, components and missiles can greatly benefit from such ground testing. The test is tailored to the customer's specification under which the item was developed and built. Acoustic and vibration military specifications for aircraft and aircraft equipment have been specifically written to reflect historical and projected levels. They are stated in terms of frequency, pressure levels, accelerations, and duration of exposure for certain phases of operation and flight. Typically, the article must survive up to 162 dB OASPL for a brief period before it is considered safe to fly. Fatigue of metal aircraft structure becomes a concern at levels above 140 dB OASPL. For the example of a shallow weapons cavity at transonic speeds discussed in Section 9.1, the SPL experienced was 170 dB. It is always wise to ensure that chamber tests have been performed and to review the results versus the specifications. It is common to subject the test object to white noise in which the energy content decreases linearly or exponentially as frequency increases. This simulates a decrease seen in actual conditions.

During flight testing of a missile externally mounted on a carrier aircraft, many problems with cracks, popped rivets, delaminations, and the like occurred on the store and adjacent structure of the carrier aircraft. Acoustic measurements showed that levels greater than 165 dB were being experienced. The missile was returned for chamber tests to 167 dB (an increase of over 20 percent in the external pressures), during which many more failures occurred. A progressive wave chamber was used, although Reference 7 (MIL-STD-810) calls for the more common reverberant chamber test, and it was later shown that the test produced much higher loads than those recorded in flight at similar SPLs. It is also possible that chamber simulations will produce lower load conditions than those experienced in flight. It is always necessary to fly an instrumented article and inspect it for failures to be certain that its design is adequate.

### **9.5.2 TEST CONCEPTS**

Sound pressure level is measured either with a microphone or a pressure transducer (see Sections 10.5 and 10.6). Calibrations of the microphones before the test and possibly after is important. The transducer must be mounted flush with the surface of the article (aircraft skin) or suspended in the region of interest. If it is mounted so that a cavity exists between the face of the transducer and the surface the cavity will act as an organ pipe, greatly amplifying any sound with a wavelength matching the cavity dimensions.

Tests should be conducted at representative operational ground and flight conditions. This may include different aircraft engine power settings, taxi conditions, takeoff and climbout, cruise at a variety of altitudes and airspeeds (particularly at the edges of the normal operating envelope and with afterburner), in various flight configurations like weapons or cargo bay doors open, landing gear, flaps, or spoilers extended, and approach and landing. Even a sudden reduction in power, a throttle "chop," can be a problem. The inlet air spillage from a chop can impact stores downstream, as was found on the F-15. It is essential that an adequate dwell time on condition for sufficient data collection be allowed, at least 30 sec to one minute. Transducers should be scattered around the area of interest so that sound level contours (also known as isobel contours) can be traced out (see Figure 9.7). Also, since vibro-acoustics data is typically of such low signal levels, it is important to define the noise level of signal processing and recording equipment to determine the percentage of the response attributable to this noise.

### **9.5.3 DATA ANALYSIS**

As with the analysis of other frequency-type data discussed in this handbook, it is most helpful to present the SPL as a function of frequency. This can be done by performing a Fourier transformation (see Section 11.3.1). To conform with standard acoustics practice, the analysis is most often shown as third-octaves. In a sound level meter or dedicated acoustics-type signal analyzer, no transformation takes place. Instead, third-octave filters specifically designed to the conventional center frequencies shown in Table 9.1 and attenuation standards will selectively analyze the entire spectrum in pieces as shown in Figure 9.8. The SPLs for each third octave can then be presented on a frequency scale as shown in Figure 9.9. This can be termed a spectrogram as opposed to a true Fourier transformation. Of course, the results of a Fourier transformation can also be presented in such a form, if desired. They can be shown as a "stair step", as in the figure, or by simply connecting the levels at the center frequencies by straight lines for a "sawtooth" type pattern.

The test data should be shown versus the specification limits. An example of this is shown in Figure 9.10 in which the "sawtooth" presentation is used. Note that the plot indicates both the reference atmospheric pressure used in the analysis as well as the test condition (configuration, transducer location, and dynamic pressure). In this case the SPL limits have been exceeded at several points in the spectrum. It must then be decided what has caused these high levels and the easiest ways to reduce them if they are considered critical.

### **NOMENCLATURE**

C	Celsius or Centigrade
dB	decibel
f	frequency
Hz	Hertz
L	level
m	meters

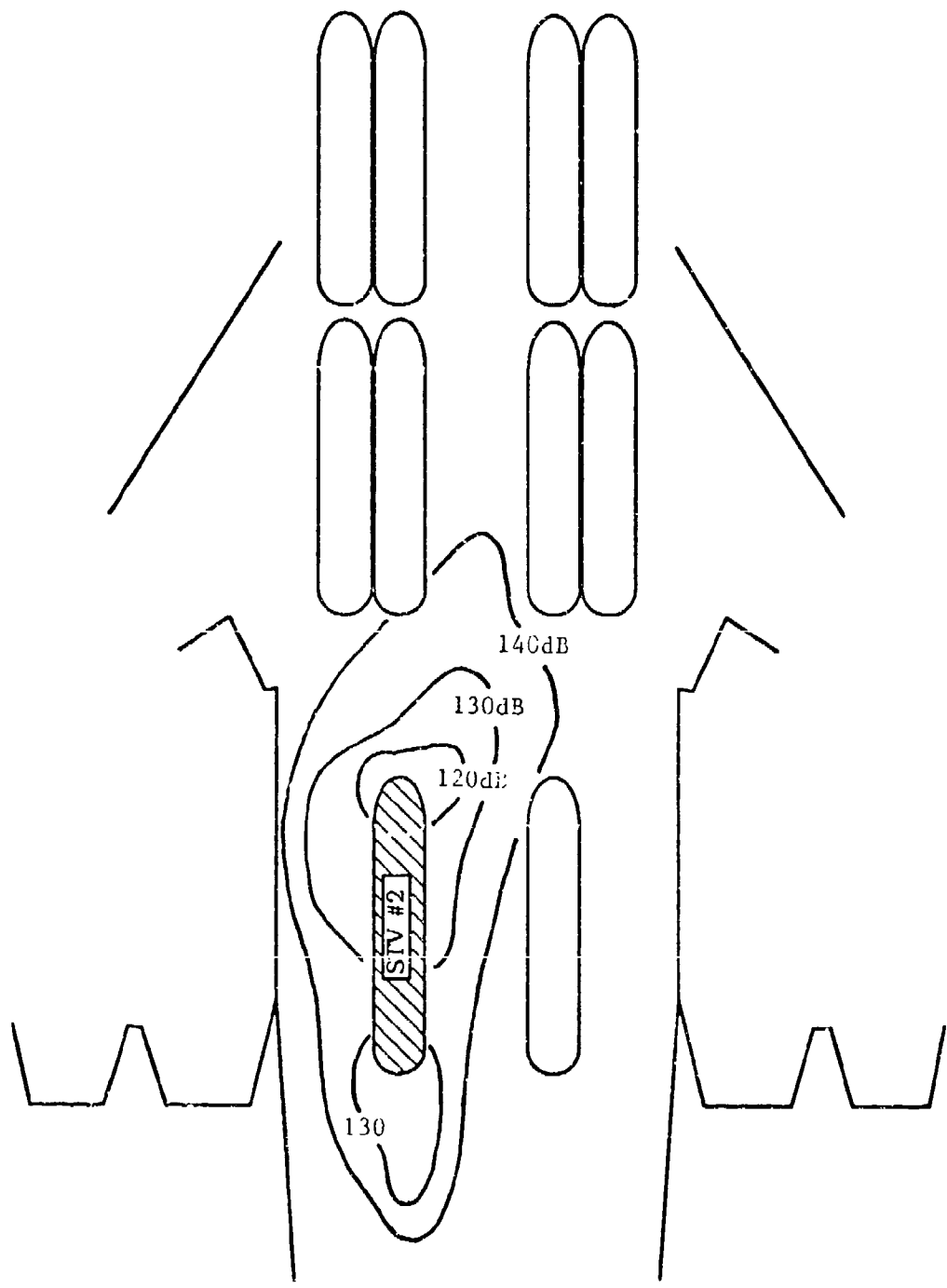


Figure 9.7 Example Sound Contour Pattern

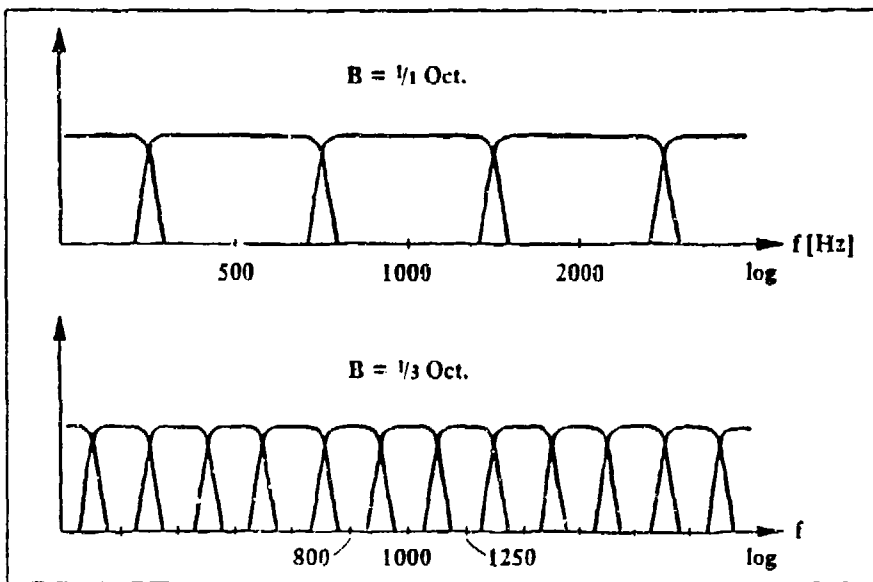


Figure 9.8 Illustration of Octave and Third-Octave Segmentation of Frequency Spectrum

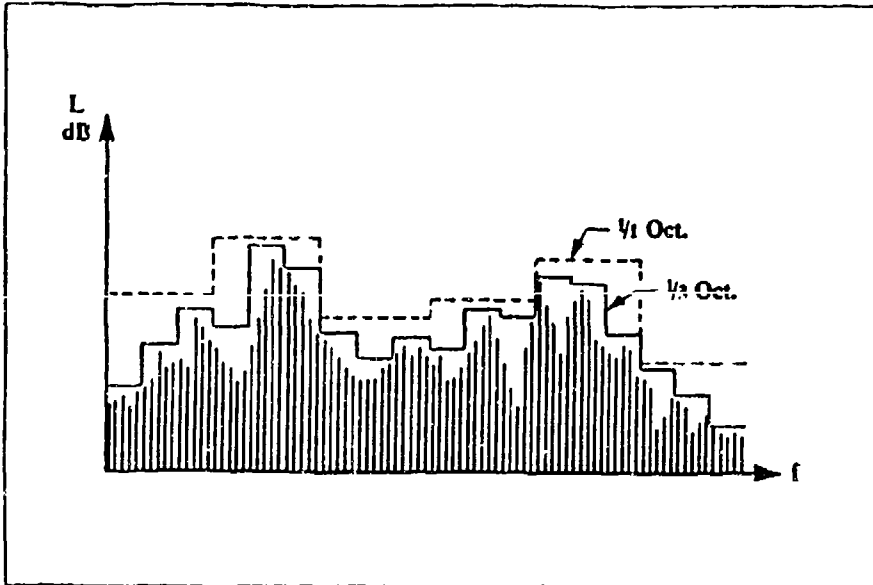


Figure 9.9 Illustration of Octave and Third-Octave SPL versus a Fourier Transform Presentation

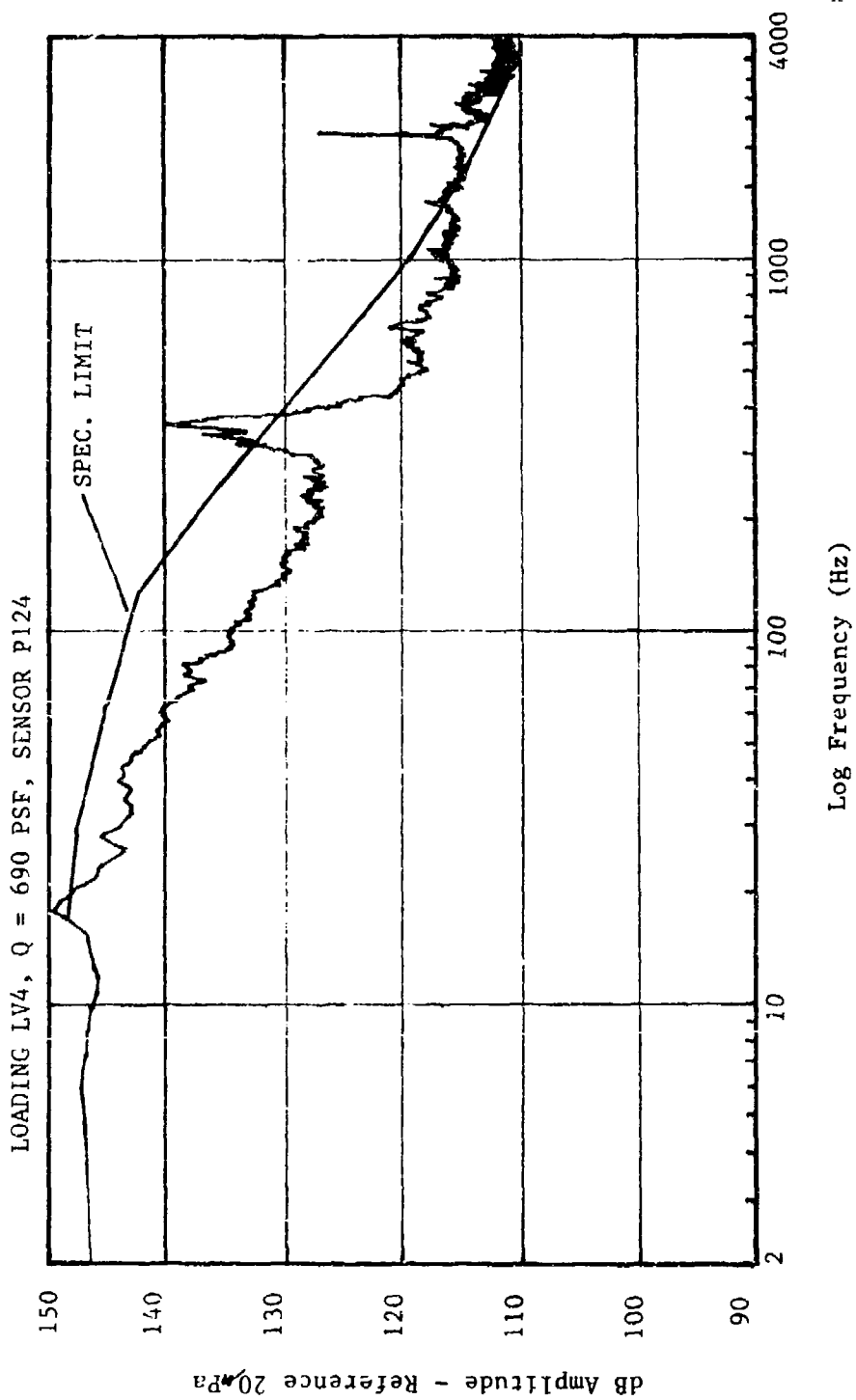
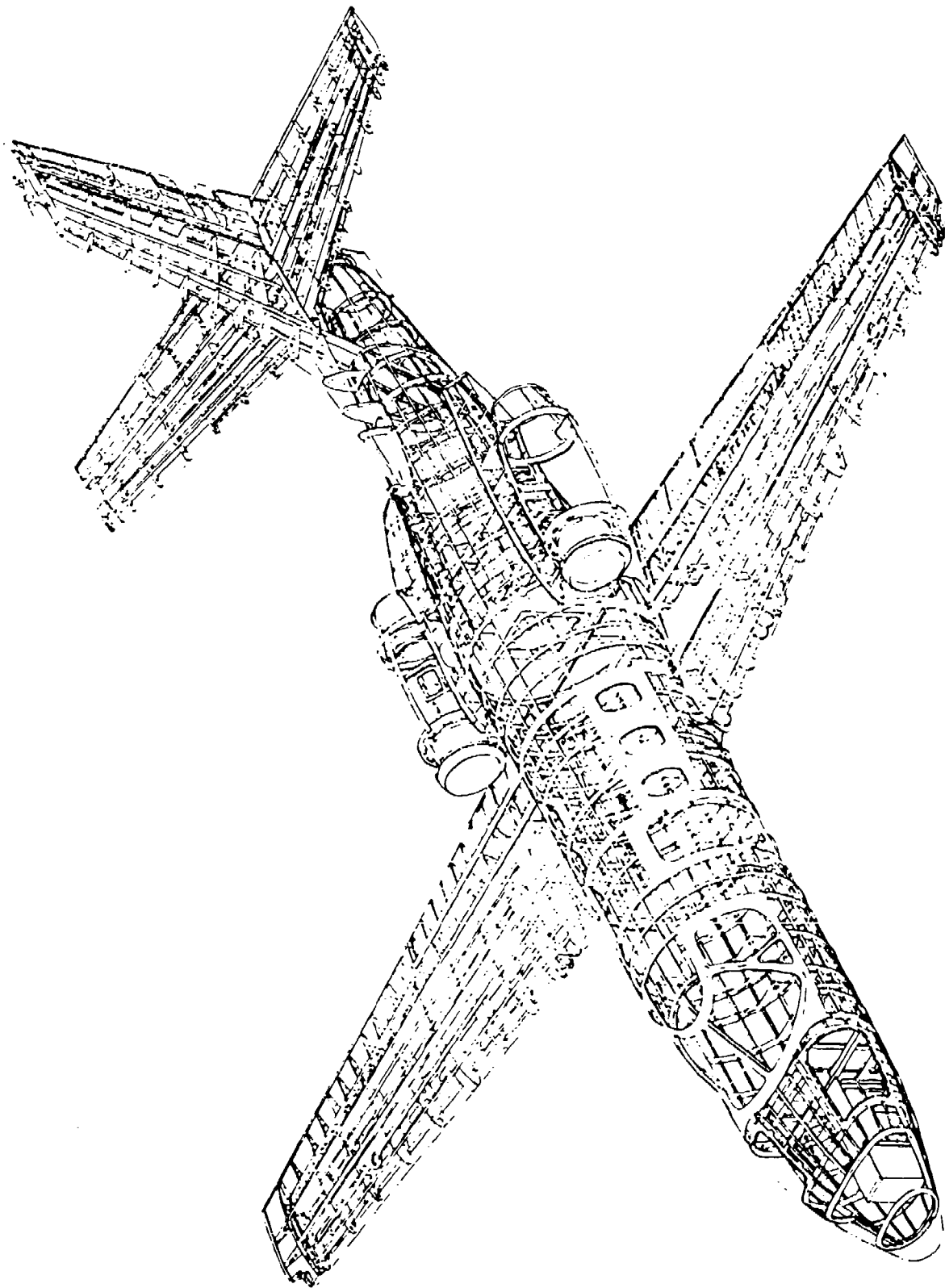


Figure 9.10 Example of SPL Test Data versus Specification Level

OASPL	overall sound pressure level
oct.	octave
P	RMS sound power
Pa	Pascal
p	RMS sound pressure, pico
PSD	power spectral density
RMS	root mean squared
SEL	sound exposure level
SPL	sound pressure level
sec	second
W	watt
$\lambda$	wave length
$\Sigma$	sum
$\mu$	micro
$\Delta$	increment of change
Subscripts	
eq	equivalent
o	reference value at 0 dB
p	pressure
w	power

## REFERENCES

1. *Measuring Sound*, (Pamphlet), Brüel & Kjaer, Naerum, Denmark, September 1984.
2. *Pocket Handbook, Noise, Vibration, Light, Thermal Comfort*, Brüel & Kjaer, Naerum, Denmark, 1986.
3. Peterson, Arnold P.G. and Gross, Ervin E., Jr., *Handbook of Noise Measurement*, GenRag Incorporated, Concord, Massachusetts, 1978.
4. Hunter, Joseph L., *Acoustics*, Prentice-Hall Incorporated, Englewood Cliffs, New Jersey, 1957.
5. Beranek, Leo L., *Acoustic Measurements*, John Wiley & Sons, New York, New York, 1956.
6. Graf, Phil A. and Drake, Michael L. *Elimination of KC-135A Aft Fuselage Acoustic Fatigue Failures*, UDR-TR-85-22, University of Dayton Research Institute, 31 January 1985.
7. Military Standard Environmental Test Methods, MIL- STD-810C.
8. Low-drag Weapon Carriage, in *Interavia Aerospace Review*, January 1990, pp. 12-13.
9. Frost, W.G., Tucker, P.B. and Wayman, G.R., Captive Carriage Vibration of Air-to-Air Missiles on Fighter Aircraft, *The Journal of Environmental Sciences*, September/October 1978.



Cessna Citation Structure

# CHAPTER 10.0

## INSTRUMENTATION

### 10.1 INTRODUCTION

While structures flight test engineers are seldom responsible for the actual installation of test instrumentation in an aircraft or the assembly of the entire instrumentation system for recording and transmission of data, they often select the transducers, choose their location, and specify required accuracies. To perform this task efficiently, it is essential that the engineer be conversant in the various transducers available and understand what happens to the data from the point at which it is sensed until it is displayed in **engineering units (EU)** for analysis. This requires at least a broad understanding of instrumentation and telemetry systems so that the structures and test range people can talk to each other with reasonable certainty of being understood. This chapter, as with all others in the handbook, just scratches the surfaces of this subject and supplemental reading as interest or project requirements dictate is strongly encouraged.

Flight test aircraft (also known as **testbeds**) are often prototype vehicles heavily instrumented with thousands of individual measurements (also known as **measurands**). Much of this instrumentation is installed at the time of construction and may not be readily accessible, if at all. The transducers and associated system equipment is identifiable by the insignia orange color used on all test system boxes and wiring. An effort is made to allow instrumentation systems to be reconfigurable to meet the requirements of the most current flight tests objectives. Such systems are very complex and the associated technology is constantly being improved. However, the structures engineer should get to know the responsible systems engineer and become somewhat familiar with the capabilities and limitations of the instrumentation package on the test aircraft.

In aircraft modified for a flight test project, the modifications necessary to conduct the test as well as instrumentation installation should take place prior to or during the test approval cycle. The structures engineers on the project should verify the "**project history**" which is the list of the instrumentation parameters that will be available as part of the instrumentation stream that is recorded on board and those telemetered to the ground. The engineer should ensure that all parameters essential to meeting the specific test objectives are being used and are within the proper data ranges. Most projects will have an instrumentation engineer assigned who is a good source for such information.

During the test planning phase, a list of **technical GO/NO-GO** parameters are decided upon by the engineers. Lack of these are parameters would make performing the test maneuvers useless in meeting the test objectives during the flight. Those measurands that are necessary to ensure that the test is conducted in a safe manner are known as **safety of flight (SOF) GO/NO-GO** parameters. They may include such things as normal acceleration at the cg or Mach number. They are measurements which are felt to be essential for monitoring on the ground when dealing with a test aircraft or equipment of uncertain characteristics. SOFs must be verified as functioning before the flight is launched. The flight will be terminated immediately should one of these critical measurands fail during the flight. A variation on the technical and SOF measurands are the **safety of test (SOT)** parameter which must be functioning to safely perform a certain type of test, although the plane may fly otherwise. An example of a SOT parameter

may be a wing tip accelerometer for a flutter flight. It is always wise to provide backups to critical measurands for redundancy. Failure of a technical GO/NO-GO of SOT measurand need not result in test termination if other test points can be performed for which the lost parameters are not necessary.

## **10.2 STRAIN GAGES**

Strain gages are the common means of measuring strain from which stress can be derived (see Section 3.2) to ensure that the limit stress of the material is not being exceeded. They can also be used to measure loads, as will be explained later. They can be employed in a static loading situation or in a dynamic application where their response can be used to measure the oscillatory motion of a structure. The strain gage employs the principle that the electrical resistance in a metal element will change with a change in length. Thus, the change in resistance of such an element bonded to a test specimen in such a way that it will experience the same deformation as the specimen under a load will be a measure of the strain within the specimen. The change in resistance is extremely small, requiring sensitive equipment to monitor it. In fact, the change in resistance is so small as to be on the order of that produced by temperature or shunting due to moisture, and so requires great care in transducer installation and use. It is clear that the strain gage is very simple in concept and structure, but some further information is needed to use them properly.

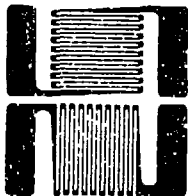
### **10.2.1 SELECTION**

The most common gages used in aircraft flight testing are small foil gages. These consist of a thin metal foil photo-etched to the desired pattern and bonded to a nonconductive but durable backing. The patterns are optimized for particular applications but usually look like that shown in Figure 10.1 (greatly enlarged). It allows any strain to be experienced by the greatest portion of the foil conductor. The gage shown in 10.1 is designed to measure strain only along its longest axis, as shown. This is a **uniaxial gage** and is suitable for components in which the stress is expected to be uniaxial or for which only the stress along the axis of the gage is of interest. The **bi-axial strain gages** have two uniaxial elements at 90 degrees to each other (Figure 10.2a) which can be aligned with known **principal stress directions** (the direction of the maximum and minimum stresses) or any direction of choice. For an application in which the **principle stress directions** are not known and multi-axial stresses are expected a **rosette strain gage** can be used (Figure 10.2b). The rosette typically has three uniaxial gage elements oriented at either 120 (delta type) or 45 degrees (rectangular type, Figure 10.2c) from each other. For pressure vessels, the **spiral gage** (Figure 10.2d) can be used. There are many other gage patterns available in many different sizes, and most manufacturers will prepare a pattern to customer specifications.

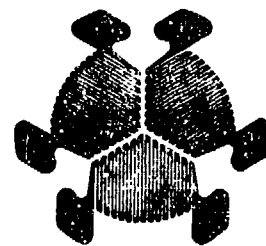
Apart from gage pattern, gage size, resistance, and temperature limits must also be considered. Special gages are manufactured for high temperature applications. A large gage will be easier to install and may be necessary for high stress situations where the strains expected could exceed the capability of a small gage (cause the gage to exceed its elastic limit and possibly break). However, a large gage will typically not be as sensitive as a small gage. Typical unstrained resistances are 120, 350, and 1000 ohms. Matching the gage material to the test article material (aluminum gage to aluminum test specimen, brass to brass, etc.) is important to avoid problems with incompatible thermal expansions.



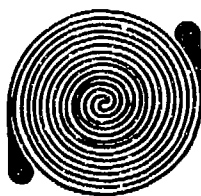
Figure 10.1 Typical Uniaxial Strain Gage Configuration



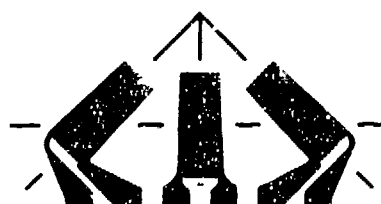
a. Bi-Axial Gage



b. Delta Rosette Gage



c. Rectangular Rosette Gage



d. Spiral Gage

Figure 10.2 Other Common Strain Gage Configurations

### 10.2.2 MEASUREMENT

Each strain gage or batch of gages will have a gage factor ( $K$ ) determined by the manufacturer prior to packaging. The gage factor permits a conversion of resistance change to strain as expressed by

$$K = (\Delta R/R)/e \quad (10.1)$$

where  $\Delta R$  is the change in resistance,  $R$  is the specified gage resistance (unstrained), and  $e$  is the strain experienced. Thus, strain can be derived from the equation and converted to stress as shown in equation 3.5. Of course, a negative value of  $\Delta R$  indicates compression. It can be seen with some thought that a gage with a higher gage factor and resistance would be more desirable than one with lower values. For the bi-axial gage already oriented with the principal axes, each leg is analyzed as a uniaxial gage using equation 10.1 for the principle strains. The associated stresses are then

$$\sigma_{\max} = E(e_{\max} + \nu e_{\min}) / (1 - \nu^2) \quad (10.2)$$

$$\sigma_{\min} = E(e_{\min} + \nu e_{\max}) / (1 - \nu^2) \quad (10.3)$$

where  $e_{\max}$  and  $e_{\min}$  (a negative value) are the measured principal strains in the appropriate legs of the bi-axial gage,  $E$  is the Young's modulus of the material (see Section 3.2.2), and  $\nu$  is the Poisson's ratio of the material (Section 3.2.2). For the rectangular rosette gage, the principal strains and stresses are derived as:

$$e_{\max,\min} = 0.5(e_a + e_c) \pm 0.5 \sqrt{(e_a - e_c)^2 + (2e_b - e_a - e_c)^2} \quad (10.4)$$

$$\sigma_{\max,\min} = E/2[(e_a + e_c)/(1 - \nu)] \pm \sqrt{[e_a - e_c]^2 + [2e_b - e_a - e_c]^2} / (1 + \nu) \quad (10.5)$$

where the  $e$ 's denote the strains in each of the three legs of the rosette and where the plus sign is used for the maximum and the minus for the minimum. For the delta rosette:

$$e_{\max,\min} = (e_a + e_b + e_c)/3 \pm \sqrt{[e_a - (e_a + e_b + e_c)/3]^2 + (e_c - e_b)^2/3} \quad (10.6)$$

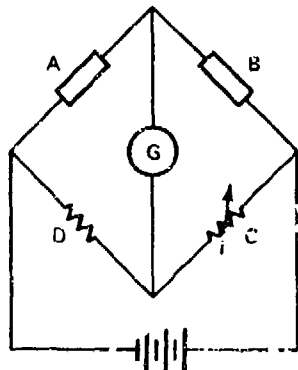
$$\sigma_{\max,\min} = E[(e_a + e_b + e_c)/[3(1 - \nu)] \pm \sqrt{[e_a - (e_a + e_b + e_c)/3]^2 + (e_c - e_b)^2/3} / (1 + \nu)] \quad (10.7)$$

Because the change in resistance is so small, a **Wheatstone bridge** is used to convert the resistance change to a voltage, amplify the signal and to provide compensation for temperature changes. The typical elements of this dc circuit are shown in Figure 10.3. The **temperature compensating gage (dummy gage)** should be identical to the active gage and bonded to a sample of identical but unstressed material and subjected to the same ambient conditions. The circuit will then automatically subtract out the stresses due to temperature variation. The adjustable resistor allows for balancing of the bridge or the zeroing-out of any **residual strain** reading in an unloaded state. Using the nomenclature for resistances from the figure

$$A/B = D/C \quad (10.8)$$

In a loaded situation the bridge will be unbalanced. For static tests it is good practice to record the zero-load strains both before and after the loading to account for "drift". The bridge used in flight testing will typically lack the galvanometer (strain meter). Some people make a point of using gages from the same package for a bridge to reduce differences introduced by manufacturing tolerance.

In the laboratory a purpose-built **strain meter** (rather than a simple volt meter) can be used into which the gage factors can be set, no-load zero offset readings can be nulled, and multiple gages can be read. In flight testing this is not available and the analysis is usually done by computer using recorded gage outputs.



A = active, or strain-measuring gage.  
 B = the temperature compensating gages.  
 C = D = Internal resistances in the meter.  
 G = Galvanometer

Figure 10.3 Typical Wheatstone Bridge Circuit.

### **10.2.3 CALIBRATION**

Gages are often used to measure loads. A load applied at a specific spot on a structure will always give the same stress/stain at another specific spot, all else remaining the same. By measuring gage output for incrementally increased loads, the strain gage can be "calibrated" so that strains read in flight can be used to determine the loads at that condition (see Section 5.2.2.1). Shears, bending moment, and torques are the components that are measured by the strain gages in such tests. This is a fairly straight forward thing when dealing with a uniaxial load in a simple component. However, measuring loads in a complex structure like a wing with distributed and varying loads requires a much more involved setup and calibration.

For loads measurement applications the gages should be applied where the stresses will be adequate to obtain good sensitivity but away from areas of local stress concentrations. Ideally, the gages intended for measurement of a particular type of load should be located where that load is dominant. In practice this is seldom a clear-cut decision. For wing applications, the gages intended for shear measurements should be placed on the shear web of the spars, the bending moment gages on the spar caps or the skin, and torque gages on the structure's torque boxes (see Figure 10.4). It is a common practice to use redundant gages in these areas, such as either side of the shear web, top and bottom of the spar caps, etc. Analogous areas should be used for structures other than a wing. Generally, as many as three to five gages (bridges) are used to derive a single force component. This is done for the sake of accuracy and to ensure that the strains in all primary components of the structure are accounted for. For example, a wing with two spars should have gages on each spar if accurate measurements are sought. The output of more than one gage is then used to derive the desired loads. This makes the calibration a very involved process.

Reference 7 provides a very detailed discussion of how a strain gage loads calibration is performed with a complete derivation of equations and discussion of assumptions. The calibration uses the principle of superposition. That is, the strain at a particular location due to loads applied simultaneously at several points on the structure is the algebraic sum of the strains due to the same loads applied individually. The individually applied calibration load can then be used to derive an equation for determining the distributed load on the structure. The calibration measurements would be used to fill the strain matrix of the following equation for shear ( $V$ ), and likewise for torque ( $T$ ) and moment ( $M$ ).

$$\begin{Bmatrix} V_1 \\ V_2 \\ \vdots \\ V_i \end{Bmatrix} = \begin{bmatrix} u_{11} & u_{12} & \dots & u_{1j} \\ u_{21} & u_{22} & \dots & u_{2j} \\ \vdots & \vdots & \ddots & \vdots \\ u_{i1} & u_{i2} & \dots & u_{ij} \end{bmatrix} \begin{Bmatrix} C_{11} \\ C_{12} \\ \vdots \\ C_{1j} \end{Bmatrix} \quad (10.9)$$

where the  $u$ 's are the nondimensional bridge outputs. An  $i$  number of shear loads are applied at various chordwise positions on the structure and the measured strains on  $j$  bridges recorded for each loading. What we are seeking is a single expression that would permit shear to be solved for having only the strain outputs from the bridges. That is

$$V = C_{11}u_1 + C_{22}u_2 + \dots + C_{1j}u_j \quad (10.10)$$

and similarly for torques and moments. Equation 10.9 gives  $j$  unknowns and  $i$  equations which can be solved simultaneously for the coefficients  $C$ , as long as  $i$  is greater than  $j$ . The same process is done with torque and bending moment loadings and the coefficients for the analogous equations to 10.10 solved. It is common to calculate the errors to be expected if the equations are solved with one or more of the original gages nonfunctional. The application of precise calibration loads generally requires fixtures, jigs, calibrated pneumatic or hydraulic load rams and the like which makes the process a major laboratory test when an entire airframe is involved. It is possible to provide a low level loads calibration using just onboard fuel and weapons to load the structure, although this is not a recommended procedure.

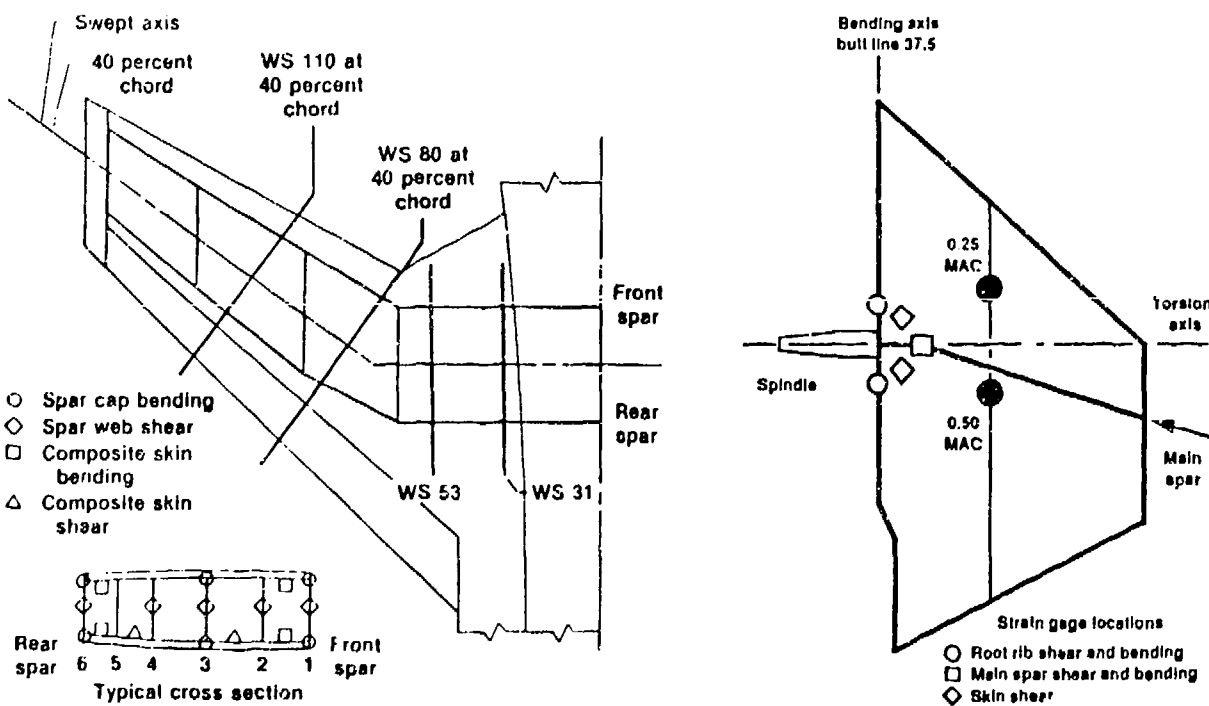


Figure 10.4 Example Strain Gage Application for Loads Measurements - X-29 Wing and Canard

Another method for calibrating the gages installed in an aircraft structure is to associate readings measured at specified flight conditions with loads analytically predicted or historically seen for that flight condition. A finite element model of the aircraft can provide predicted loads at the strain gage locations for exactly specified flight conditions like altitude, airspeed, and maneuver. The measured stresses at these actual conditions in flight will then be a measure of the loads which are assumed to be the same as those predicted mathematically or seen previously (perhaps on another aircraft of the same model). The problem with this method is that predictions are just that, and will vary from the actual loads by some unknown percentage. The ability of the pilot to fly the conditions precisely will also add some uncertainty to the calibrations. The method should not be used on a prototype airframe or one that has been substantially modified. A precise ground loads test approach is still considered the best calibration method. It is much more practical to apply this approach to components, such as actuators or support members. In this case it may be advisable to use up to eight gages per bridge for linearity and to render the output as much a unique function of the load as possible.

#### **10.2.4 INSTALLATION**

The bonding of the strain gage to the surface of the test item is extremely important for accurate strain readings. The surface should be carefully prepared before cementing the gage. This is done by removing any paint or other coatings, lightly sanding and polishing the bare material, followed by a thorough cleaning. Several cements are suitable, some dictated by the test environment. The gage must be protected against damage during the cementing and excessive cement and trapped air bubbles must be avoided. Alignment marks typically must be made so that the gage is properly aligned (often of paramount importance) but these must not be under the gage itself. Care must be taken not to place the gage at an area of potential stress concentrations (such as weld joints, cutouts, sharp corners, edges or doubler plates, severe buckling areas, etc.) which could produce confusing results. This entire process takes much practice for a proper gage application.

The gage will usually have tiny wires from the small solder pads on the gage itself to bigger pads where larger, more durable wires can be soldered. These larger wires must be secured so that they cannot be pulled out and then a stress-relieving loop added as an extra precaution (see Figure 10.5). The wiring should be shielded to reduce contamination of the signal by the surrounding electrical environment. The gage is protected against moisture with a coat of varnish or other substance that will dry to a hard surface. In flight testing, the gage and wires immediately adjacent are "potted" or covered with a thick, durable coating or a rubber-like compound. This is particularly important for gages mounted external to the aircraft. Even with these measures the strain gage is very easily damaged or the wires pulled loose. For this reason it is a common practice to mount redundant or backup gages for each primary gage. For a structure with many gages installed, just about any of the gages can be used to measure the strain for which another gage is primarily installed, although the measurement will not be as efficient.

### **10.3 ACCELEROMETERS**

The piezoelectric accelerometer is now the widely accepted means of measuring structural accelerations. These transducers are available in very small sizes with outstanding frequency range, resolution, and linearity, and are extremely durable. The piezoelectric device contains a piezo-material element which generates a small electrostatic charge when compressed or stressed by force or acceleration. Since the charge is proportional to the applied force it can be used as a measure of the force. The orientation of the element will determine whether the generated charge (measured as picoCoulombs or pC) is positive or negative.

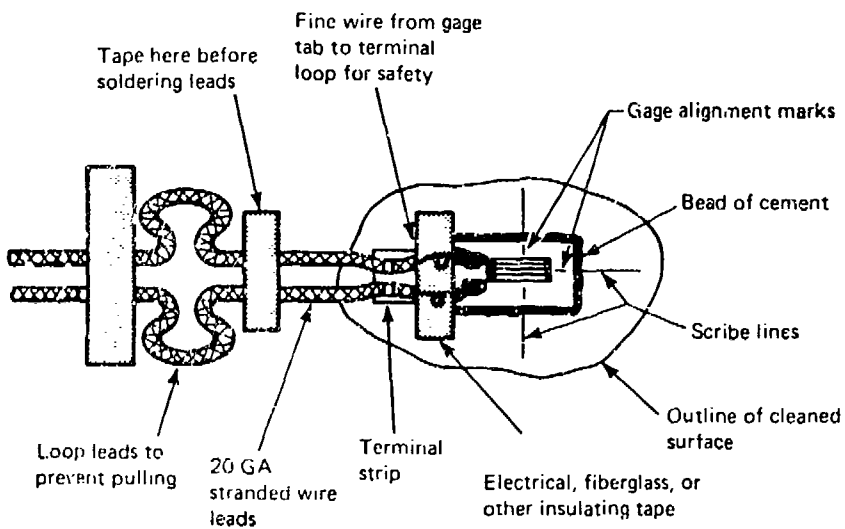


Figure 10.5 Example Strain Gage Installation

The basic structure of the piezoelectric accelerometer is shown in Figure 10.6. The piezo-material is highly preloaded between the case or sleeve and a seismic mass. The inertia of the mass will act as the force transmitted to the piezo-material. The greater this mass the greater will be the sensitivity of the transducer. A **triaxial accelerometer** is simply three accelerometers assembled as a single unit with the sensors precisely oriented to three mutually orthogonal axes. The "triax" is very useful for testing vibration environments at an internal location and greatly reduces installation difficulties where three axes accelerations must be obtained. For the more "dirty" installations, a carefully machined block with three mounting points for accelerometers in the mutually orthogonal pattern has the advantage of quick installation and lower initial expense and maintenance than a triax. Accelerometer packaging has continued to be reduced until some are less than half a gram in weight.

The **piezo-resistive accelerometer** is based on an element analogous to a strain gage, the output of which is a function of the acceleration. This device has high accuracy but has many other limitations that has reduced its usefulness over the past decade or so. The **servo accelerometer** is also a very specialized device beyond the limited scope of this text.

### **10.3.1 SELECTION**

The three basic types of accelerometer designs are illustrated in Figure 10.7. The choice of **compression accelerometers**, **upright** or **inverted**, will depend upon mounting application or restraints. The upright design is most frequently used because the case is more shallow and the coaxial cable from the transducer can be secured to the mounting surface closer to the transducer. The inverted design sees use in ground vibration tests (see Section 7.7). The **shear mode transducer** is also of shallow design and may have a through-the-case mounting screw method.

Frequency range and resolution are the most important criteria for selection, although most accelerometers today are good for a wide range of applications. Transducers that respond to very high frequencies are usually good down to only around 3 to 5 Hz at the low end. More generally, they should not be trusted below about 20 percent of the natural frequency of the

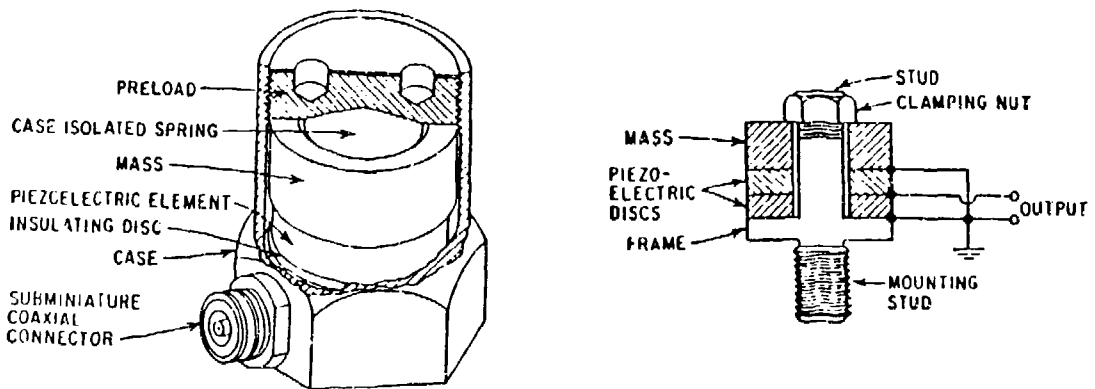


Figure 10.6 Common Piezoelectric Accelerometer Components

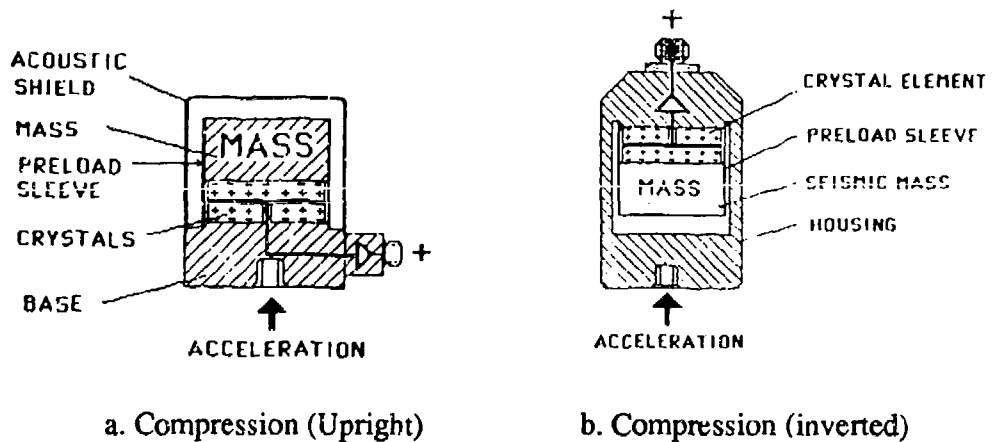


Figure 10.7 Three Common Accelerometer Configurations

transducer itself. For good resolution at very low frequencies an accelerometer with a larger seismic mass must be used which in turn makes it unsuitable for high frequency applications. The user should assure that the linearity of the response and the frequency resolution is adequate for the entire frequency range of interest. The natural frequency of the transducer itself must be beyond the frequency range of interest, and this is generally the case. **Sensitivity** (mv/g), where g is the acceleration due to gravity, should also be considered to ensure that the anticipated acceleration level can be faithfully transduced by the device. Lastly, the mass of the transducer must not add significantly to the mass of the structure and thus change its modal characteristics. One method which has been used to check this is by comparing the response of the structure with the accelerometer, and then with a second accelerometer placed on top of the first. Adverse changes in frequencies and amplitudes will indicate that the first device alone is probably adding too much mass. The device and associated wiring must also be capable of withstanding the inflight environment and be properly shielded against unwanted outside electrical signals.

#### **10.3.2 MEASUREMENT**

Because the high impedance charge output of the piezo-device is so small, it is necessary to pass the signal through a signal conditioner to make it suitable for read-out instruments or recording. The conditioner may also filter, digitize, or provide other signal processing functions (see Chapter 12.0). This will typically be a **charge amplifier** for our applications in which a charge mode type of transducer is used. A **voltage mode** transducer incorporates an impedance converter within the transducer itself to maximize the signal-to-noise ratio and eliminate the capacitance of the coaxial cable so that only a power source is required.

The transducer **scale factor** allows the measured signal to be associated with an acceleration as determined during the calibration of the device. The scale factor is provided with each unit and must be set in the charge amplifier sensitivity setting for correct readings. This will be in units of  $\mu\text{C/g}$  or mv/g.

#### **10.3.3 CALIBRATION**

Accelerometers must be periodically recalibrated. The high frequency response in particular tends to deteriorate with age. The typical calibration is usually performed using a special laboratory calibration accelerometer which is carefully preserved just for this purpose and is in turn precisely calibrated against a universally accepted standard. Most users send their accelerometers to the manufacturer for calibration. However, as the price of the accelerometers normally used for aircraft structures applications have continued to fall, it is now more practical to discard the device rather than accept the time and expense of a recalibration.

#### **10.3.4 INSTALLATION**

There are many methods for mounting accelerometers with varying ease and suitability depending upon applications. The transducer will be supplied with a small threaded mounting stud and matching hole in the case of the unit. If it is practical to prepare a threaded mounting point in the structure to be tested then the stud mount can be used. This is probably the most widely suitable approach and allows the transducer to be easily installed and removed. Placing a thin film of silicon grease at the cleaned interface of the transducer and structure will improve coupling and frequency response. Care must be taken not to over-torque the device during installation as it can introduce errors. In aircraft ground vibration test applications in which many devices need to be mounted or moved around, the stud mount is usually impractical.

Where the stud mount is not practical but a permanent installation is required, a variety of cements can be used. Dental cement is frequently used as it dries to a very hard surface (high natural frequency) and has a very high bonding strength. Whatever is used, it is important that the glue film not be excessive. The cement may tend to shift the transducer resonance to a lower frequency and this should be considered to ensure that it is still beyond the frequency range of interest. For installations in which the transducer is expected to be moved around or is a temporary installation, beeswax or tape can be used. The wax must be softened with a hot air hand blower, and again, an excessive amount must be avoided. Double-backed duct tape is the easiest application method. Wax and tape are less desirable from a resonance perspective but is usually adequate for aircraft ground tests. If high frequency vibrations are to be measured then these methods should be avoided. Small and inexpensive mounting blocks are now appearing in which the transducer can be simply slid in and out. Many of these can be quickly cemented to the structure for a ground test and eliminate the uncertainties of other temporary installation methods. Magnetic transducer mounts are widely suspect and are usually impractical for aircraft uses anyway.

For all mounting techniques, it is important that the base of the device be flush with the structure to be tested, or at least not edge-mounted. This may require that a specially fabricated shim be installed so that the base is flat against the mount and properly aligned with the desired acceleration axis (see Figure 10.8 for an example). It is important that the shim's natural frequency be much greater than the frequency range of interest. A metal or phenolic material is commonly used. There are a number of special purpose jigs and other tools to ensure that the accelerometer is properly aligned with the desired axis.

The coaxial cable from the accelerometer must be taped or glued down to prevent it from flopping around from structural motion. This flopping introduces noise into the signal, can cause it to work loose from the transducer, and can wear the cable to failure. A small stress relieving loop in the cable near the transducer is a good idea to avoid failures from an over-stressed cable during surface motion. If the cable-to-transducer connection is likely to be subjected to moisture, like rain or condensation, then it should be sealed. Care in shielding and grounding will help ensure that the local electromagnetic environment does not corrupt the accelerometer signal. An annoying limitation of the accelerometer is that there is no easy way to check the integrity of the transducer while in place on the test article, apart from striking the adjacent structure or jumping up and down on the aircraft.

#### **10.4 FORCE TRANSDUCERS**

The typical mechanical force transducer or load cell used today is nearly identical to the accelerometer. The standard configuration of the piezoelectric force sensor is illustrated in Figure 10.9. When a precise measure of the force and its frequency content is necessary for use in a frequency response plot (see Chapter 11.0) then this sort of force transducer should be chosen over a calibrated strain gage.

Some standard piezoelectric force sensor designs are shown in 10.10. The compression-tension-impact model is most often seen incorporated into the impact hammer used for vibration testing (see Section 7.8.2.1) while the force link may be used in a ground vibration test placed between the shaker and the structure under test (Section 7.6.3). The force ring has little application in aircraft tests. All the discussions of the operation, measurement, calibration, and installation for the accelerometer also apply to the force sensor. Sensitivity (mV/lb) should be considered in the same way as with the accelerometer. Expected loads must fall within the linear response range of the transducer. The shock rating should be compared with the anticipated

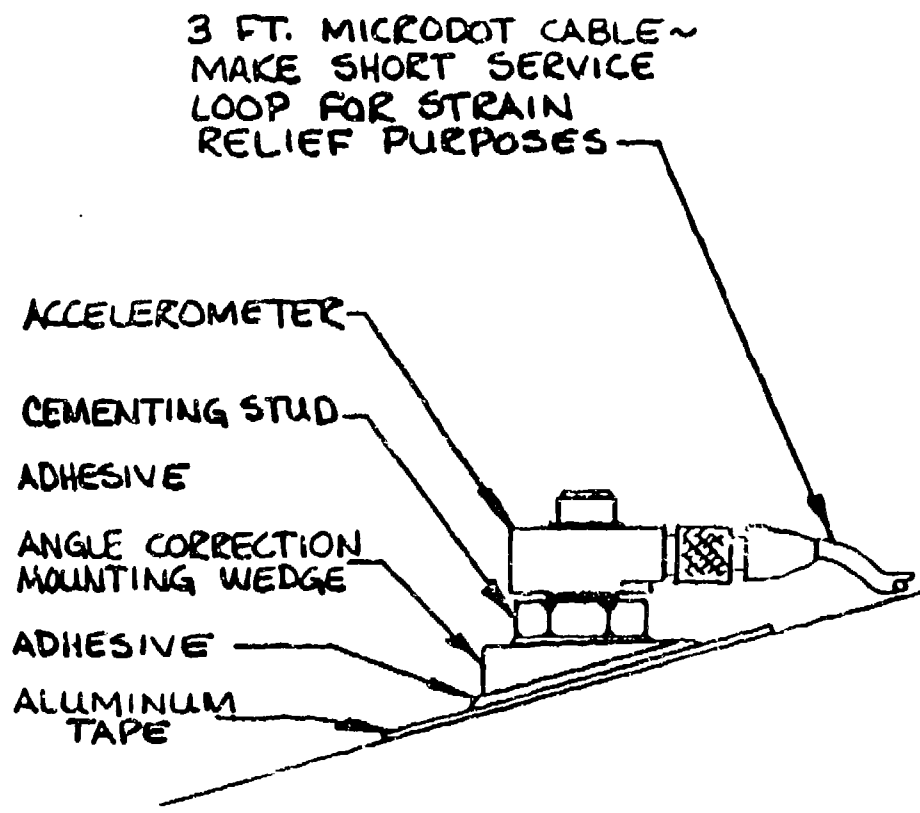


Figure 10.8 Example of Shim Mounted Accelerometer

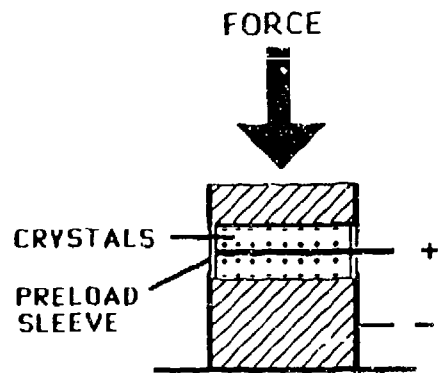


Figure 10.9 Force Transducer Components

accelerations. When used during a ground vibration test or similar application, the natural frequencies of the device must be considered the same as for an accelerometer.

## **10.5 PRESSURE SENSORS**

The pressure sensors typically used in structures testing to measure acoustic pressures (see Chapter 9.0) are piezoelectric devices (see Figure 10.11) and the piezoresistive device incorporating tiny strain gage bridges (Figure 10.12). It can be seen that the piezoelectric type is much like the force sensor but for the diaphragm across the top. The diameter of the diaphragm and the number of piezo-elements determines the sensor's sensitivity. The piezoresistive devices can come in extremely small sizes, as small as 0.03 inches in diameter. The flat-package configuration typically used in flight test applications is shown in the figure. This transducer is often mistakenly referred to by the manufacturer name of **Kulite**. The flat-package form is easily cemented to the surface of a structure. The cylindrical type typically require that a hole be drilled in the structure and the device cemented in from the back so that the diaphragm is flush with the surface; a much more involved operation.

## **10.6 MICROPHONES**

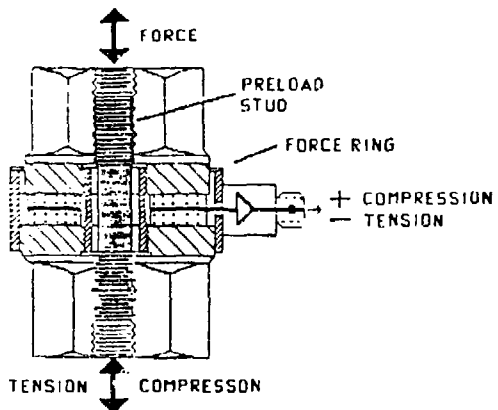
Microphones are also pressure sensing devices but incorporate many more features than the simple piezoelectric sensor which makes them superior in frequency response. Because of this, such microphones are sometimes called **Dynamic Pressure Transducers (DTP)**. However, they need repeated calibration, are less durable, and are generally larger than the piezo pressure sensors.

Figure 10.13 shows a typical measuring microphone which incorporates a diaphragm and a perforated plate as a damper. The **ceramic microphone** uses a ceramic piezoelectric element to generate the measurement signal. The **condenser microphone** uses the variation in electrical capacitance between the diaphragm and a backplate to generate the signal when a polarizing voltage is applied. This type of microphone is less suitable for very low frequency sound pressure measurements. Since the sensor will be oscillating with the structure, this will be sensed as an incoming pressure wave which is not a true environmental input. To correct for this an accelerometer is incorporated into the microphone to automatically cancel the portion of the signal produced by sensor motion. Most such devices are omni-directional so that only pressure waves perpendicular to the surface will be faithfully measured.

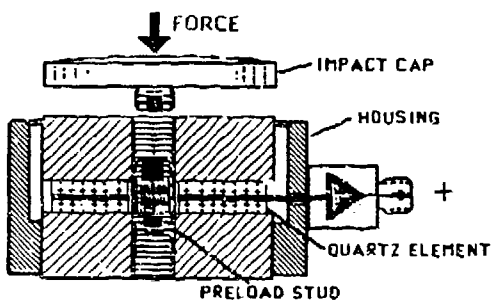
It is important that the face of the microphone be flush with the surface of the structure under test. If a cavity exists between the surface and the face of the instrument an organ pipe sort of arrangement is created. Any pressure front with a wave length identical to the dimensions of this cavity will be artificially amplified and provide erroneous readings. The device can extend beyond the surface if a precise measurement on the surface is not necessary, such as in measuring the general sound pressure levels in a bomb bay or avionics compartment. Calibration is usually performed with a precision sound generating device that fits over the face of the transducer. Such things can be purchased and the calibration done by the user. Most of the other sensor considerations already discussed are applicable to the microphone.

## **10.7 OTHER COMMON TRANSDUCERS**

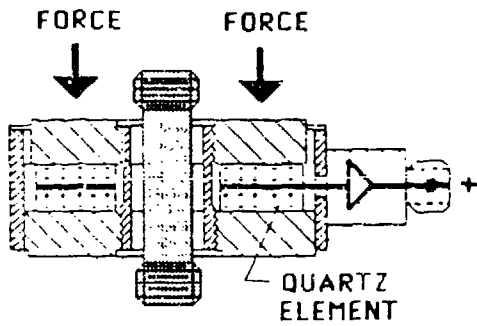
There are many other instrumentation transducers that the flight test engineer may come across which have little application to structures testing. However, there are a few which require a short introduction as they occasionally have a small role to play in loads and flutter tests.



a. Compression-Tension-Impact



b. Force Link



c. Quartz Force Ring

Figure 10.10 Common Force Transducer Configurations

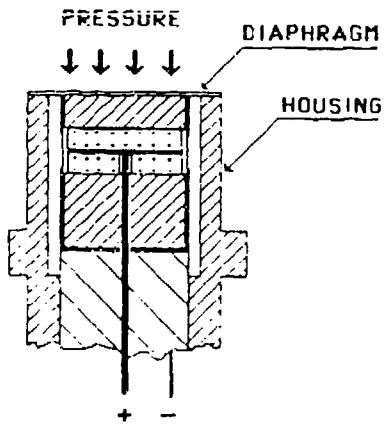


Figure 10.11 Pressure Transducer Components

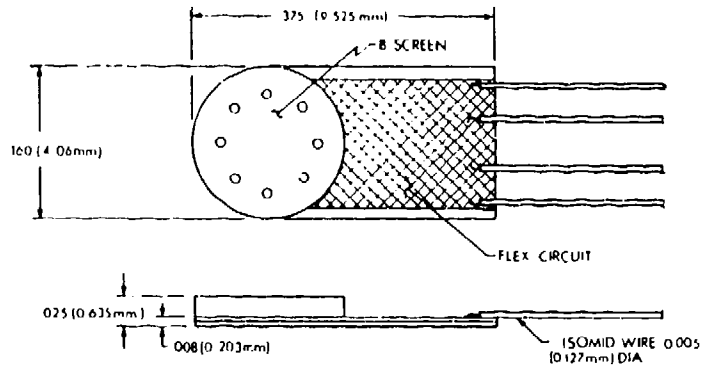


Figure 10.12 Typical Small Piezoelectric Pressure Transducer

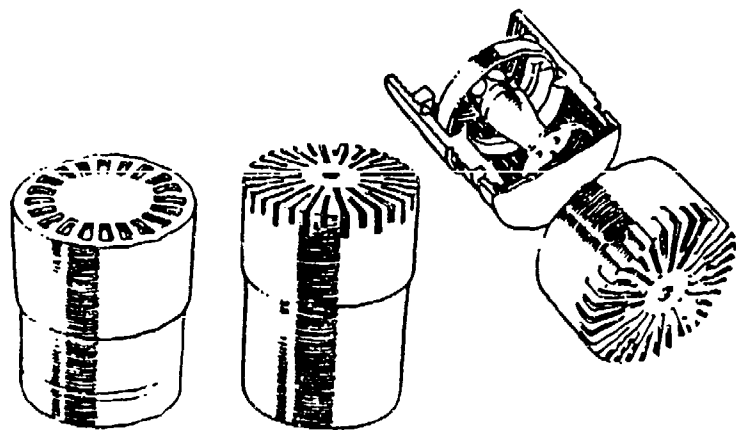


Figure 10.13 Common Measurement Microphones and Components

### **10.7.1 THERMOCOUPLE**

The very small voltage proportional to temperature produced at the junction of two dissimilar metals provide a simple but effective means of measuring temperatures on a surface. This may be important where high temperatures can cause a reduction in the modulus of the material and a loss of strength. These devices are easy to install, are inexpensive, but may be nonlinear. It is important with these devices to avoid dissimilar metals in cable runs and plugs. Another simple method of obtaining temperature information is with a resistance device or RTDs. These consist of a single material element as opposed to the two materials in the thermocouple.

### **10.7.2 DISPLACEMENT TRANSDUCERS**

The displacement of a control surface or other structure may need to be monitored to detect any tendency to divergent oscillations caused by flutter or structural feedback. This is frequently done with a rotary or linear displacement transducer. The typical position transducers used are potentiometers, linear variable differential transformer (LVDT), and strain gage bending beams. One form of this is the "string pot" which uses a string between the moving part and the transducer fixed to a nonmoving member. These are essentially potentiometers that have a rotating component attached to a brush contact. The motion of the contact causes a change in output voltage. By calibrating the displacement of the object under test against this voltage a relationship can be determined. Actually, a position transducer can be any electromechanical device that produces an electrical output proportional to some physical variable and need not be a string pot configuration. Another common form of position transducer is the strain gage bending beam, the output of which is also calibrated to the displacement of the object it is attached to. The position transducer function has also been performed by lasers and photocells. As with other transducers, the position transducer typically requires signal conditioning for power and signal amplification (see Section 10.8). The transducer may not be at the moving surface itself but buried within the control system, perhaps at a pulley or bellcrank.

### **10.7.3 TIME CODE GENERATORS**

It is seldom necessary to time-sync structures test data, however knowing the range time at which an event occurred is often required for locating the associated data on a magnetic tape or to associate the data with other events on the aircraft. The time is produced by a digital time code generator or TCG. During the flight, range time will be displayed digitally in the control room. This is the same time that will be recorded on tape and is synced to the aircraft TCG, although after the sync the control room time may be locally generated to avoid problems with telemetry interruptions. The display is produced by a time code generator that can either count the time itself or repeat the time recorded on tape during a playback of the flight's data. The time can be altered by controls on the face of the instrument. Range time is generally set to an international standard and processed using a recognized format, generally IRIG-B.

Range time is traced out at the edges of the stripchart recorder page using a binary number system called slow code. This a numbering system uses ones and zeros (on and off) to represent whether a digit is active or not. The progression of digits is with each succeeding digit twice the value of the proceeding digit, beginning at 1 (1, 2, 4, 8, 16, etc.). Groups of digits then form a number. Figure 10.14 is an example of slow code and, reading the digit groups from left to right where the U denoting units, T denoting tens, and H denoting hundreds, represents the 191st day, 14th hour, 8th minute, 32nd second at the right hand reference mark.

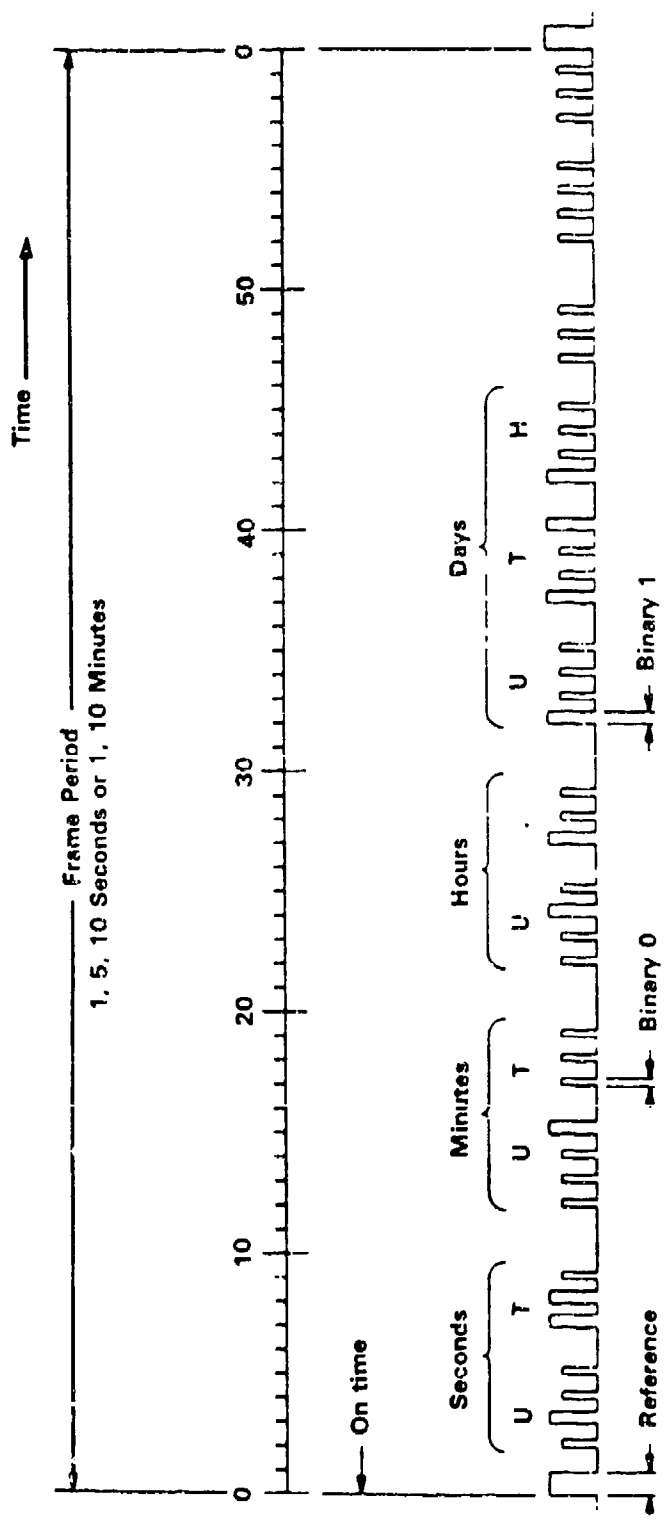


Figure 10.14 Example SCR Show Code Traces

#### **10.7.4 DISCRETES**

Some data need be no more than on/off information, such as the weight-on-wheels switch on or off. The test engineers may be provided with an **event switch** which allows them to mark an event, like the beginning of a test maneuver. Such data are called **discretes** and are handled as a binary, a 1 for on and a 0 for off.

### **10.8 INSTRUMENTATION SYSTEMS**

The basic components of the typical instrumentation system are shown in Figure 10.15. The system allows multiple transducer signals to be compiled in an efficient manner for recording, transmission, and later display for analysis. The signals must first be processed by the **signal conditioner**. This instrument may provide power or excitation to the transducer, completion networks such as Wheatstone bridge components for strain gages, provisions for calibration prior to flight, amplification of the signals, and any necessary filtering. All data comes out as voltage levels, usually 0 to 5 VDC. These signals are then coded, to allow them to be distinguished from one another, in a manner unique to the type of system being used (see Sections 10.8.1 and 10.8.2). The **multiplexer** or **mux** mixes these signals so that multiple transducer signals can be combined sequentially into just a few magnetic tape tracks or radio transmission channels. A **demultiplexer** allows the individual signals to be recovered later for display.

The radio transmission of data is termed **telemetry**. Tape recording of data aboard the aircraft as well as on the ground at the receiver station allows redundancy in the event that something happens to one of the systems during the flight or a tape is lost or damaged after the flight. The aircraft tape is generally the best source of data for later analysis because it would not have noise introduced by the radio transmission and reception process or actual **loss of signal (LOS)** which produce **dropouts**. Dropouts are erroneous data usually identified by an excursion of the data to **bandedge**, either the upper or lower limits of the transducer output. The tapes typically used store data on 14 or 28 tracks (physical locations on the tape width), that is 14 or 28 channels of multiplexed data which may contain hundreds of measurands each.

Aircraft tapes can be run at different speeds (measured in inches per second or ips) with the fastest speed giving generally better data resolution. However, the faster the tape is run the quicker it will be exhausted and the less that can be accomplished on the flight. To save tape, the aircrew is often instructed to turn the tape on before a specific test maneuver and then off again after the event. This means that the tape is not running for the entire flight which typically has only 50 percent of the time devoted to actual test accomplishment.

Data can be displayed in an unprocessed form such as on a **stripchart recorder (SCR)**, a scrolling paper plotter with usually eight parameters to a page. The minimum and maximum input voltage signal corresponds to some minimum and some maximum equivalent engineering units for the measurand and this is what is displayed on the SCR; a simple linear conversion. A variation on the SCR is the **visicorder** which traces out high frequency data (the SCR begins to attenuate a response at about 60 Hz) on light-sensitive paper. More and more data is now being presented on television screens in either a digital (tabular or "tab") or plotted format. Data may need to be subjected to second-generation processing such as the combining of parameters or transformation to the frequency domain prior to display to be truly useful to the engineer. Dedicated processing systems are used to perform these functions. The most current telemetry data processing system at AFFTC is called **IFDAPS**.

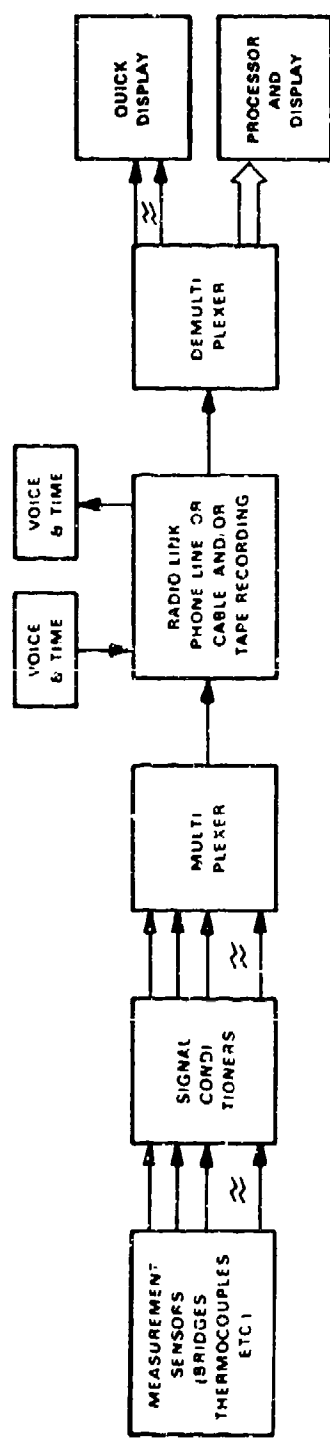


Figure 10.15 Typical Instrumentation System Configuration

There are two basic types of instrumentation systems used at AFFTC; the **FM** (frequency-division multiplex), and the **PCM** (pulse code modulation) systems. The basic nature of these systems will now be discussed.

### **10.8.1 FM SYSTEMS**

The FM systems are analog instrumentation techniques and are typically used where a high frequency response is required, such as for flutter measurands. Each transducer signal modulates a separate **subcarrier oscillator** (SCO) or **voltage control oscillator** (VCO) whose output frequency shifts in relation to the voltage from the associated transducer. This process is known as frequency-division multiplexing. **Discriminators** later filter for each distinct frequency in order to recover the individual transducer data for display (see Figure 10.16).

### **10.8.2 PCM SYSTEMS**

The basic components of a PCM system are illustrated in Figure 10.17. This is a digital technique in which the data is converted to a binary (see Section 10.7.3) and encoded into a digital signal during the mixing process. This encoding may use the amplitude of the analog signal to determine the binary representation as Figure 10.18 illustrates. Some typical terms used in this digital processing is the **bit** (binary digit, a single pulse or absence of pulse), and a **word** (a group of bits representing a single sample of information from a single channel). The number of bits comprising any word is a measure of the data resolution. A ten-bit system would have 1024 binary numbers possible to represent amplitudes between the bandedges. Increasing the bits/word from ten to twelve will produce an increase in data resolution.

PCM uses time-division multiplexing, or sampling of each parameter in turn at a specific sample rate. This sampling can be performed mechanically with a **syncro** in the **commutator** as suggested by Figure 10.19. A **decommutator** reverses the process so that the signal can be analyzed as individual data channels. More commonly today, a digital encoding routine is used to mix the data signals and later to separate them out again. The sampling rate is usually set at about five times the highest frequency of interest for fidelity. A **frame** refers to a block of data from the signal produced by a single syncro revolution, or one complete sampling cycle with a word from each channel. Today, the frame length, or words per syncro, is programmable.

The encoding of the commutator output into a digital form involves the use of a **analog-to-digital converter** (ADC). The actual transducer outputs are analog signals which must be interpreted and coded into a digital format. PCM systems usually have a lower signal-to-noise ratio than FM systems. It also lends itself more easily to the current digital signal processing methods.

## **NOMENCLATURE**

A	one leg of Wheatstone bridge
ADC	analog-to-digital converter
AFFTC	Air Force Flight Test Center
B	one leg of Wheatstone bridge
C	one leg of Wheatstone bridge, coefficient
cg	center of gravity
D	one leg of Wheatstone bridge
E	Young's modulus
EU	engineering units

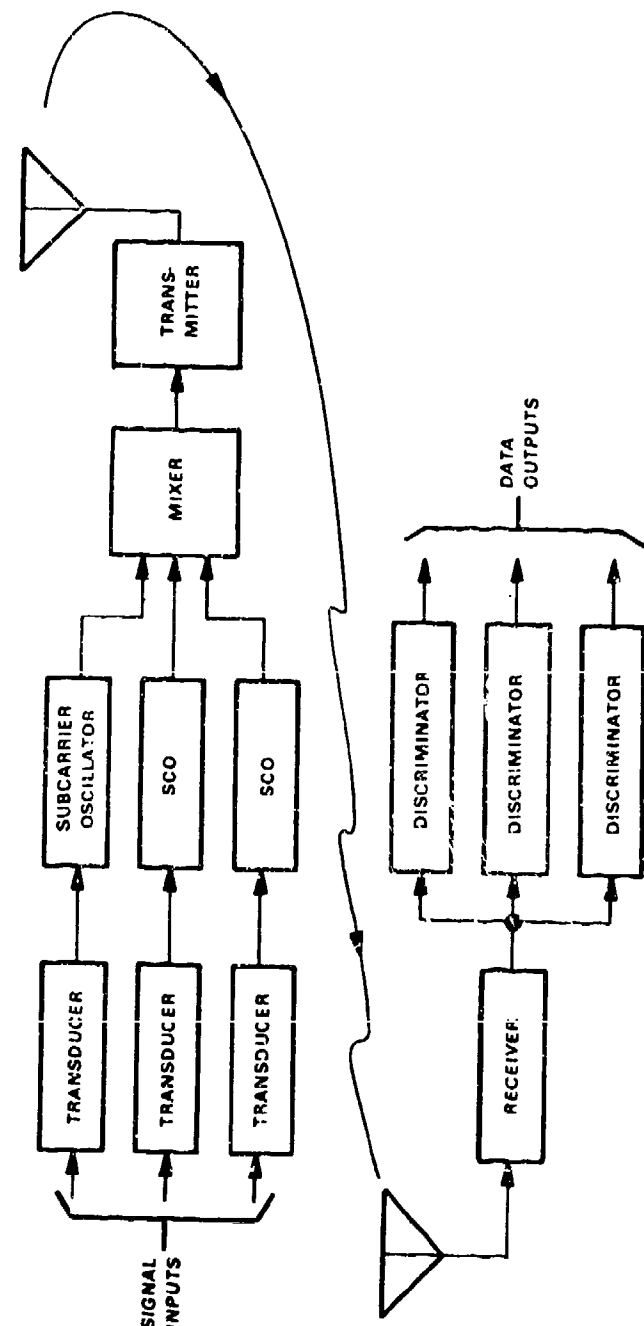


Figure 10.16 Basic FM System Components

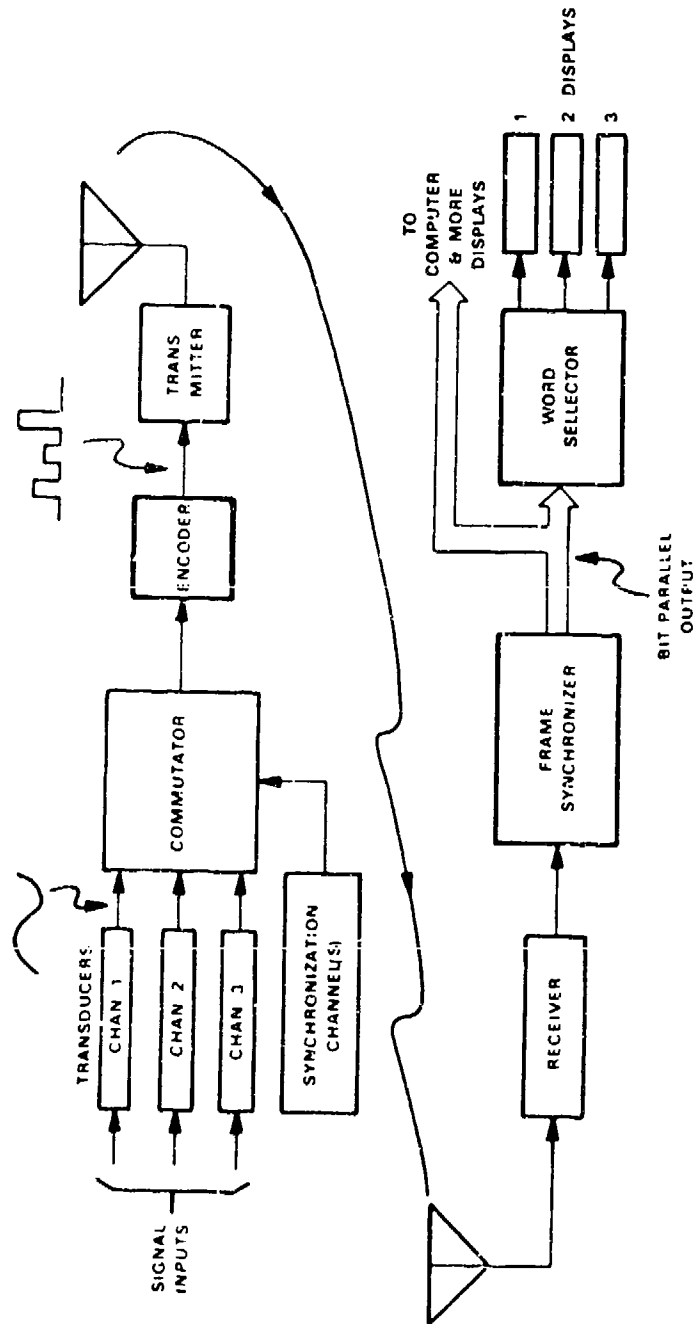


Figure 10.17 Basic PCM System Components

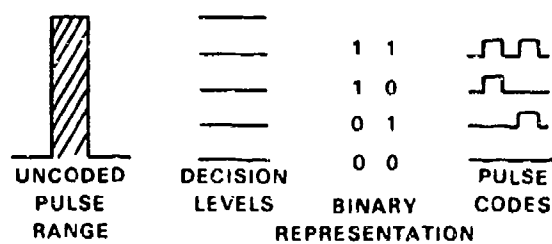


Figure 10.18 Example of PCM Encoding

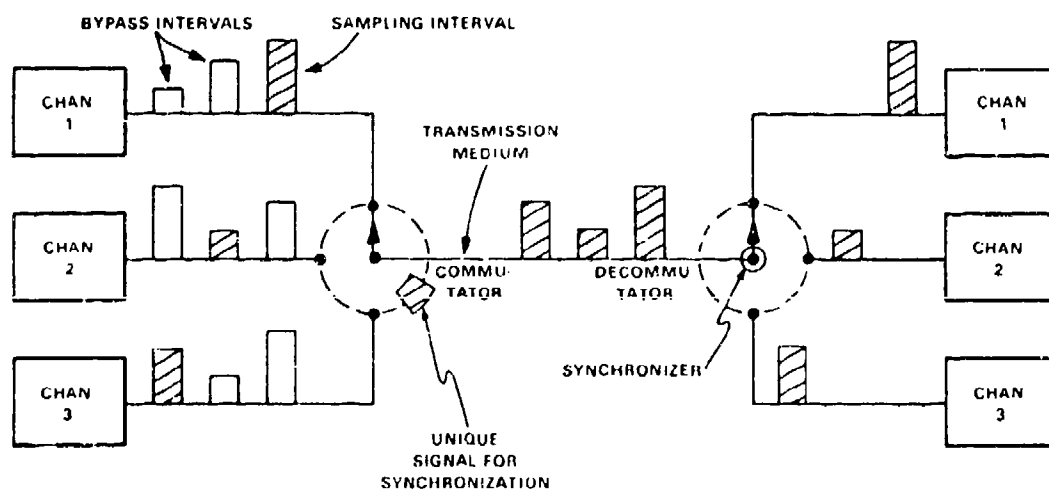


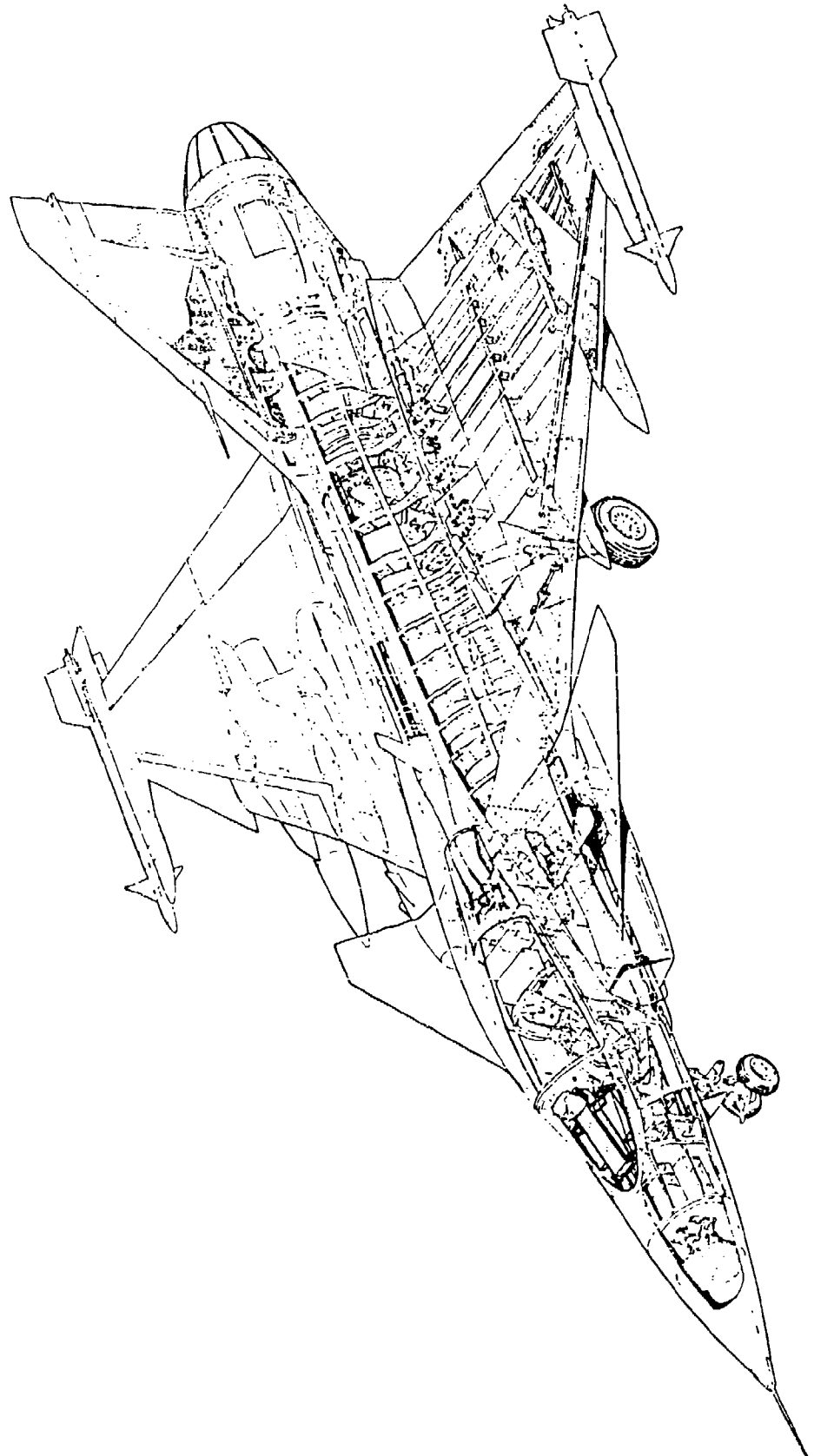
Figure 10.19 Illustration of Commutator Function

e	strain
FM	frequency division multiplex
G	galvanometer
g	acceleration due to gravity
H	hundreds digit
Hz	Hertz
ips	inches per second
K	gage factor
LOS	loss of signal
LVDT	linear variable differential transformer
M	moment, mass
mm	millimeter
mux	multiplexer
mv	millivolts
PCM	pulse code modulation
pC	pico Coulomb
R	resistance
RTD	resistance device
SCO	subcarrier oscillator
SCR	scripchart recorder
SOF	safety of flight
SOT	safety of test
T	torque, tens digit
TCG	time code generator
U	shear, units digit
u	nondimensional Wheatstone bridge output
V	shear
VCO	voltage control oscillator
VDC	volts direct current
WS	wing station
$\Delta$	increment of change
v	Poisson's Ratio
$\sigma$	stress
Subscripts	
a	one leg of rosette
b	one leg of rosette
c	one leg of rosette
i	matrix row counter
j	matrix column counter
max	maximum
min	minimum

## REFERENCES

1. McKinley, Joe, *Fundamentals of Stress Analysis*, Matrix Publishers, 1979.
2. Petterson, Arnold P.G. and Bross, Erwin E., Jr., *Handbook of Noise Measurement*, GenRad Incorporated, Concord, Massachusetts, 1978.
3. Davis, Harmer E., Troxell, George E. and Wiskocil, Clement T., *The Testing and Inspection of Engineering Materials*, McGraw-Hill Book Company, New York, New York, 1955.
4. Stiltz, Harry L, *Aerospace Telemetry*, Prentice-Hall Incorporated, Englewood Cliffs, New Jersey, 1961.

5. Strock, O.J., *Telemetry Computer Systems, An Introduction*, Instrument Society of America, 1983.
6. Doeblin, Ernest O., *Measurement Systems: Application and Design*, McGraw-Hill Book Company, New York, New York, 1983.
7. Skopinski, T.H., Aiken, William S., Jr. and Huston, Wilbur B., *Calibration of Strain Gage Installations in Aircraft Structures for the Measurement of Flight Loads*, NACA Report 1178, 1954.
8. Sims, Robert, McCrosson, Paul, Ryan, Robert and Rivera, Joe, X-29A Aircraft Structural Loads Flight Testing, *Society of Flight Test Engineers 20th Annual Symposium Proceedings*, 18 to 21 September 1989.



Saab-Scania JAS39 Gripen Cutaway

# CHAPTER 11.0

## FREQUENCY RESPONSE DATA ANALYSIS

### 11.1 INTRODUCTION

Test data must be presented in a format that permits complete and relatively simple analysis. The dynamic response of a structure can be displayed in the time or the frequency domain. The response can also be expressed as an equation of motion but this is seldom done with aircraft structures, either in flight or in ground tests, because the complexity of the structure and the presence of nonlinearities and other noise makes the extraction of the necessary parameters from the test data extremely difficult, at best. The sought after modal parameters are typically extracted from plots, known collectively as **frequency response functions (FRFs)** in the frequency domain.

The principle objective of frequency response test data analysis is the determination of the frequency, amplitude and damping of the response modes observed and a measure of the reliability of the results. The frequency may be used in correlating the test results with predictions in order to identify the modes of response. The damping allows an evaluation of how close the mode is to instability.

### 11.2 TIME DOMAIN

The analysis of a single degree of freedom (SDOF), **unforced response (transient impulse response)** in the time domain is relatively easy and so will be presented first. Figure 11.1 shows a typical time history trace for a damped system of this type. The dotted line in the figure describes the classical exponential damping decay envelope. The response may be displacement, velocity, or acceleration. Analysis of such a response should follow the removal of any average zero-offset of the response, the so-called **dc component**. This operation is **dc suppression**. Some typical definitions related to the figure (see also Chapter 4.0) are the **damping rate ( $\sigma$ )**, the **damping ratio, or damping coefficient ( $\zeta$ )** which is the actual damping divided by critical damping, the period ( $T$ ) or time between successive pulses, the **natural frequency ( $\omega_n$ )**, the damped natural frequency ( $\omega_d$ ), the **residue (R)** which is indicative of mode's strength, and the **structural damping (G)**. Common relationships between these terms are

$$\sigma = \zeta \omega_n \quad (11.1)$$

$$T = 2 \pi / \omega_d \quad (11.2)$$

$$G = 2 \zeta \quad (11.3)$$

$$\omega = 1/T \quad (11.4)$$

When the damping is extracted from flight test data both structural damping and aerodynamic damping is measured. This is then called the **total system damping**, also denoted with a  $G$ .

### **11.2.1 LOGARITHMIC DECREMENT METHOD**

By counting a fixed number of cycles on the time history and determining the amplitude of the initial and final cycle used, the damping can be determined using the following equation. This is the log decrement (log dec) method.

$$G = \ln(A_0/A_N)/(\pi N) \quad (11.5)$$

where  $N$  is the number of cycles used in the analysis,  $A_0$  is the amplitude of the first cycles used, and  $A_N$  is the amplitude of the final cycle used

This equation can be quickly applied to a response like Figure 11.1 which is representative of those often produced real-time on strip chart recorders with a single mode dominating the damped impulse response to some excitation. A trace of real structural response flight test data will seldom be a "clean" as that shown in the figure. As long as a single mode is clearly dominant, a drawn french curve line fit to the general decay will allow a log dec analysis by pulling the points from the drawn line adjacent to the trace peaks. An even quicker way to simply approximate the damping is to determine the number of cycles to the cycle that is nearest to one half the amplitude ( $N_{1/2}$ ) of the first cycle used. Equation 11.5 then becomes

$$G = 0.22/N_{1/2} \quad (11.6)$$

### **11.2.2 LOGARITHMIC (PEAK) AMPLITUDE METHOD**

The log amp or peak amp method provides a means of "curve fitting" a damping to test data that does not display a clean exponential damping envelope. The method entails plotting natural logarithms of the absolute value half cycle amplitudes versus the associated half cycle number (see Figure 11.2). By using the slope of the best straight line fit to the data points, equation 11.7 can be used to determine the damping.

$$G = 2(\text{slope})/\pi \quad (11.7)$$

Although not accomplished quickly and cumbersome for use in a mission control room, this method is superior to the logdec technique because it uses all of the available data, not just two peaks.

### **11.2.3 MULTIPLE DEGREE OF FREEDOM RESPONSES**

The analysis techniques presented in Sections 11.2.1 and 11.2.2 are useful only with time histories that have SDOF responses or ones that are almost entirely dominated by a single mode. Figure 11.3 is an example of a response that has more than one mode present. Clearly the log decrement or log amplitude methods cannot be used. The solution to this problem is to curve fit the best equation of motion to this response. The coefficients of the equation will provide the frequency response parameters sought.

One form of the equation to be fitted to data of any number of degrees of freedom is a sum of sinusoids, or

$$y(t) = C + \sum_{n=1}^N A_n e^{-\zeta_n t} \sin(f_n t + \phi_n) \quad (11.8)$$

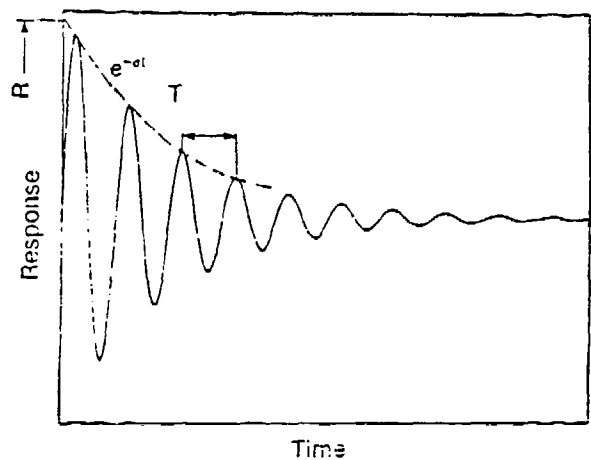


Figure 11.1 Damped Impulse Response Time History

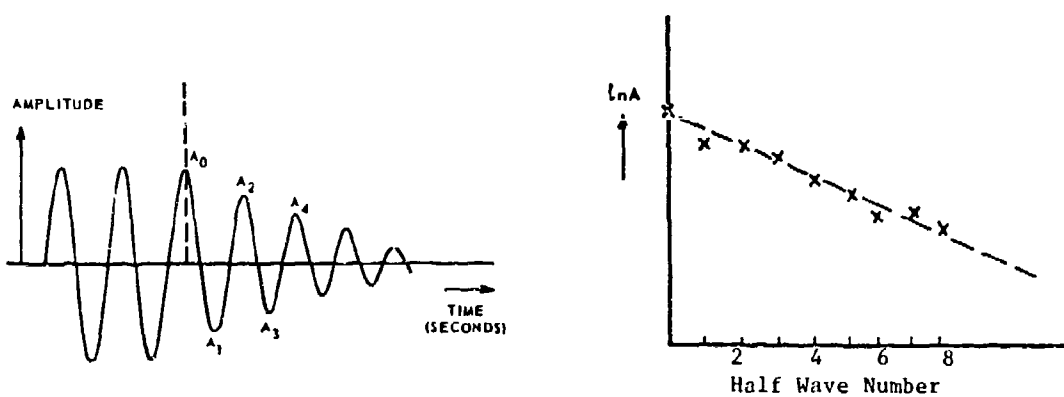


Figure 11.2 Log Amplitude Plot

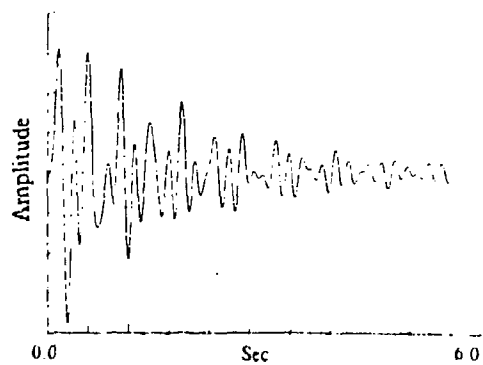


Figure 11.3 MDOF Impulse Response Function

where  $A_n$  is the amplitude of mode  $n$  in  $y(t)$  units,  $C$  is the **zero offset** correction in  $y(t)$  units,  $t$  is time in seconds,  $y(t)$  is the value of the transient at  $t$ ,  $n$  is the mode number,  $N$  is the maximum mode number,  $\phi_n$  is the **phase angle** of mode  $n$  in radians,  $f_n$  is the natural frequency of mode  $n$  in radians/second, and  $\zeta_n$  is the damping ratio of mode  $n$ .

There are a number of successful ways of arriving at the equation's coefficients that will result in the best representation of the experimental data. One of the easiest approaches is the **Least Squares Curve Fit** method. Put simply, this technique requires an initial guess at the coefficients. The difference between the calculated response and the measured response is used to correct the initial coefficients and another calculation and comparison is made. This iteration process is continued until the square of the difference between the two has been reduced to a pre-selected level.

#### **11.2.4 RANDOM DECREMENT METHOD**

The structural response time history produced by frequent random excitations would normally display no discernible individual modes from which damping and frequency can be determined (see Figure 11.4). To extract such data, a time history data crossing of a selected trigger level serves to represent an impulse excitation for subsequent structural response (the transient response due to an initial displacement). One may utilize a percentage of the RMS (root mean squared) value of the entire output signal as the trigger level. The triggering may be with a positive slope crossing of the trigger level, a negative slope crossing, or both. A signature

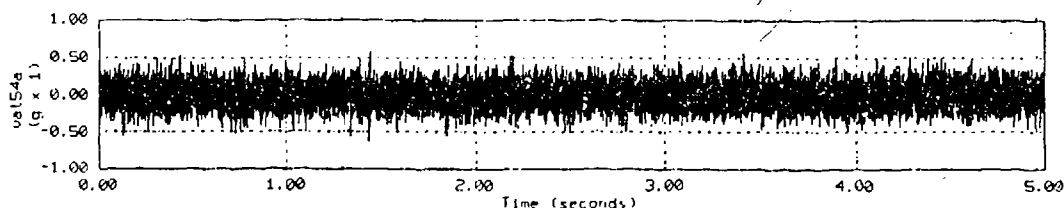


Figure 11.4 Random Excitation Response Time History

length of data is taken at each subsequent crossing of the trigger level and each is averaged with the previous signature(s).

Assuming linear superposition (see Section 10.2.3), sufficient **ensemble averages** will permit the signature to converge to the structural response due to a single excitation with extraneous noise averaged out (see Section 12.4.2). The final signature will then be in the form of a single or sum of damped sinusoidal functions. The quality of the signature and any subsequent analysis will increase with the number of averages used. This, then, is the essence of the Random Decrement or **Randomdec** method. The final signature can be used to find the desired modal parameters by the methods described in this section. Using frequency domain analysis on a Randomdec signature is not advised because more errors would be introduced to data that has already been greatly manipulated.

### 11.2.5 CORRELATION FUNCTIONS

Correlation functions provide another means of extracting useful modal data from random vibration data or data with random or "white" noise superimposed on the signal. Correlations are produced by an averaging technique that will produce the structural response in the same way as that with the Randomdec method. True random noise averages out.

Put simply, correlation functions are produced by multiplying two time histories point-by-point, repeating the process after shifting one of the histories by a time increment, and finally averaging all of the products. An **auto-correlation** results from using the same time history twice in this process (input or output response). **Cross-correlations** result from using two different histories, typically the input and output response. Since flight test data will seldom have the input signal recorded (or even completely known), attention will first focus on the auto-correlation of the output waveform.

The auto-correlation algorithm for a continuous output function,  $x(t)$ , is

$$R_{xx}(\tau) = \lim_{T \rightarrow \infty} (\frac{1}{T}) \int_{-T/2}^{T/2} x(t) x(t + \tau) dt \quad (11.9)$$

Since digitized test data is a discrete, noncontinuous data stream, equation 11.5 needs to be expressed as a summation or in a discrete form, such as

$$R_{xx}(\tau) = R_{xx}(mT) = \frac{1}{P-m} \sum_{K=1}^{P-m} (x_K y_{K+m}) \quad (11.10)$$

$$m = 0, 1, 2, 3, \dots, M$$

where  $P$  is the total number of data points,  $m$  is the correlation shift or "lag" number,  $M$  is the maximum number of time shifts to be performed, and  $T$  is the sampling period (inverse of the data sampling rate). Plotting the result of this calculation gives a waveform like that in Figure 11.5b. Since this waveform is symmetric about zero, the left side of the plot is generally neglected. The auto-correlation would then look like Figure 11.1 and can be analyzed by the techniques discussed previously. The correlation function can also be produced by plotting the sums of the time-lag products against the time shift or lag number. This number can be converted to time by equation 11.11.

$$\Delta t = (\text{lag number}) / (\text{sample rate}) \quad (11.11)$$

The algorithm for the cross-correlation (where  $y(t)$  is the input signal or any other response signal) are

$$R_{xy}(\tau) = \int_{-\infty}^{\infty} x(t) y(t + \tau) dt \quad (11.12)$$

or

$$R_{xy} (mT) = \frac{1}{P-m} \sum_{k=1}^{P-m} x_k y_{k+m} \quad (11.13)$$

$$m = 0, 1, 2, 3, \dots, M$$

and

$$R_{yx} (mT) = \frac{1}{P-m} \sum_{k=1}^{P-m} y_k x_{k+m} \quad (11.14)$$

$$m = 0, 1, 2, 3, \dots, M$$

By itself, the cross-correlation function can identify periodic functions which are common in the two time histories and time delays between the two signals while the auto-correlation tends to identify a sinusoidal or periodic function within a noisy time response.

Time domain correlation functions are seldom used by themselves because they are so subject to signal processing-induced errors and noise. They are, however, often used in producing power spectral densities (see Section 11.3.2) and transfer functions with which better analysis can be performed.

#### 11.2.6 LISSAJOUS FIGURES

A useful means of displaying two undamped sinusoidal waveforms in a manner that permits determination of relative frequency, amplitude and phasing is a cross-plotting or "beating" of the two signals (not to be confused with the beating described in Section 4.4.3). The resulting display is formed as shown in Figure 11.6 and is called a Lissajous figure. They are common displays on oscilloscopes in laboratory investigations.

Relative phase is determined as shown in the figure or by employing the equation

$$\text{phase } \phi = \sin^{-1}(y_{\text{intercept}}/y_{\text{max amplitude}}) \quad (11.15)$$

Relative frequencies are determined visually as shown in Figure 11.7 and the relative amplitudes by examining the gain settings on the display instrument for each channel necessary to produce a symmetric diagram.

Some figures used to manually "tune" modes are shown in Figure 11.8. In a ground vibration test (GVT, see Chapter 7.0), for example, a resonance occurs when the structural acceleration response 90 degrees out of phase with the excitation force. This can be determined by beating the excitation force signal against the signal from the response transducer and slowly increasing the forcing frequency until a Lissajous like Figure 11.8c is obtained. If a flutter mechanism in an aircraft wing is bending coupling with torsion with a 90 deg phase difference then flutter susceptibility increases as the Lissajous resulting from the beating of a bending and a torsion response expands from a line to a circle (Figure 11.8c again). This can be used during a flutter flight test although setting of instrument gains often prove difficult in such circumstances. Collapsing to a line from a circle is possible by integrating one of the signals.

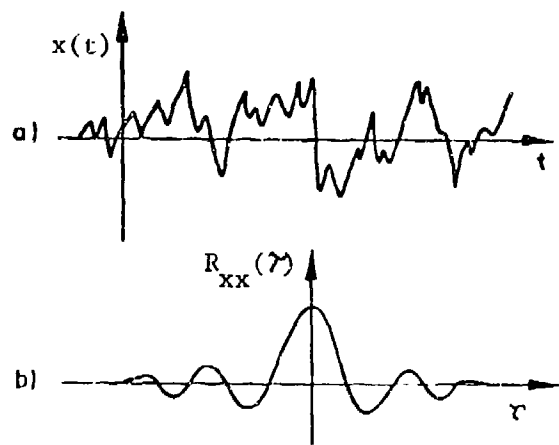


Figure 11.5 a. Original Random Response Time History (SDOF)  
b. Associated Auto-Correlation Function

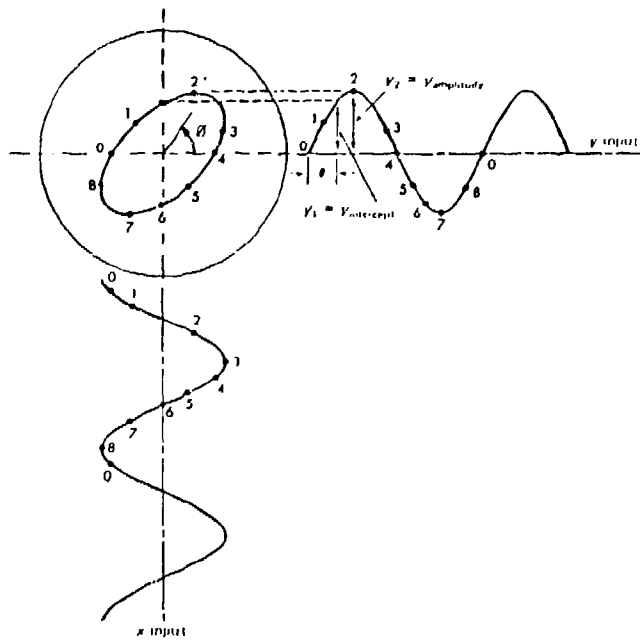


Figure 11.6 Sample Lissajous Construction

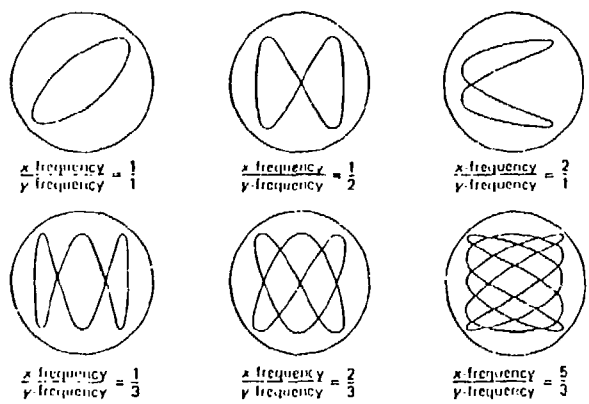
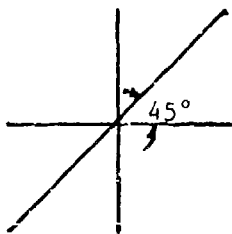
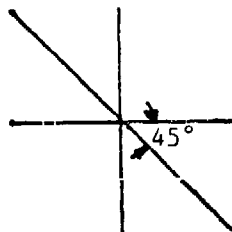


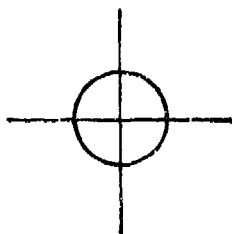
Figure 11.7 Lissajous Displays for Sinusoidal Inputs at Various Frequency Ratios



a. Line, Positive 45° Slope, In Phase



b. Line, Negative 45° Slope, 180° Out of Phase



c. Circle, 90° Out of Phase

Figure 11.8 Important Lissajous Figures  
(Same Frequency and Amplitude for Both Signals)

## **11.3 FREQUENCY DOMAIN**

Frequency domain modal analysis of test data provides many advantages over time domain analysis. MDOF systems can be analyzed with ease and the relative dominance of modes readily observed. Many forms of data presentation are available, some more suitable for a particular application than others. Manipulation of the data to remove errors introduced by the acquisition method, noise, and improving resolution is relatively easily done with many techniques available (see Chapter 12.0).

### **11.3.1 FOURIER TRANSFORMATIONS**

When the input frequency to a system is known at every instant of time, it is possible to measure frequency response functions directly. Since this is seldom the case, the heart of the frequency domain methods is the ability to transform data from the time domain. This must be done by numerical methods since continuous functions for defining the frequency response are also seldom available. The most widely used means for performing this transformation is the Fourier transformation.

Engineers are usually introduced to the Fourier transformation in the series form in which a complex waveform is represented by a series of sine and cosine functions. That is

$$f(t) = A_0/2 + \sum_{k=1}^{\infty} [A_k \cos(k \omega_0 t) + B_k \sin(k \omega_0 t)] \quad (11.16)$$

where

$$A_0 = 2/T \int_0^T f(t) dt \quad (11.17)$$

$$A_k = 2/T \int_0^T f(t) \cos(k\omega_0) dt \quad (11.18)$$

$$B_k = 2/T \int_0^T f(t) \sin(k\omega_0) dt \quad (11.19)$$

and where  $f(t)$  is a periodic function,  $\omega_0$  is the fundamental frequency of the function, and  $T$  is the period of  $f(t)$ . Representation in the frequency domain requires the identities

$$\text{dc component amplitude} = A_0/2 \quad (11.20)$$

$$\text{Amplitude at any frequency} = \sqrt{A_n^2 + B_n^2} \quad (11.21)$$

The  $B_n$  component is actually an imaginary term and the  $A_n$  the real term. For plotting purposes, the transformed result is generally multiplied by its complex conjugate, or

$$\text{Amplitude} = \text{Re}^2 + \text{Im}^2 \quad (11.22)$$

This results in the units of the measured values being plotted as squared terms,  $g^2$  for example. This is essentially an **auto spectrum** rather than a simple transform, and looks like Figure 11.9 in which the discrete calculated amplitudes are plotted at each frequency as **spectral lines**. A pure auto spectrum would possess both positive and negative values, one the mirror image of the other. Because the data we seek can be obtained from just a single side of the spectrum, the positive side is usually the only one plotted. The contribution of the negative side can be accounted for by multiplying the displayed side by two. If the amplitude of the dynamic response in the frequency domain is important, in environmental vibration tests for example (see Chapter 9.0), it is absolutely essential to know whether the spectrum is multiplied by two or not.

The transformation of a single sine wave component would appear as a single spectral line at the associated frequency. Referring to Figure 11.9, the spectral lines on either side of the resonant (peak) line are due to nonlinearities of real structures or signal processing considerations (see Chapter 12.0). The **dc** component (direct current, borrowed from electrical applications) is generally removed by displaying only the spectrum to the right of its line or by subtracting the average of the time domain data (zero offset) prior to transformation. This is done because the magnitude of this component is generally much greater than the rest of the response and scaling makes analysis of the relatively smaller magnitudes in the rest of the spectrum difficult. It is also normally of no interest.

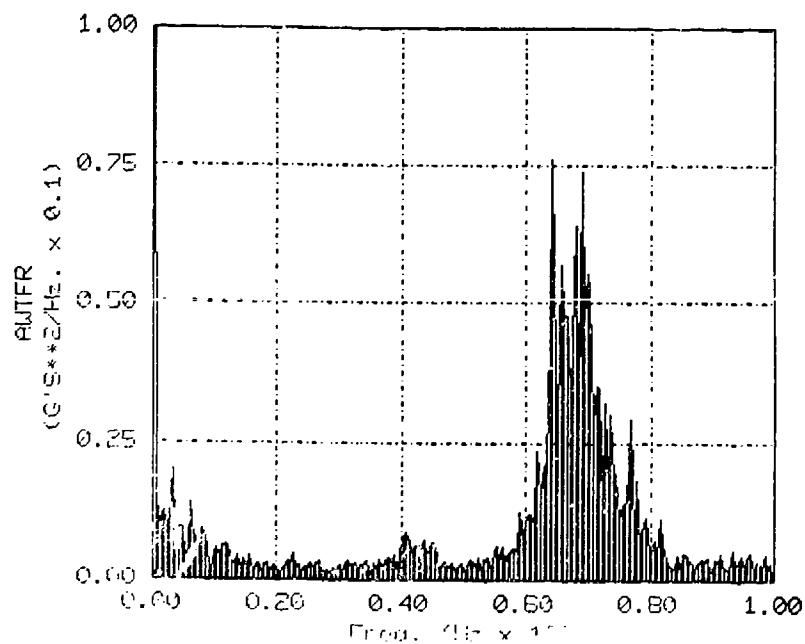


Figure 11.9 Typical Fourier Transformation Results

The principle difficulties in implementing an algorithm such as equation 11.16 in practice is the unlimited frequency range specified and the requirement to evaluate integrals of the unknown continuous expression for  $f(t)$ . These problems can be circumvented by numerical integration techniques which essentially sums the area under the time history of  $f(t)$ . Thus

$$A_o = \frac{2}{N} \sum_{k=0}^{N-1} f(k \Delta t) \quad (11.23)$$

$$A_o = \frac{2}{N} \sum_{k=0}^{N-1} f(K \Delta t) \cos(n \omega_0 K \Delta t) \quad (11.24)$$

$$B_n = \frac{2}{N} \sum_{k=0}^{N-1} f(K \Delta t) \sin(n \omega_0 K \Delta t) \quad (11.25)$$

where

$$T = N \Delta t \quad (11.26)$$

and  $\Delta t$  is the time between data points ( $N$  total). This permits the transformation of discrete data and is called the **Discrete Fourier Transformation (DFT)**.

For computer applications, a more tractable form of the transformation is

$$F(\omega) = \int_{-\infty}^{\infty} f(t) e^{-i\omega t} dt \quad (11.27)$$

which, for an input signal ( $x$ ) or an output signal ( $y$ ) shall be denoted as

$$S_x(\omega) = F[x(t)] \quad (11.28)$$

$$S_y(\omega) = F[y(t)] \quad (11.29)$$

In a DFT format (see Reference 5) we have

$$x_n = \left(\frac{1}{N}\right) \sum_{k=0}^{N-1} x_k \omega_N^{kn} \quad (11.30)$$

where  $N$  is the number of data points,  $X_n$  is the array of complex transformed values,  $x_k$  is the time domain data points (complex), and  $X_0$  is the dc term. Also

$$\omega_n = e^{-2\pi i / N} \quad (11.31)$$

The associated **Inverse Fourier Transformation (IFT)** to return to the time domain is

$$x_n = \sum_{k=0}^{N-1} X_k \omega_N^{-kn} \quad (11.32)$$

A pure IFT will reproduce the time history unless DFT averaging, widowning, and other data smoothing work has been employed (see Chapter 12.0). An IFT of such a DFT from random data will appear as an impulse response rather than the original time history. This and the fact that random noise is eliminated in the averaging process will improve a time domain analysis of the resulting IFT. An example of an IFT from processed data is presented in Figure 11.13, as discussed in Section 11.3.4.

Since test data is almost always real, computational speed can be increased by employing a special case form of equation 11.30. That is,

$$x_{N-n} = \frac{1}{N} \sum_{k=0}^{N-1} x_k \omega_N^{kn} \quad (11.33)$$

By employing mathematical reductions and recognizing certain symmetries in the computations, the number of operations by the computer can be significantly reduced. These methods produce the **fast Fourier transformation or FFT**.

### **11.3.2 AUTO SPECTRUMS**

Auto spectrums were first introduced in the last section. Correlations in the frequency domain are done in an analogous manner to those in the time domain (Section 11.2.5) with the averaging of FFT outputs (or **instantaneous spectra**) of two channels, inputs only, or a combination. This produces the auto spectrums or **auto power spectrums**. It can also be generated by taking a Discrete Fourier Transformation of the auto correlation function (see Section 11.2.5), or

$$G_{xx}(\omega) = F[R_{xx}(\tau)] \quad (11.34)$$

$$G_{xy}(\omega) = F[R_{xy}(\tau)] \quad (11.35)$$

where the equation 11.35 formulation is called the **cross power spectrum**. However, the auto spectrums are more frequently derived in the manner described in the previous section, or

$$G_{xx}(\omega) = S_x(\omega) S_x(\omega)^* \quad (11.36)$$

$$G_{yx}(\omega) = S_y(\omega) S_x(\omega)^* \quad (11.37)$$

where the asterisks denotes the complex conjugate. Note that

$$G_{yx}(\omega) = G_{xy}(\omega) \quad (11.38)$$

which is true for similar functions.

The auto spectrums provide essentially the same information as the time domain correlations. Additionally, the auto spectrum can be used to determine the power or energy content as a function of frequency. The cross spectrum is a measure of the power shared between two signals but can also be used to analyze the phase relationship between the signals.

### 11.3.3 POWER SPECTRAL DENSITY

As a means of accentuating the resonant peaks in the auto spectrum plot, the amplitude can be divided by its frequency resolution (see Section 12.2.1) to produce a power spectral density plot ( $\Phi$ ). For example

$$\Phi_{xx}(\omega) = G_{xx}(\omega)/\Delta f \quad (11.39)$$

This operation has the effect of amplifying peaks while reducing the level of noise, leakage, and other undesirable signal processing consequences (see Chapter 12.0). The amplification process increases the accuracy and ease of the damping calculations. The units of the magnitude axis are now the square of the response divided by frequency (i.e.  $g^2/\omega$  or  $g^2 \text{ sec}$ ). The resulting plot is called a Power Spectral Density or PSD. These plots are widely employed in modal analysis and provide a means of maintaining consistency within the field. The name is derived from the electrical engineering field and the earlier electrical methods for producing the PSD.

There are alternative ways to produce the PSD. In a general formulation

$$\Phi_{yy}(\omega) = (1/2\pi) \int_{-\infty}^{\infty} R_{yy}(\tau) e^{-i\omega\tau} d\tau \quad (11.40)$$

$$\Phi_{xx}(\omega) = \operatorname{Re}[F(R_{xx}(mT))] \quad (11.41)$$

That is, for the output

$$\Phi_{xx}(\omega) = T \left[ R_{xx}(0) + 2 \sum_{m=1}^{M-1} R_{xx}(mT) \cos m\omega T + R_{xx}(mT) \cos M\omega T \right] \quad (11.42)$$

A similar formulation can be made for the output.

A cross spectral density (CSD) can also be defined.

$$\Phi_{xy}(\omega) = (1/2\pi) \int_{-\infty}^{\infty} R_{xy}(\tau) e^{-i\omega\tau} d\tau \quad (11.43)$$

Note that  $\Phi_{xy}(\omega) = \Phi_{yx}^*(\omega)$ .

### 11.3.4 HALF POWER METHOD

The most common technique for determining the damping of a mode in the frequency domain is by use of the half power method. This approach is based upon the following approximation for the damping of a single structural mode.

$$G \approx (\Delta\omega/\omega_0)/\sqrt{|A|_{max}^2/|A|^2 - 1} \quad (11.44)$$

where  $|A|_{max}$  is the maximum response amplitude at  $\omega_0$ , and  $|A|$  is the response at some  $\omega$  where

$$\omega = \omega_0 + \Delta\omega/2 \quad (11.45)$$

where ( $\omega \ll \omega_0$ )

For  $|A|/|A|_{\max} = 1/\sqrt{2}$  (or 0.707), then

$$G \approx \Delta \omega / \omega_n \quad (11.46)$$

The half power method applied to a plot such as the imaginary portion of the frequency response (see Section 11.3.8) will use this criteria as shown in Figure 11.10 where

$$\sigma = \zeta_r \omega_d \quad (11.47)$$

The residue is a measure of a mode's energy content and is defined as

$$R \approx 2 |A_{\max}| \sigma_r \quad (11.48)$$

Also, a quality factor can be defined as

$$Q = \omega_0 / \Delta \omega \quad (11.49)$$

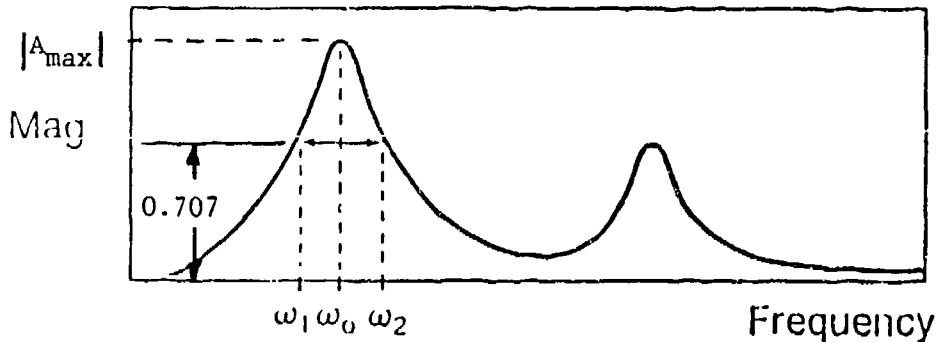


Figure 11.10 Half Power Damping From a Non-Squared FRF

When the magnitude of a response plot is squared, as in an auto spectrum or a PSD (see Section 11.3.3), then 1/2 of the resonance used instead of 0.707 (see Figure 11.11). If the plot is further modified by showing the magnitude on a log scale then the  $\Delta\omega$  is then found as before, depending on whether the amplitude was initial squared or not. Data can be plotted using  $20\log(\text{magnitude ratio})$ , where the ratio is determined by dividing by some convenient reference magnitude, or just  $\text{Log}(\text{magnitude})$  for a transfer function (see Section 11.3.6). This results in units of decibels (dB). Now -3dB down would be the required amplitude for the analysis (Figure 11.12) if the original amplitude was not squared, and -6dB (half the power) is used when the original magnitude was squared.

The half power method assumes that the only one mode is influencing the results; the mode being analyzed. The fidelity of the damping result is a function of how pure the mode appears or how close other modes are to the one being analyzed. It may be necessary to extrapolate the skirts of the mode in order to do a half power analysis where close modes are clearly expanding the skirt. This sort of analysis of one mode at a time versus a curve fit of the entire FRF is termed **peak picking**.

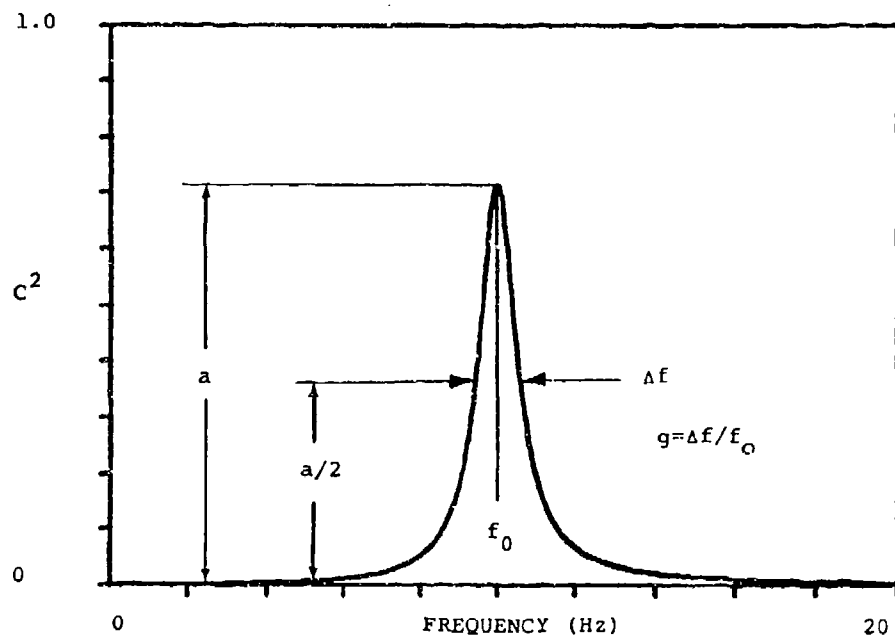


Figure 11.11 Half Power Method From a Squared FRF

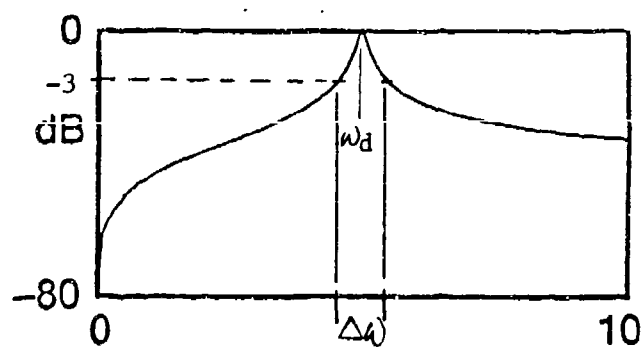
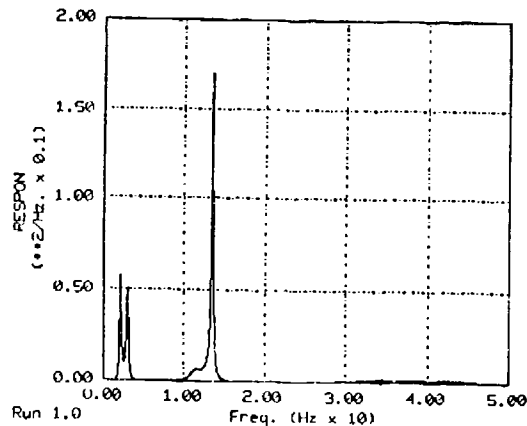
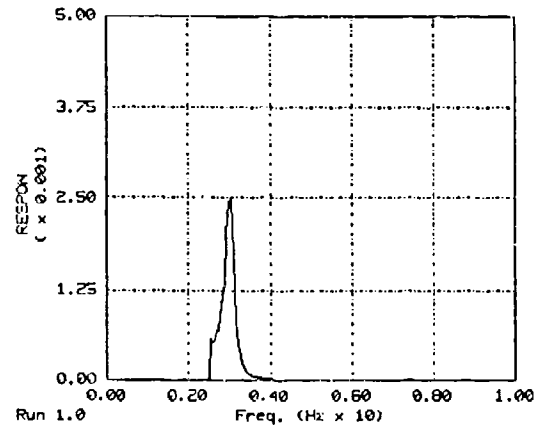


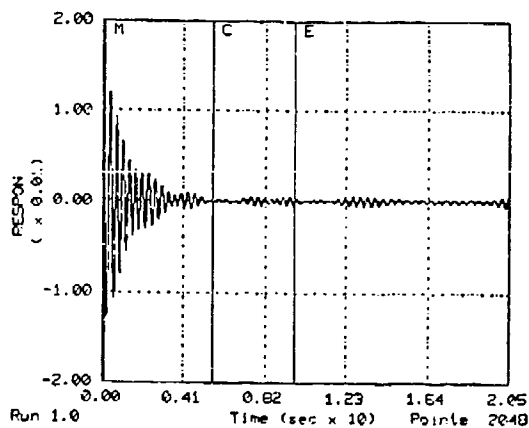
Figure 11.12 Half Power Applied to Decibel Scale (Non-Squared FRF)



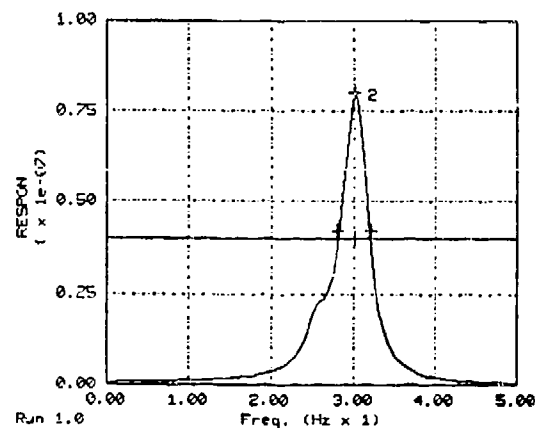
a. Original PSD



b. Bandpass Filter Isolation of Single Mode from a.



c. IFT of b. Showing Exponential Analysis Window Notation



d. Resulting PSD Showing Half Power

Figure 11.13 Half Power Method Using an IFT for Smoothing

Figure 11.13 shows an analysis method that uses several of the techniques discussed so far. The portion of the original PSD (11.13a) of interest is isolated (11.13b) using a narrow band pass window function (Section 12.4.1). An IFT of b) produces an auto correlation function which may be seen as the single decay shown in the figure or as a series of beating-type responses typical of close modes and analogous to a transient response. The first damped response, if several beat responses are present, is the dominant mode and it is the damping of this which is most important. The mode is marked with a line at the peak of the response or beginning of the decay portion (M, at zero in this case) and a line to mark the lowest response level at the end of the decayed portion (C, for cut-off, in the figure). An exponential window (Section 12.4.1.5) is used to force the decay to zero. The choice of the E line shown in the figure dictates the shape of the exponential envelope superimposed on the decay and forces the response to 2 percent of the response at M at the selected point. The closer the E is to the cut-off, the sharper the decay will be. All of this serves to isolate and smooth a single mode, or several if such is included in the IFT cut-off. The PSD of the selected mode is shown in 11.13d and shows how the peak of the resulting smoothed mode is chosen, the half power line is then automatically calculated and drawn on the plot, and the skirt crossings marked. While this approach may be the only means of extracting useful damping data from poorly excited response data with close modes, it is about the limit of the processing you want to do without losing confidence in the resulting damping and frequency values.

### **11.3.5 OTHER COMMON PRESENTATIONS**

The dynamic response relationships introduced in Section 4.4.1 provide important information when plotted in the frequency domain. Figure 11.14 provides examples of these functions. The compliance, mobility and inertance plots identify resonances as maximum value "spikes", while the apparent stiffness, impedance and apparent mass identify resonances at the minimum "valleys". antiresonances or nodes (see Section 4.5.2). The apparent mass (inverse of inertance) displayed as logarithmic amplitude is simply the mirror image of the inertance plots so that they are analyzed in an inverse manner (valleys being resonances, etc.). Note that the phase shifts 180 deg at resonance for inertance and 90 deg for compliance and mobility. This fact is used to separate "true" modes from "false" modes (spikes produced by structural nonlinearities or signal processing errors). Note that at resonance the real component of inertance has a value of zero, and the imaginary component has a local minimum (negative spike).

Figure 11.14 also illustrates for inertance how a logarithmic amplitude (dB) allows more detail in low energy modes while a linear display allows resonances to be seen more easily. This is generally true for most frequency domain plots.

These relationships provide another way of extracting modal parameters. Using compliance (displacement divided by force or  $x/f$ ), the following relationship can be defined

$$G = \frac{|x/f|(f_0)}{|x/f|(0)} \quad (11.50)$$

where  $|x/f|(f_0)$  is the amplitude of the compliance at the resonant frequency, and  $|x/f|(0)$  is the static compliance or the magnitude at zero frequency. Figure 11.15 shows how stiffness and mass can be obtained from the displacement, velocity and acceleration plots. For frequencies much less than the resonant frequency, the slope of the curves (called the stiffness line) are proportional to the stiffness ( $k$ ) as shown. These slopes are 0, 1, and 2 for displacement, velocity and acceleration, respectively. For frequencies much greater than the resonant frequency, the slope of the curves are proportional to the mass (termed the mass line), as shown, where the

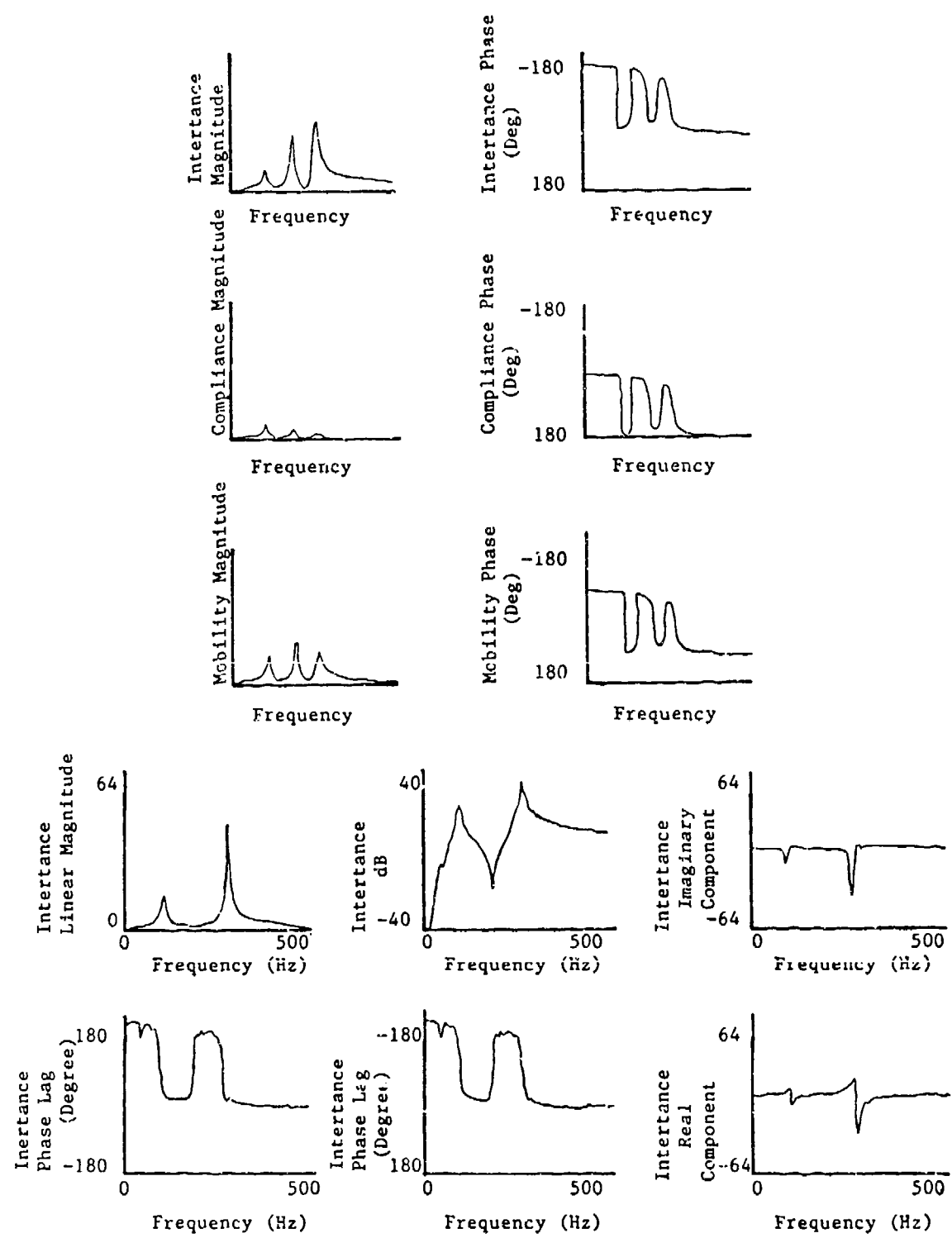


Figure 11.14 Common Data Presentations

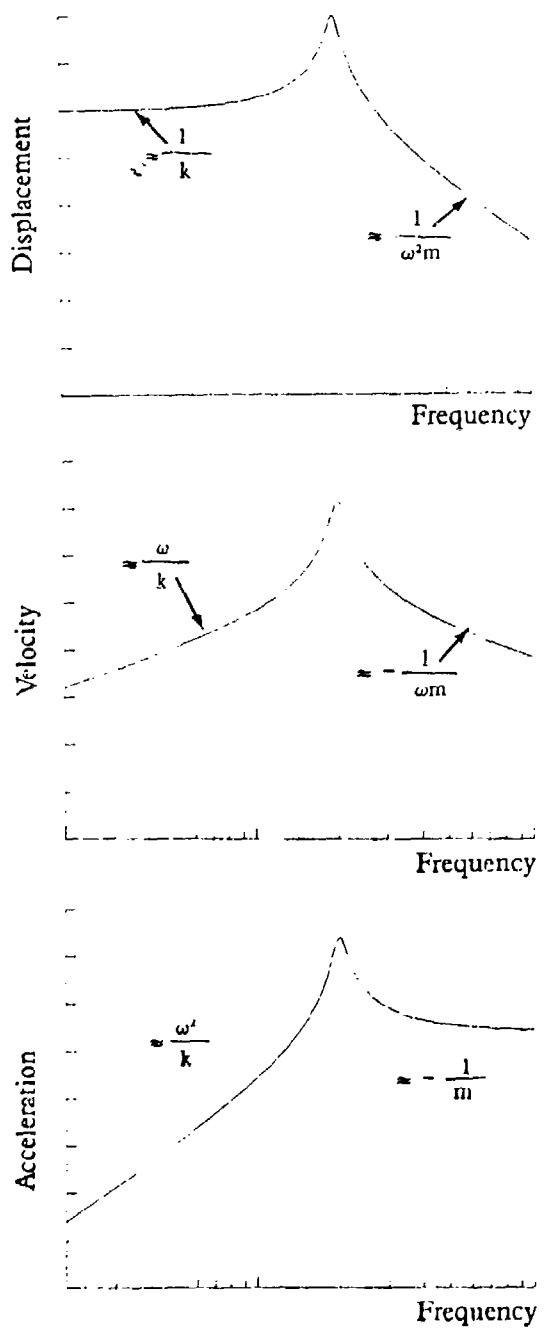


Figure 11.15 Modal Parameters From Simple Response Plots

slope are -2, -1, and 0 for displacement, velocity and acceleration, respectively. All of this naturally assumes that the data is clean and only one mode is affecting the response at the frequency of interest.

### 11.3.6 TRANSFER FUNCTIONS

A transfer function is a mathematical model of a system (the structure in our case) that transforms the input excitation into the output response, as shown by Figure 11.16.

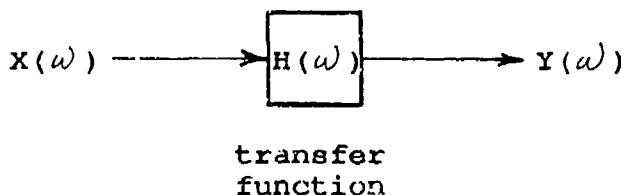


Figure 11.16 Diagram of Transfer Function Operation

It can be defined as

$$H(\omega) = Y(\omega)/X(\omega) \quad (11.51)$$

or, using the notation from Section 11.3.2, as

$$H(\omega) = G_{xy}(\omega)/G_{xx}(\omega) \quad (11.52)$$

Similarly, in the Laplace domain (see Section 11.3.9)

$$H(s) = Y(s)/X(s) \quad (11.53)$$

Or, using power spectral densities

$$H(\omega) = \Phi_{xy}(\omega)/\Phi_{xx}(\omega) \quad (11.54)$$

and

$$|H(\omega)|^2 = \Phi_{yy}(\omega)/\Phi_{xx}(\omega) \quad (11.55)$$

This last equation allows the elimination of the input power spectral density if the input can be assumed to be sufficiently flat in the frequency range of interest (such as free air turbulence excitation). That is

$$|H(\omega)|^2 = \Phi_{yy}(\omega) \cdot \text{constant} \quad (11.56)$$

The power of the transfer function rests in its ability to predict the response to any input, if it can be so defined, by reforming equation 11.51 as

$$Y(\omega) = H(\omega)X(\omega) \quad (11.57)$$

This chapter deals principally with modal parameters derived more or less manually from response plots. However, there are many transfer function curve fitting routines that can be used to extract the parameters which provide the modal data. These are very mathematically intensive and too lengthy to detail here. A few curve fitting routines allow some correction for modal contribution from response outside the frequency range being analyzed. These are called the **residuals**. Curve fitting in the frequency domain has the advantage of being able to fit only those portions of the spectrum of interest and thus eliminate those areas with noise or signal processing problems, and to obtain a better fit.

### **11.3.7 COHERENCE FUNCTION**

The coherence function can be formed using the power spectral densities (see Section 11.3.3) or the auto spectrums (Section 11.3.2), as shown in equations 11.58 and 11.59, respectively.

$$v_{xy}(\omega) = |\Phi_{xy}(\omega)|^2 / [\Phi_{xx}(\omega)\Phi_{yy}(\omega)] \quad (11.58)$$

$$v_{xy}(\omega) = |G_{xy}(\omega)|^2 / [G_{xx}(\omega)G_{yy}(\omega)] \quad (11.59)$$

It is used when both the input and response functions are known, most often when attempting to form a transfer function (previous section). The coherence between single input and single output signals has been called **ordinary coherence**.

The ordinary coherence function will always be between 0.0 and 1.0, as shown in Figure 11.17, and shows the amount of response due to the input alone, and how much is due to noise or parasitic excitation and leakage (see Section 12.3.3). At 1.0 the response is due entirely to the input (perfect correlation) with no noise present. Conversely, at 0.0 there is no correlation at all. A value of greater than 0.7 is considered acceptable and modal parameters extracted from the FRFs at corresponding frequencies should be reliable. A value of less than 0.7 is considered unacceptable and the test should be repeated with different excitations of the data analyzed again in an effort to reduce noise and processing errors.

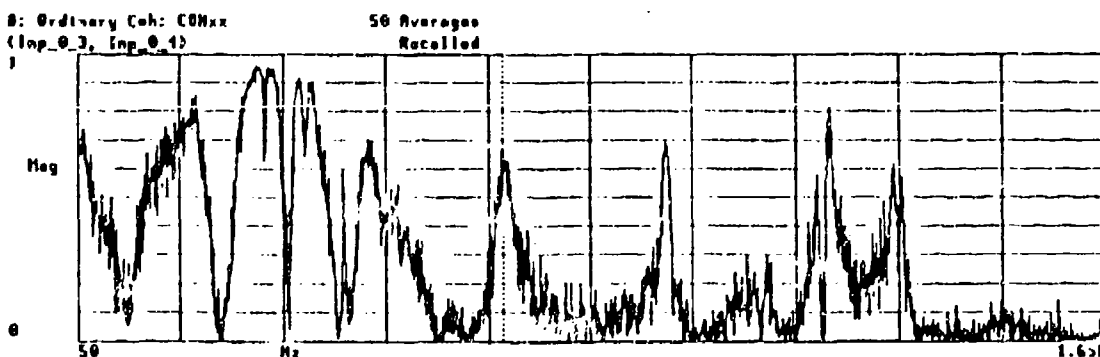


Figure 11.17 Example of Ordinary Coherence Function

When more than one input and output are involved, other coherence functions can be defined. **Partial coherence** is essentially an ordinary coherence function but with one or both of the signals "conditioned" by removing the potential contributions from other influences, such

as from other forcing functions. It is most often used to see if another input is correlated in any way with the input of interest and thus influencing the output signal. In the case of a coherence between two inputs, a low value of coherence would indicate little or no correlation. This allows an evaluation of how much unknown or undesirable inputs are influencing the response. A **multiple coherence** is done between a single output and all known input signals. This allows an evaluation of how much unknown or undesirable inputs are influencing the response. A multiple coherence would involve a matrix of input cross spectrums,  $[G_{yx}]$ , in which each element is a cross spectrum of an input  $i$  with an input  $j$ , one for each  $G_{yx}(i,j)$ . This matrix is then augmented with an array of output-input cross spectrums,  $\{G_{yy}\}$  to produce

$$[G_{yxx}(i)] = \begin{bmatrix} G_{yy}(i,i) & G_{yx}(i,1) & G_{yx}(i,2) & G_{yx}(i,3) & \dots \\ G_{yx}(1,i) & G_{xx}(1,1) & G_{xx}(1,2) & G_{xx}(1,3) & \dots \\ G_{yx}(2,i) & G_{xx}(2,1) & G_{xx}(2,2) & G_{xx}(2,3) & \dots \\ G_{yx}(3,i) & G_{xx}(3,1) & G_{xx}(3,2) & G_{xx}(3,3) & \dots \\ \vdots & \vdots & \vdots & \vdots & \ddots \\ \vdots & \vdots & \vdots & \vdots & \ddots \end{bmatrix} \quad (11.60)$$

Our multiple coherence for output  $i$ ,  $v_M(i)$  can now be determined by using the determinant of this matrix and the matrix of input cross spectrums.

$$v_M = \frac{1 - \text{DET}[G_{yxx}(i)]}{G_{yy}(i,i) \text{DET}[G_{xx}]} \quad (11.61)$$

### **11.3.8 CO/QUAD METHOD**

Another way of analyzing frequency domain data is by examining the real and imaginary parts of the frequency response. These are shown in Figure 11.18 for a single mode, and other forms have already been presented in Figure 11.8. Notice that at resonance the mobility has only real amplitude while the compliance and inertance has only imaginary amplitude. The real part of the response is in phase or **coincident (CO)** with the forcing function and the imaginary part is out of phase with the response (**quadrature or QUAD**). The peak of the QUAD will occur at the resonance frequency, the same as the CO zero or axis crossover.

The peak of the CO can be used to find the damping by using the real or imaginary portions of the compliance, mobility and inertance as indicated in Figure 11.19, and with the equation

$$G = [(f_a/f_b)^2 - 1]/[(f_a/f_b)^2 + 1] \quad (11.62)$$

Damping derived from the QUAD has been presented in Section 11.3.4.

### **11.3.9 NYQUIST PLOTS AND CIRCLE FIT**

If the two curves of Figure 11.18 are plotted against each other then a plot like Figure 11.20 will result for a SDOF. Plots for acceleration, velocity (mobility) or displacement (compliance) would be identical but for a 90 deg rotation of the trace each time. When examining the imaginary and real axes alone in the Argand plane a circle is seen. This is called a Nyquist or Polar plot

and can also be produced by plotting magnitudes at the corresponding phase angles as in Figure 11.21. The circle is easily plotted by employing the simple geometric identities

$$\text{Re} = \text{mag}(\cos \varphi) \quad (11.63)$$

$$\text{Im} = \text{mag}(\sin \varphi) \quad (11.64)$$

At a phase angle of  $90^\circ$  the amplitude is maximum with the real component zero. This condition corresponds to resonance, so the frequency of this point is the resonant frequency. Larger diameters represent lower damping than small diameter circles.

Real data for a MDOF system would appear more like Figure 11.22a. The distortion and offset of the circle are the effects of coupling between off-resonant modes (vector OA in Figure 11.22b) or the presence of non-linear restoring and damping forces. The peak response is found as shown in Figure 11.22b and the damping by equation 11.65. Using the notation of Figure 11.22b

$$\zeta = 2(\omega_c - \omega_d)/\omega_0 \quad (11.65)$$

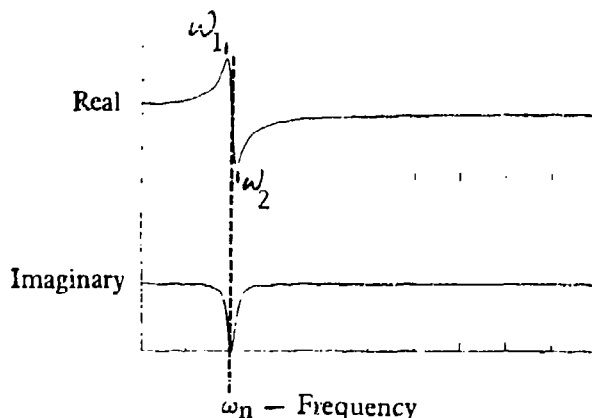


Figure 11.18 CO/QUAD Elements

### 11.3.10 LAPLACE (S-PLANE) TRANSFORMATION

Analysis is occasionally done in the s-domain where s is the Laplace variable defined as

$$s = \sigma \pm j\omega \quad (11.66)$$

or

$$s = \zeta_n \pm j\omega_n \sqrt{1 - \zeta^2} \quad (11.67)$$

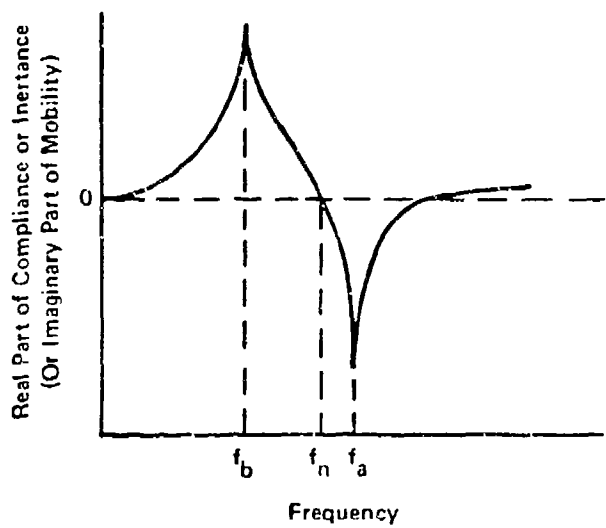


Figure 11.19 Determining Damping From Real or Imaginary Response

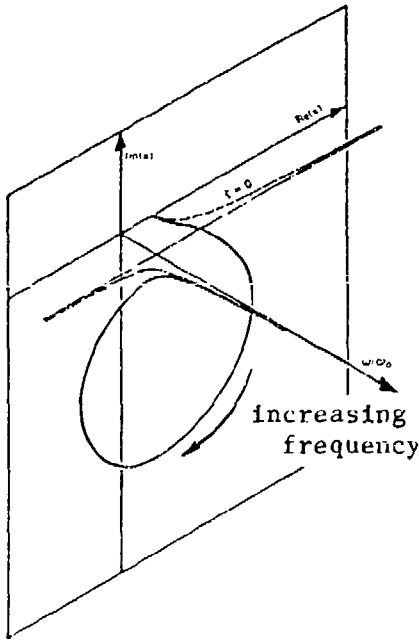


Figure 11.20 3-Axis Frequency Response Plot

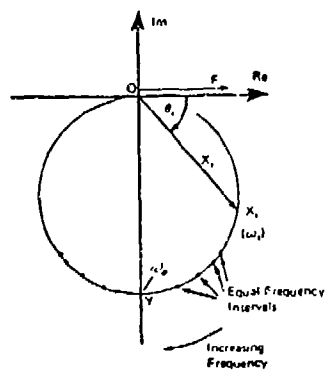


Figure 11.21 SDOF Nyquist Plot

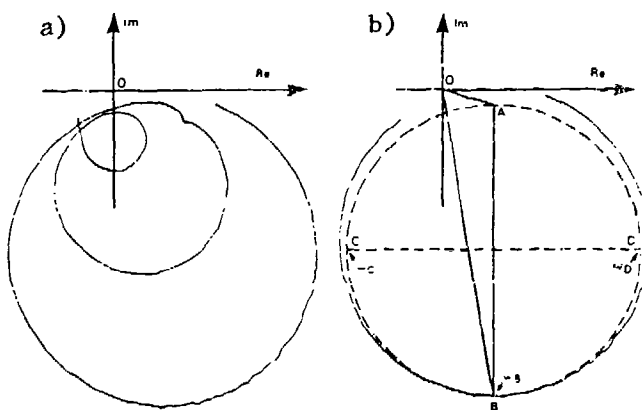


Figure 11.22 Nyquist Plot Analysis

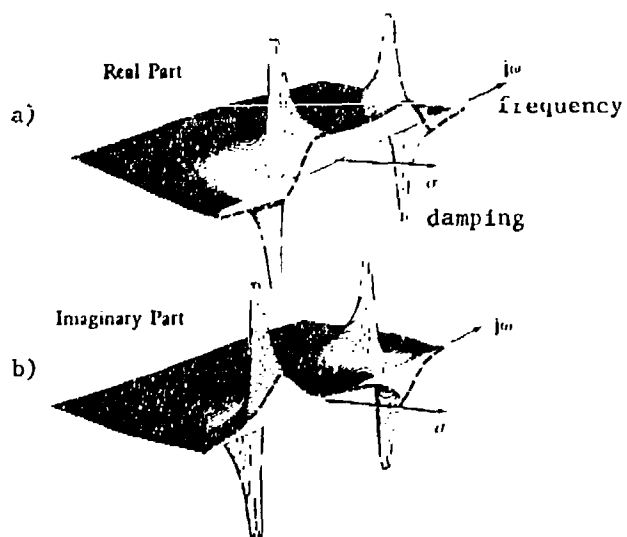


Figure 11.23 S-Plane Representations (SDOF)

and is plotted in Figure 11.23a and b where only negative values of  $\sigma$  (damping axis) is shown. Note in the figure that the dashed line is the frequency response function and the surface represents the transfer function.

For a continuous function the Laplace transformation is defined as

$$x(s) = \mathcal{L}x(t) = \int_0^{\infty} e^{-st} x(t) dt \quad (11.68)$$

The transformation of a transfer function can be cast in partial fraction form in which the roots of the denominator terms are called poles and the roots of the numerator terms are zeros. For example

$$H(s) = \frac{2(s+1)(s-2)}{(s+3)(s+1+j)(s+1-j)} \quad (11.69)$$

For the purpose here only the poles are of interest and these are the peaks of Figures 11.23. The poles and zeros can be shown as in Figure 11.24 in which a pole-zero analysis can be performed. For the purposes here this need only involve the following identities.

$$\zeta = \cos \beta = \sigma / \omega_n \quad (11.70)$$

and  $\omega_n$  is equal to the distance from the origin to the pole or

$$\omega_n = \sigma / \cos \beta = \omega_d / \sin \beta \quad (11.71)$$

Some modal analysis techniques (particularly those that utilize transfer functions) operate on frequency response data as a Laplace transform by assuming that the structural damping is negligible and setting  $\sigma = 0$  on equation 11.66. This just leaves amplitude versus frequency, as has been dealt with in previous sections of this chapter.

### 11.3.11 BODE PLOTS

If the real and imaginary parts of the frequency response, like that of the s-plane definition (Figure 11.24), can be replotted as magnitude and phase, where phase ( $\phi$ ) is

$$\phi = \tan^{-1} \omega / \sigma \quad (11.72)$$

and magnitude is

$$A(\omega)^2 = \text{Re}(\omega)^2 + \text{Im}(\omega)^2 \quad (11.73)$$

The result would appear as a Bode plot (Figure 11.25). As with Figure 11.23, the dashed line is the frequency response function and the surface represents the transfer function.

It is more typical to examine the positive axis alone and also to define the amplitude as a decibel (dB) value to accentuate peaks, as explained in Section 11.3.4. The result is as shown in Figure 11.26.

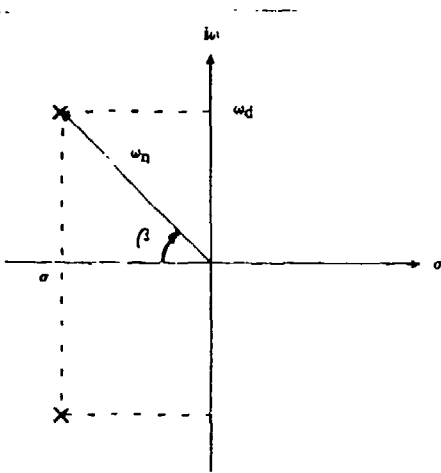


Figure 11.24 Example S-Plane (Root-Locus) Analysis (SDOF)

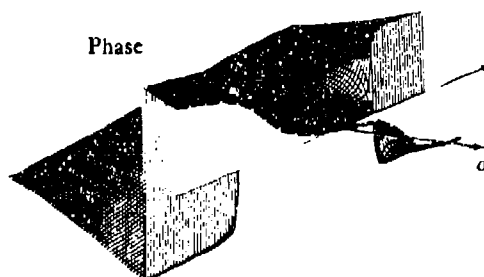
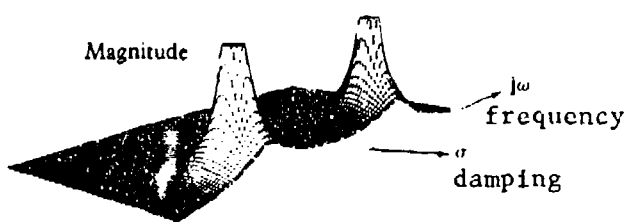


Figure 11.25 Magnitude and Phase Diagrams

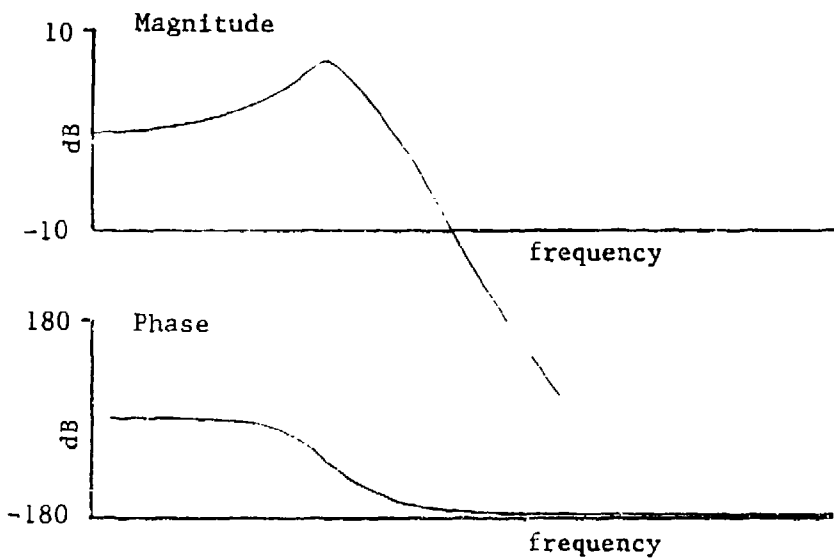


Figure 11.26 SDOF Bode Plot

sibility plot (or T-plot). The magnitude plot may show many peaks but a true resonant peak must occur at plus or minus 90° of phase. It is then an easy matter to cross-reference peaks in the magnitude plot to phase at the same frequency to verify resonance. This is particularly useful in examining the results of a frequency sweep during a ground vibration test (see Chapter 7.0).

### 11.3.12 Z-PLANE TRANSFORMATION

For test data analysis the Laplace transformation defined by equation 11.68 is impractical because there is seldom a continuous function defining the frequency response. The z-transform provides a discrete technique which is analogous to the s-plane. It is defined as

$$X(z) = \sum_{n=-\infty}^{\infty} x(n)z^{-n} \quad (11.74)$$

or the limits  $n = 0$  to  $\infty$  for a one-sided transformation. The inverse is

$$x(n) = [1/(2\pi j)] \oint_c X(z)z^{n-1}dz \quad (11.75)$$

where

$$Z = e^{sT} \quad (11.76)$$

and where  $T$  is the sampling rate for the data. Clearly then,  $z$  has the characteristics of a sampled Laplace transformation.

The z-plane will look like Figure 11.27 where lines of constant  $\sigma$  in the s-plane map into circles of radius  $e^{\sigma T}$ , and lines of constant  $\omega$  become radial rays at an angle  $\omega T$  and a constant  $\zeta$  becomes a logarithmic spiral. For system analysis, the consideration of roots falling within the unit circle is important for stability (see Reference 3).

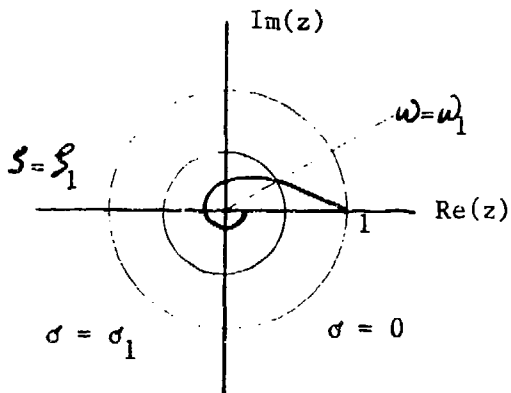


Figure 11.27 Example Z-Plane

### NOMENCLATURE

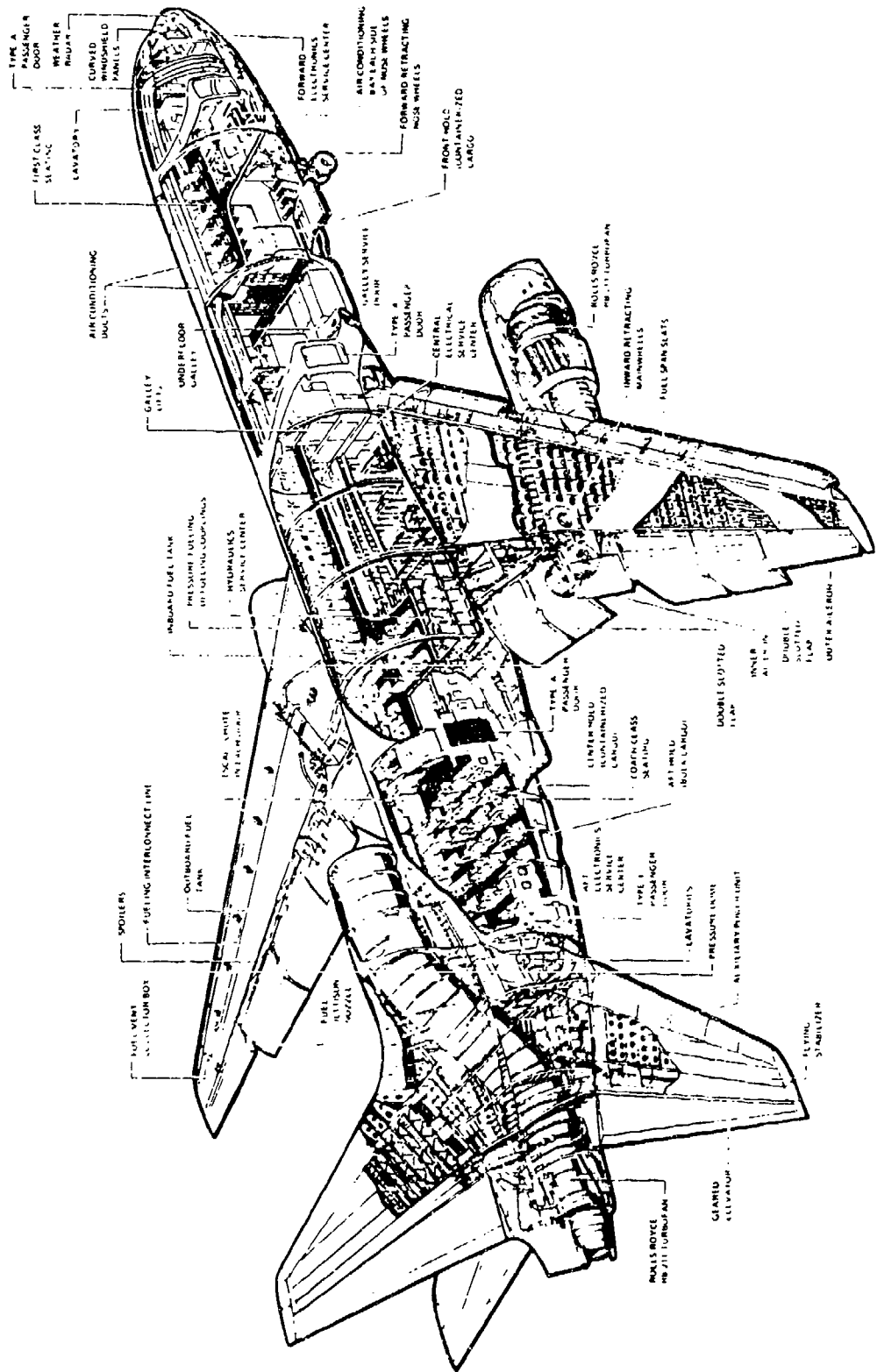
A	amplitude, constant
B	constant
C	zero offset, constant
CO	coincident part
CSD	cross spectral density
DET	determinant
DFT	Discrete Fourier Transformation
dB	decibel
dc	direct current (zero offset)
deg	degrees
dt	derivative with respect to time
e	exponential constant
F	Fourier transformation
FFT	fast Fourier transformatior
FRF	frequency response function
f	frequency
f(t)	periodic function
G	structural or total system damping
GVT	ground vibration test
G <sub>xx</sub>	input auto spectrum (or output G <sub>yy</sub> )
g	acceleration due to gravity
H	transfer function
IFT	inverse Fourier transformation
Im	imaginary part
i	imaginary number
j	imaginary number
K	counter maximum value
k	counter, stiffness
M	maximum number of time shifts

MDOF	multiple degrees of freedom
m	correlation shift or lag number, mass
mag	magnitude
N	number of cycles
n	mode number
P	total number of data points
PSD	power spectral density
Q	quality factor
QUAD	quadrature part
R	residue
Re	real part
RMS	root mean squared
R <sub>r</sub>	residue
R <sub>xx</sub>	auto-correlation (also R <sub>yy</sub> )
R <sub>xy</sub>	cross-correlation (also R <sub>yx</sub> )
SDOF	single degree of freedom
S <sub>x</sub>	Fourier transformation of input (also S <sub>y</sub> for output)
s	Laplace variable
T	period
t	time (seconds)
X	output function
Y	input function
Δ	increment of change
β	angle
υ	coherence
ζ	damping ratio
w	frequency
π	pi
τ	integration variable, function of time
Φ <sub>xx</sub>	input power spectral density (also output O <sub>yy</sub> )
Φ <sub>xy</sub>	cross spectral density (also O <sub>yx</sub> )
σ	damping rate
φ	phase angle
∞	infinity
Σ	summation
ℒ	Laplace transformation
Subscripts	
d	damped
k	counter
i	matrix row counter
j	matrix column counter
M	multiple
max	maximum
N	with respect to Nth cycle
n	natural, with respect to mode n
o	with respect to first mode or cycle
1/2	with respect to half amplitude cycle
Superscript	
°	degrees
*	complex conjugate

## REFERENCES

1. *The Fundamentals of Modal Testing*, Application Note 243-3, Hewlett-Packard Company, 1986.

2. *Flutter Testing Techniques*, NASA SP-415, October 1975.
3. *Linear Control Theory, Analysis and Design*, J.J. D'Azo and C.H. Houpis, McGraw-Hill Book Co., 1981.
4. *Feedback and Control Systems*, Schaum's Outline, J.J. DiStefano, A.R. Stubberud and I.J. Williams, McGraw-Hill, 1967.
5. *MASSCOMP Array Processor Programming Manual*, John Sundman, Massachusetts Computer Corporation, 1985.
6. *Modal Testing: Theory and Practice*, D.J. Ewins, John Wiley and Sons Inc., 1984.
7. *Digital Time Series Analysis*, R.K. Otnes and L. Enochson, John Wiley and Sons, 1972.
8. *Understanding Vibration Measurements*, George F. Lang, Application Note 9, Rockland Scientific Corp., December 1978.
9. *Advanced Engineering Mathematics*, C. Ray Wylie, McGraw-Hill Book Company, New York, 1975.



Lockheed L-1011 Cutaway

# CHAPTER 12.0

## SIGNAL PROCESSING

### 12.1 INTRODUCTION

Structures testing most often uses digitized data. This refers to the time sampling of an analog, continuous voltage signal and recorded as binary numbers representing the signal's amplitude. The binary numbers are sequentially recorded for time reference. The digitizing processing can create errors or present limitations which must be understood in order to determine the validity of the data. Any data signal must be processed in some manner for presentation and this can lead to errors and general corruption. Some processing methods permit the data to be corrected and "smoothed" for easier analysis. This chapter will highlight some of the more common concepts and processing techniques currently employed in instrumentation data manipulation.

All of the information in this chapter is in simplified, summary form. Whole books have been written on this subject. For detailed work in this area, many worthy references are provided at the end of the chapter.

### 12.2 RESOLUTION

It is important to determine the required resolution of critical parameters during the planning for a test. The required frequency and damping resolutions should determine sampling and digitization parameters, not the other way around.

#### 12.2.1 FREQUENCY RESOLUTION

For a digitized block or frame of time history data will consist of  $N$  equally spaced samples. In most cases, this block is a base two number like 1024. When a Fourier transformation is performed, this number will be halved because at each frequency amplitude and phase information is present. A plot of amplitude alone from a block of 1024 points will have only 512 spectral lines (see Section 11.3.1). The bandwidth (BW) is then represented by this  $N/2$  data block. The sampling rate (SR) must be at least twice the maximum frequency that can be resolved, per Shannon's Sampling Theorem, or

$$f_{\max} = SR/2 \quad (12.1)$$

or

$$f_{\max} = (N/2).T \quad (12.2)$$

where  $T$  is the period of the time record. In practice, the sampling rate is typically five or more times the maximum frequency of interest for the purpose of practical frequency resolution for modal analysis. Figure 12.1 illustrates how at least five data points are necessary to identify a mode (full cycle) with any certainty in the time domain as well as in the frequency domain (modal peak).

**Rayleigh's Criterion** states that the lowest frequency resolution or the minimum resolvable frequency obtainable is inversely proportional to the sample period,

$$F_{\min} = \Delta f = 1/T \quad (12.3)$$

or, using other identities associated with a frequency domain analysis

$$\Delta f = SR/N \quad (12.4)$$

For a **baseband** analysis, one in which the lower frequency of the bandwidth is zero, the BW would become  $f_{\max}$ , the maximum frequency resolution obtainable would be

$$\Delta f = BW/(N/2) \quad (12.5)$$

So, to analyze up to the maximum desired frequency requires that the SR increase. However, this is detrimental to frequency resolution in the frequency domain unless the block size (N) is not also increased.

### **12.2.2 DAMPING RESOLUTION**

The analysis of damping with the half power method (see Section 11.3.3) has a practical minimum damping that can be resolved. The worst case half power analysis using the best positioning of the spectral lines is shown in Figure 12.2. From this it can be concluded that

$$G_{\min} = \Delta f/f \quad (12.6)$$

where  $f$  is the center frequency and damping ( $G$ ) is defined in Chapter 4.0, or using relationships that have already been established

$$G_{\min} = SR/fN \quad (12.7)$$

So, an increase in block size alone will increase damping resolution, but an increase in SR will decrease resolution. Also, lower frequencies will have lower damping resolution than higher frequencies for the same processing parameters. Although the theoretical  $G_{\min}$  can be obtained with only three spectral lines included in the **spectral lobe** as shown in Figure 12.2, experience has shown that at least five spectral lines (like Figure 12.3) with at least three above the half-power line (see Section 11.3.3) are necessary in the lobe to get a reliable estimation of damping. So, twice the  $G_{\min}$  of equation 12.7 should probably be used in reality.

### **12.2.3 AMPLITUDE RESOLUTION**

If the frequency of a response is not a multiple of  $\Delta f$  then a spectral line representing the amplitude of the mode will fall between two lines which are actually produced in the frequency domain plot, as suggested by Figure 12.3. The amplitude would only be partially represented by the two adjacent spectral line. Only an increase in frequency resolution can reduce this problem. Section 12.3.1 discusses an error source that can further reduce amplitude resolution.

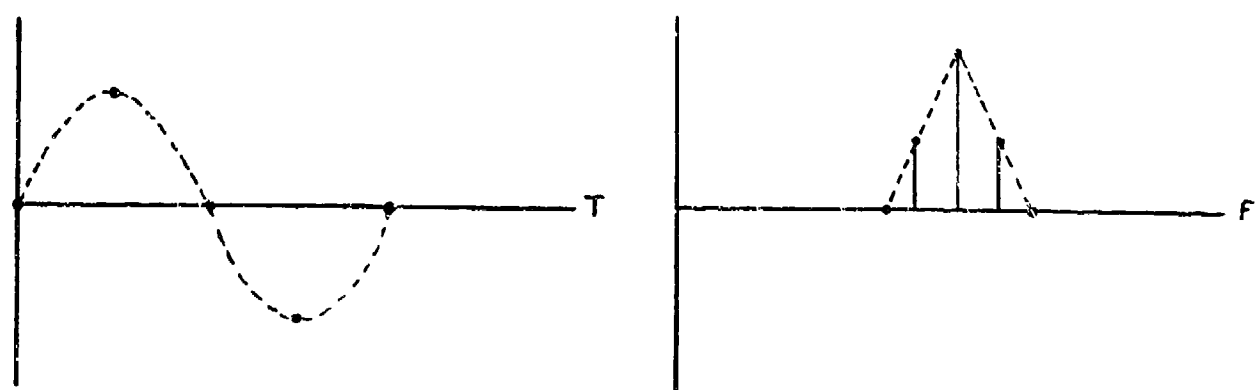


Figure 12.1 Points Required to Define a Mode

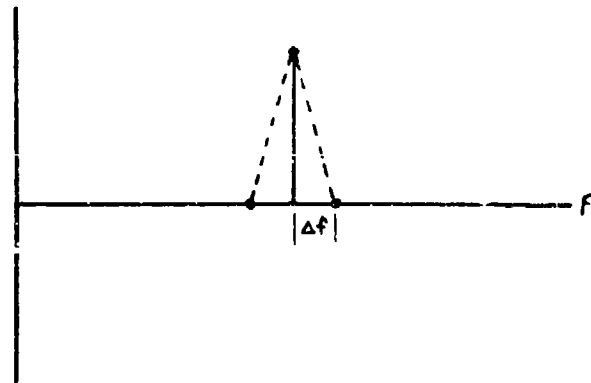


Figure 12.2 Illustration of Minimum Damping Resolution

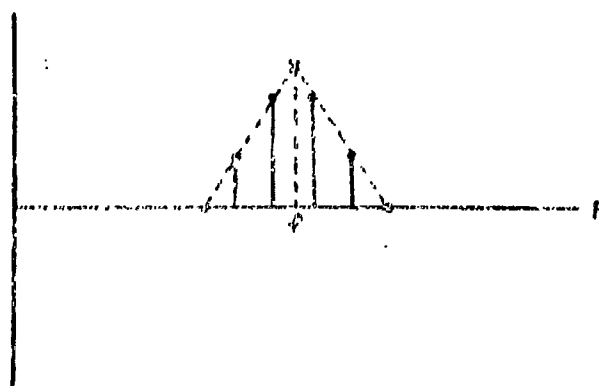


Figure 12.3 Illustration of Worst-Case Amplitude Error

#### **12.2.4 RANGING**

The sensitivity of recording or analysis equipment should be set so that the anticipated signal level is about half the setting chosen. This is termed **half-ranging** and ensures that the data is not **under-ranged** or **over-ranged**. Over-ranging can lead to **clipping** of the data where the maximum values measured are simply not recorded and are cut-off at the maximum sensitivity level. Under-ranging can produce noisy data with poor frequency response results because the full dynamic range of the equipment is not be utilized.

### **12.3 ERROR**

A total data error of five percent is considered good for flight test data. A smart test engineer will attempt to quantize the accuracy of data by considering resolution, errors, and effects of processing. This section will provide some basis for assessing the quality of the data in the presence of the multiple errors produced in flight testing.

#### **12.3.1 QUANTIZATION**

The resolution of a signal amplitude represented by a binary word depends upon how many bits are used (see Section 10.7.3). A 12 bit word would have greater amplitude resolution than a 10 bit word. This is a fundamental limitation of the analog-to-digital converter (ADC) equipment and establishes one element of the error band for the data. The actual error is

$$E = \pm 0.5(U_r/2^M) \quad (12.8)$$

where  $U_r$  is the maximum range for the engineering unit that is encompassed by the signal voltage range, and  $M$  is the number of bits in the binary word. So, if the maximum range is 100 g's with a word of 10 bits, the quantization error is 0.05 g's.

#### **12.3.2 ALIASING**

If frequency components greater than one half of the sampling frequency (the Nyquist or "folding" frequency,  $f_N$ ) are recorded (recall Shannon's Sampling Theorem), a significant frequency or amplitude error is possible. A frequency higher than signal  $f_N$  may be misinterpreted at a lower frequency or even as zero frequency because of the relationship between sampling rate and the period of the signal. Figure 12.4 shows that for a mode at exactly the sampling frequency,  $f_s$ , a false response is shown at zero Hertz in the frequency domain. Sampling at higher frequencies has the potential for misrepresenting a waveform as a lower frequency as the bottom plot in 12.4 indicates. Aliasing is then a folding back of higher frequency components into the frequency range of interest. The practical result is a response at less than the true frequency of a mode beyond the Nyquist frequency, thus allowing a misinterpretation of the data. Figure 12.5 shows a way of determining the potential aliased sources for a suspect response. The response at  $2/3f_N$  could be folded down from the crossings of the diagonal lines, or  $4/3f_N$ ,  $8/3f_N$ ,  $10/3f_N$ , etc. Examining ground vibration or modal analysis data for a mode at these frequencies can provide insight into the source of a suspicious response.

The simplest solution to the aliasing problem is to analog filter out (low pass, see Section 12.4.8) all of the frequency content above one half the sampling rate prior to the ADC. If the ADC is aboard the test vehicle, the filter will also have to be on the vehicle. Because filters have practical limitations on their ability to completely attenuate signals above the Nyquist frequency,

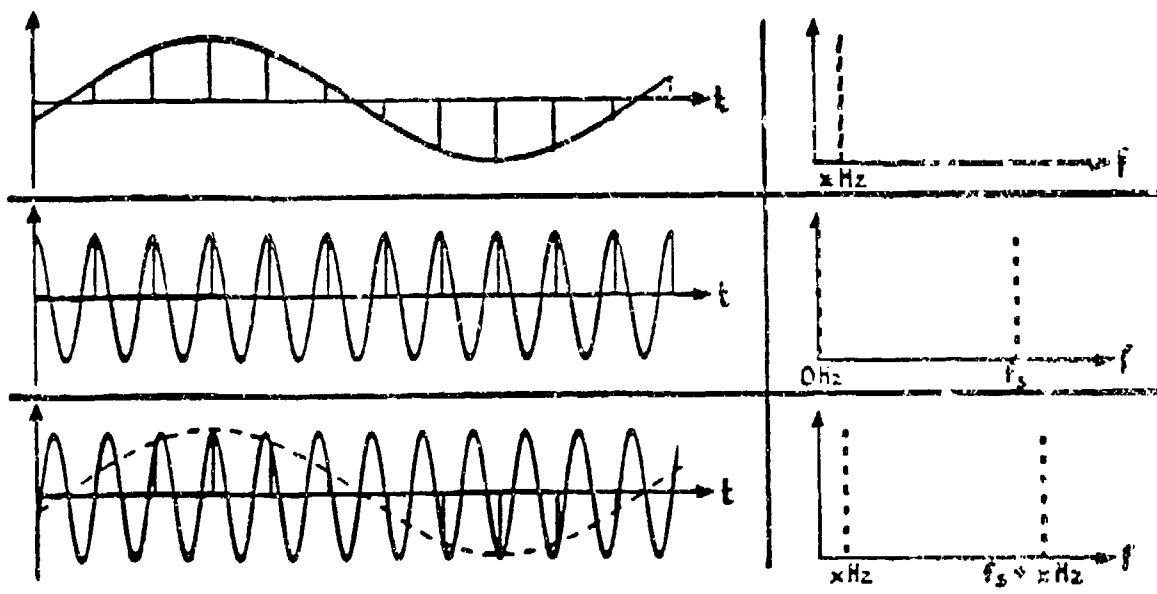


Figure 12.4 Examples of Aliasing Error

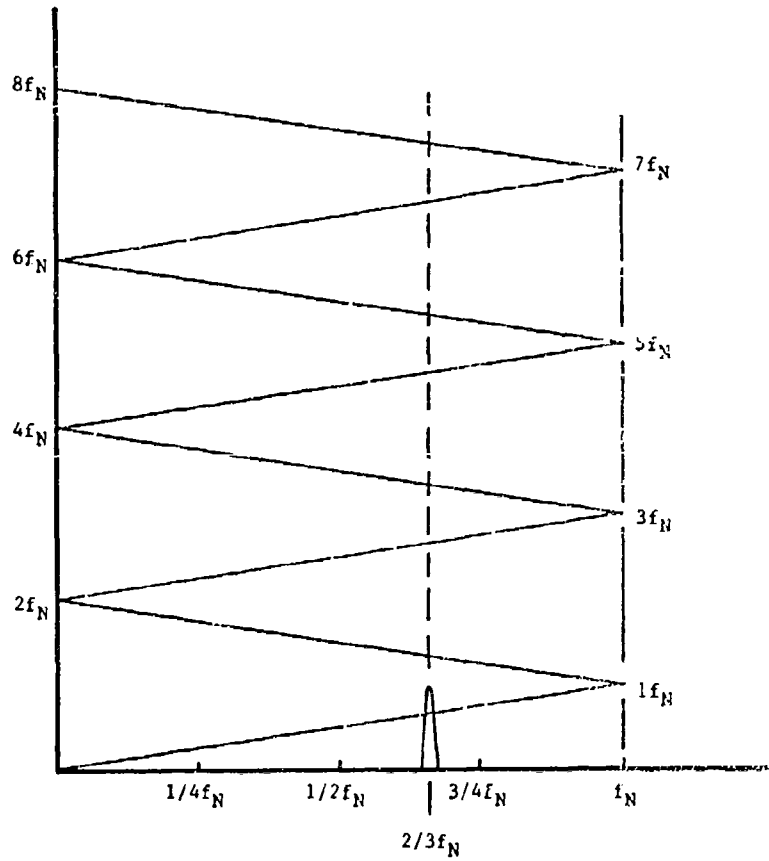


Figure 12.5 Aliasing Fold-Down Chart

the sample rate is generally set at greater than twice the filter cutoff frequency (see Section 12.4.8). A factor of 1.25 times the highest frequency of interest has been used successfully in the past.

### **12.3.3 LEAKAGE**

The assumptions entailed in the Fast Fourier Transformation (FFT, see Section 11.3.1) include the requirement for the analog signal to be periodic and with a period equal to that of the time sample, or periodic within the window being transformed and continuous throughout time. This is because the FFT must operate on a finite portion of the signal in a discrete fashion. For a signal which is not periodic within the frame, the FFT will be based on a distorted wave form as shown in Figure 12.6. The result is a smearing of modal energy which is referred to as leakage in the frequency domain and wrap around in the time domain. Energy from the non-periodic parts of the signal (the theoretical single mode spectral line) will "leak" into the periodic parts of the spectrum (adjacent spectral lines), or the response leaks out of the current data sample into the next.

Leakage is most readily seen as the expanding of the "skirt" on either side of the mode's peak, as shown in Figure 12.7, instead of a clean peak. This will produce an over-estimation of the damping. Amplitudes will also be truncated. Leakage is also seen as large dips in a coherence plot (see Section 11.3.6) in the vicinity of the modal peaks. Besides producing falsely high damping values, small signals close to the primary mode may be masked within the exaggerated skirt. One approach to reducing this error is to increase the frequency resolution. But, this is not always practical. Another method is windowing, covered in Section 12.4.1.

### **12.3.4 OTHER SOURCES OF ERROR**

There are many other sources of error that may need to be tracked if there is a great concern about accuracy in a reading. The transducers themselves will have measurement tolerances and drift that provides the first source of error to be accounted for. Bit drop-out refers to the failure of one bit in the ADC to be set. This is usually easily identified as a discrete band edge excursion of the data (see also Section 10.8). Drop-outs are particularly troublesome when transforming data to the frequency domain. Such a sharp data excursion is interpreted as an impulse response with infinite frequency content and will result in a broad band noise being superimposed on the frequency response plots. The ADC reference voltage may drift during the sample periods. Aperture error or clock jitter may result in the measured value not being assigned to the correct time. Digitizer error may cause a random setting of a bit. This is commonly seen as a narrow band of clipped noise apparently superimposed on the signal. One very common source of error or noise is the electrical noise occurring at harmonics of the power line frequency, usually 60 cycles.

An ever-present noise that contaminates structures flight test data are due to unknown excitations, the nonstationary nature of the flight environment, and necessary restrictions on the length of the test points. The myriad sources of line noise, transmission noise, and structural nonlinearities (rattles) will produce a low level clutter that will generally be at an average level called the noise floor. If the signal-to-noise (S/N) ratio is fairly low then it may become difficult to clearly discern the important data and analyze it properly. When this happens, more fundamental measures must be taken such as boosting the signal, reducing the transmission range, shielding instrumentation cables and sensors, and attempting to locate and eliminate component rattles in the test article. Since the sensitivity of an ADC is frequently set in advance of a test, it is possible that an important signal is below the noise floor of the processor. It is also

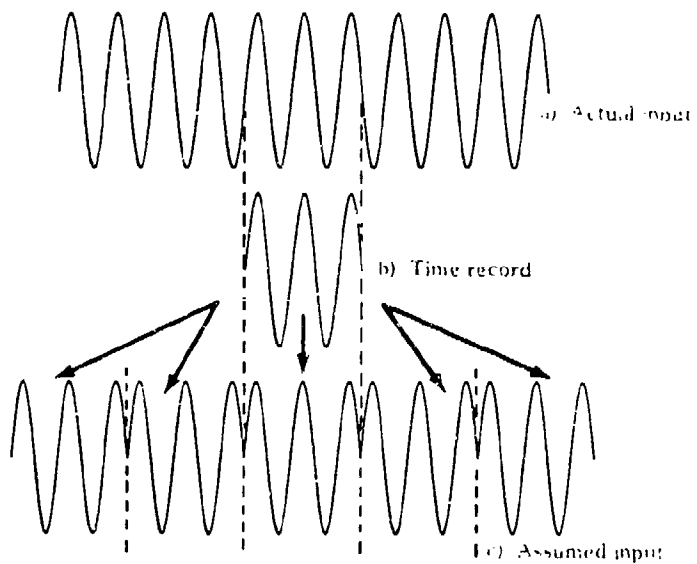


Figure 12.6 Distorted Waveform Producing Leakage

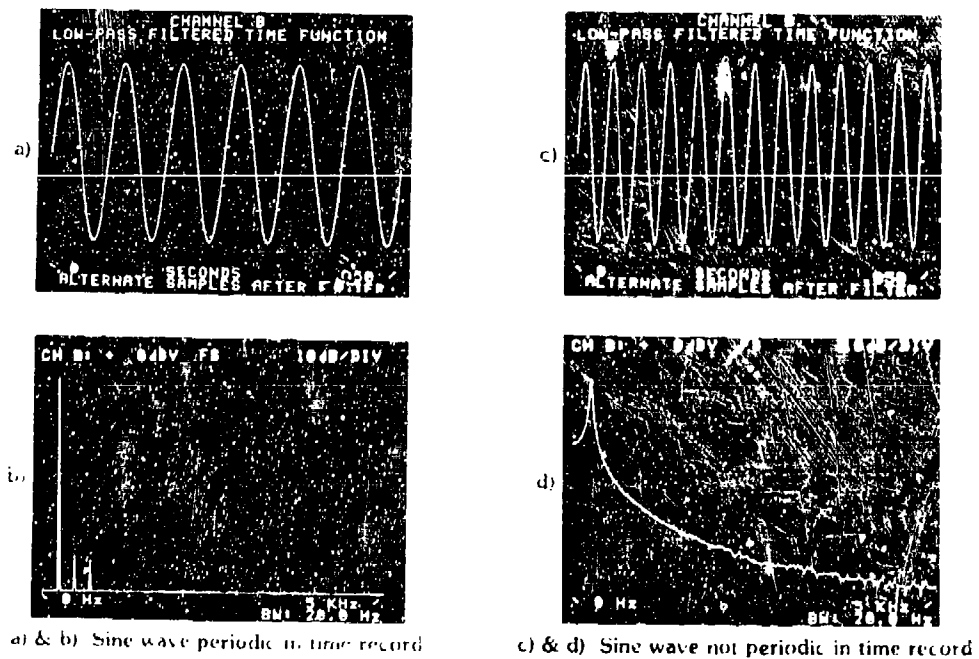


Figure 12.7 Illustration of Leakage Error

possible to set the sensitivity so high that a normal signal can cause an overload and be clipped so that its entire value is not reproduced. The sharp change in the response produced by clipping will also produce a broad band noise in the frequency domain as does drop-outs. An overload of the ADC may take several sampling increments to recover. This is usually evident as an apparent loss-of-signal (LOS).

A Fourier transform may produce a relatively large amplitude response at 0 Hz. This is the dc response, is the zero offset of the data in the time domain. Its amplitude may well cause more important responses to be scaled so small as to be difficult to analyze. For this reason the dc component is generally filtered prior to plotting. This can be done simply by subtracting the mean value of the entire data sample from each point in the sample.

## **12.4 PROCESSING TECHNIQUES**

The methods discussed in this section are used to smooth data, removing errors to facilitate data analysis. Caution must be taken to ensure that you know the consequences of employing a particular technique. A general warning is in order against using more than two processing methods on any single block of data. The data may look better but the results may be getting farther from the true parameter values being sought. Time and funds permitting, the same data should be processed separately using more than one technique and the results compared.

### **12.4.1 WINDOWING**

Multiplying the analog signal by a weighting function to force the response signal to become periodic within the window for the reduction of leakage (see Section 12.3.3) or the reduction of discontinuities at the boundaries of the sample is known as windowing. The result is an improvement in the frequency domain of amplitude and frequency resolution accuracy, and makes damping analysis easier. There are a number of different window functions, each with their own special applications. Windowing the data also creates problems and limitations that must be considered. Only the most common windows are discussed.

#### **12.4.1.1 HANNING WINDOW**

This window is a bell-shaped curve (Figure 12.8) that is typically used with undamped or slowly decaying signals. Its mathematical form is

$$w(t) = [1 - \cos(2\Delta t/N)]/2 \quad (12.9)$$

The result is to force the signal to zero at the window boundaries and retain the actual amplitude only at the center. In the frequency domain, this window does cause an artificial increase in the damping(s) because it tends to slightly reduce the amplitude of a resonant peak while also spreading out the skirt a little. The worse this error can get is  $0.5 \Delta f/f$ , however the error decreases as the frequency resolution increases. A true analytical correction for this artificial damping is beyond the scope of this text, but an adequate frequency resolution should reduce the error to a negligible level. The Hanning window gives very good frequency resolution but generally poor amplitude accuracy. The Hamming Window is similar to the Hanning Window except that the mathematical form of the function is slightly different. Applying these windows to a signal that is already periodic in the window will only unnecessarily distort the signal and produce misleading data. Random noise is a frequent subject for the Hanning window.

#### **12.4.1.2 FLAT TOP WINDOW**

Examining the Hanning window in the frequency domain (Figure 12.9) it can be seen that the passband shape (essentially a filter) has a relatively sharp peak. This will tend to produce large amplitude errors except very close to the peak. It can be seen in the figure that the flat top window has a flatter peak and so will produce less amplitude error for a broader range of frequencies. However, the skirts are wider and this reduces the ability to resolve small spectral components. Therefore, the flat top window gives very good amplitude accuracy at the expense of frequency resolution. This window (Figure 12.10) is generally applied to an input signal.

#### **12.4.1.3 UNIFORM WINDOW**

As shown in Figure 12.11, this window, also known as the rectangle and boxcar window, gives equal weighting to all portions of the signal so actually contributes nothing. It is analogous to isolating a sampling frame. It is generally used only with self-windowing signals (impulse, shock response, sine burst, chirps, and noise bursts inputs, see Section 7.8) which are already periodic within the sample when the analysis routine demands that some window function be defined.

#### **12.4.1.4 FORCE WINDOW**

This window is primarily used with data obtained during impact testing (see Section 7.8.2.1) and is shown in Figure 12.12. The force window modifies the input or force signal from the impactor transducer to ensure that it begins at unity and eliminates any unwanted signal (noise) before and after the input. Since the force window is essential a bandpass filter, it will not have the perfectly square form shown in the figure, but will have some slope associated with the rise and decay (see Section 12.4.7). Using the force window with a stationary signal like a continuous sine wave will result in large errors.

A variation of the force window is one that is similar to the uniform window but does not extend all the way to the beginning and end of the block. The effect is to eliminate a small portion of the initial and trailing portion of the block to reduce leakage effects. While this is usually only employed with data that is not adversely effected by the loss of this data (such as with turbulence excitation), occasionally the window is applied to a doubled block consisting of the initial sampled block appended to itself. Thus, the middle of the new block includes the beginning and end of the initial block and this data is not lost.

#### **12.4.1.5 EXPONENTIAL WINDOW**

This algorithm has the form

$$x = Ae^{-\alpha t} \quad (12.10)$$

where  $\alpha$  is the damping coefficient of the exponential curve to be used. The window modifies a decaying response to ensure a smooth decay to zero within the window, as shown in Figure 12.13. The time needed to reduce the amplitude by  $1/e$ , the time constant, should be about a quarter of the window length. The damping represented by the exponential window function is added to that of the signal and so will result in an apparent increase in damping of the convoluted waveform. This additional damping must be subtracted out for correct damping values. Problems are likely to arise if the added damping is significantly greater than the actual structural

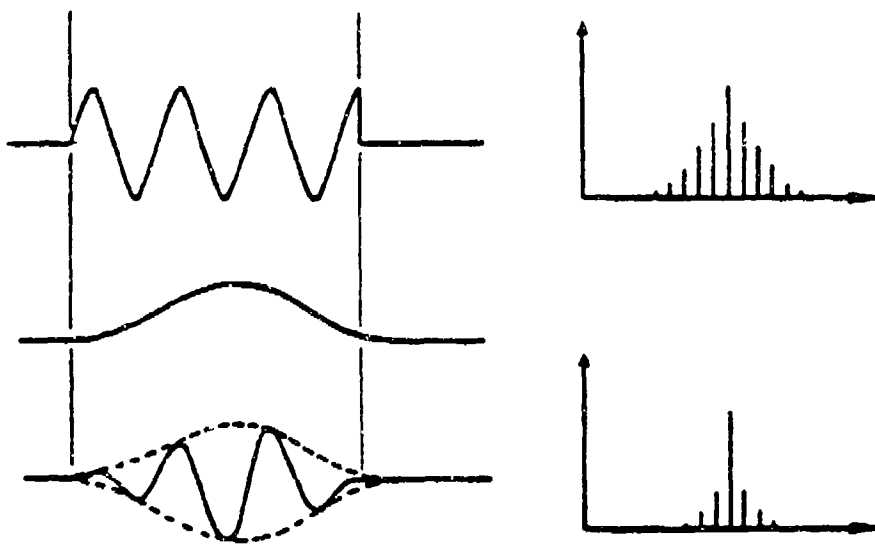


Figure 12.8 Application of Hanning Window

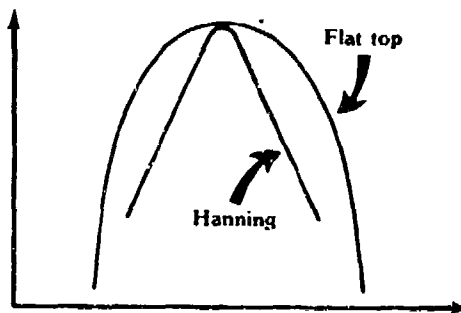


Figure 12.9 Comparison of Hanning and Flat Top Windows

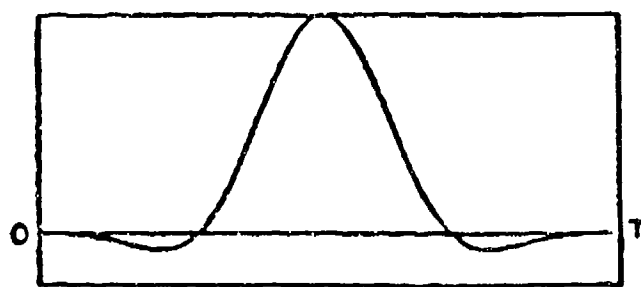


Figure 12.10 Flat Top Window

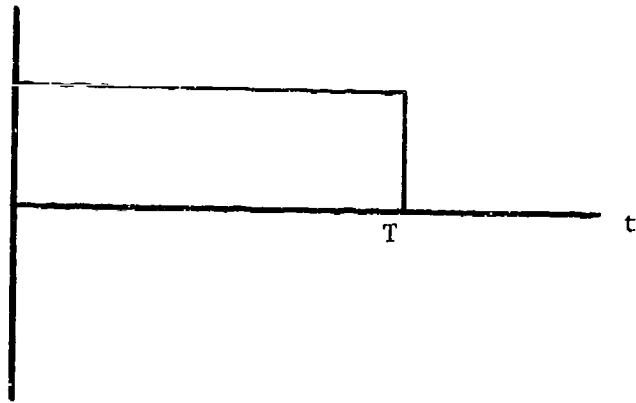


Figure 12.11 Uniform Window

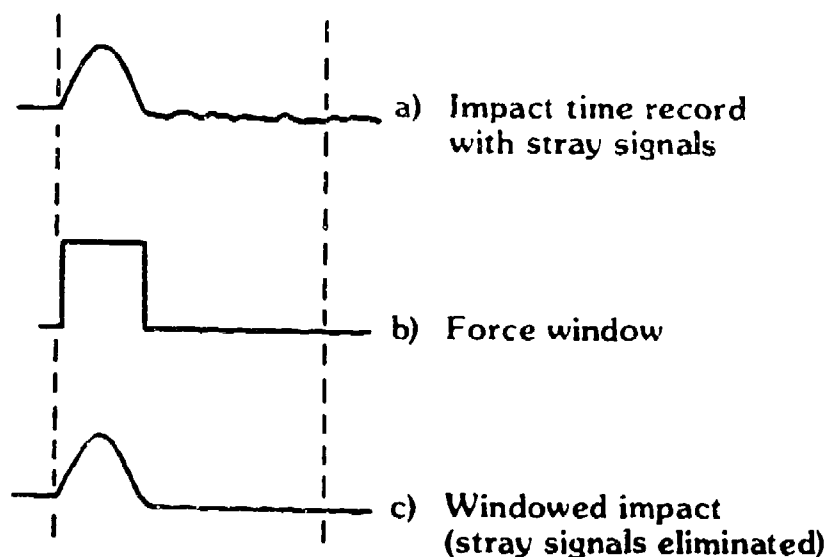


Figure 12.12 Application of Force Window

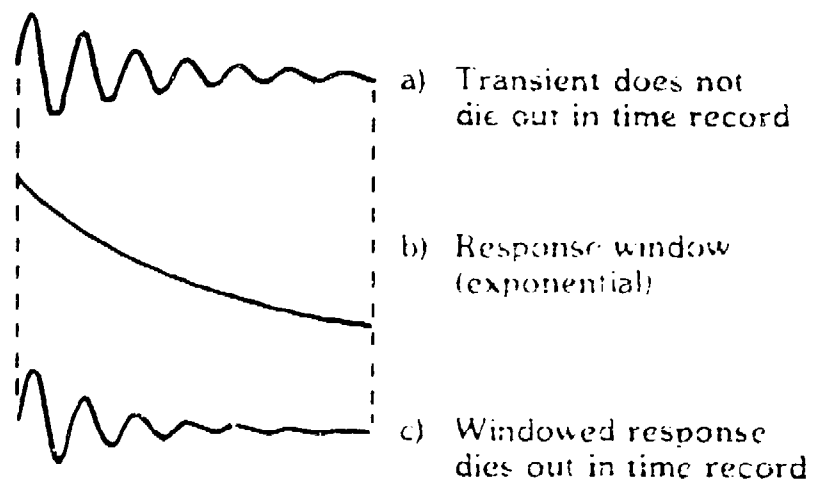


Figure 12.13 Application of Exponential Window

damping. The tendency to increase the damping can also result in the inability to discern closely spaced modes in the frequency domain. The setting of any "noise tail" on the response to zero by application of the window will be beneficial.

The exponential window can be used as a smoothing function even when applied to multiple degree of freedom time history data. A frequency response plot from such smoothed data will be much easier to analyze. It is essential that the dc (zero offset) component be removed before applying this window. As with the force window, using the exponential with a continuous signal will produce large errors.

#### **12.4.2 ENSEMBLE AVERAGING**

The averaging of time domain or frequency domain responses will tend to reduce the influence of nonlinearities, noise and distortion effects. This ensemble averaging is permitted as long as the nature of the input excitation does not vary. An example of this is the use with random excitation such as discussed in Section 11.2.4. The number of averages required or desired is strongly dependent upon the excitation and the test subject.

##### **12.4.2.1 RMS AVERAGING**

A root mean squared or RMS average (also known as **power averaging**) will only give a better estimate of the true signal plus the noise. Naturally, as with any averaging technique, the more averages that are taken the more accurate the final result. However, some practical limit can usually be established, after which further average has no apparent effect.

##### **12.4.2.2 LINEAR AVERAGING**

**Linear averaging** requires that a time domain trigger be used to start the sampling period. The triggering will usually be chosen as some signal level well above the noise floor. It ensures that the periodic part of the signal will always be the same in each time record while the noise will not, thus allowing the noise to average out.

##### **12.4.2.3 OVERLAP AVERAGING**

Instead of simply averaging consecutive data blocks, it is possible to use part of the last block in the next average. This overlapping of blocks allows many more averages from a given data sample and, when averaging with either of the techniques described in the previous two sections, produces a much better final result to facilitate analysis (see Figure 12.14). The triggering described in Section 12.4.2.2 will likely result in an overlap, although perhaps not with a uniform shift delta.

#### **12.4.3 ADDING AND SUBTRACTING SPECTRA**

Spectrums can be produced for a single response or for a sum or difference of responses. This later method may be useful in discerning close structural modes or to increase the resolution on like modes. For example, if the response signals from transducers located in like positions on the opposite wings are added then antisymmetric modes would not appear in the spectra because their opposite phases at identical frequency would cause them to cancel out. Conversely, symmetric modes would show an increase in magnitude. Subtracting the same signals would

because their opposite phases at identical frequency would cause them to cancel out. Conversely, symmetric modes would show an increase in magnitude. Subtracting the same signals would enforce antisymmetric modes but cause symmetric modes to cancel out. This simplifies both the identifying of modes with respect to their phase as well as separating the symmetric and antisymmetric modes that are often inseparable by other means.

#### **12.4.4 ZOOM TRANSFORM**

If an FFT of 0 to 60 Hz has been done with a data block of 1024 points this would be a frequency resolution of 0.12 Hz (see Section 12.2.1). The subject under test may be such that there is great modal density (close modes) in one part of this bandwidth that cannot be adequately discerned with this resolution. Simply increasing the block size to increase the resolution is not always practical from a computer capacity or a time perspective. In this case it is desirable to "zoom" on the dense region and perform the transformation again with the consequently increased frequency resolution (see Figure 12.15). If 1024 lines are used for a 10 to 15 Hz bandwidth, now the resolution is 0.01 Hz. The measurement must be taken again to obtain more points in the region of interest.

This zoom procedure has also been called Band Selectable Fourier Analysis (BSFA) or simply Band Selectable Analysis (BSA) and is only useful when the data can be taken again with the new bandwidth. Recorded data has generally already been sampled and digitized for a specific block size. In these cases, only a magnification of the desired region is possible with no increase in resolution. An added benefit of zooming is the reduction of leakage effects and broad band (white or impulsive) signal components. Data acquisition time may also increase.

#### **12.4.5 ZERO INSERTION**

Inserting zero amplitude data points at the end of the time domain data block allows an increase in the block size (sampling period) without increasing the sample rate and without sampling the data again. This has the effect of increasing the frequency resolution and the damping resolution (more points in the frequency domain, see Section 12.2) without affecting the validity of the frequency domain data. Doubling the block size with zero insertion will double the frequency and damping resolution. Inserting the zeros in the frequency domain to artificially increase the block size and then transforming back to the time domain has the effect of increasing the sample rate (time resolution, more points in the time domain) which reduces the frequency and damping resolution. It is important that the insertion be made at a point where the real data is approximately zero itself. Otherwise, the sharp discontinuity in the data will be seen as a broad band noise superimposed on the frequency response plot (see Section 12.3.4).

#### **12.4.6 DECIMATION**

This is the elimination of a set number of equally distributed time domain data points from the data record. An example would be removing every other point, or reducing a block from 1024 to 512. For this example, it has the effect of halving the sample rate and consequently reducing the maximum frequency that can be resolved. However, it also results in a smaller frequency resolution and an improvement in the damping resolution in the frequency domain (see Section 12.2). An essential precaution is to apply an anti-aliasing filter at about half the new sample rate before decimating.

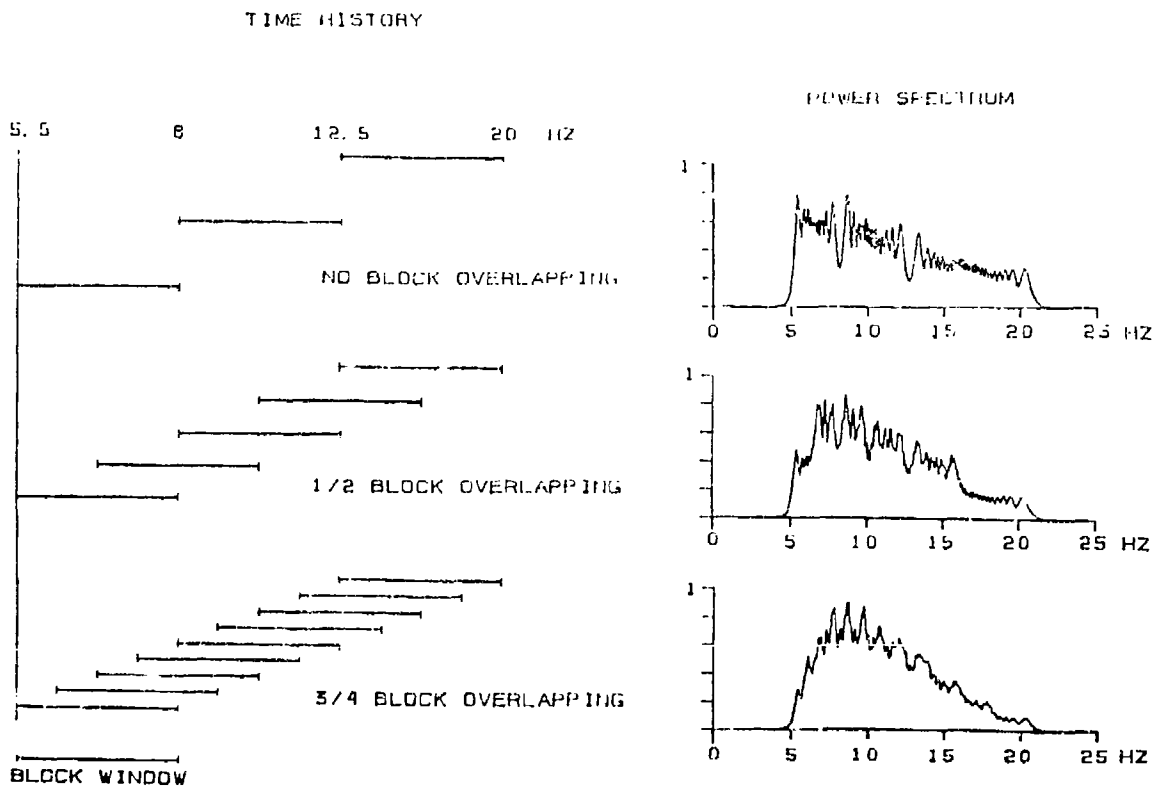


Figure 12.14 Illustration of Overlap Averaging and Result

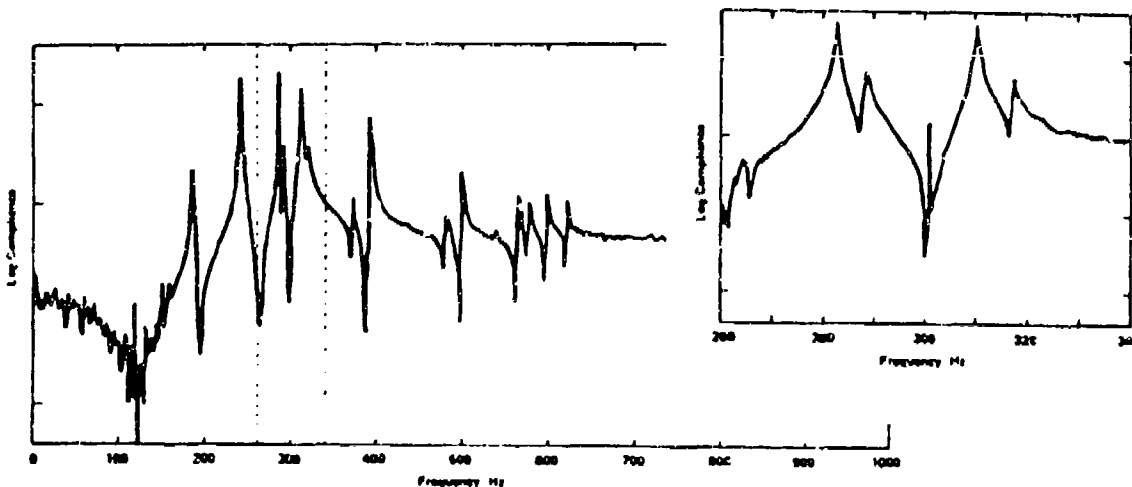


Figure 12.15 Example of Zoom Transform Application

#### **12.4.7 CUT-OFF**

Similar to the force window, this is simply setting the data points within the time domain block beyond a designated cut-off to zero. It is used where a signal of interest has clearly ceased (the structure has damped out, for example) and only noise remains. Otherwise, a sharp discontinuity in the data will result with the consequences discussed in the Section 12.4.5 if the cut-off is not set at a point where the data is naturally zero, or nearly so. Removing this noise will provide a much improved frequency domain plot or improve a time domain curve fit.

#### **12.4.8 FILTERING**

Filters are either analog or digital devices that only allow a specified frequency range of signals to pass. A **high pass filter** only pass signals above a certain level and **low pass filters** only pass those below a certain frequency. In combination, these are called **bandpass filters**. Filters permit undesired parts of a signal to be eliminated to prevent errors, to eliminate noise, or to permit a more practical scaling of the presented data.

Design limitations do not permit the realization of perfect filters where the signal drops to zero instantly at the desired frequency. Instead, there is a decay of the signal, called **roll-off**. This roll-off will begin before the frequency set as the cutoff to ensure that the signal is significantly attenuated at the required frequency. If a true signal amplitude is required up to the cutoff then the filter should be set slightly higher than this frequency. How quickly the roll-off occurs varies from one type of filter to the next, and may be very important to a certain application. A rapid roll-off or sharp "skirts" are generally desired. Digital filters will usually provide better characteristics than analog filters, but the latter are often necessary for such uses as anti-aliasing filters which is done prior to digitization.

Figure 12.16 illustrates several of the terms frequently used when discussing filters commonly used in structures tests. Here,  $B$  is the **cutoff frequency** and  $R$  is the **rejection frequency**. Other characteristics that must be considered in the choice of filters are **ripple power** (small oscillation in the passband), **sidelobe power** (caused by amplitude modulation), and **noise bandwidth**. Filters are rated by dB/octave to indicate how quickly they roll-off. For example, one may wish the amplitude to be reduced by one half in one octave or 3 dB/octave. A digital filter can be set to pass whatever frequency range is required by the application. For analog filters, a series or bank of narrow bandpass filters are needed if a broad spectrum is to be covered selectively (see Figure 12.17). Another type of filter passes just a narrow band but can be swept across a broad spectrum as an alternate way to provide a frequency domain plot without an actual transformation. This is called a **tracking filter**. Examples of how filters are used are presented elsewhere in this chapter.

Filters may be used to remove all spectral components but for the region of interest in a frequency response plot, such as around one mode or a group of modes. The result can then be transformed back to the time domain (IFT, see Section 11.3.1), smoothed with a window such as with an exponential window, and transformed back to the frequency domain for final analysis. This is shown in Figure 11.13. Another example is isolating a mode(s) in the frequency domain, transform to the time domain for smoothing or analysis, and then subtract this mode(s) from the initial data. This eliminates all contributions from this mode(s) that may be overshadowing higher frequency but lower energy modes and allows these other modes to be more easily extracted and analyzed.

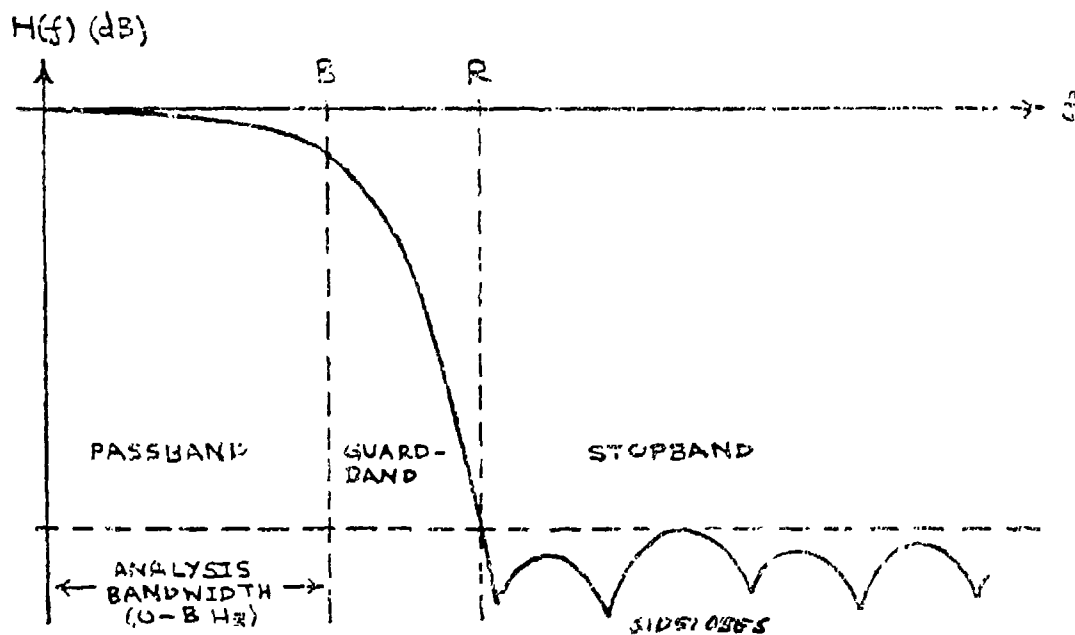


Figure 12.16 Filter Characteristics

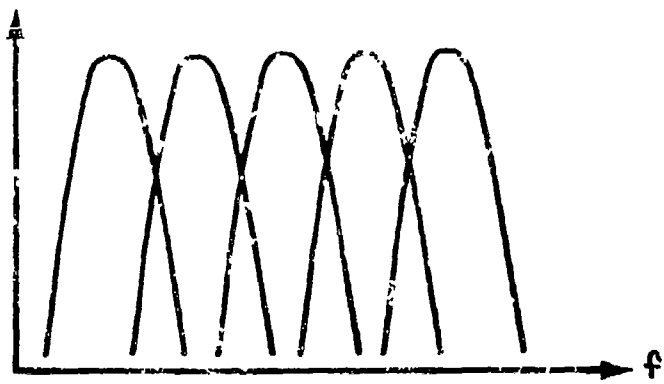


Figure 12.17 A Bank of Harmonic Passbands

One problem with filters which is annoying in frequency response analysis is called "ringing." This appears as a damped sinusoidal response resulting from an electronic resonance within the filter. Ringing has been observed to be excited by specific frequencies unique to each filter.

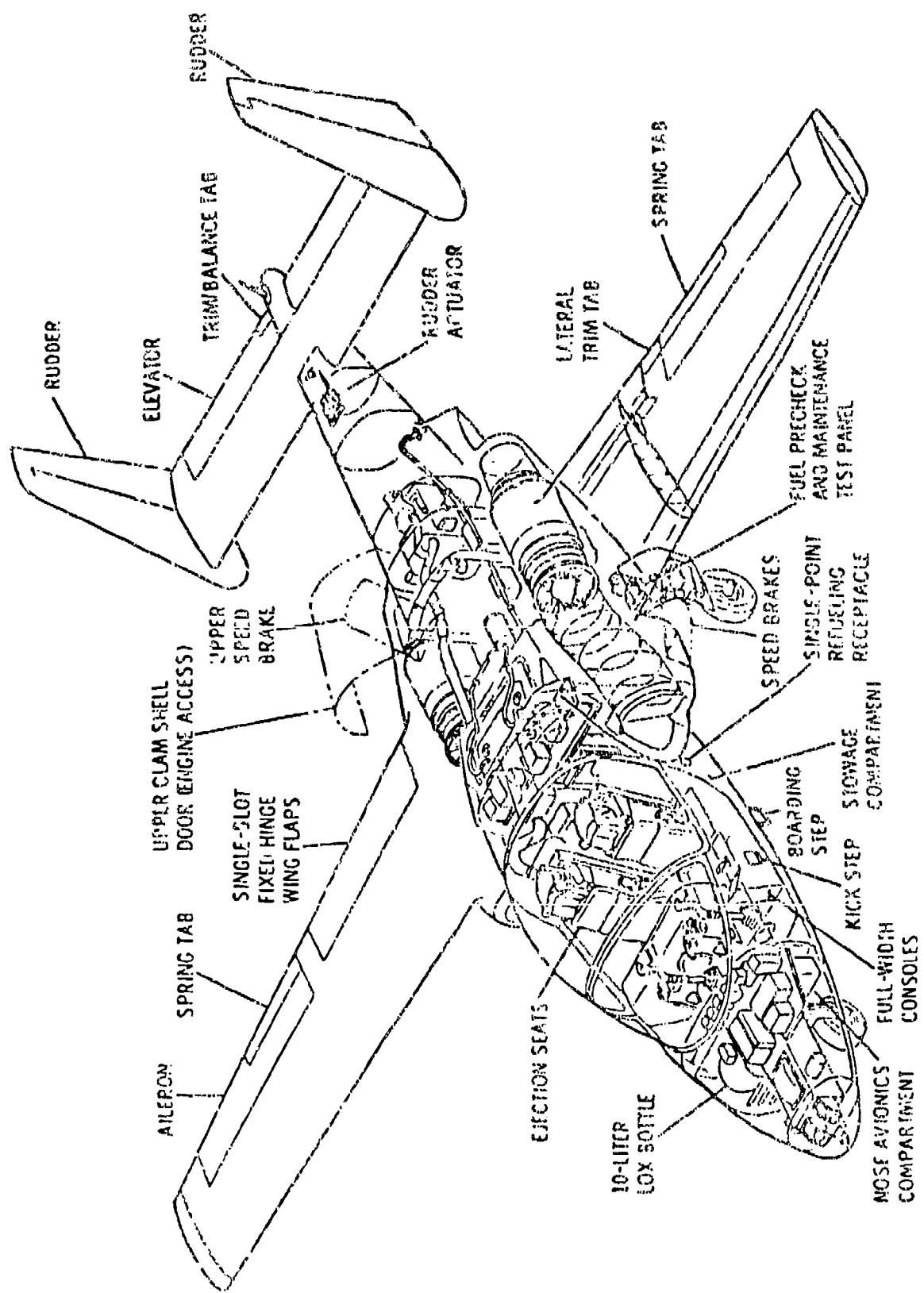
## NOMENCLATURE

A	amplitude
ADC	analog-to-digital converter
BSA	Band Selectable Analysis
BSFA	Band Selectable Fourier Analysis
BW	bandwidth
dB	decibel
dc	direct current
E	quantization error
e	exponential constant
FFT	fast Fourier transformation
f	frequency
G	total system damping
g	acceleration due to gravity
Hz	Hertz
IFT	inverse Fourier transformation
LOS	loss-of-signal
M	number of bits in a binary word
N	block size
RMS	root means square
S/N	signal-to-noise ratio
SR	sample rate
T	period of time record
t	time
U	engineering unit quantity
w	weighting function
x	function
$\Delta$	increment of change
$\alpha$	damping coefficient
Subscripts	
$\max$	maximum
$\min$	minimum
N	Nyquist
r	range
S	Sampling

## REFERENCES

1. Otnes, Robert K. and Enockson, Loren, *Digital Time Series Analysis*, John Wiley & Sons, New York, New York, 1972.
2. Haidl, G. and Steininger M., *Excitation and Analysis Techniques for Flight Flutter Tests*, AGARD Report No. 672, AGARD, London, England, January 1979.
3. Rabiner, Lawrence R. and Gold, Bernard, *Theory and Application of Digital Signal Processing*, Prentice-Hall Incorporated, Englewood Cliffs, New Jersey, 1975.

4. *The Fundamentals of Signal Analysis*, Application Note 243, Hewlett-Packard Company, Palo Alto, California, 1985



T-46A Aircraft

# CHAPTER 13.0

## FLIGHT TESTING AT AFFTC

### 13.1 INTRODUCTION

In order to conduct and support flutter, loads, aeroservoelastic, vibration and acoustics tests, the AFFTC relies upon the structural engineers of the 6510 Test Wing for engineering expertise in airframe structures technology. The Test Wing ensures the availability of a lead structures engineer and any number of additional engineers needed to support an individual test project. This structures team should be involved early in the test planning phase. Responsibilities for the conduct of the test and the reporting of results is set in this phase. The charter of the team requires that its engineers ensure the safe and effective conduct of all structures tests, whether conducted by the contractor, the Air Force, or as a joint effort, if any AFFTC resources are to be used. In the case of certifying aircraft modifications or store configurations, the structures engineers will ensure that the proper decision regarding the need for flight testing has been made, and will sign off on those tests where additional flight testing is not required.

The flight testing of modern aircraft is a lengthy and expensive process that requires careful planning and teamwork to achieve optimum results as efficiently as possible. This chapter will outline the process by which this is done at the AFFTC. While often slow and frustrating, and certainly far from perfect, this process has evolved over decades of experience to ensure smart and safe flight testing.

### 13.2 RESPONSIBLE ORGANIZATIONS

The 6510 Test Wing is an organization within the AFFTC, which is in turn an organization within Air Force Systems Command, a major command of the USAF. The mission of the AFFTC is to conduct and support tests of manned and unmanned aerospace vehicles. As a part of this AFFTC responsibility, flutter and loads testing normally occurs prior to other tests on a new airframe since flutter can have drastic consequences, and the intent is to avoid flutter while performing other less hazardous tests. Other structures tests are then performed. When substantial modifications are made to an airframe already in service, or if new configurations of stores are to be flown, AFFTC may have the responsibility for testing and certifying these modifications or configurations.

Normally, all new aircraft or missiles will be tested for flutter, loads, and other aeroelastic phenomena. Whether the testing is done by the contractor with Air Force support or by the Air Force with contractor support is normally decided by the System Program Office (SPO). Research programs are occasionally managed by an Advanced Development Program Office (ADPO). These organization, normally based at Wright-Patterson AFB, Ohio for projects involving airframes, has the ultimate acquisition and development authority over the project. The Program Office pays the bills. AFFTC is responsible to them. However, the AFFTC has veto authority over any decisions involving aircraft that will be tested using AFFTC resources (the range, crews, etc.). Therefore, if the Program Office decides to test a new configuration for performance, handling, etc., the AFFTC must certify ("sign off") that the aircraft is safe to fly without additional structures testing in the new configuration. Specifically for stores, the 3246th Test Wing at Eglin AFB will also play a role in this decision.

The organization which will act as the lead agency for the conduct of the test is termed the **Responsible Test Organization (RTO)**. The Test Wing may establish a **Combined Test Force (CTF)** which consists of both USAF and contractor personnel working jointly toward program success.

### **13.3 AIRCRAFT MODIFICATIONS**

The structures engineer may be asked to review modification documentation to ensure that all relevant analysis has been satisfactorily completed on any aircraft modifications (mods). Temporary modifications for the purpose of a development test effort are termed "Class II" and extremely superficial modifications are "Class III" mods. A **Class I** mod involves a permanent change to the aircraft fleet. Documentation should include drawings plus a statics and dynamics analysis. The analysis must include the flight environment stated in military specifications, particularly MIL-A-8861 and MIL-A-8870.

Any change to a military aircraft requires a considerable amount of documentation and coordination for approval. The electrical load, electromagnetic compatibility, and weight-and-balance impact must be reviewed and documented. Each mod must be approved by the **Deputy Commander for Maintenance (DCM)** prior to and after installation. This is referred to as the **Configuration Control Board (CCB)**. Complex installations involving many aircraft systems may require ground testing to ensure proper and safe functioning prior to flight. Dedicated flight tests may also be mandatory. The Class II modification office under the DCM is a vital source of information and assistance in this area.

Most changes in electrical equipment on an aircraft, including instrumentation changes, require an **electromagnetic compatibility/electromagnetic interference (EMC/EMI)** ground test. This is to verify that the normal aircraft electrical systems do not adversely affect the new equipment, and that the new equipment does not affect the pre-existing equipment. An EMC/EMI problem can be analogous to turning on a newly installed car radio and finding that the windshield wipers automatically begin to operate at the same time.

#### **13.3.1 ANALYSIS**

Modifications or onboard equipment designed at AFFTC are often analyzed for the effects of flight loads by the structures team using dedicated computer software. Dynamics analysis and flutter analysis can also be done by the Branch but this has become rare in recent years because of the prohibitive time and manpower this would require. Generally, the team does not attempt to analyze the effects of the modification on the aircraft structure and aerodynamics since this would require detailed mathematical models of the aircraft. If this is deemed necessary then the original manufacturer or an independent contractor is generally hired to do the analysis with Air Force review.

#### **13.3.2 FLIGHT TESTS**

Flight tests of aircraft modifications will follow the general pattern of those outlined in this handbook. Testing will be reduced to concentrate on the mod and its effects on the rest of the aircraft. Load paths, stress concentrations, mass re-distributions, and down stream airflow effects should be considered in making this assessment. Instrumentation will concentrate on the modified structure but must include some measurands on the flight vehicle as a whole to see the effects of the mod throughout the machine. Testing may be waived entirely depending on the

nature of the mod and whether similar mods have been flown previously on a similar structure at similar flight conditions.

The modified structure and added articles (stores, pallets, etc.) must be specifically designed to withstand the load spectrum for taxi, landing, in-flight gusts, and maneuvering (both symmetric and asymmetric) scenarios. Any cuts to the pressure vessel must be thoroughly documented and analyzed. It is strongly advised that the test engineer contact the engineers at the aircraft depot and consult with them about material problem in the areas intended to be modified or at the normal load and maneuver conditions intended for operation. Certain inspections may be necessary to ensure that the aircraft structure is sound (particularly for an old aircraft) before testing is allowed to proceed. Flight testing normally consists of testing the aircraft to the flight manual limits of normal load (positive and negative), roll rate, and steady-heading sideslips. Strain gage instrumentation is advisable but not always necessary.

A flutter analysis is usually required for significant changes to structural stiffness or mass distribution. A flutter speed of at least 115 percent of red-line airspeed is mandatory unless a restricted flight envelope is accepted. Flight testing can consist of as little as approaching the red-line dynamic pressure and Mach conditions while performing control raps. Control surface positions and wing/en pannage tip accelerations should be monitored and a damping evaluation performed.

External protuberances can have a profound effect on internal acoustics, airframe buffet, airflow over critical surfaces, structural fatigue life, aircraft stability and control, plus stall speed and post-stall characteristics. Wind tunnel tests are common in assessing potential trouble areas. Tufting is advisable for initial flight testing to help visualize airflow disturbances. For serious situations it may be necessary to add acoustic instrumentation and pressure taps to assist in analysis. Common handling quality and approach to stall tests should also be done.

## **13.4 TEST PLANNING**

### **13.4.1 PRELIMINARY PLANNING**

It is best if the flight test engineer can be part of the initial design reviews prior to prototype construction or the test airframe modification. This provides the opportunity to understand the design philosophy and the analysis techniques used. Flight test experience gives the flight test engineer (FTE) insights that the design engineer may not have and FTE comments can be very helpful in avoiding difficulties later in the flight test phase. These design reviews are conducted at the contractor's plant and are termed the **Preliminary Design Review (PDR)** and the **Critical Design Review (CDR)**. Following the CDR, changes in the design become very difficult to initiate, such as additional instrumentation in the prototype, so that it becomes urgent for a structures FTE to be present at this important review.

Later, the Program Office will begin periodic reviews of the test plans, both by mail and in meetings. These meetings are generally called **Test Plan Working Groups (TPWGs)** or **Technical Interchange Meetings (TIMs)** and the structures FTE should attend those meetings touching on the field. This ensures that relevant issues are given the proper attention. The engineer must consider whether the plan is actually executable and will provide the necessary data to meet the test objectives. A broad picture of all the testing in the program (generally large projects), The RTO and required test resources will be described in the **Test and Evaluation Master Plan (TEMP)**. This document is prepared with inputs from all agencies involved with

the project and will be changed during the course of the program as required. When coming onto an already established project, becoming familiar with the TEMP should be an early priority.

#### **13.4.2 THE TEST PLAN**

The test matrix and instrumentation requirements are all included in the Test Plan. This document also contains procedures for conducting the test, **flight test techniques (FTTs)**, flight maneuvers, personnel, equipment requirements, and data requirements. The contents of this document are outlined in AFFTCR 80-1. The first portion of the test plan is the Test Objectives section which details the purpose(s) of the test. All of the subsequent sections contain information on procedures and requirements that will be necessary to accomplish the test.

The test engineer is advised to read test plans from prior projects to become familiar with test planning and the Test Plan format. The Test Plan should contain information on the number of personnel needed to conduct the test, their identity, and roles they will play. As a minimum, a strip chart operator for each critical strip chart, a computer operator, a test director, and an aircraft controller are required. All support equipment and aircraft modifications needed to support the test are also detailed in sections of those names. Finally, the amount and types of data (the Data Requirements) to be analyzed, the methods used to analyze them, and the responsible organizations are discussed.

The Test Plan may specify a control room layout that details locations of strip charts, personnel, and the data analysis computer. Each CTF is required by AFFTCR 55-23 to develop an Operating Instruction (OI) for control room procedures. The control room layout is designed to allow sufficient space for all strip chart and computer operators, and also to provide the structures test director access to all critical charts and to the computer.

#### **13.4.3 THE REVIEW CYCLE**

Once the Test Plan has been prepared, a **Technical Review Board (TRB)** is convened. The purpose of the TRB is to critique the test plan to ensure that the test objectives can be met following the procedures outlined, that the procedures can be accomplished, and that the requirements can be met.

Normally, when a structures type Test Plan is reviewed, the Wing Chief Engineer acts as board chairman. The Structural Dynamics Branch (DOES) chief (or anyone so assigned) is a board member as well as a Flight Dynamics Branch (DOEF) representative. A representative from the appropriate branch of Test Operations (bomber, fighter, etc.) is required to determine whether the maneuvers and test points called for are within the capability of the aircraft. These are the minimum board members.

Members of the CTF, if applicable, that attend the TRB often include the **CTF Unit Test Safety Officer (UTSO)**, the lead airframe engineer, the structures engineers working on the project and a higher level CTF manager to represent the CTF director. Sometimes the **Test Safety Office** representative may be invited in order to obtain background information for the succeeding Safety Review Board and to recommend changes to make the SRB go more smoothly. The contractor and Program Office involved may send a structures engineer.

The **Safety Review Board (SRB)** follows the TRB. One of the principle tasks of the SRB is to assign a risk level. The risk assessment is either low, medium, or high (hazardous) risk, based upon the maneuvers involved, the predicted behavior of the aircraft, and the proximity of

test points to the edge of the test envelope. The risk assessment will often be increased based upon the confidence (or lack of confidence) in the analytical model and ground tests results. Each hazard requires detailed examination and explanation of minimizing procedures in **Test Hazard Analysis (THA)** sheets which become part of the safety package that results from the SRB. The general safety approach (minimum altitudes, chase aircraft, abort criteria, etc.) is outlined in the AFSC Form 5028, Test Project Safety Review, and amended when necessitated by subsequent test plan changes by any number of Form 5028b's, which also becomes part of the safety review package. The principle purpose of the SRB is to assess a risk level, but the board may recommended changes to the test plan to minimize the risk. A very detailed outline of safety issues is contained in AFFTCR 127-3.

For a flutter test, the DOES and DOEFS representatives from the TRB normally function as SRB members as well as the Test Safety Office representative (chairman) and a Test Pilot School (TPS) representative. Lead structures engineers, the CTF UTSO, and contractor engineers normally attend also, but they are not board members.

After the SRB, the Commander of AFFTC is briefed regarding the program objectives and the risk assessment. The Test Safety Officer, CTF UTSO, lead structures engineer, or project pilot may together or one alone conduct the briefing. Contractor engineers may attend the briefings to the Commander if it is believed that they will have something to contribute. The path from test plan writing to TRB to SRB to the Commander's briefing is normally termed the "test approval cycle".

#### **13.4.4 FINAL PREPARATIONS**

During, or immediately following the test approval cycle, the **CTI Deputy Commander for Operations (DO)** will begin to schedule resources to support the test, with the leg work actually done by the responsible engineers. These will normally include a control room to conduct the test, needed strip charts, the data analysis computer, the aircraft and stores (if any), and any other support equipment needed. If a CTF is not involved, the structures engineer may need to perform these tasks.

When all of the data has been gathered to the satisfaction of the engineers involved, the program will be terminated and the aircraft, stores, and any other equipment needed for the test will be released for use on other programs.

### **13.5 CONDUCT OF THE TEST**

AFFTCR 55-23 contains a detailed guide to flight test conduct, but a brief overview is in order.

#### **13.5.1 PRE-FLIGHT BRIEFING**

Pre-flight briefings should be conducted to review the operating limitations safety considerations (the AFSC Form 5028 and any 5028b's) and, most importantly, the "flight cards". These are the cards that the pilots take along to guide them through the test mission. The pilot should understand completely the maneuvers to be flown, and the test point progression. The "chase" pilot, a pilot who will follow the test aircraft in the safety chase aircraft to identify emergencies (loose or detached test aircraft components, etc.), will be fully briefed either during the pre-flight briefing or immediately thereafter.

### **13.5.2 CONTROL ROOM OPERATIONS**

Each CTF is required by AFFTCR 55-23 to write an **Operating Instruction (OI)** defining all control room setups and procedures. A mock room setup should be conducted. All strip charts, computers, chairs, tables, headsets, etc., that will be used in the test should be in place to verify that a workable arrangement has been designed. Actually playing some data through the system to verify that the data recording and display systems are properly setup is essential.

During or following the mock setup, a ground check of the telemetry is made to ensure the operational status of all instrumentation devices, the telemetry system, antennas, TM encoders, decoders (for encrypted data), etc. All transducers should read their proper steady state values. The ranges for parameters on the strip charts should be checked and any changes made to allow easier readability and to allow accurate display of data.

Prior to the test, strip chart operators and computer operators should be trained in the proper use of the equipment. They must be briefed on the purpose of the test, test conduct, and their roles during the test. Responsible engineers will verify that any project computer software functions properly, and they will create directories, files, charts for recording run numbers, etc. prior to the test.

Control room operations should be well-defined and orderly to prevent confusion during the flight. A set of operating instructions should be created that will detail the roles of all test personnel, the criteria for test termination, and the procedures in the event of an emergency. All personnel involved directly with the test should be briefed on the contents of the instructions and given a copy to use as a reference.

### **13.6 TEST REPORTS**

Most structures programs will result in the production of a technical report which may be the responsibility of the Air Force lead structures engineer or the contractor. The technical report will contain details of the aircraft configuration, test instrumentation, test conduct, results, and conclusions based upon those results. Lower level efforts or preliminary results may be reported in a letter report or a **Preliminary Report of Results (PRR or "PR squared")**. The format for all AFFTC reports is contained in AFFTC-TIH-88-002 with other pertinent information regarding them found in AFR 80-14 (with AFSC and AFFTC supplements).

Following any structures project a **Lessons Learned** paper may be submitted by the lead engineer and approved by the DOES chief. The **Lessons Learned** paper should contain information about new techniques used to conduct the tests, old techniques that did not work, or possibly suggestions for better techniques. Problems encountered with particular data analysis methods should be discussed, and solutions presented. These **Lessons Learned** papers are designed to be read by lead engineers on other programs to learn from the mistakes or suggestions of others.

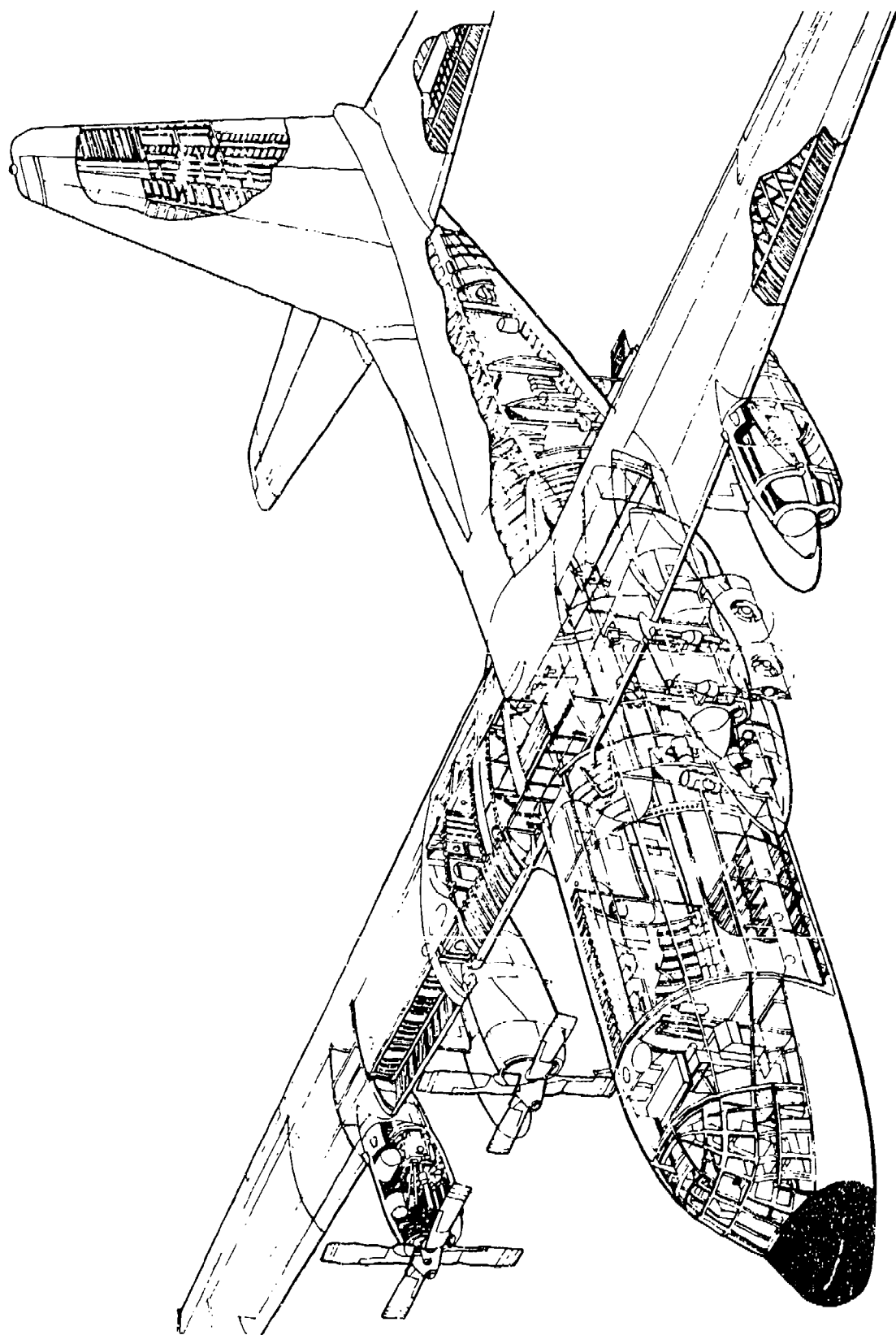
### **NOMENCLATURE**

ADPO	Advanced Development System Office
AFFTC	Air Force Flight Test Center
CCB	Configuration Control Board
CDR	Critical Design Review
CTF	Combined Test Force
DCM	Deputy Commander for Operations

DO	Deputy Commander for Operations
EMC/EMI	Electromagnetic Compatibility/Electromagnetic Interference
FTE	Flight Test Engineer
FTT	Flight Test Techniques
PDR	Preliminary Design Review
PRR	Preliminary Report of Results
RTO	Responsible Test Organization
SPO	System Program Office
SRB	Safety Review Board
TEMP	Test and Evaluation Master Plan
THA	Test Hazard Analysis
TIM	Test Interchange Meeting
TPS	Test Pilot School
TPWG	Test Plan Working Group
TRB	Technical Review Board
UTSO	Unit Test Safety Office

## REFERENCES

1. AFSCR 23-4.
2. *Test Control and Conduct*, AFFTC Regulation 55-23.
3. *Research and Development Test Plan*, AFFTCR 80-1.
4. *Research and Development - Test and Evaluation*, AFR 80-14, AFSC Supplement 1, AFFTC Supplement 1.
5. *Safety Planning and AFFTC Tests*, AFFTC Regulation 127-1.
6. Stroface Joseph F., *The Author's Guide to Writing AFFTC Technical Reports*, AFFTC-TIH-88-002, AFFTC, Edwards AFB, California, May 1988.



Lockheed C-130H Cutaway

# INDEX

## A

A weighting	9-6
Accelerance	4-11
Accelerometer	7-1, 10-7
Calibration	10-10
Compression	10-18
Frequency range	10-18
Installation	10-10
Linearity	10-10
Measurement	10-10
Natural frequency	10-8
Reference	7-9
Roving	7-31
Scale factor	10-10
Sensitivity	10-10
Servo	10-8
Shear mode	10-8
Tri-axial (triax)	7-1, 9-2, 10-8
Voltage mode	10-10
Accessory gearbox	1-10
Accumulator	1-13
Acoustic chamber tests	
Progressive wave chamber	9-8
Reverberant chamber	9-8
Active Control System (ACS)	5-14
ADAM (Analogue and Digital Aeroversoelasticity Methods)	8-10
Advanced Development Program Office (ADPO)	13-1
Aerial refueling (AR)	1-15
Acroacoustics	9-1
Aerodynamic	
Center (a.c.)	2-9, 2-14, 2-15
Quasi-static	6-13
Quasi-steady	6-13
Stiffness	6-12
Aeroversoelasticity (ASE)	8-10
Analysis	8-10
Flight test	8-15
Ground test	8-12
Acrothermoelasticity	6-16
Afterburner	1-12
Aileron	1-4, 2-20, 6-10, 6-12
Reversal	6-15
Roll	5-10

Airbrake	1-6
Aircraft	
Geometry	1-1
Tail	1-3, 2-14
Airfoil	2-8
Oscillating	6-6
Airloads (see Load)	
Airspeed	
Calibrated (CAS)	2-4
Calibration	2-4, 6-23
Equivalent (EAS)	2-4
Indicated (IAS)	2-4
Indicator	1-20
True (TAS)	2-8
Aliasing	12-4, 12-16
Altimeter	1-20
Altitude	
Density	2-4
Pressure	2-4
AM-2 runway repair mat	
American method	6-9
Amplitude resolution	12-2, 12-4, 12-6
Analog-to-digital converter (ADC)	10-20, 12-6
Angle of attack (AOA)	2-9, 2-13, 2-15, 5-8, 6-28
Anhedral	1-2
Animated mode shape	7-1
Antinode	4-17
Antiresonance	4-17, 7-18, 11-17
Aperture error	12-6
Area, wing	1-1
Argand plane	11-23
Arrestment tests	5-17
Aspect ratio	1-1
Asymmetric mode	7-18
Atmosphere	2-1
Attitude indicator	1-20
Augmentor	1-13
Auto power spectrum or auto spectrum	11-9, 11-12
Autopilot	1-15
Auxiliary power unit (APU)	1-13
Avionics	1-8
Averaging	12-1
Ensemble	11-1, 12-13
Linear	12-13
Overlap	12-13
Power	12-13

# INDEX (Continued)

RMS	12-13	<u>C</u>
Axes		
Body fixed	2-13	California Bearing Ratio
Directional	2-13, 2-15	(CBR) 5-15
Lateral	2-13, 2-15	Camber 2-8
Normal	5-2	
Vertical	5-2	Canard 1-6, 2-14
<b>B</b>		Center of
Backlash (see Freeplay)		Gravity (cg) 2-13, 2-14
Band Selectable Analysis		Pressure (c.p.) 2-9
(BSA)	12-14	Centering tendency 6-3
Band Selectable Fourier		Chaff 1-20
Analysis (BSFA)	12-14	Characteristic polynomial 8-8
Bandedge	10-18	Charge amplified 10-10
Bandwidth	8-5, 12-1, 12-2	Chirp (see Sine input)
Barometric pressure	2-1	Chord 1-1
Baseband analysis	12-2	Circuit breakers 1-13
Beating	4-12, 11-14	Circulation 2-9, 2-11
Bending	3-1	Circle fit method 11-23
Bernoulli Equation	2-4	Class II modification 13-2
Binary numbers	10-16, 12-4	Clipping error 12-4
Bit	10-20, 12-4	Clock jitter error 12-6
Drop-out error	12-20	Closed-loop 8-3
Bleed air	1-10	Coalescence 6-1
Block	12-1	Coherence 6-26, 11-21
Diagram	8-3	Ordinary 11-21
Diagram algebra	8-3	Multiple 7-22, 11-21
Size	12-1, 12-2	Partial 7-22, 11-21
Blockage	6-18	Coincident (CO) 11-23
Blower	7-7	Cold-working 3-8
Node plot	8-8, 11-26	Combined Test Force (CTF) 13-2, 13-13
Bonker	6-22	Combustion section 1-10
Boom refueling	1-15	Commutator 10-20
Boundary layer	2-9, 2-11, 6-13	Compensation 8-6, 8-8
Turbulent	2-11	Dynamic 8-6
British method	6-10	Gain 8-6, 8-8
Brittleness	3-10	Lag 8-6, 8-8
Buffet	5-8, 5-10, 6-15, 6-23,	Lead 8-6, 8-7
	13-6	Lag-Lead 8-6, 8-10
Bump and dip test	5-15	Compliance 11-17, 11-23
Burst	6-23	Dynamic 4-11
Burst-and-decay	6-22	Mechanical 6-4
Butt line (BL)	1-6	Composites 3-5
Buzz	6-13	Compressibility, 2-4, 2-12, 6-7
Bypass ratio	1-10	compressible flow 1-10
		Compressor
		Computational fluid
		dynamics (CFD) 2-11

## INDEX (Continued)

Configuration Control		Hysteretic	4-2, 6-9
Board (CCB)	13-2	Inherent	6-3
Control		Matrix	4-13, 6-12
Reversal	6-14	Error	12-6
Room	13-4	Proportional	4-2
Pulse	6-19	Rate	11-1
Rap	6-19	Ratio	4-5, 11-1
Coordinates		Resolution	12-2,
Natural	4-16	Structural	4-2, 6-3, 6-15
Principle	4-16	Total system	6-3
Transformation	4-15	Viscous	6-12
Coordinated test	2-15	Viscous damping coefficient	6-12
CO/QUAD method	7-18, 11-22	Data bus	1-8
Corner point	5-4	Data error	12-4
Correlation function		Deadbeat	4-5, 6-26
Auto-correlation	11-5	Decade	9-6
Cross-correlation	11-5	Decibel (dB)	8-8, 9-3, 11-14, 11-17
Frequency domain	11-12	Decimation	12-14
Time domain	11-4	Decoupled	4-15
Corrosion	3-8	Degree of freedom (DOF)	4-1, 6-1, 6-17
Electrochemical	3-9	Single	4-3, 6-13, 11-1
Coupling	4-15, 6-1	Multiple	4-13, 11-2, 11-6, 11-23
Crack	3-10	Delamination	3-8
Creep	3-8	Diffuser	1-13
Critical Design Review		Digitizer error	12-6
(CDR)	13-6	Dihedral	1-2
Cross point measurement	7-9	Direct current (dc)	11-1, 11-9, 11-10, 12-13
Cross power spectrum (see power spectral density)		Discrete	10-18
Curve fitting	7-23, 11-2, 11-20	Discriminator	10-20
Cut-off	12-14	Displacement transducer	10-16
		Divergence	6-14
		Divergent response	4-5, 6-1, 6-3, 6-4, 6-9
		Dome mode	8-1
<b>D</b>		Dorsal	6-10
Damage tolerance	5-7	Doublet	1-6
Damper	4-1	Aerodynamic	2-16
Viscous	4-2	Control	6-19
Damping	2-24, 6-2, 6-9, 6-24, 6-28	Lattice method	2-16
Acrodynamic	6-3, 6-12	Downwash	2-9
Aeroelastic	6-3	Drag	2-9, 2-11
Coefficient	11-1	Coefficient	2-11
Coefficient of viscous damping	4-2	Form	2-11
Coulomb	4-2	Induced	2-9
Critical	4-5, 11-1	Interference	2-11
Equivalent	6-12	Parasite	2-11
Factor	4-5	Profile	2-11

## INDEX (Continued)

Skin friction	2-11	Electronic warfare (EW)	1-22
Total	2-11	Elevated-g roll	5-10
Wave	2-11	Elevator	134, 2-14
Driving point measurement	7-9	Elcvon	1-6
Drop tanks	1-15	Empennage	1-3
Dropouts	10-18	Engine pressure ratio (EPR)	1-20
Ductility	3-10	Engineering units (EU)	10-1
Durability	3-10, 5-7	Ensemble averaging (see Averaging)	
Dutch roll mode	2-16	Environmental control system (ECS)	1-8, 1-10, 1-13
Dye penetration	3-10	Euler coordinates	8-10
Dynamic		Event switch	10-18
Balance	6-4	Excitation	
Pressure ( $\dot{q}$ )	2-4, 6-23, 6-24	Aircraft	6-18
Pressure Transducer (DPT)	10-13	Base	7-5
Response	6-16	Exfoliation	3-9
Dynamical matrix	4-17	Exhaust gas temperature (EGT)	1-20

### E

Eddy current	3-10
Effective mass	7-7, 7-28
Eigensolution	6-9, 6-14
Eigenvalue	4-17, 6-9
Eigenvector	4-17, 6-9, 6-10
Ejection seats	1-15
Elastic	
Axis	6-19, 7-8, 7-12
Limit	3-4
Range	4-1
Elasticity	3-11
Modulus of	3-3, 6-16
Electrical bus	1-13
Electrodynamic Exciter	6-20
Electrodynamic Shaker	6-20, 7-1, 7-5
Armature	7-5
Attachment to structure	7-18
Characteristics	7-15
Force drop at resonance	7-18
Multishaker techniques	7-22
Physical Features	7-15
Selection	7-7
Sting	7-2
Stroke	7-7
Suspension	7-2, 7-17
Electromagnetic compatibility/electromagnetic interference (EMC/EMI)	13-2

### F

FACES	6-6
Factor of safety	3-4, 5-7
Failure modes, flight control system	8-15
Fast Fourier transformation (FFT)	11-12
Fatigue	3-8, 5-7, 6-13, 13-3
Sonic	9-1
Feedback	8-3
Fillet	1-8
Filters	12-16
High pass	12-16
Low pass	12-16
Ripple	12-16
Ringing	12-16
Roll-off	12-16
Sidelobe	12-16
Skirts	12-16
Tracking	12-16
Finite element modeling (FEM)	3-5
Flap	1-3
Flaperon	1-3
Flexibility matrix	4-15
Flexure	6-6
Flight	
Cards	13-5
Control system (FCS)	5-1

# INDEX (Continued)

Computer	1-15	Fast Fourier Transformation (FFT)	11-12, 12-6
Mechanics	2-12	Inverse Fourier Transformation (IFT)	11-11, 12-16
Operating limits (FOL)	5-1	Series	11-9
Flight data recorder	3-9	Transformation	11-9, 12-1
Flight Test Techniques (FTT)	13-4	Frame	10-20, 12-1
Flootation system	7-5	Free-free condition	7-1
Flow straighteners	2-9	Free-play	6-4, 6-28, 7-4
Flutter	6-1, 8-1	Frequency	4-4
Aileron rotation/wing bending	6-4	Cutoff	12-16
Bending-torsion	6-3	Damped natural	4-4, 11-1
Binary	6-1	Division multiplex (FM)	10-20
Body freedom flutter	6-2	Domain analysis	11-6
Critical flutter mode	6-3, 6-26	Folding frequency	12-4
Data Reduction	6-25	Line	12-6
Determinant	6-7	Natural	11-1, 11-4
Divergent	6-3	Nyquist	12-4
Examples	6-3	Rejection	12-16
Explosive	6-10	Resolution	12-1, 12-10, 12-14, 12-18
Flight test	6-18	Response Function (FRF)	7-2, 11-1
Incipient	6-23	Undamped	4-4
Limit Cycle Flutter (LCF)	6-15	Fretting	3-9
Margin	6-10, 6-26	Fundamental Mode	4-13
Match point analysis	6-10	Fuse plugs	5-17
Mechanism	6-1, 6-26	Fuselage	1-6
Mode	6-2	Fuselage station (FS)	1-6
Panel	6-13		
Prediction	6-6		
Propellor whirl flutter	6-5		
Quaternary	6-1		
Quinary	6-1		
Speed	6-3		
Store	6-16		
Suppression	6-6		
Ternary	6-1		
Flutteron	6-21		
Fly-by-wire	1-15, 5-1, 6-22		
Force transducer	10-11		
Compression-tension-impact	10-11		
Force link	10-11		
Force ring	10-11		
Sensitivity	10-11		
Forward-swept wing	6-14		
Fourier			
Discrete Fourier Transformation (DFT)	11-11, 11-12		
		G	
		Gain (see also Compensation)	8-5, 8-6
		Crossover frequency	8-10
		Margin	8-8, 8-10
		Generalized	
		Coordinates	4-15
		Modal matrix	4-16, 6-6
		Generator	1-13
		GO/NO-GO parameters	
		Safety of flight	10-1
		Safety of test	10-1
		Technical	10-1
		Ground Resonance Test	
		(GRT)	7-3, 8-12, 8-13
		Ground vibration test (GVT)	6-6, 6-7, 6-18, 7-1, 8-13, 11-6

# INDEX (Continued)

Aircraft suspension	7-1, 7-4	Inertia	4-2
Configuration	7-3	Matrix	4-13
Excitation techniques	7-12	Moment of	4-2
Preparation	7-2	Polar moment of	4-3
Survey	7-1, 7-20	Inertial navigation system	
Transducer installation	7-12	(INS)	1-20
Wand	7-20	Influence coefficient matrix	4-15
G-suit	1-20	In-homogeneous materials	3-7
Gust	5-12, 6-15	Inlet	1-6
Loads flight tests	5-12	Instantaneous spectra	11-12
Probe	6-23	Instrumentation systems	10-18
		Intake	1-6
		Intercom	1-20
		Interphone	1-20
		Inter-turbine temperature	
		(ITT)	1-20
Half power damping method	11-13, 12-4	In-vacuo analysis	6-7
Hamilton's Principle	4-10	Inverse square law	9-3
Harmonics	4-13	IRIG-B	10-16
Harmonic function	4-7, 6-12	Ironbird	8-12
Heads-up display (HUD)	1-20	Isobei contours	9-9
Heavy Store Oscillation	6-15	Isolator mounts	9-2
Helix angle	6-15	Isotropic materials	3-5
Hooke's Law	3-3		
Horizontal situation indicator (HSI)	1-20		
Horizontal stabilizer	1-3		
Hot spots	7-12		
Hump mode	6-10	J	
Hydraulics	1-13	Jump phenomenon	4-13
Hypersonic	2-10		
		K	
I		KE-method	6-12
Ibrahim Time Domain	7-23	Kinetic heating	3-5
Identification friend-or-foe (IFF)	1-20	K-method	6-9
IFDAPS	10-14	Knots	2-4
Impact testing	7-13	Kulite	10-13
Tips	7-14		
Weight	7-14		
Impedance	4-11, 7-9, 11-17	L	
Electrical	7-9	Lag (See also Compensation)	11-5
Mechanical	7-9	Lag-lead (See also Compensation)	
Mismatch	7-9	Lagrangian	4-10
Incidence, wing	1-2	Landing gear	1-6
Indicial response	8-5	vertical load factor	5-16
Inertance	4-11, 11-17	load tests	5-16
		Laminar flow	2-9, 2-11

# INDEX (CONTINUED)

Laplace	4-10, 8-6	<b>M</b>
Transformation	11-26	
Variable	11-23	
Lateral-directional		<b>Mach</b>
Axes (see Axes)		Box method
Control system	8-3	Number
Lead (See also Compensation)		Critical
Leading edge extension (LEX)	6-15	Magnaflux
Leakage error	7-18, 12-8, 12-16	
Lessons Learned	13-6	<b>Manifold</b>
Least squares curve fit	11-4	
Lift	2-8, 2-9, 2-11, 5-2	<b>Maneuver</b>
Coefficient	2-9	Asymmetric
Lifting line theory	2-11	Load Control (MLC)
Limit Cycle		Speed
Oscillation (LCO)	6-15, 6-26	Symmetric
Test	8-12	Margin of safety
Linear variable differential		Mass
transformer (LVDT)	10-16	of air
Lincarity check	7-20	Apparent
Lissajous figures	6-22, 7-18, 11-6	Balancing
Load	5-6	Effective
Airload	5-1	Line
Alleviation system	5-13	Lump
Asymmetric normal load	5-2	Matrix
Cell	7-9, 7-13, 10-11	Point
Correction	5-11	Matrix Iteration
Design limit load	3-4, 5-7, 5-8, 5-11	Maxwell's Reciprocity
Environmental	5-1	Theorem
Gust	5-12, 5-11	Mean aerodynamic chord
Inertia	5-1	(MAC)
Landing gear	5-14	Mean chord line
Limit load factor	5-2	Measurand
Live	5-1	Mechanical
Reaction	5-1	Fuse
Side	5-2	Vibration
Ultimate	3-4, 5-7	Microphone
Vertical	5-1	Ceramic
Vertical load factor ( $n_z$ )	5-2, 5-7	Condenser
Logarithmic		Mission computer
Amplitude (log amp)		Mobility
method	11-2	Mode
Decrement (lod dec)		Antisymmetric
method	11-2	Characteristic
Longitudinal axes	2-13	Close
Loss-of-signal (LOS)	10-18, 12-8	Complex
		False
		Local
		Natural
		Normal

# INDEX (CONTINUED)

Real	4-11	Oil-canning effect	6-13, 8-3
Shape	4-16, 6-13	Open-loop	8-3
Symmetric	7-20	Operating inputs	7-22
Tuning	11-6	Operating Instruction (OI)	13-7
Visualization	7-23	Orthogonal	4-16
Modal		Transformation	4-16
Analysis	4-13	Orthogonality	
Parameters	7-23	Check	7-23
Motion sensors, aircraft	8-1, 8-3	Cross-orthogonality	7-23
Accelerometer	8-1	Orthotropic materials	3-5
Gyro	8-1	Outriggers	1-8
Multiplexer (mux)	10-18	Overall sound pressure level (see Sound)	
Multiple-input, multiple-output (MIMO)	8-3	Over-design	5-8
Multipoint data	7-22	Overdamped	4-5
Multipurpose display (MPD)	1-20	Overload error	12-6
 <u>N</u>		Overload Warning System (OWS)	5-2
Nacelle	1-6	Over-g	5-11
NASTRAN	3-5, 6-6	Overtones	4-13
Newton's Second Law of Motion	4-2	Oxidation	3-9
Nichol's plot	8-8	 <u>P</u>	
Node	3-5, 4-17, 7-9, 8-4	Panels	2-12
Line	7-23	Parameter	
Noise	12-6	Estimation	7-23
Floor	12-6, 12-13	Extraction	7-23
Pink	9-3	Identification	7-23
Random	9-3	Peak	
White	9-3	Amplitude method	11-2
Non-destructive inspection (NDI)	3-9	Picking method	11-14
Nonlinearities	6-6, 7-2, 7-20, 12-6	Perfect Gas Law	2-1
Normal load factor	6-6	Period of oscillation (T)	4-4, 11-1
Notch filter	8-15	Phase	
Nozzle	1-13	Angle	4-7, 11-4, 11-6
Nozzle pressure ratio (NPR)	1-20	Crossover frequency	8-10
Nyquist		In phase	4-8
Path	8-10	Margin	8-8
Plot	8-10, 11-23	Shift	4-11
Stability Criterion	8-10	Phugoid mode	2-16
 <u>O</u>		Piezoelectric	10-7
Octave	9-3	Piezo-resistive	10-8
Third-octave	9-3	Pilot induced oscillation (PIO)	2-16
		Piston theory	2-12
		Pitch	2-13
		Pitot-static boom	2-4
		Pitting	3-9

## **INDEX (Continued)**

	<u>R</u>
PK-method	6-10
Planform, wing	1-1
Plant	8-3
Plasticity	3-11
Plunge	6-2
P-method	6-12
Poisson's Ratio	3-3, 10-4
Polar	
Coordinates	8-10
Plot	8-10, 11-23
Pole	8-6, 11-26
Pole-zero	8-6, 11-26
Plot	8-7, 11-27
Poly Reference	7-23
Position error	2-4
Power spectral density (PSD)	11-12, 11-14
(See also Auto spectrum or auto power spectrum)	
Cross spectrum or cross power spectrum	11-12
Cross spectral density (CSD)	11-13
Pre-flight briefing	13-5
Preliminary Design Review (PDR)	13-3
Preliminary Report of Results (PRR)	13-6
Preload	7-4
Pressure	
Distribution	2-6
Gradient	2-6, 2-11
Sensor	10-13
Taps	5-8
Probe and drogue refueling	1-15
Project history	10-1
Proof test	5-7
Proportional force method	7-18
Propulsion	1-10
Pull-up	5-10
Pulse code modulation (PCM)	10-20
Push-over	5-10
.	
<b><u>Q</u></b>	
Quadrature (QUAD)	11-23
Quality factor	11-14
Quantization error	12-6
Quill	7-8
Radome	1-6
Raleigh's Criterion	12-2
Quotient	4-17
Random decrement (Randomdec) method	11-4
Random input	7-18
Burst	7-20
Periodic	7-19
Pseudo-random	7-19
Pure	7-18
Rate-of-climb indicator	1-20
Ram air turbine (RAT)	1-13
Ranging	12-2
Half-ranging	12-2
Over-ranging	12-4
Under-ranging	12-4
Rectangular coordinates	8-10
Receiver	1-15
Reciprocity	7-2
Reduced	
Frequency	6-9, 6-13, 6-18
Velocity	6-9
Relative wind	2-13
Reservoir, hydraulic	1-13
Residue	11-1, 11-14
Resilience	3-11
Resistance device (RTD)	10-16
Resonance	4-8, 4-11, 4-17
Response	
Forced	4-7
Free	4-4
Impulse	11-1
Steady-state	4-7, 7-1, 7-17
Transient	4-7, 7-1, 7-19, 11-1
Unforced	11-1
Responsible Test	
Organization (RTO)	13-2
Right half-plane (RHP)	8-7
Rigid body mode	2-16, 7-1, 7-4
Rise time	8-5
Risk level	6-25, 13-4
Roll	2-13, 2-15
Effectiveness	6-15
Rolling pull-out (RPO)	5-10
Rollup	2-17

# INDEX (Continued)

Root-locus	8-6	S-N diagram	3-8
Roving	7-1	Sound	9-1
Rudder	1-3, 2-15	Chamber tests (see Acoustic chamber tests)	
Kicks	5-10	Data analysis	9-9
Reversals	5-10	Equivalent continuous	
Ruddervator	1-6	sound level	9-6
Rust	3-9	Exposure level (SEL)	9-6
<b>S</b>			
Safety chase aircraft	6-25, 13-5	Far field	9-3
Safety Review Board (SRB)	13-4	Free field	9-3
Sample rate (SR)	12-1, 12-2, 12-14	Infrasound	9-2
Sand pattern	7-23	Intensity	9-2
Schlieren	2-6	Near field	9-8
Separated flow	2-9, 6-14	Overall sound pressure	
Self-operating input	7-12	level (OASPL)	9-6
Self-windowing signals	12-9	Power level	9-6
Settling time	8-5	Pressure	9-3
Shannon's Sampling Theory	12-1, 12-4	Pressure level (SPL)	9-3
Shear	3-1,	Semireverberant field	9-3
Modulus	3-4, 4-3	Testing	9-8
Shimmy, landing gear	5-17	Ultrasound	9-2
Shock isolator	9-4	Source	2-11
Shock wave	1-10, 2-7, 2-12, 6-13	Spalls	5-15
Normal	2-7	Span	1-1
Oblique	2-7	Spectral lobe	12-2
Short period mode	2-16	Spectrogram	9-9
Sideslip	2-15, 5-10	Speed of sound	2-7
Signal conditioner	10-18	Speedbrake	1-6, 6-6, 6-23, 6-25
Signal-to-noise ratio (S/N)	7-16, 7-19, 12-6	Spin	2-16
Signature	11-4	Spiral mode	2-16
Length	11-4	S-plane	8-6, 8-6, 11-23
Sine input	7-17	Spoiler	1-3
Chirp	7-18	Spring	4-1
Dwell	7-18	Constant	4-1
Fast Sine Sweep	7-18	Spring-mass-damper system	4-4
Stepped sine	7-18	Stability	
Sweep	7-17	Artificial	2-15
Single-input, single-output		Axes	2-13
(SISO)	8-3	and Control	2-12
Singlet	6-19	Dynamic	2-16
Sink	2-11	Derivative	2-17
Skirt, modal	12-6	Static	2-14
Slat	1-3	Stabilator (Stab)	1-3, 2-14
Slip plate	7-5	Stable system	6-3
Slow code	10-16	Stagnation point	2-6
		Stall	2-9
		Standard	
		Atmosphere	2-1
		Day	2-1

## INDEX (Continued)

Static pressure test	5-7	Stripchart recorder (SCR)	10-18
Stationarity	7-4	Structural	
Stator	1-10	Coupling	8-1
Steady-heading sideslip	2-15	Feedback	8-1
Step input	6-19, 8-6	Fuse	7-8
Step relaxation input	7-16	Mode vibration (SMI) test	8-12
Stick		Subcarrier oscillator (SCO)	10-20
Fixed	2-16, 6-19	Subsonic	2-7
Free	2-16, 6-19	Superposition, principle of	10-5
Stiffener	6-13	Supersonic	2-7, 2-12
Stiffness	4-1, 6-7, 6-28	Sweep	
Aerodynamic	6-12	Excitation	6-19, 6-24
Apparent	4-11, 11-17	Wing	1-1
Dynamic	4-11	Sweet spots	8-1
Line	11-17	Syncro	10-20
Stop-drill	3-8	System	
Strake	1-8	Error	8-5
Strain	3-1, 10-2	Minimum phase	8-7
Hardening	3-8	Non-minimum phase	8-7
Meter	10-4	Program Office (SPO)	13-1
Principal	10-4		
Residual	10-4		
Strain gages	5-8, 10-2		
Calibration	10-5		
Dummy	10-4		
Gage factor (K)	10-3		
Installation	10-7		
Rosette	10-2		
Selection	10-2		
Spiral	10-2		
Temperature compensation	10-4		
Uniaxial	10-2		
Streamline	2-6		
Strength	3-11		
Stress	3-1		
Analysis	3-4		
Axial	3-1		
Compression	3-1		
Concentration	3-1		
Limit	3-4		
Principal	3-1, 10-4		
Residual	3-1		
Shear	3-1		
Tension	3-1		
Ultimate	3-4		
Visualization	3-9		
String pot	10-16		
Strip theory	2-12		
		<b>T</b>	
		Tail hook	1-6
		Taper	1-1
		Taper ratio	1-1
		Taxi	
		Loads	5-15
		Tests	5-15
		Technical Interchange	
		Meeting (TIM)	13-3
		Technical Review Board	
		(TRB)	13-4
		Telemetry	10-18
		Tension	3-1
		Test and Evaluation Master	
		Plan (TEMP)	13-3
		Test Hazard Analysis (THA)	13-5
		Test plan	13-4
		Test Plan Working Group	
		Meeting (TGPW)	13-3
		Test planning	13-3
		Test repository	13-6
		Testbed	10-1
		Thermal	
		Expansion	3-5
		Stresses	3-5
		Thermocouple	10-16

# INDEX (Continued)

<b>Third-Octave (see Octave)</b>			
<b>Thrust</b>			
Reverser	1-13	Underdamped	4-5
Vectoring	1-13	Unit Test Safety Officer (UTSO)	13-4
<b>Thruster</b>	7-8	Unstable system	4-5, 6-1, 6-4, 8-1
<b>Thunderstorm penetration speed</b>	5-12	Unsteady flow	2-9, 6-1, 6-6, 6-13
<b>Time</b>		Upwash	2-9
<b>Code generator (TCG)</b>	10-16		
<b>Constant</b>	4-5		
<b>Delay</b>	8-5	<b>V</b>	
<b>Domain analysis</b>	11-1	V-f plot	6-10
<b>Tinic-invariant systems</b>	8-3	V-G plot	6-10
<b>Time-variant systems</b>	8-3	V-g diagram	5-2
<b>Torque</b>	4-3	V-n diagram	5-2
<b>Torsion</b>	3-1	V-q plot	6-10
<b>Toughness</b>	3-11	Ventral	1-6
<b>T-plot (see Transmissibility Plot)</b>		Fin	1-6
<b>Trailing cone</b>	2-4	Vertical tail	1-3
<b>Transfer function</b>	7-22, 8-3, 8-6, 8-8, 11-20	Vibration table	7-5
<b>Transformation matrix</b>	4-16	Vibro-acoustics	9-1
<b>Transient performance</b>	8-6	Viscous damping factor	4-5
<b>Transonic</b>	2-7, 6-6, 6-7, 6-23	Visicorder	10-18
<b>Transmissibility</b>	4-7	Voltage control oscillator (VCO)	10-20
Plot (T-plot)	11-26	Vortex	4-11, 6-15, 6-28
<b>Transponder</b>	1-20	Generators (VG)	2-9, 6-14
<b>Transport delay</b>	8-5	Tip	2-9
<b>Triggering</b>	11-6, 12-13	Sheet	2-12
<b>Trim</b>	2-16	V-tail	1-6
Tab	1-3, 6-5		
<b>T-tail</b>	1-3	<b>W</b>	
<b>Tufts</b>	2-6, 13-3	Wand	6-20
<b>Tuning modes</b>	7-18	Washin	1-2
<b>Turbine</b>	1-10	Washout	1-2, 2-17
<b>Turbojet</b>	1-10	Water line (WL)	1-6
<b>Turbofan</b>	1-10	Wavelength	9-2
<b>Turboprop</b>	1-10	Weight	
<b>Turbulence</b>		And balance	2-14
Penetration speed	5-12	Design	5-11
Random	6-15, 6-22, 6-25	Empty	2-14
<b>Twang test</b>	7-17	Gross	5-2, 5-11
		Standard	5-11
		Wheatstone bridge	10-4, 10-18
<b>U</b>		Wheel spin-up	5-15
<b>UFAPS</b>	6-6	Wind tunnel test	6-18, 13-3
<b>Ultrasonic inspection</b>	3-10	Windown turn	5-10
<b>Undamped</b>	4-5	Windup turn	5-10, 6-27

## INDEX (Concluded)

Window, data	12-4	<u>Y</u>	
Windowing	12-8	<u>Yaw</u>	
Boxcar	12-9	Adverse	2-15
Exponential	12-9	Axes	2-13, 2-15
Flat top	12-9	Damper	2-17
Force	12-9	Yield	3-4
Hanning	12-8	Young's Modulus	3-3, 4-2, 10-4
Hamming	12-8	<u>Z</u>	
Rectangle	12-9	<u>Zero</u>	
Uniform	12-9	Insertion	12-14
Wing	1-1	Offset	11-1, 12-13
Loading	5-7	Polynomial	8-6
Station (WS)	1-1	Zoom transformation	12-14
Winglet	1-2	Z-plane	
Word	10-20, 12-4	Analysis	11-28
Work	6-2	Inverse	11-28
Work-hardening	3-8	Transformation	11-28
Wrap around	12-6		
<u>X</u>			
X-ray	3-10		